RELIABILITY OF FLEXIBLE DOLPHINS

DETERMINATION OF THE PARTIAL SAFETY FACTORS FOR PARAMETERS IN FLEXIBLE DOLPHIN DESIGN

Master of Science Thesis

I.J.M. Schrijver

RELIABILITY OF FLEXIBLE DOLPHINS

DETERMINATION OF THE PARTIAL SAFETY FACTORS FOR PARAMETERS IN FLEXIBLE DOLPHIN DESIGN

Master of Science Thesis

For the degree of Master of Science in Civil Engineering at Delft University of Technology

I.J.M. Schrijver

June 13, 2016

Faculty of Civil Engineering and Geosciences – Delft University of Technology

Student	I.J.M. (Ilona) Schrijver	
	Zuideindseweg 13	
	2645 BD Delfgauw	
	06 – 15634614	
	Ilona_schrijver@hotmail.com	

Assessment Committee

Chairman	Prof. Dr. Ir. S.N. Jonkman	TU Delft
Daily supervisor	Dr. Ir. K.J. Bakker	TU Delft
Daily supervisor	Ir. D.J. Jaspers Focks	Witteveen+Bos
Supervisor	Dr. Ir. J.G. de Gijt	TU Delft
Supervisor	S.H.J. van Es, MSc	TU Delft
External supervisor	Prof. Dr. Ir. R.D.J.M. Steenbergen	TNO
External supervisor	Ir. A.A. Roubos	Havenbedrijf Rotterdam

ABSTRACT

The subject of this master thesis is introduced by the lack of regulations for the design of flexible dolphins. Currently, the design of flexible dolphins is based on the Eurocode, which does not cover all aspects which are of importance in dolphin design. Consequently, different countries and associations developed their own guidelines, which often do not coincide and are used interchangeably by different advisers. Nowadays, there is no uniform design approach for the design of flexible dolphins. The partial safety factors used in dolphin design are therefore not consistent and often subject of debate.

This master thesis starts with a literature review on the available design models which are nowadays most often used in flexible dolphin design. The oldest model which is still frequently used in the preliminary design stage, is the empirical method of Blum. The simplicity of this model also introduces several limitations. Some more advanced models are D-Sheet Piling and D-Pile Group, which approach the behaviour of the soil by bi-linear and non-linear springs along the pile. However, research reveals that the Finite Element Method approaches the behaviour of laterally loaded piles best. With Plaxis 3D it is possible to assign a different soil model to the each individual layer of soil, resulting in a relatively accurate approximation of the soil behaviour. However, because of the complexity of Plaxis 3D and the lack of probabilistic tools, this model is not considered to be the most appropriate for this master thesis.

In order to determine which of the two springs models, D-Sheet Piling or D-Pile Group, is most appropriate for the derivation of the partial safety factors, a comparison between the models was made based on the results obtained from performed tests. It was demonstrated that both models tend to overestimate the bending moments which develop in laterally loaded piles, whereas D-Pile Group seems to give a better approximation of the deformations. However, it was found that under some conditions, D-Pile Group overestimates the reliability of the structure. Therefore, D-Sheet Piling was considered to be most suited for the determination of partial factors for dolphin design.

To determine the partial safety factors for flexible dolphins, a reliability analysis was carried out with the probabilistic toolbox Prob2B. With this toolbox a FORM-analysis was performed on a flexible mooring dolphin from practice. The evaluations were performed with respect to three different limit states, namely structural failure of the cross-section of the pile, excessive deformations and soil mechanical failure. After the evaluation of the initial mooring dolphin design, modifications were introduced to the soil structure in order to examine the sensitivity of the influence factors and partial safety factors to changes.

From the probabilistic evaluations with respect to structural failure, it was concluded that the reliability of the structure is mainly defined by the exerted mooring load and the structural parameters of the pile. The soil hardly has any influence on the reliability of the structure. Only the most upper soil layer prevents the development of the bending moment in the structure, and an increasing strength of this layer therefore introduces a higher reliability.

With respect to the deformations of the structure, it was concluded that again the mooring load strongly contributes to the reliability of the dolphin. Furthermore, the strength of the upper soil layers is of importance. The influence of the soil on the reliability of the structure appears to decrease with increasing depth. Moreover, it was concluded that the influence of the different variables is most sensitive to changes in strength and layer thickness.

The final limit state which was evaluated, was soil mechanical failure. As a result of the lateral load exerted on the pile, a passive wedge develops at the rear side of the structure. At a certain point, this wedge is fully developed and soil mechanical failure of the structure is induced. From the probabilistic analysis it was found that the mooring load also has a large, but smaller, influence on the reliability of flexible dolphins with respect to this limit state. Furthermore, it could be concluded that the soil parameters which have most influence on the reliability are the weight of the soil and the angle of internal friction.

Finally, a recommendation has been made for a set of partial safety factors for flexible mooring dolphin design. It was proposed to apply partial factors equal to 1.30 on the characteristic mooring load and the stiffness of the soil. Furthermore, it was recommended to apply a partial safety factor equal to 1.15 on the characteristic value of the friction angle of the soil and to apply a factor equal to 1.05 on the mean wall thickness of the pile. For the other parameters, a partial safety factor equal to 1.00 was recommended.

PREFACE

This report has been established in response to my thesis study, where research has been done on the partial safety factors for parameters in flexible dolphin design. The research was conducted at Witteveen+Bos within the department of geotechnical engineering and at Delft University of Technology, faculty of Civil Engineering and Geosciences at the department of Hydraulic Engineering.

I would like to express my gratitude to Witteveen+Bos and Ir. D.J. Jaspers Focks for providing the resources and support during my stay at Witteveen+Bos, and to TNO with in particular Dr. Ir. W.M.G. Courage for providing the probabilistic calculation tools. Furthermore, I would like to thank all the members of my assessment committee for their guidance and support, which were of great value for this thesis.

Delfgauw, June 2016
Ilona Schrijver

TABLE OF CONTENTS

NOMENCLATURE

Probabilistic calculations

α_i	Influence factor of parameter
β	Reliability index
$\gamma_{calc,i}$	Partial safety factor over the characteristic value for the calculated reliability
$\gamma_{RC2,i}$	Partial safety factor over the characteristic value for the target reliability of RC2
$\gamma_{R,i}$	Partial safety factor for resistance
$\gamma_{S,i}$	Partial safety factor for solicitation
μ_i	Mean parameter value
P_f	Probability of failure
$P_{f,i}$	Probability of failure for a failure mechanism
R	Resistance
S	Solicitation
σ_i	Standard deviation of parameter
u_i*	Standard normal equivalent design value of parameter
V_i	Coefficient of variation of parameter
$X_{char,i}$	Characteristic parameter value
X_i*	Design parameter value
Z	Limit state function

Greek

α	Rheological coefficient	[-]
β	Correlation between cone resistance and pressiometric modulus	[-]
γ_{sat}	Saturated unit weight of soil	[kN/m^3]
γ_{unsat}	Unsaturated unit weight of soil	[kN/m^3]
δ	Deformation	[mm]
ε	Strain	[-]
ε_y	Yield strain	[-]
θ	Rotation	[deg]

ρ_{grains}	Density of grain	[kg/m^3]
ρ_{water}	Density of water	[kg/m^3]
σ_n'	Effective normal stress	[kPa]
σ_x	Meridional stress	[kN/m^2]
τ_{cr}	Critical shear strength	[kPa]
$\tau_{x\theta}$	Shear stress	[kPa]
φ	Angle of internal friction	[deg]

Latin

A	Absorbed energy	[kN m]
c	Cohesion	[kPa]
C_C	Berth configuration coefficient	[-]
C_E	Eccentricity coefficient	[-]
C_M	Added mass coefficient	[-]
C_S	Softness coefficient	[-]
D	Pile diameter	[m]
E	Young's modulus of steel	[kN/m^2]
E_N	Normal berthing energy	[kN m]
E_M	Pressiometric modulus of Ménard	[kN/m^2]
E_M^{ref}	Pressiometric modulus at reference pressure of 100 kPa	[kN/m^2]
EI	Flexible rigidity	[kN m^2]
F_b	Berthing force	[kN]
F_m	Mooring load	[kN]
F_{MBL}	Minimum breaking load of mooring lines	[kN]
$F_{mooring}$	Mooring load	[kN]
F_R	Impact berthing force	[kN]
f_y	Yield strength of steel	[N/mm^2]
k_h	Horizontal subgrade reaction of soil	[kN/m^2]
k_p	Bending stiffness of the pile	[kN/m]
k_s	Stiffness of the structure	[kN/m]
l	Pile length	[m]
m	Mass of vessel (displacement in tones)	[t]
M	Bending moment	[kN m]
n	Porosity	[-]
q_c	Cone resistance	[kPa]
s	Deflection	[m]
t	Wall thickness	[mm]
v	Berthing velocity	[m/s]
V	Shear force	[kN]
V	Volume of soil	[m^3]
W_d	Weight of dry soil	[kN]
W_{el}	Elastic section modulus	[m^3]
x	Distance	[m]

1

INTRODUCTION

1.1 Problem description

The Dutch landscape is characterized by their many inland waterways and adjacent ports, which form an important link in the transport chain in Western Europe. In these ports and along the river banks a lot of flexible dolphins are constructed, which have to provide safe mooring conditions for the barges and seagoing vessels. Distinction can be made between two different types of dolphins:

- Breasting dolphins have to protect underlying structures such as quays or jetties;
- Mooring dolphins have to provide facilities to secure a ship by ropes.

The impact forces or mooring forces exerted on flexible dolphins are absorbed by deformations of the structure and the soil.

So far there do not exist regulations that explicitly cover the design of flexible dolphins. Currently, mooring and breasting dolphins are designed based on the Eurocode (EN 1997), but this code does not provide sufficient guidance on a number of areas. On these aspects several countries and associations developed their own guidelines, which often do not coincide on all points and are used interchangeably by different advisers. This means that there is no uniform design approach for the design of flexible dolphins. The partial factors used in dolphin design are therefore not consistent and usually subject of debate.

The application of different design approaches and inconsistent partial factors may lead to conservative designs. This means that a lot of money can be saved, especially for large dolphins.

The problem of lack of a consistent design approach was also encountered by CUR Committee 206 of the SBRCURnet. They are therefore elaborating a new recommendation for the design of flexible dolphins. However, still no research has been done on the partial safety factors that can be applied to obtain a safe and robust design, what led to the start of this master thesis.

1.2 Objective

The main objective of this master thesis is to determine the partial safety factors that have to be applied on the design of flexible dolphins. These factors will be determined based on the results of tests that have been carried out by Witteveen+Bos and Royal HaskoningDHV commissioned by the Port of Rotterdam.

To reach the main objective, several research questions have been formulated at the start of this master thesis, which should be answered throughout this study:

1. Which models and guidelines are mostly used in the Netherlands for the design of flexible dolphins?
2. Which model provides the best approximation of the behaviour of flexible dolphins and how can this model be used in the determination of the reliability of the structure and the derivation of partial safety factors for parameters in flexible dolphin design?
3. What is the influence of the parameters involved in flexible dolphin design on the reliability of the structure and how sensitive are these influences to changes in the soil structure?
4. What are the required partial safety factors for flexible dolphin design with respect to the different failure mechanisms?

1.3 Outline of the thesis

The structure of this report broadly follows the order of the defined research questions. Chapter 2 starts with a literature review on the design models which are present-day most often used in Dutch dolphin design. It starts with a contemplation of the most simplified model and at the end of the chapter the most advanced model is considered. In Chapter 3, the literature review continues with an elaboration on the probabilistic analysis methods which can be used for the evaluation of the reliability of flexible dolphins and for the determination of partial safety factors. The chapter ends with an overview of the most commonly applied design codes in guidelines in flexible dolphin design.

In chapter 4 the most important starting points of the research are defined. First, it is determined which model and analysis method are most appropriate for this research to obtain the intended results. Subsequently the probabilistic model input is defined.

In chapter 5 a probabilistic analysis is performed for a flexible mooring dolphin from practice. The results contain a set of partial safety factors for the design of flexible dolphins in accordance with reliability class 2. However, these partial factors are determined based on specific conditions. Therefore, a sensitivity analysis is conducted in Chapter 6, in order to examine the sensitivity of these obtained factors to changes in the soil structure.

Chapter 7 is the final chapter of this master thesis. In this chapter the final conclusions are presented together with a set of recommended partial safety factors for flexible mooring dolphin design. At the end of this chapter also some recommendations are made for future research.

2

LITERATURE REVIEW – DESIGN MODELS

2.1 Introduction

Different models and methods are available for flexible dolphin design. The models and methods which are most frequently used in the Netherlands are introduced in this chapter. The characteristics of the methods are discussed, as well as the advantages and the limitations. The methods which are considered are:

- Empirical model – Method of Blum (section 2.2)
- P-y curves (section 2.3)
- D-Sheet Piling – Single Pile module (section 2.4)
- D-Pile Group (section 2.5)
- Finite Element Methods – Plaxis 3D (section 2.6)

2.2 Empirical model – Method of Blum

The original method of Blum (1931) was developed for the analysis of sheet pile walls. After some modifications, the method of Blum became in 1932 applicable for the problem of laterally loaded piles (Blum, 1932). This method has already been applied for over 80 years in engineering practice. The principle of Blum's method is that the toe of the pile is assumed to be a clamped edge. At this edge a concentrated reaction force is imposed which replaces the soil reaction on the pile below this clamping. The theoretically necessary penetration depth t_0 is obtained by considering a force equilibrium and a bending moment equilibrium at the toe of the pile. For homogeneous soils the required penetration depth can be calculated with equation 2.1 (Ruigrok, 2010).

$$\frac{24P}{f_w} = t_0^3 \frac{t_0 + 4b}{h + t_0} \tag{2.1}$$

In which:

P = Horizontal force at static loading [kN]

f_w = Soil resistance = $\gamma\lambda_p$ [kN/m^3]

λ_p = Passive pressure coefficient = $\frac{1+sin\varphi}{1-sin\varphi}$ [-]
φ = Angle of internal friction of the soil [deg]
γ = Volumetric weight of the soil above water table [kN/m^3]
t_0 = Theoretically necessary penetration depth [m]
b = Width of the pile perpendicular to the direction of the force [m]
h = Height where load P is applied [m]

The real penetration depth has to be sufficiently larger than the theoretically required penetration depth in order for the pile to be fully clamped. To obtain the real penetration depth, the theoretical penetration depth should be increased by 20%.

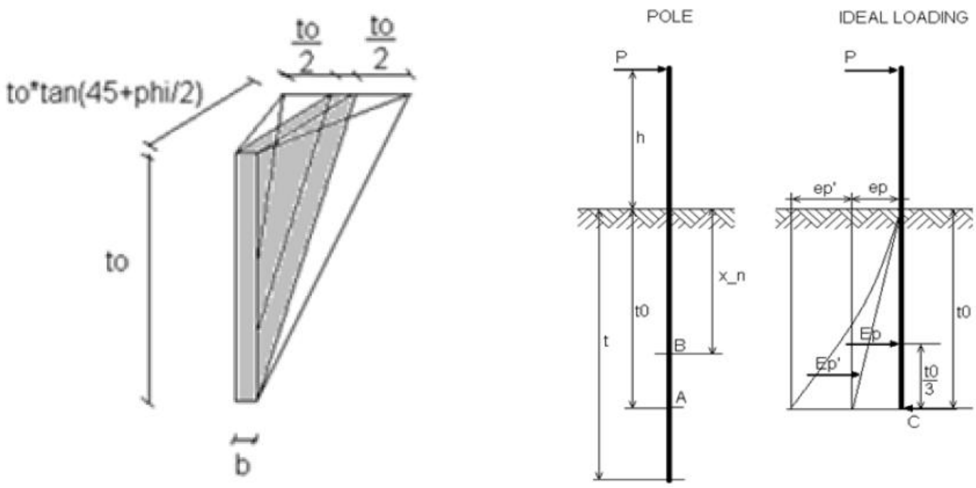

Figure 2.1 - Model of Blum (Ruigrok, 2010)

For the determination of the required penetration depth of the piles, only a few input parameters are required. This makes the method of Blum a very simple model. However, due to this simplicity also some limitations are introduced:

- Only homogeneous, non-cohesive soils are considered;
- The method is an ultimate strength model, it assumes that the full passive resistance is mobilized;
- No calculations under working loads are possible, only failure loads can be considered;
- Only static loads can be considered;
- Differences in cross-section of the pile cannot be taken into account.

In 1961 Brinch-Hansen developed a method similar to the method of Blum. It is also an ultimate strength model, but layered and cohesive soils can be taken into account. For a description of the Brinch-Hansen method and other empirical models, reference is made to Ruigrok (2010).

2.3 P-y curves

2.3.1 Beam model of Hetenyi

A laterally loaded pile is a typical soil-structure interaction problem, a solution for the reaction of the pile cannot be obtained without considering both the deformation of the pile and the soil (Reese, et al., 2006). In his beam model, according to which a pile under lateral load is considered to act, Hetenyi (1946) considered a linear relationship between the pile deflection and the soil response. In his book he derived a differential equation for the beam column on a foundation which is given by equation 2.2. For the derivation of this equation reference is made to Reese et al. (2006).

$$E_p I_p \frac{d^4 y}{dx^4} + P_x \frac{d^2 y}{dx^2} + E_{py} y = 0 \qquad (2.2)$$

In which:

E_pI_p	= Bending stiffness of the pile [kN m^2]
y	= Lateral deflection of the pile [m]
P_x	= Axial load on the pile [kN]
E_{py}	= Stiffness of the soil [kN/m^2]

In case there is no axial load present, the second term on the right hand side can be eliminated. The response of a laterally loaded pile, without the presence of an axial loading, is shown in Figure 2.2. In this figure also the mathematical relationships are included.

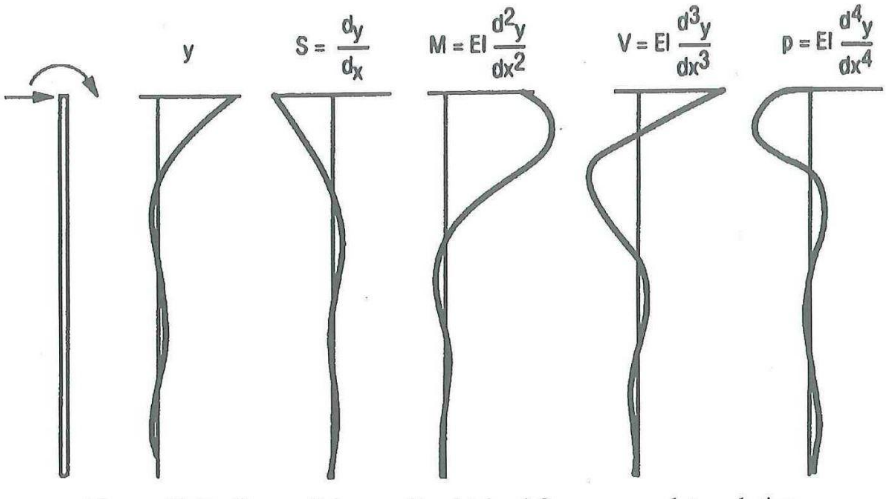

Figure 2.2 - Response of a laterally loaded pile according to Hetenyi (Reese, et al., 2006)

For his derivation, Hetenyi made some simplifications, which lead to limitations for the applicability of the differential equation. First of all, the method is only applicable for straight piles with an uniform cross-section which consist of a homogeneous and isotropic material. Furthermore, Hetenyi assumed a linear relation between the deflection of the pile and the soil response what means that the soil must have a uniform modulus of subgrade. This is not a realistic assumption. In addition to this no layered soils can be considered. Moreover, the soil is considered to form an elastic foundation for the pile, what means that plasticity of the soil is not taken into account. Finally, the largest limitation for the application of the model for the design of dolphins is that only static situations can be considered in which the proportional limit of the pile material is not exceeded.

Hetenyi's derivation formed the basis for the development of the p-y curves. This method is based on the non-linear reaction between the deflection of the pile and reaction of the soil and therefore will lead to more realistic solutions for the design of dolphins.

2.3.2 Characteristics of p-y curves

The p-y method is a modulus of subgrade reaction method which uses non-linear load-deformation curves. They describe the relationship between the passive earth pressure and the pile displacement that is needed to mobilize this (HTG, 2015). A typical p-y curve is shown in Figure 2.3a. It represents a situation where a short-term static loading is applied to a pile. The first part of the curve, between the origin and point *a*, shows that a linear relation exist between the deflection of the pile and the reaction of the soil for small pile deflections. As the deflection of the pile increases this relation becomes non-linear. This is represented by the part of the curve between points *a* and *b*, which shows an increasing soil resistance at a decreasing rate with respect to the pile deflection. The last part of the curve, after point *b*, indicates that the soil will behave plastically for large pile deflections.

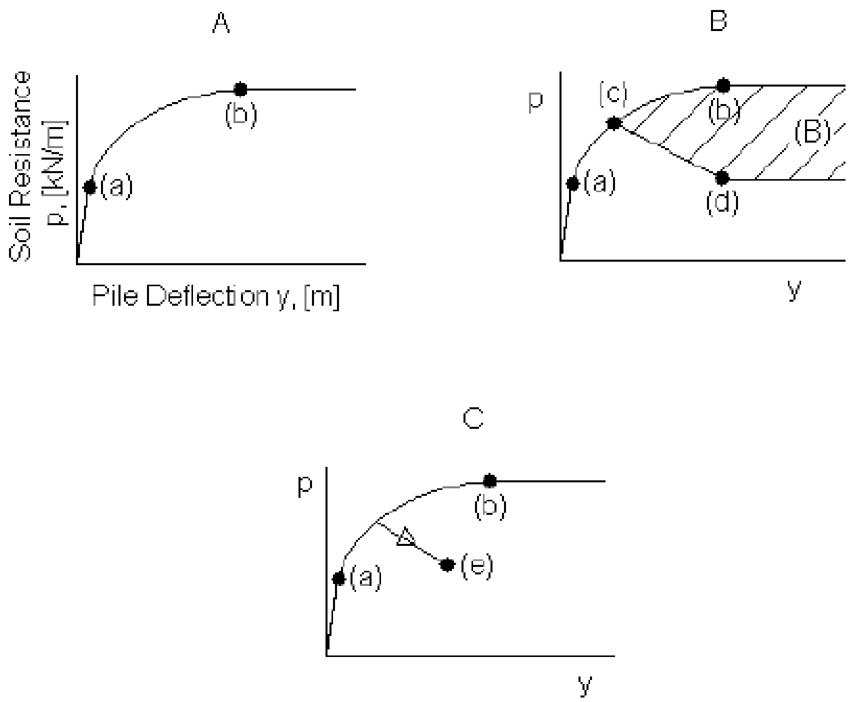

Figure 2.3 - Typical p-y curves for: (a) short-term static loading; (b) cyclic loading; (c) sustained loading (Ruigrok, 2010)

For the design of dolphins not only static, but also dynamic and cyclic loading have to be taken into account. At some point, these cyclic loads will lead to a decrease in soil resistance, as is reflected by the shaded area of the p-y curve in Figure 2.3b. For cohesive soils this loss of resistance can be explained by two different mechanisms (Reese, et al., 2006):

1. Due to subjection of the clay to repeated strains of large magnitude the soil around the pile is distorted what leads to a loss of shearing strength of the soil;
2. An enforced flow of water occurs in the vicinity of the pile what will cause scour around the pile.

Compared to the loss of resistance for cohesive soils, the loss of resistance for cohesionless soils is not nearly as significant. For these soils the decrease in soil resistance can be explained by the change of void ratio what will result in settlement of the ground surface. If the pile is cycled in the same direction with loads that cause deflection of more than a few millimetres, the cohesionless soil will collapse behind the pile and pile deflection will be "locked in" (Reese, et al., 2006).

Comparing the p-y curve for short-term static loading with the one for cyclic loading (Figure 2.3a and Figure 2.3b) it can be can be seen that for small deflections the cyclic loading has little or no effect on a p-y curve. Only for larger deflections, from point *c* to point *d*, a reduction in soil resistance will occur.

In the p-y curve in Figure 2.3c the possible effect of sustained loading is depicted. This effect is mainly of importance for normally consolidated clay. For these clays the effect of dissipation of excess pore water pressure due to a lateral load is largest. The deflection of the pile will increase as more pore water pressure is dissipated. It is assumed that the decrease in soil resistance is compensated for by a shift in resistance towards other elements along the pile. Because no or little excess pore water pressure is present in granular soils or overconsolidated clays, the effect of sustained loading on the behaviour of the piles is not significant for these soils.

2.3.3 Ultimate soil resistance

To obtain the ultimate soil resistance against deflection of a laterally loaded pile, two models have to be used. The first model is a strain wedge model which considers the development of an upward moving passive wedge at the rear side of the pile. The resistance against sliding of the wedge is provided by the friction forces along its sliding surfaces and the weight of the wedge. At a greater depth the resistance against an upward moving wedge will be such that only horizontal movement of the soil will occur. This horizontal flow of soil around the pile is considered by the second model. These two failure models are schematized in Figure 2.4.

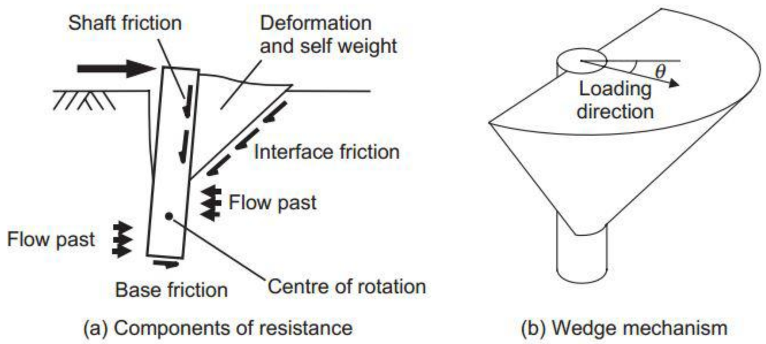

Figure 2.4 - Collapse mechanisms in the soil around a pile (Fleming, et al., 2008)

According to Reese distinction has to be made between the ultimate soil resistances for cohesive soils and cohesionless soils. Therefore these are described separately.

In this master thesis only the ultimate soil resistance according to Reese et al. (2006) will be considered. For other methods to determine the ultimate soil resistance at greater depth reference is made to Verhoef (2015).

Cohesive soils

For the determination of the ultimate soil resistance of cohesive soils two assumptions are made (Reese & Van Impe, 2001). First of all the soil is assumed to be saturated. This assumption appears to be justified by the fact that the water content in partially saturated clays can change over time. Secondly, it is assumed that the undrained-strength approach will lead to useful answers.

The assumed passive failure wedge for cohesive soils is shown in Figure 2.5. The ultimate soil resistance can be found by solving the force equilibrium for F_p by taking into account the weight of the wedge, W, and the frictional forces that act on the sliding surfaces of the wedge, F_t, F_s, F_n and F_f, and by finally differentiating F_p with respect to the depth of the wedge, H. This leads to an ultimate soil resistance according to equation 2.3.

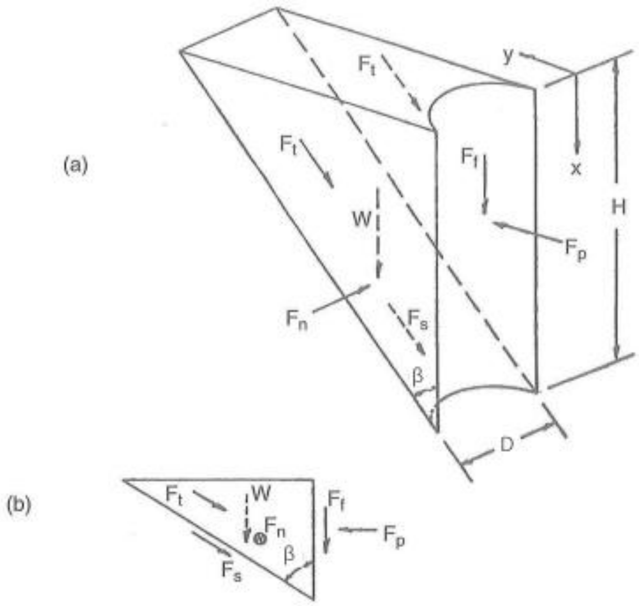

Figure 2.5 - Assumed passive wedge-type failure for cohesive soils (Reese, et al., 2006)

$$p_{u1} = c_a D[\tan\beta + (1+\kappa)\cot\beta] + \gamma D H + 2c_a H(\tan\beta\sin\beta + \cos\beta) \qquad (2.3)$$

In which:

p_{u1}	= Ultimate resistance near the ground surface per unit of length along the pile [kN/m]
c_a	= Average undrained shear strength over the depth, H [kN/m^2]
β	= Angle of the inclined plane with the vertical [deg]
κ	= Reduction factor for shearing resistance along the face of the pile [-]
γ	= Unit weight of soil [kN/m^3]
D	= Diameter of the pile [m]

H = Depth below the ground surface [m]

For cyclic loading the factor κ can be set to zero. If the soil is assumed to behave in an undrained mode β can be taken equal to 45° (Reese & Van Impe, 2001).

The model for the computation of the ultimate soil resistance at greater depth is shown in Figure 2.6a . It shows a cylindrical pile surrounded by 5 blocks of soil. Due to a horizontal movement of the pile, block 5 is moved laterally and in this block a stress is generated which causes it to fail. The stress is transmitted through block 4 and on around the pile to block 1. It is assumed that blocks 1, 2 and 4 will fail by shearing, whereas block 3 is assumed not to distort. It is assumed that at each side of the pile a resistance will develop equal to $cD/2$. The ultimate resistance of cohesive soils at greater depth can then be defined as:

$$p_{u2} = (\sigma_6 - \sigma_1 + c)D = 11cD \qquad (2.4)$$

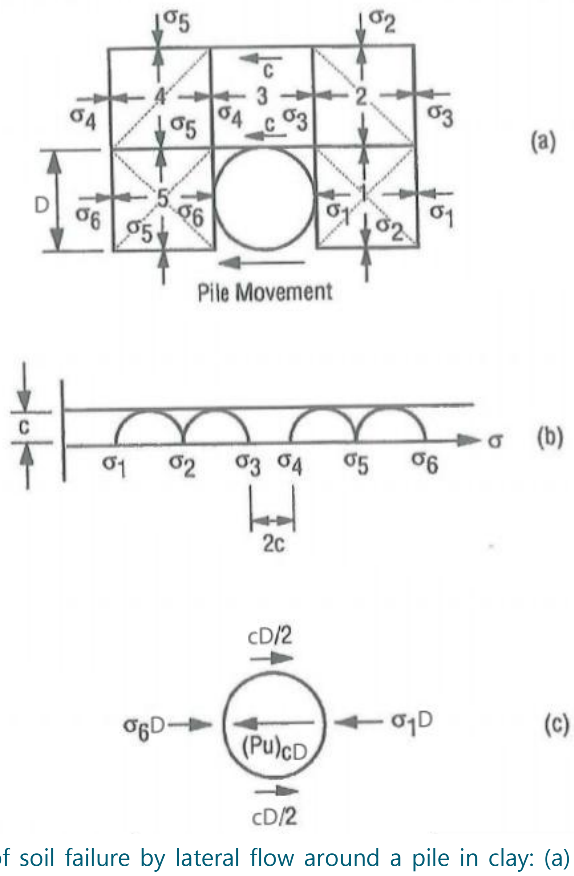

Figure 2.6 - Assumed mode of soil failure by lateral flow around a pile in clay: (a) section through the pile; (b) Mohr-Coulomb diagram; (c) forces acting on a section of a pile (Reese, et al., 2006)

Note

The passive wedge model for cohesive soils assumes plane sliding surfaces. However, tests by Reese et al. (1975) show that the contours of the rise of the ground surface at the front of a pile do not correspond to this. Also, O'Neill and Dunnavant (1984, 1985) found that the response of the soil to a laterally loaded pile could best be characterized by a nonlinear function of the pile diameter, whereas equation 2.3 indicates a linear relation. This means that the passive wedge model for cohesive soils might underestimate the amount of mobilized soil (Reese & Van Impe, 2001).

Cohesionless soils

For the determination of the ultimate soil resistance of cohesionless soils it is assumed that the soil is fully drained (Reese & Van Impe, 2001). This assumption appears to be valid for most granular soils. The assumed passive failure wedge for cohesionless soils is shown in Figure 2.7. The ultimate soil resistance of these soils can be determined in a similar way as for cohesive soils, namely by solving the force equilibrium for F_p and by differentiating this force with respect to the depth, *H*. Finally the equation for the ultimate soil resistance near the ground surface for cohesionless soils is equal to equation 2.5.

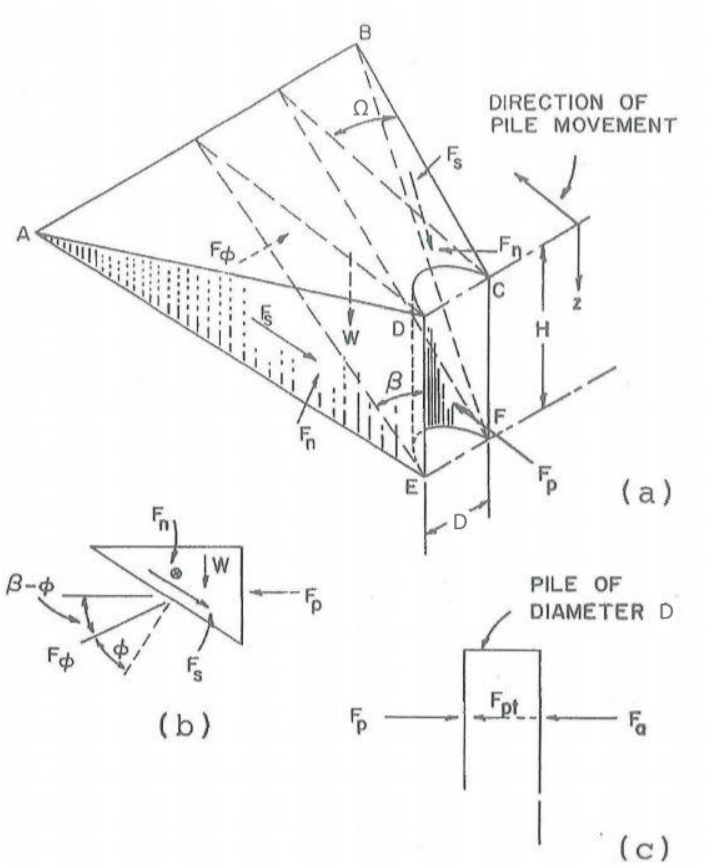

Figure 2.7 - Assumed passive wedge-type failure for cohesionless soils (Reese, et al., 2006)

$$p_{u1} = \gamma H \left[\frac{K_0 H \tan\varphi \sin\beta}{\tan(\beta-\varphi)\cos\Omega} + \frac{\tan\beta}{\tan(\beta-\varphi)}(D + H\tan\beta\tan\Omega) + K_0 H \tan\beta\,(\tan\varphi\sin\beta - \tan\Omega) - K_a D \right] \tag{2.5}$$

In which:

K_0 = Coefficient of earth pressure at rest [-]

K_a = Minimum coefficient of active earth pressure = $\frac{1-\sin\varphi}{1+\sin\varphi}$ [-]

φ = Friction angle of the soil [deg]

Ω = Angle of the wedge [deg]

For the determination of the ultimate soil resistance at greater depth a similar model can be used as the one used for cohesive soils (Figure 2.8a). When the minimum active pressure is smaller than the stress σ_1 at the back of the pile, failure of the soil due to slumping will occur. Under assumption of the states of stress according to Figure 2.8b, the ultimate soil resistance for horizontal movement of the soil is equal to:

$$p_{u2} = K_a D\gamma H(\tan^8\beta - 1) + K_0 D\gamma H \tan\varphi \tan^4\beta \tag{2.6}$$

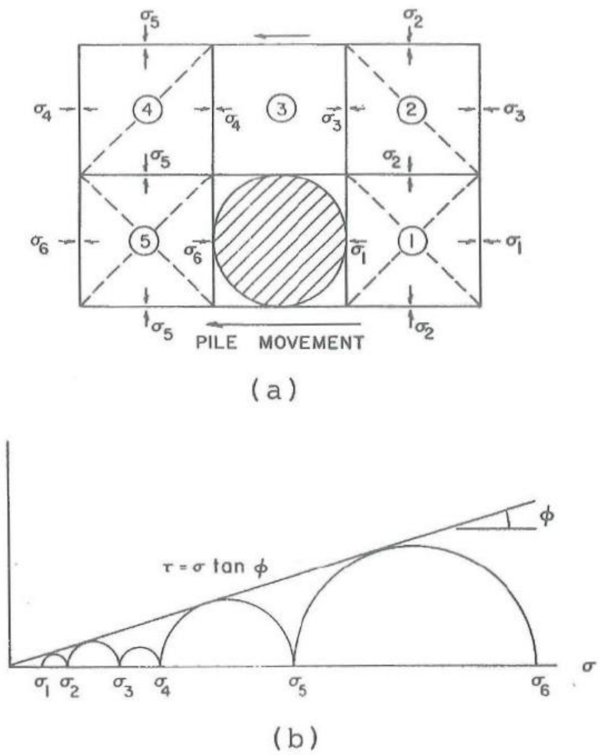

Figure 2.8 - Assumed mode of soil failure by lateral flow around a pile in sand: (a) section through the pile; (b) Mohr-Coulomb diagram (Reese, et al., 2006)

2.3.4 Modification for sloping grounds

Breasting dolphins, but particularly mooring dolphins may often be found in sloping grounds. These sloping grounds may influence the soil-structure interaction significantly, because the horizontal earth pressure at one side of the pile is reduced with respect to the pressure at the other side. It is assumed that at greater depth the horizontal movement of the soil, the flow-around failure of the soil, will not be influenced by the sloping ground. Therefore only the equations for the ultimate soil resistance according to the passive wedge model have to be modified.

Cohesive soils

The ultimate soil resistance near the ground surface if the pile is pushed downhill, with a slope angle equal to θ, can be expressed as

$$p_{u1} = (2c_a D + \gamma DH + 2.83 c_a H)\left(\frac{1}{1+\tan\theta}\right) \tag{2.7}$$

In case the pile is pushed uphill, the ultimate soil resistance can be expressed as

$$p_{u1} = (2c_a D + \gamma DH + 2.83 c_a H)\left(\frac{\cos\theta}{\sqrt{2}\cos(45+\theta)}\right) \tag{2.8}$$

Cohesionless soils

The ultimate soil resistance for cohesionless soils in sloping grounds, for which the slope angle θ is smaller than the angle of friction of the soil φ, can be determined using:

$$\begin{aligned} p_{u1} = \gamma H \Bigg[&\frac{K_0 H \tan\varphi \sin\beta}{\tan(\beta-\varphi)\cos\Omega}\left(4{G_1}^3 - 3{G_1}^2 + 1\right) + \frac{\tan\beta}{\tan(\beta-\varphi)}\left(DG_2 + H\tan\beta\tan\Omega {G_2}^2\right. \\ &+ K_0 H \tan\beta\,(\tan\varphi\sin\beta - \tan\Omega)\left(4{G_1}^3 + 3{G_1}^2 + 1\right) - K_a D\Bigg] \end{aligned} \tag{2.9}$$

With:

$$K_a = \cos\theta \frac{\cos\theta - (\cos^2\theta - \cos^2\varphi)^{0.5}}{\cos\theta + (\cos^2\theta - \cos^2\varphi)^{0.5}} \tag{2.10}$$

The factors G_1 and G_2 differ for the situation where the pile is pushed downhill or uphill. In case the pile is pushed downhill, these factors are equal to:

$$G_1 = \frac{\tan\beta\tan\theta}{\tan\beta\tan\theta + 1} \tag{2.11}$$

$$G_2 = 1 - G_1 \tag{2.12}$$

For piles being pushed uphill, these factors are equal to:

$$G_1 = \frac{\tan\beta\tan\theta}{1 - \tan\beta\tan\theta} \tag{2.13}$$

$$G_2 = 1 + G_1 \tag{2.14}$$

Modification of p-y curves by p-multipliers

Nimityongskul (2010) performed a series of full scale tests to investigate the influence of sloping grounds on p-y curves. He captured the relation between the p-y curves for sloping grounds and the curves for horizontal grounds in so called p-multipliers. With these p-multipliers the behaviour of laterally loaded piles in sloping grounds can be analyzed using a design flow chart Nimityongskul published (Verhoef, 2015):

1. Select the p-y curve for a laterally loaded pile in horizontal ground
2. Define appropriate p-multipliers
3. Construct the new p-y curves
4. Perform the analysis of the laterally loaded pile with the renewed p-y curves

From the tests, Nimityongskul found that the effect of the slope on p-y curves is larger as the displacements increase and becomes steady at large soil displacements. Therefore he developed a p-multiplier which depends on the soil displacement. Nimityongskul derived the p-multiplier from seven p-y curves at a distance of one to seven feet below the ground surface. The multiplier is only valid until 7 feet (=2.13 m, =7D) beneath the soil surface. Below this depth Nimityongskul considers the multiplier to be equal to 1.0 (Verhoef, 2015). The results for Nimityongskul's p-multipliers are shown in Figure 2.9.

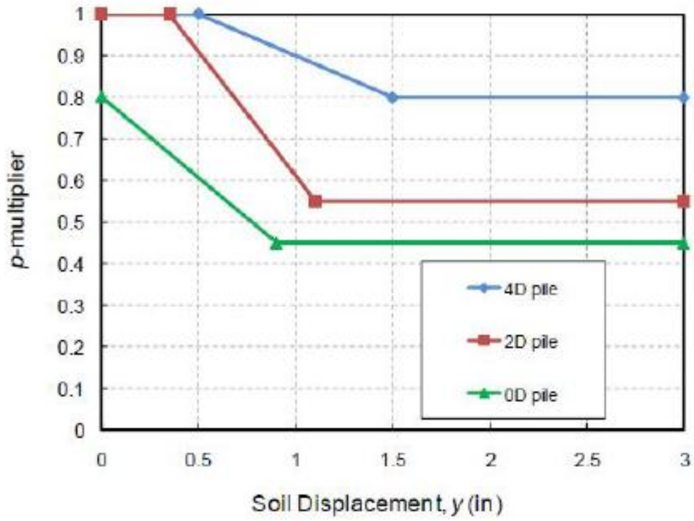

Figure 2.9 - Proposed p-multipliers by Nimityongskul (1 inch = 2.54 cm) (Verhoef, 2015)

In her master thesis report, Verhoef (2015) recommends to analyze the behaviour of laterally loaded piles in sloping grounds according to the design flow chart of Nimityongskul. Because his design flow chart was based on only one p-y ratio, which was concluded to be considerably conservative, Verhoef expanded the amount of available p-y ratios. The p-multipliers she obtained are depicted in Table 2.1.

Table 2.1 - p-multiplier obtained by Verhoef (2015) (Verhoef, 2015)

Sand ratios			**Clay ratios**		
Depth	**Slope**	**Multiplier**	**Depth**	**Slope**	**Multiplier**
z = 0	Slope 1:4	0.67	z = 0	Slope 1:4	0.88
	Slope 1:3	0.55		Slope 1:3	0.78
z = -1D	Slope 1:4	0.72	z = -1D	Slope 1:4	0.88
	Slope 1:3	0.6		Slope 1:3	0.78
z = -2D	Slope 1:4	0.78	z = -2D	Slope 1:4	0.91
	Slope 1:3	0.63		Slope 1:3	0.85
z = -3D	Slope 1:4	0.78	z = -3D	Slope 1:4	0.82*
	Slope 1:3	0.69		Slope 1:3	0.85*
*) These values are considered to be not realistic					

For a more extensive explanation of the p-multipliers and for a description of other methods that take into account sloping grounds, reference is made to Verhoef (2015).

2.3.5 Modification for layered soils

The p-y curve described so far are only applicable to homogeneous soils. However, in many cases the soil near the ground surface is layered. If these layers intersect the sliding plane of the upward moving passive wedge, the p-y curves have to be modified. This can be done by the method of Georgiadis (1983), which is based on the determination of the equivalent depth of all layers existing below the upper layer (Reese & Van Impe, 2001).

According to the method of Georgiadis, the p-y curves of the upper layer are similar to those for homogeneous soils. The effects of the upper layers on the p-y curves of the lower layers are accounted for by the equivalent depth, H_2, of the overlying layers based on strength parameters (Yang & Jeremic, n.d.). The equivalent depth can be determined by equating the summation of the ultimate resistances of the upper layer to the summation as if the upper layer had been composed of the same material as the second layer. This means that the following two equations have to be solved simultaneously for H_2 (Reese & Van Impe, 2001):

$$F_1 = \int_0^{H_1} p_{ult1} dH \tag{2.15}$$

$$F_2 = \int_0^{H_2} p_{ult2} dH \tag{2.16}$$

The p-y curves for the second layer can be determined with the equivalent layer thickness H_2 and the soil parameters of the second layer.

2.4 D-Sheet Piling – Single Pile Module

With D-Sheet Piling the behaviour of laterally loaded piles can be analysed by using the single pile module (Deltares, 2014). With this module the bending moments and the deflection of the pile under applied forces and moments can be determined.

D-Sheet Piling is a spring model in which the soil is modelled by bi-linear springs along the pile. The subgrade reaction of the soil is limited by the minimum (active) and maximum (passive) pressure that can develop in the soil. The ultimate horizontal soil resistance against lateral movement of the pile can be calculated using the Brinch-Hansen method, whereas the modulus of subgrade reaction may be determined using the Ménard theory. For the calculation of the ultimate soil resistance according to Brinch-Hansen and the modulus of subgrade reaction according to Ménard, reference is made to Appendix A.

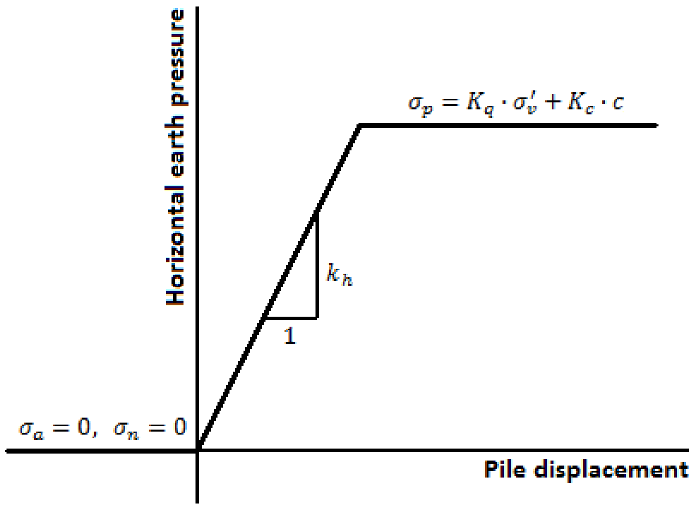

Figure 2.10 - Bi-linear spring curve used in D-Sheet Piling with limits according to Brinch-Hansen

To analyse the behaviour of laterally loaded piles and the surrounding soil with D-Sheet Piling, only a limited amount of input parameters is required. Besides the geometry and the pile properties, only the unit weight, cohesion, angle of internal friction and the modulus of subgrade reaction of Ménard of the soil have to be known. This makes D-Sheet Piling a very easy and quick method to determine the pile-soil interaction.

The simplicity of D-Sheet Piling also introduces some limitations of the model. The main limitation of the software is that the soil is modelled by bi-linear springs, whereas in practice the stiffness of the soil decreases with increasing deformation and increases with the depth. However, by generating multiple layers for one soil layer with increasing stiffness over the depth, this negative influence on the pile behaviour can be reduced. Another limitation is that within D-Sheet Piling only horizontal soil layers can be introduced leaving that sloping ground surfaces cannot be considered. Furthermore, only static, lateral loadings can be applied.

2.5 D-Pile Group

With D-Pile Group the three-dimensional behaviour of single piles and pile groups can be analyzed (Deltares, 2014). It is based on a mass-spring model in which lateral and axial soil springs describe the relation between the pile and the surrounding soil. The soil springs applied in D-Pile Group are non-linear and based on p-y curves derived from full scale tests. In case plasticity is involved, hysteresis is included in the load-displacement model.

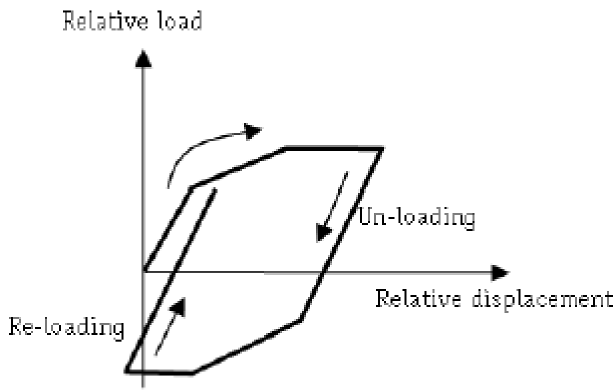

Figure 2.11 - Force-displacement relation between pile and surrounding soil (Deltares, 2014)

In D-Pile Group several models are available to analyse the interaction between pile and soil. For single piles the Cap model has to be used. With this model only static loading can be considered. However, for the analysis of the pile-soil interaction under dynamic loading, a Dynamic model is available which can be used when the reaction of the pile is dominated by inertia effects. The dynamic analysis performed by the model is based on the Cap model.

For the analysis of the behaviour of a single pile with D-Pile Group, the required amount of input parameters is limited. Regarding the soil, for sand only the unit weight, angle of internal friction, cone resistance and coefficient of horizontal subgrade reaction are required, whereas for clay only the unit weight, undrained shear strength, empirical constant *J* and the strain at 50% of the failure load have to be known. This makes D-Pile Group an easy and cheap method to model the pile-soil behaviour. Another advantage of D-Pile Group is that the soil is modelled by non-linear springs what will model the behaviour of the soil more accurate compared to D-Sheet Piling.

D-Pile Group also has its limitations. First of all it is not possible to model sloping ground surfaces. Furthermore, the coefficient of horizontal subgrade reaction is considered constant over the depth within each soil layer. Also, lateral loads can only be applied at the top of the pile.

P-y curves

The p-y curves which define the non-linear soil springs that are used by D-Pile Group in the analysis of the pile and soil behaviour, can be user defined or defined by the American Petroleum Institute (*API*). With the *API* p-y curves it is possible to perform analyses for both drained and undrained sand and for undrained clay. The *API* p-y curves for both clay and sand are modelled by five parallel elasto-plastic springs which are chosen such that the resulting multi-linear spring characteristic used by D-Pile Group corresponds best with the one obtained from the full scale tests (Deltares, 2014). The p-y curves used by D-Pile Group and the equations which describe the *API* p-y curves are included in Appendix B.

2.6 FEM – Plaxis 3D

Plaxis 3D is a finite element method developed for the analysis of deformation, stability and groundwater flow in geotechnical structures in which three-dimensional effects play a significant role (Brinkgreve, et al., 2015). In Plaxis 3D several models are available to model the soil, such as Mohr-Coulomb, Hardening Soil (HS) and Hardening Soil Small Strain (HSsmall). The HSsmall model is considered to be most suitable for modelling laterally loaded dolphins in clayey and sandy soils because it takes into account the differences in deformation over the length of the pile, it accounts for the stress-dependency of the soil stiffness (Plaxis bv, 2015). The HSsmall model is a second order model which describes the reaction of the soil by a hyperbolic stress-strain curve.

The yield surface of a HSsmall model is not fixed but can expand due to plastic straining. As a result hardening of the soil can be modelled. There are two main types of hardening, namely shear hardening and compression hardening. Shear hardening is used to model irreversible plastic strains due to primary deviatoric loading, whereas compression hardening is used to model irreversible plastic strains due to primary compression (Plaxis bv, 2015).

Because Plaxis 3D is an advanced model, a lot of input parameters are required. The parameters regarding the soil are (Plaxis bv, 2015):

m	Stress dependent stiffness according to a power law [-]
E_{50}^{ref}	Reference stiffness modulus [kN/m^2]
E_{oed}^{ref}	Tangent stiffness for primary oedometer loading [kN/m^2]
E_{ur}^{ref}	Reference Young's modulus for unloading/reloading [kN/m^2]
ν_{ur}	Poisson's ration for unloading/reloading [-]
c	Cohesion [kN/m^2]
φ	Angle of internal friction [deg]
ψ	Angle of dilatancy [deg]
G_o	Initial shear modulus [kN/m^2]
$\gamma_{0.7}$	Shear strain level at which the secant shear modulus G_s is reduced to 70% of G_0 [-]

In Plaxis 3D a tubular pile is modelled as a plate element. These elements are characterized by four parameters, namely the pile diameter, wall thickness, Young's modulus and the unit weight of the material. The pile can be modelled to behave as an elastic or elasto-plastic material. (Plaxis bv, n.d.)

Along tubular piles, both on the inside and the outside, interfaces can be activated. These interface allow for the modelling of the soil-structure interaction, they simulate the thin zone of shearing material at the contact between the pile and the surrounding soil (Brinkgreve, et al., 2015). The strength reduction factor, R_{inter},, relates the interface strength (wall friction angle and adhesion) to the soil strength (friction angle and cohesion).

With respect to D-Sheet Piling and D-Pile Group, Plaxis 3D approaches the real soil behaviour the best. However, the program also has some disadvantages. The program requires a lot of different input parameters what makes it very complex to use. Furthermore, Plaxis 3D has large calculation times, what makes that the program is very time-consuming and expensive to use. Therefore, for the (first) design calculations often D-Sheet Piling and D-Pile Group are used.

3

LITERATURE REVIEW – RELIABILITY ANALYSIS

3.1 Introduction

Partial safety factors can be determined based on results obtained from probabilistic calculations. Therefore, this chapter starts with an overview of the available probabilistic calculation methods. In section 3.3 it is discussed how these probabilistic calculation methods can be combined with the models and methods which are described in chapter 2. In the last paragraph of this chapter, the design codes and guidelines are discussed which are frequently used for dolphin design in the Netherlands. The principles of the codes and guidelines are discussed, as well as the partial factors which have to be applied according to these design codes and guidelines.

3.2 Probabilistic analysis

3.2.1 General

The reliability of a structure can be expressed as the complement of the probability of failure, it is the probability that no failure occurs. The boundary between failure and non-failure is defined by the limit state. At these states the difference between the loads on the structure and the strength of the structure is equal to zero. By using the limit states reliability functions can be expressed which in their general form can be written as

$$Z = R - S \tag{3.1}$$

in which R is the strength of the structure (resistance) and S is the load on the structure (solicitation). The probability of failure can be described as

$$P_f = P(Z \leq 0) = P(S \geq R) \tag{3.2}$$

The reliability of the structure can be expressed as

$$P(Z > 0) = 1 - P_f \tag{3.3}$$

An analysis of the reliability in which the probability of failure is calculated with equation 3.2 is known as a structural reliability analysis (CUR-publicatie 190, 2002).

Currently it is common to express the reliability in terms of a reliability index, β, which expresses the distance of the mean margin of safety from its critical value (Z = 0) in units of standard deviation (Baecher & Christian, 2003):

$$\beta = \frac{\mu_Z}{\sigma_Z} = \frac{\mu_R - \mu_S}{\sqrt{\sigma_R^2 + \sigma_S^2 - 2\rho_{RS}\sigma_R\sigma_S}} \tag{3.4}$$

The correlation coefficient ρ_{RS} is equal to zero when the variables are uncorrelated. The reliability index can be related to the probability of failure by means of the standard normal cumulative distribution function, Φ:

$$P_f = \Phi(-\beta) \tag{3.5}$$

The loads on a structure and the structural parameters that determine the strength of the structure can be described as random variables. In order to determine the structural safety of a structure, a level-classification of calculation methods is retained (CUR-publicatie 190, 2002).

Level III: These methods calculate the probability of failure by considering the probability density functions of all strength and load variables. (Fully probabilistic)

Level II: This level entails linearising the reliability function in a carefully selected point. The probability distribution of each variable is approximated by a standard normal distribution. (Fully probabilistic with approximations)

Level I: The level I calculation is a design method according to the standards, which consider an element sufficiently reliable if a certain margin is present between the representative values of the strength and the loads. This margin is created by taking partial safety factors into account in the design. (Semi-probabilistic)

These three levels are discussed in more detail in paragraphs 3.2.2, 3.2.3 and 3.2.4, as well as some developed and frequently used methods for the different levels. The descriptions are mainly based on CUR-publication 190 (1997).

3.2.2 Level III methods

Level III methods are characterized as fully probabilistic methods in which no simplifications and approximations are introduced. The foundation of the level III failure probability calculations lies in a mathematical formulation of the probability of failure, which involves failure. When the joint probability density function ($f_{R,S}(R,S)$) of the strength and the load is known, the probability of failure can be calculated by means of integration:

$$P_f = \iint_{Z<0} f_{R,S}(R,S)\, dR\, dS \tag{3.6}$$

Given that Z<0 if R<S, this can be solved by solving the convolution-integral which in this case reads

$$P_f = P(S > R) = \int_{-\infty}^{\infty} \left(1 - F_S(R)\right) f_R(R) dR \tag{3.7}$$

Usually, the strength and the load are functions of one or more random variables. In such a case the reliability function can be written as

$$Z = g(X_1, X_2, \dots, X_n) \tag{3.8}$$

The integral that describes the probability of failure can seldom be determined analytically. However, in order to solve for the failure probability various numerical methods exist. One of them is the Monte Carlo method.

Monte Carlo method

In the Monte Carlo method random numbers between zero and one are drawn from an uniform probability density function. These uniform random numbers are transformed to an arbitrary distribution by means of inversion:

$$F_X(X) = X_u \tag{3.9}$$

$$X = F_X^{-1}(X_u) \tag{3.10}$$

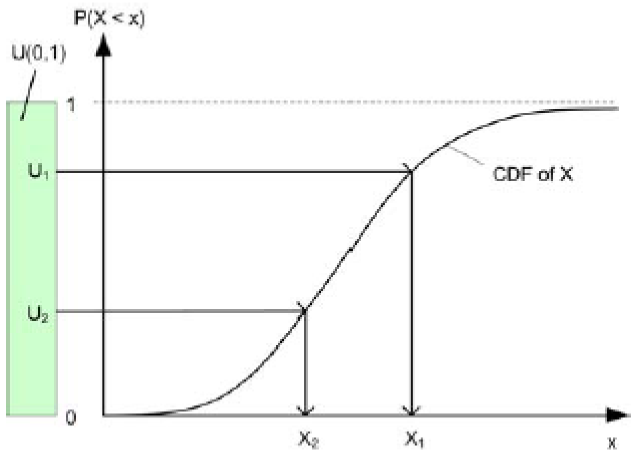

Figure 3.1 - Generating samples from a distribution by using its inverse CDF (Schweckendiek, 2006)

For some distributions the inverse probability density function is not known analytically. For these cases the base variables of a statistical vector can be drawn from a known joint probability distribution function, which must be formulated as the product of the conditional probability distributions of the base variables of the vector.

$$F_{\vec{X}}(\vec{X}) = F_{X_1}(X_1) \cdot F_{X_1|X_2}(X_1|X_2) \dots F_{X_m|X_1,X_2,\dots,X_{m-1}}(X_m|X_1, X_2, \dots, X_{m-1}) \tag{3.11}$$

By taking m realisations of the uniform probability distribution between zero and one, a value can be determined for every X_i:

$$\begin{gathered} X_1 = F_{X_1}^{-1}(X_{u_1}) \\ X_2 = F_{X_2|X_1}^{-1}(X_{u_2}|X_1) \\ \vdots \\ X_m = F_{X_m|X_1,X_2,\ldots,X_{m-1}}^{-1}(X_{u_m}|X_1, X_2, \ldots, X_{m-1}) \end{gathered} \tag{3.12}$$

For statistically independent base variables this can be simplified to

$$X_i = F_{X_i}^{-1}(X_{u_i}) \tag{3.13}$$

For statistically dependent variables further transformations are necessary in order to determine the arbitrary distribution.

For reliability analysis the probability of failure can be determined by repeating this procedure for a large number of times. The probability of failure can then be estimated with

$$P_f \approx \frac{N_f}{N} \tag{3.14}$$

in which N is the number of simulations of the random vector X and N_f is the number simulations for which failure occurs, so for which $Z(X)<0$.

The relative error of this simulation can be written as

$$\varepsilon = \frac{\frac{N_f}{N} - P_f}{P_f} \tag{3.15}$$

For the expectation of the relative error it holds that $E[\varepsilon]=0$ and the standard deviation is equal to

$$\sigma_\varepsilon = \sqrt{\frac{1 - P_f}{n\, P_f}} \tag{3.16}$$

Provided that the number of simulations is sufficiently large, the relative error is normally distributed. For the simulation to be sufficiently reliable, it is required that the relative error ε is smaller than the acceptable error E:

$$k \cdot \sigma_\varepsilon < E \tag{3.17}$$

For the required k and E the required number of simulations N can be estimated with

$$N > \frac{k^2}{E^2}\left(\frac{1}{P_f} - 1\right) \tag{3.18}$$

If a reliability of 95% has to be obtained (k=2) with an acceptable error of 10% (E=0.1), the required number of simulations amounts to

$$N > 400\left(\frac{1}{P_f} - 1\right) \tag{3.19}$$

From eq. 3.18 it follows that the minimum required number of simulations is inversely proportional to the probability of failure. When the reliability that has to be achieved is high, a large number of simulations has to be performed. This is because the convergence slows down as a higher reliability is reached. To improve the efficiency of the failure probability calculations more advanced methods can be applied. An example is Importance Sampling. This method increases the failure space relative to the total integration space so that when drawing random numbers from the Importance Sampling probability distribution function, more points are found in the failure area. For a more extensive description, and for a description of other more advanced methods, reference is made to Schweckendiek (2006).

3.2.3 Level II methods

The level II approach is a first order method which uses the first terms of a Taylor series expansion to linearize the limit state function. This linearization is carried out in a carefully selected point.

First Order Second Moment Method (FOSM)

The First Order Second Moment method is a called is second moment method because the highest order statistical result used in the method is a form of the second moment (Baecher & Christian, 2003). It is a mean value approximation method which linearizes the limit state function in the mean values. When the variables are uncorrelated, the expressions for the mean value and the standard deviation become

$$\mu_Z = Z\left(\mu_{x_1}, \mu_{x_2}, \dots, \mu_{x_n}\right) \tag{3.20}$$

and

$$\sigma_Z = \sqrt{\sum_{i=1}^{n} \left(\frac{\partial Z}{\partial x_i}\right)^2 \sigma_{x_i}^2} \tag{3.21}$$

Since the limit state function is written as $Z = R - S$, the reliability index β for uncorrelated variables can be expressed as

$$\beta = \frac{\mu_Z}{\sigma_Z} = \frac{\mu_R - \mu_S}{\sqrt{\sigma_R^2 + \sigma_S^2}} \tag{3.22}$$

The limit state function of a structure can also be formulated in terms of safety factors ($R/S < 1$). However, for this limit state FOSM will not give the same results as it will for a limit state function written in terms of margins of safety ($R - S < 0$). This means that the method is not indifferent to the formulation of the limit state. This is also illustrated in Figure 3.2. In this figure both methods start from the same point, but they go in different directions and meet the failure line at different points. Another limitation of FOSM is that the method is only suitable for uncorrelated normally and lognormally distributed variables. Due to these limitations, FOSM is not a very accurate method and therefore not applied very often. However, it might give a good indication for the reliability of a structure.

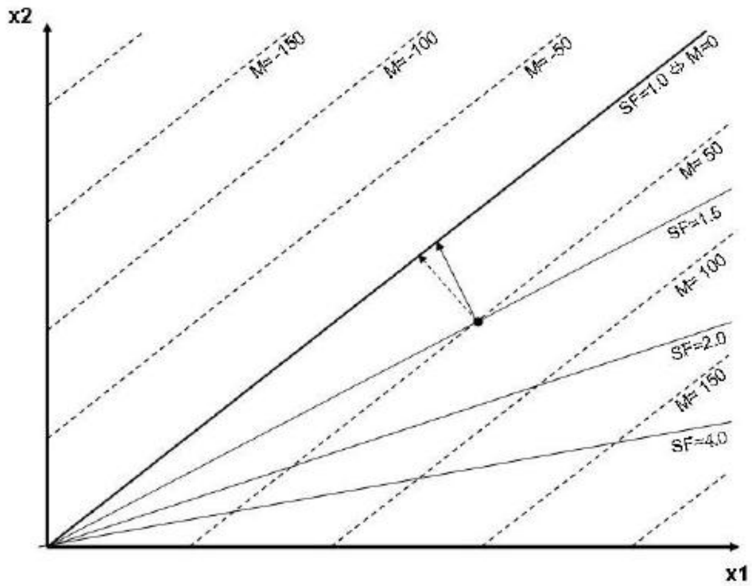

Figure 3.2 - Factor of safety reliability (SF) compared to margin of safety reliability (M).

Hasofer-Lind method

The FOSM involves some approximations which may lead to an overestimation of the reliability and which may therefore not be acceptable. One assumption the method makes is that it makes little difference where the partial derivatives are evaluated. Another assumption is that the margin of safety or the factor of safety is known and can be used to determine the reliability. However, these assumptions are often not valid. Hasofer and Lind addressed these concerns by proposing a different approach which is also known as the First Order Reliability Method (FORM) (Baecher & Christian, 2003).

The Hasofer-Lind method reformulates the problem by transforming the random variables to equivalent standard normally distributed variables which have a mean equal to zero and an unit standard deviation:

$$u_i = \frac{x_i - \mu_{x_i}}{\sigma_{x_i}} \tag{3.23}$$

Values which are not normally distributed have to be transformed to their normal equivalent first before eq. 3.23 can be applied. One method to do this is the Rosenblatt transformation, which will not be described here any further.

The Hasofer-Lind method suggests that the reliability index can be interpreted geometrically as the distance between the point defined by the expected values of the variables and the closest point on the failure criterion (Baecher & Christian, 2003). This means that the distance between the origin of the u-space and the failure criterion has to be minimized in order to find the design point (see Figure 3.3):

$$\beta = \min\left(\sqrt{u_1^2 + u_2^2 + \cdots + u_n^2}\right) \tag{3.24}$$

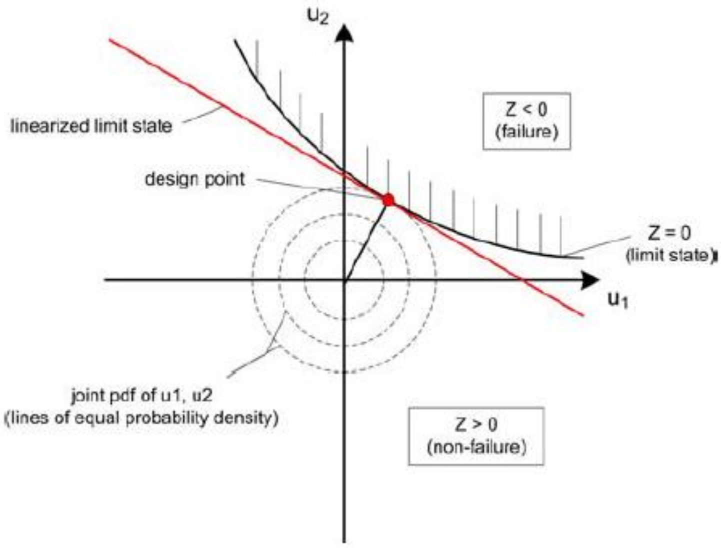

Figure 3.3 - Design point and linearized limit state for two dimensions in u-space (Schweckendiek, 2006)

The minimization problem can be elaborated by using e.g. the Lagrangian Multiplier Approach or the Taylor Series Approach. These approaches lead to a similar solution for the reliability index:

$$\beta = \frac{\mu_Z}{\sigma_Z} = \frac{Z(x_i^*) + \sum\left(\frac{\partial Z(x_i^*)}{\partial x_i}\right)(\mu_{x_i} - x_i^*)}{\sqrt{\sum\left(\frac{\partial Z(x_i^*)}{\partial x_i}\right)^2 \sigma_{x_i}^2}} \tag{3.25}$$

The superscript star indicates that the unit factor is evaluated at the design point. However, this point is not known in advance but has to be found iteratively. For this procedure the Rackwitz algorithm can be applied. However, first a normalized unit vector α has to be defined which is called the influence factor:

$$\alpha_i = \frac{\frac{\partial Z(x_i^*)}{\partial x_i}\sigma_{x_i}}{\sqrt{\sum\left(\frac{\partial Z(x_i^*)}{\partial x_i}\right)^2 \sigma_{x_i}^2}} \tag{3.26}$$

The Rackwitz algorithm then proceeds in six iterative steps (Baecher & Christian, 2003):

1. Assume the initial values of the design point (e.g. the mean values)
2. Compute Z and α at the assumed design point, u_i^*
3. Compute the new design point-approximation: $x_i^* = \mu_{x_i} - \alpha_i \beta \sigma_{x_i}$
4. Substitute the new design point (u_i^*) into Z and solve for β
5. Evaluate the new values of $u_i^* = -\alpha_i \beta$
6. Repeat steps 2 through 5 until the process converges

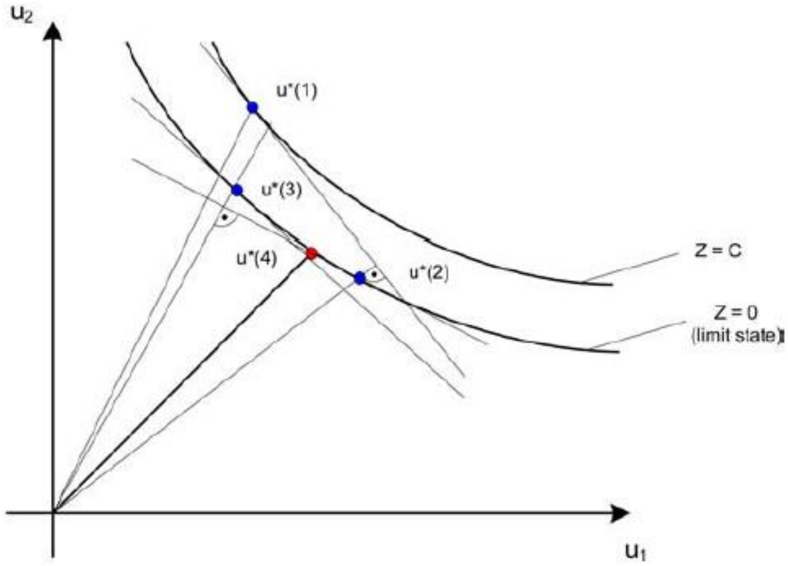

Figure 3.4 - Graphical representation of the Rackwitz algorithm (the numbers in brackets show the iteration steps) (Schweckendiek, 2006)

When the design point in u-space is obtained from the reliability analysis, the design point in the original x-space can be obtained by transforming the values again:

$$x_i = \sigma_{x_i} u_i + \mu_{x_i} \tag{3.27}$$

Second Order Reliability Method (SORM)

A limitation of FORM is that the method is only accurate for linear limit state functions. The magnitude of the error is determined by the degree of non-linearity of the limit state function. In some cases this error may be reduced by applying the Second Order Reliability Method. Just as the FORM, this method also works in the u-space.

SORM approaches the real limit state function by a second order expansion of the linearized limit state function in the design point (Courage & Steenbergen, 2007):

$$Z_{2nd} = \beta + \sum \alpha_i u_i + \frac{1}{2} \sum \sum \frac{\partial^2 Z}{\partial u_i \, \partial u_j} (u_i - u_i^*)(u_j - u_j^*) \tag{3.28}$$

Subsequently the coordinate system is rotated (transformation of u_i to v_i). The v_1-direction is chosen such that it goes through the design point. This transformation leads to:

$$v_1^* = \beta \quad and \quad v_k^* = 0 \quad with \; k = 2, \dots, n \tag{3.29}$$

$$\alpha_1 = -1 \quad and \quad \alpha_k = 0 \quad with \; \alpha = 2, \dots n \tag{3.30}$$

The limit state function can now be written as:

$$Z_{2nd} = \beta - v_1 + \frac{1}{2} \sum \sum \frac{\partial^2 Z}{\partial v_i \, \partial v_j} (v_i - v_i^*)(v_j - v_j^*) \tag{3.31}$$

In most cases, the considered problem has n dimensions. For these cases a matrix G can be defined:

$$G_{ij} = \frac{\partial^2 Z}{\partial v_{i+1}\,\partial v_{j+1}} \quad with\ i, j = 1, \dots, n-1 \tag{3.32}$$

The main curvatures in the $v_2,\dots,\ v_n$-space, which are stored in the vector κ, can be determined by solving:

$$Det\|G - \kappa I\| = 0 \quad with\ I = unity\ matrix \tag{3.33}$$

Now the probability of failure can finally be estimated with

$$P_f = \Phi(\beta)\prod_{i=1}^{n-1}(1 - \beta\kappa_i)^{-1/2} \tag{3.34}$$

As mentioned, SORM may not always lead to more accurate results. As the curvature increases, two design points may be found instead of one. This means that the applicability of the method is limited to small curvatures. Furthermore, for irregular shaped LSF the method may lead to severe errors when local curvatures are applied. This is illustrated in Figure 3.5 Figure 3.5 - SORM result for an arbitrary irregular LSF . Because the form of the non-linearities is often not known, SORM is not often used in practice.

Another disadvantage of SORM is that the method is more time consuming than FORM, because the number of evaluations per iteration step is larger. Also, for a large number of random variables the computational efficiency of SORM reduces with respect to the efficiency of a Monte Carlo simulation (Maier, et al., 2001).

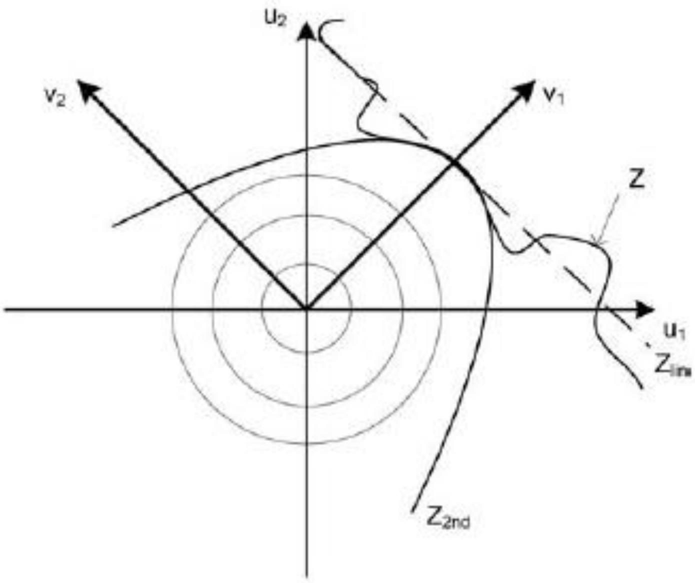

Figure 3.5 - SORM result for an arbitrary irregular LSF (Schweckendiek, 2006)

3.2.4 Level I methods

The level I method is a design method according to the standards. The essence of these standards is that design parameters are obtained by dividing a representative value of the strength by a factor and by multiplying a representative value of the load by a factor. For this the following must apply:

$$\frac{R_{rep}}{\gamma_R} > S_{rep} \cdot \gamma_S \tag{3.35}$$

The factors γ_R and γ_S are the partial safety factors. For the most common strength and load parameters these are recorded in the standards.

It is plausible that for failure the values of the strength and the load are close to the values for the design point. This results in two expressions that can be used to determine the partial safety factors for the resistance parameters and the load parameters respectively:

$$\gamma_R = \frac{R_{rep}}{R^*} = \frac{1 + k_R \cdot V_R}{1 + \alpha_R \cdot \beta \cdot V_R} \tag{3.36}$$

$$\gamma_S = \frac{S^*}{S_{rep}} = \frac{1 + \alpha_S \cdot \beta \cdot V_S}{1 + k_S \cdot V_S} \tag{3.37}$$

When a 5% reliability has to be obtained, k is equal to 1.64.

3.3 Probabilistic calculations with software models

3.3.1 Probabilistic model of Bakker

The method of Bakker is a First Order Second Moment reliability-analysis for geotechnical structures, which relates the probability of failure to the factor of safety. The method is based on the finite element method according to Plaxis, of which the Mohr-Coulomb model is used. The method of Bakker is applicable to undrained layered soils (Technische Adviescommissie voor de Waterkeringen [TAW], 2004).

The method of Bakker is implemented in three different spreadsheets: *ARBEID*, *UNDRAINE* and *SOMARBEID*. These spreadsheets are rather complicated. Because this method will not be used in the remainder of this research, no further description will be provided. For a more elaborate description of the method reference is made to TAW (2004).

3.3.2 Prob2B

Prob2B is a probabilistic toolbox which performs reliability calculations resulting in a reliability index and a probability of failure. It sends stochastic input parameters to a deterministic external program and processes the output parameters using probabilistic techniques. (Courage & Steenbergen, 2007).

As a first step, for each individual variable the mean value, standard deviation and type of distribution need to be determined. Also the correlation coefficients have to be determined when parameters are statistically dependent. When all parameters are described, the limit state functions have to be defined for each individual limit state. Prob2B evaluates the defined limit state functions based on the output parameters of the external program. For this evaluation several different probabilistic methods are available, e.g. FORM or Crude Monte Carlo. In this way the probability of failure and the reliability of the structure can be determined by choosing a suitable method.

3.4 Safety in currently available codes and guidelines

3.4.1 Available codes and guidelines

Eurocode 7 (also referred to as EN 1997) is part of the European standards and provides common structural design rules for the design of geotechnical structures. Part 1 of this code is intended to be used as a general basis for the design of these structures. However, the European codes do not explicitly cover the design of flexible dolphins. To cover this gap, different international institutes have developed their own codes which all take into account different design methods. The codes on dolphin design which are currently applied and assumed to be effective are:

- NEN 9997: Dutch guideline on the geotechnical design of structures
- EAU 2012: German guidelines for dolphin design
- BS 6349: British standards for maritime structures
- PIANC 2002: Guidelines from the International Navigation Association for the design of fender systems

These guidelines will be further elaborated in section 3.4.3 to 3.4.6, but first more insight will be given in the European guidelines which form the basis of these codes.

3.4.2 European guidelines – Eurocode

According to Eurocode 7 Part 1 (Geotechnical design - General guidelines) structural reliability analysis has to be performed for the design of geotechnical constructions. The design of the structure has to be verified based on relevant limit states. The limit states that should be considered are:

- EQU: loss of equilibrium of the structure or the ground;
- STR: internal failure or excessive deformation of the structure;
- GEO: failure or excessive deformation of the ground;
- ALS: extreme situations (Accidental Limit State).

For the ultimate limit states the verification of the strength has to be based on design values of the load and the resistance. The combination of partial safety factors that has to be applied to obtain these design values is dependent on the design approach that has to be used (NEN-EN 1997-1, 2005).

- Design approach 1: Partial safety factors are applied to actions and to ground strength parameters.
- Design approach 2: Partial safety factors are applied to actions or to the effect of actions and to ground resistances.

- Design approach 3: Partial safety factors are applied to actions or to the effect of actions from the structure and to ground strength parameters.

For some parameters the partial safety factors depend on the reliability class that has to be achieved. The reliability class that has to be obtained depends on the consequences of failure of the structure. In case the structure is appointed to Consequence Class 1, also a Reliability Class 1 has to be maintained for the design. The consequence classes are defined in Eurocode 0 (NEN-EN 1990+A1+A1/C2, 2011):

Table 3.1 - Definitions of consequence classes

CC1	**CC2**	**CC3**
• Low consequence for loss of human life • Economic, social or environmental consequences are small or negligible	• Medium consequence for loss of human life • Economic, social or environmental consequences are considerable	• High consequence for loss of human life • Economic, social or environmental consequences are considerable

3.4.3 NEN 9997 – Dutch guideline on geotechnical design of structures

According to the Dutch national guideline geotechnical calculations have to be performed according to design approach 3. This means that the verifications on the limit states have to be carried out using the following set of partial factors:

$$(A1 \text{ or } A2) + M2$$

The partial factors *A*1 have to be applied in case structural loads are considered whereas the factors *A*2 have to be applied in case of geotechnical loads. The partial factors *A*1 and *A*2 for verification of structural and geotechnical limit states are displayed in Table 3.2.

Table 3.2 - Partial factors on actions and the effect of actions (NEN 9997-1+C1, 2012)

Load		**Symbol**	**Combination**		
			A1	***A2***	
				Remainder	**Sheet pile**
Permanent	unfavourable	γ_G	1.35 [a b]	1.0	1.0
	favourable		0.9	1.0	1.0
Variable	unfavourable	γ_Q	1.5 [a]	1.3 [a]	1.1 [a]
	favourable		0	0	0

[a]) The factors shown in the table account for RC2. To obtain the partial factor for RC1 a multiplication factor of 0.9 has to be applied, to obtain the partial factor for RC3 a multiplication factor of 1.1 has to be applied.
[b]) This value is only normative in case of small variable loads. In other cases a partial factor of 1.2 is applied.

The design of flexible dolphins is not explicitly covered within the Eurocode or a Dutch national annex. To be able to perform geotechnical verifications it is therefore often assumed that flexible dolphins behave in a similar way as regular piles or a sheet pile wall. With respect to the behaviour of the soil, the flexible dolphins can be compared best with a sheet pile wall because in both cases the strength of the soil is derived from a passive wedge. The *M2* factors which have to be applied on the soil parameters are represented in Table 3.3. Besides the partial factors for sheet pile walls also the factors that have to be used for the verification of the overall stability are presented to give a complete overview.

Table 3.3 - Partial factors on soil parameters (NEN 9997-1+C1, 2012)

Soil parameter	**Symbol**	***M2***					
		Sheet pile wall			**Overall stability**		
		Safety class			**Safety class**		
		RC1	**RC2**	**RC3**	**RC1**	**RC2**	**RC3**
Angle of internal friction	γ_{φ}'	1.15	1.175	1.20	1.20	1.25	1.3
Effective cohesion	γ_c'	1.15	1.25	1.40	1.3	1.45	1.6
Undrained shear strength	γ_{cu}	1.5	1.6	1.65	1.5	1.75	2.0
Unit weight	γ_{γ}	1.0	1.0	1.0	1.0	1.0	1.0
Stiffness	E'	1.3	1.3	1.3	1.3	1.3	1.3

The assumed similarity between dolphins on the one hand and regular piles and sheet pile walls on the other is not entirely correct. Especially in the case of berthing dolphins, the use of the partial factors for sheet pile walls might result in an overestimation of the safety. However, the application of the partial factors concerning the overall stability might result in a very conservative result on the safety.

3.4.4 EAU 2012 – German guideline on dolphin design

The German national guideline on verification of the safety of earthworks and foundations (DIN 1054) makes a subdivision in the limit state regarding the failure or excessive deformation of the ground (GEO):

- GEO-2: Failure or very large deformation of the ground;
- GEO-3: Loss of overall stability.

For these two limit state conditions different design approaches have to be considered. Design approach 2 should be used for the geotechnical analysis of limit states STR and GEO-2 , whereas design approach 3 should be used for analyzing limit state GEO-3. The partial safety factors that should be applied for the design of dolphins in the ultimate limit state are depicted in Table 3.4. When serviceability limit states are considered, the characteristic values of the actions and resistance should be applied.

Table 3.4 - Partial safety factors for verifying the ultimate limit state of a dolphin (HTG, 2015)

Load	**Actions**	**Resistances**	
		Soil	**Steel**
	γ_Q	$\gamma_{R,e}$	γ_M
Loads from berthing manoeuvres	1.00	1.00	1.00
Mooring forces (line pull) and contact forces	1.20	1.15	1.10
Wave, wind and current loads	1.20	1.15	1.10
Ice loads	1.00	1.10	1.10

Flexible breasting dolphins are designed as elastic structures which fully exploit the yield strength of the steel. The safety margin for unforeseen berthing procedures is formed by the unused plastic reserve of the pile. Therefore the safety factors that have to be applied in case the flexible dolphin is loaded by breasting forces are equal to 1.00.

In the design of mooring and breasting dolphins also fatigue due to wind and wave loads on a vessel has to be considered. For the anticipated design life time at least twice the number of load cycles should be assumed. Also local scour due to currents or propeller wash has to be accounted for.

3.4.5 BS 6349 – British Standard for maritime structures

According to the national annex on Eurocode 7, BS EN 1997-1, geotechnical structures in the United Kingdom have to be designed according to design approach 1. This means that the verification on the limit states have to be carried out using one of the following sets of partial factors:

- Combination 1: $A1 + M1$
- Combination 2: $A2 + M2$

The partial factors $M1$ and $M2$ have to be applied to the soil parameters. These factors for verification of structural and geotechnical limit states are depicted in Table 3.5.

Table 3.5 - Partial factors for soil parameters for the STR and GEO limit state (BS-EN1997-1, 2004)

Soil parameter	**Symbol**	**Set**	
		M1	***M2***
Angle of internal friction	γ_{φ}'	1.0	1.25
Effective cohesion	γ_{c}'	1.0	1.25
Undrained shear strength	γ_{cu}	1.0	1.4
Unconfined strength	γ_{qu}	1.0	1.4

The British Standard makes a distinction in partial safety factors that have to be applied on loads based on the limit state that will be considered. For the actions acting on the structure three different sets of factors are considered:

- Static equilibrium for overall global factors (i.e. not involving the strength of the structure or the ground) should be verified using the design values for EQU, Set A.
- Design of structural members not involving geotechnical actions should be verified using the design values for STR, Set B.
- Design of structural members (footings, piles, basement walls, etc.) should be verified by using the least favourable of the effects from STR/GEO Set B and STR/GEO Set C.

The partial safety factors on permanent and variable actions for ultimate limit states are depicted in Table 3.6 and Table 3.7 respectively.

Table 3.6 - Partial safety factors on permanent actions (BS6349-2, 2010)

Actions	**Symbol**	**EQU (Set A)**	**STR/GEO (Set B)**	**STR/GEO (Set C)**
Permanent actions including geotechnical actions				
Unfavourable	$\gamma_{G,sup}$	1.05	1.35	1.0
Favourable	$\gamma_{G,Inf}$	0.95	1.0	1.0

Table 3.7 - Partial safety factors on variable actions (BS6349-2, 2010)

Actions	**Symbol**	**EQU (Set A)**	**STR/GEO (Set B)**	**STR/GEO (Set C)**
Variable persistent actions				
Ship berthing loads	γ_Q	1.4	1.4	1.3
Mooring loads	γ_Q	1.4	1.4	1.3
Wave, wind and current loads	γ_Q	1.4	1.4	1.3
Variable transient actions				
Abnormal berthing loads	γ_Q	1.2	1.2	1.2

Flexible dolphins absorb the energy of impact caused by berthing or mooring vessels by lateral deflection of the pile. Due to this deflection the stress in the steel pile increases. Under abnormal energy conditions the pile should operate at 80% of the yield stress (BS6349-4, 1994) what means that γ_M = 1.25 for the yielding strength of the steel.

3.4.6 PIANC 2002 – Guidelines from the International Navigation Association for the design of fender systems

In contrast to the NEN, EAU and British Standards, the PIANC is no national guideline but a guideline which can be applied in different countries. It is mainly a guideline for the design of fenders, but also some guidance on design of flexible dolphins is provided. It gives some advice on partial safety factors that can be applied in the limit state design method for flexible dolphins.

The load factor that has to be applied depends on the capacity of the pile to resist overloads by plastic yielding:

- $\gamma = 1.25$ when no plastic yielding is possible.
- $\gamma = 1.0$ when plastic yielding is possible until a displacement of at least two times the maximum elastic displacement.

For the material factor on steel normally a factor 1.0 can be adopted. For the soil parameters the partial factors indicated by the geotechnical specification should be used (PIANC, 2002).

4

STARTING POINTS

4.1 Introduction

This chapter contains the most important starting points for this master thesis. The first section includes a description and the results of performed full scale tests. In section 4.3 these test results are used to establish which of the available design models is most suitable for this research. Furthermore, the analysis method is discussed. Subsequently, the model parameters are described and their probabilistic distributions are defined. Also the correlations are determined for the parameters which are relevant for this research. Probabilistic evaluations are based on limit state functions. Therefore, these limit state functions had to be defined for the relevant failure mechanisms, which is done a section 4.5. The reliability which is required with respect to these failure mechanisms is determined in section 4.6.

4.2 Full scale tests

4.2.1 Description of the performed tests

To gain more insight in the behaviour of flexible dolphins subjected to static and dynamic loading due to mooring and breasting vessels, full scale tests were performed in the Port of Rotterdam (Beneluxhaven). During these tests, tubular piles were loaded dynamically, statically and statically to failure. By monitoring the development of the stresses and strains in the piles and the surrounding soil and by monitoring the deformation of the piles and soil, conclusions could be drawn on the behaviour of flexible dolphins.

During the tests, in total eight piles were considered. Based on their slenderness these piles were subdivided into three different types of piles (Van der Meer & Peters, 2015):

- Type 1: Full-length class 4 piles.
- Type 2: Traditional assembled piles with a class 3 part in the ground and a reduced wall thickness part on top.
- Type 3: Very slender full-length class 4 piles filled with sand.

The characteristics of the different classes are given in Table 4.1.

Each pile was composed out of sections with different wall thicknesses and steel grades, resulting in six different pile configurations. Furthermore, distinction was made based on the geometry: three piles were located in a slope whereas other piles were positioned in a horizontal bottom. Moreover, two of the tested piles were filled with sand after installation of the piles.

Table 4.1 - Limit values of section classes (CUR-publicatie 211E, 2014)

Class	Limits	Characteristics
1 – Plastic	$D/t\varepsilon^2 < 50$	• Full plastic moment allowed • Section is able to develop a plastic hinge • Plastic redistribution allowed
2 – Compact	$50 < D/t\varepsilon^2 < 70$	• Full plastic moment allowed
3 – Semi-compact	$70 < D/t\varepsilon^2 < 90$	• Full elastic moment allowed (yield limit in outer fibre)
4 – Slender	$D/t\varepsilon^2 > 90$	• Limited effectiveness, buckling stress (below yield limit) allowed in outer fibre
The parameter ε, which is used in the expression for the limits can be expressed as $\varepsilon = \sqrt{(235/f_y)}$.		
Note that D/t = 90 as a commonly used limit below which buckling was not likely to occur, is not valid.		

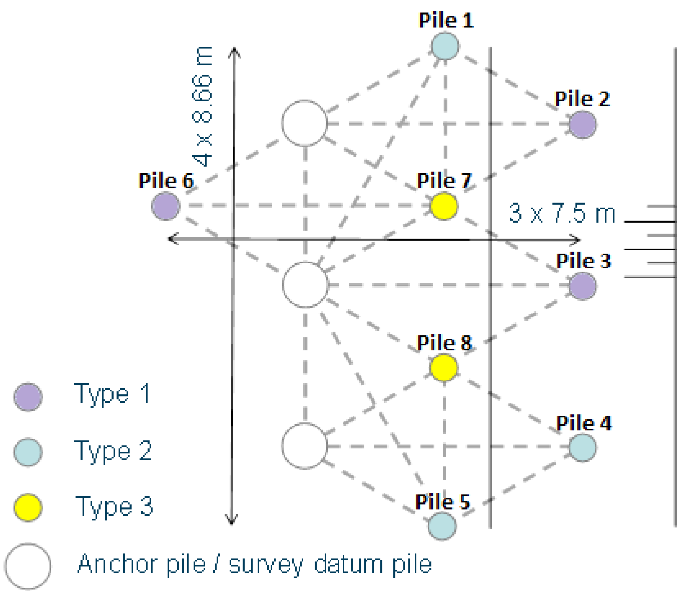

Figure 4.1 - Plan view of the pile configuration (Van der Meer & Peters, 2015)

During the tests, piles one to six were subjected to a dynamic loading. These loads were applied by a crane which was connected to the considered pile by cables and pulleys. Furthermore, piles one to six and pile eight were loaded statically. Finally, all eight piles were loaded statically to failure. For the application of these static loads, use was made of hydraulic jacks. To be able to apply the lateral loads, a frame was designed which vertically rested on three piles. The horizontal load was predominantly taken by a heavier anchor pile. To enable the use of the frame, the piles were placed in a group with identical intermediate distances, resulting in a plan view according to Figure 4.1. The distance between the tested pile and the anchor pile was always equal to 15 meters so that passive soil wedges were not expected to interfere (Van der Meer & Peters, 2015).

To measure the strains in the piles due to the loading, each pile was equipped with glass fibre optic strain fibre gauges in longitudinal and circumferential direction. The circumferential strain fibre gauges were located at the level of the bottom surface and near the transition in wall thickness above the bottom surface to measure the ovalisation of the pile. The longitudinal strain fibre gauges were located at the front and the rear of the pile (in the direction of the loading) to measure the strains from which the internal forces in the piles and its deflection could be determined. Moreover, each pile was provided with a 20 m long SAAF, which measured the angular rotation of the pile with respect to a reference point. With these rotations the deflection of the pile under static loading could be determined.

To perform geotechnical measurements regarding the occurring stresses and strains in the soil, SAAFs of 10 m long and water pressure meters were installed at close distance of the pile. During the dynamic tests the development of the water pressure was measured at three different levels below the bottom surface. With the SAAFs in the soil the deformation of the soil during the static failure tests was measured to get an indication of the failure behaviour of the soil.

4.2.2 Results of the tests

4.2.2.1 Section forces and pile displacements

The behaviour of laterally loaded piles can be approached by a bi-linear relation: up to the point of plasticity the behaviour of the pile can be described by a linear relation between force and displacement or bending moment and curvature, which is shown in Figure 4.2. With this relation, the bending moments acting in a pile can directly be derived from the measured strains. Since the piles used during the tests are all classified as class 3 or class 4 piles, the behaviour of the loaded piles can be described by the elastic branch of the relation between bending moments and curvature, resulting in

$$M = \frac{\varepsilon}{\varepsilon_y} \cdot W_{el} \cdot f_y \tag{4.1}$$

in which the yield strain ε_y is equal to the yield strength f_y divided by the Young's modulus E.

The shear forces acting in the piles can directly be derived from the bending moments as these forces are characterized by the change in bending moment according to

$$V = \frac{dM}{dx} \tag{4.2}$$

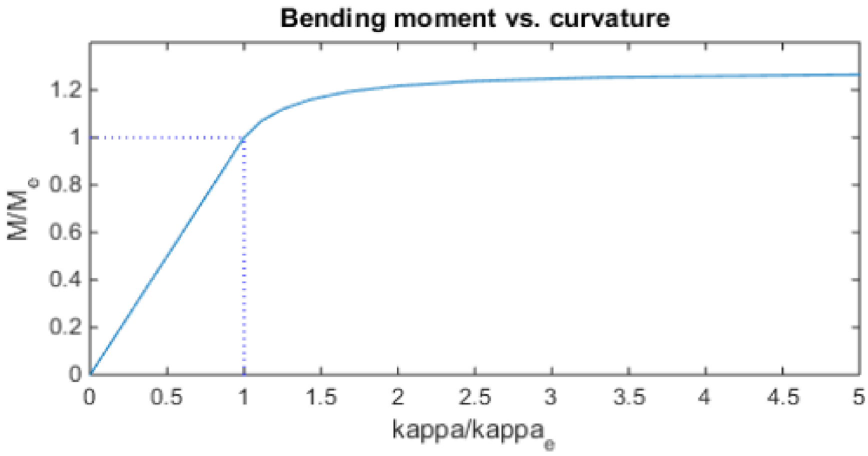

Figure 4.2 - Relation between bending moments and curvature

The first theorem of the bending moment plane (Dutch: *eerste stelling van het momentenvlak*) states that the rotation of the pile is equal to the area underneath the reduced bending moment diagram:

$$\theta = \int \frac{M}{EI} dx \tag{4.3}$$

With this relation the displacement of the laterally loaded piles can be derived from the bending moments found from the measured strains. During the full scale tests also other methods are used to determine the displacement of the loaded piles. These methods show similar results and therefore justify the use of the method which determines the displacement from the strain fibre gauges as is described above.

Figure 4.3 shows the results of pile 1 subjected to a lateral loading of 30 tons. Distinction is made between static and dynamic loading. For the results for other piles reference is made to Appendix C.

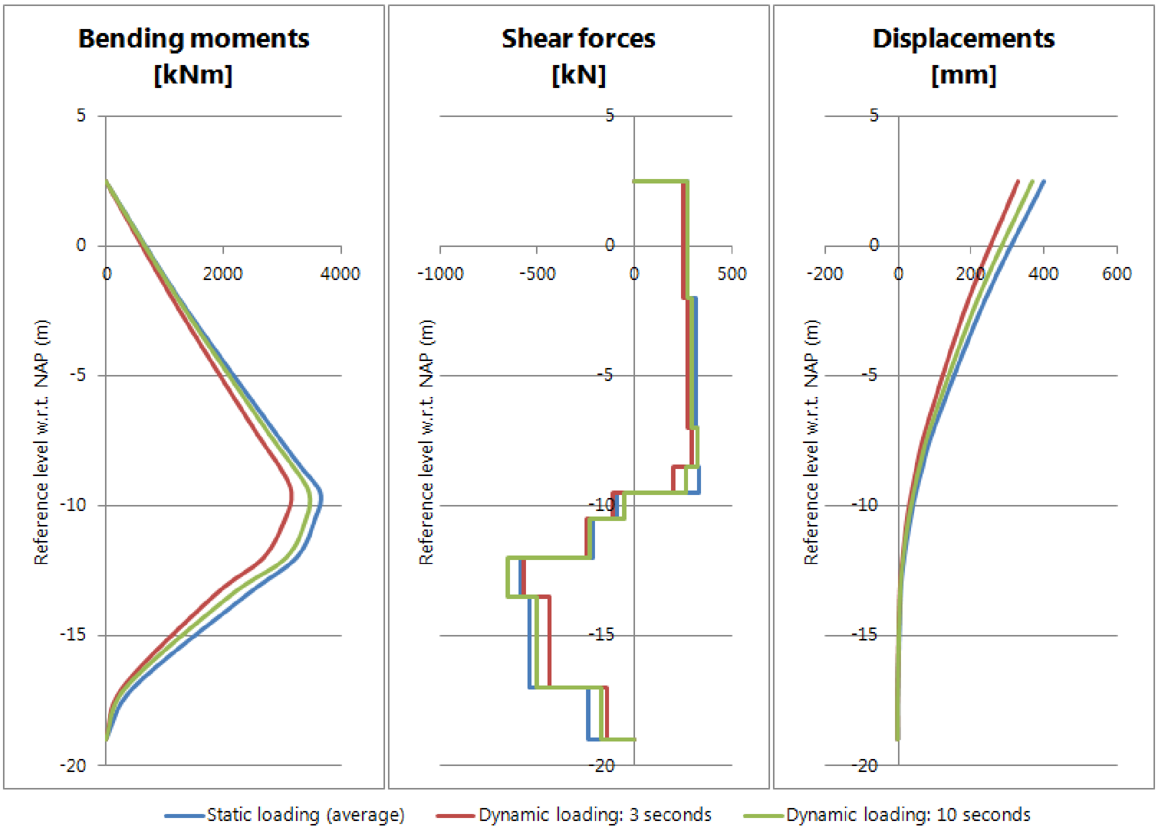

Figure 4.3 - Section forces and displacements of pile 1 (F = 30 kN)

During dynamic lateral loading of a pile, the soil surrounding the pile is loaded fast and short. As a result, the soil will not be able to consolidate and water overpressures will develop, indicating undrained soil behaviour (Verruijt, 2010). Due to this undrained behaviour, the stiffness of the soil increases. As the duration of the loading increases and approaches static loading conditions, more water can escape from the pores and the passive soil resistance gradually decreases again, allowing for larger pile deformations and larger bending moments in the pile. This behaviour is also shown by the results of the performed full scale tests. The measurements show that the deformations of the piles and the bending moments in the piles increase as the duration of the loading increases.

4.2.2.2 Failure loads

The eight piles tested during the performed full scale tests were designed such that they failed by local buckling. The load at which this failure occurred, is determined in two different ways: it is derived from the strains measured by the strain gauges and it is determined from the jack stroke.

Due to the sheltered conditions in which the full scale tests are performed, the influence of wind, waves and currents on the behaviour of the piles can be neglected. The applied lateral load can be considered to be the only external load exerted on the piles, what would result in a continuous shear force over the upper sections of the pile, which is equal to the applied load. However, the shear force diagrams obtained from the measured strains show some small discontinuities, which can be explained by small measurement inaccuracies that are amplified in the determination of the shear forces from the bending moments. Therefore the failure loads derived from the measured strains cannot be considered as completely reliable.

The failure load can also directly be determined from the jack stroke, which appears to give more reliable results. These results on the failure load for the eight tested piles are given in Table 4.2.

Table 4.2 - Failure loads

Pile	Failure load [kN]
1	693
2	700
3	697
4	688
5	723
6	620
7	360
8	302

4.2.2.3 Other test results

Water pressures

During the dynamic tests, the development of the water pressure in the soil near the piles was measured at three different levels in order to indicate the undrained behaviour of the soil and to register the development of passive failure wedges. Whereas the development of water overpressures indicate undrained soil behaviour, the development of water underpressures can be related to failure of the soil. During the development of passive failure wedges, the soil starts to shear. Due to this shearing, the soil volume tends to increase and water is sucked into the pores, resulting in water underpressures (Van der Meer & Peters, 2015).

During the performed tests, a few of the measurements show a very clear response, as, for example, the measurements made near pile 2 while the pile was subjected to a loading of 30 tons during 15 seconds. The results of these measurements are depicted in Figure 4.4. The upper water pressure meter first shows the development of an overpressure. When the maximum loading is reached, the water pressure suddenly drops and the soil fails (see also Figure 4.5). The middle water pressure meter only shows a development of overpressures, no underpressure occurs so the passive failure wedge has not yet reached this point. The lowest water pressure meter shows no response to the loading of the pile, indicating that the deformations of the pile and the soil at this point are negligible.

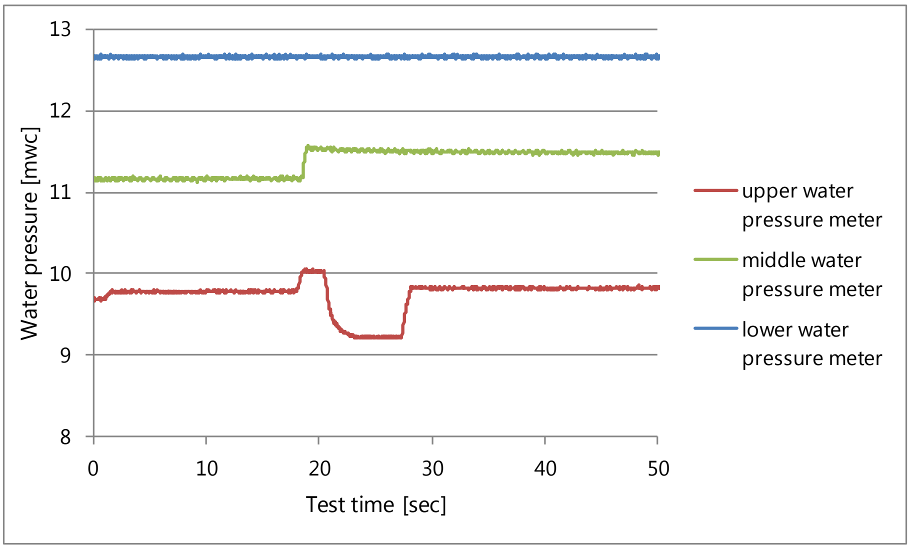

Figure 4.4 - Water pressure registration near pile 2 during dynamic loading (30 tons, 15 seconds)

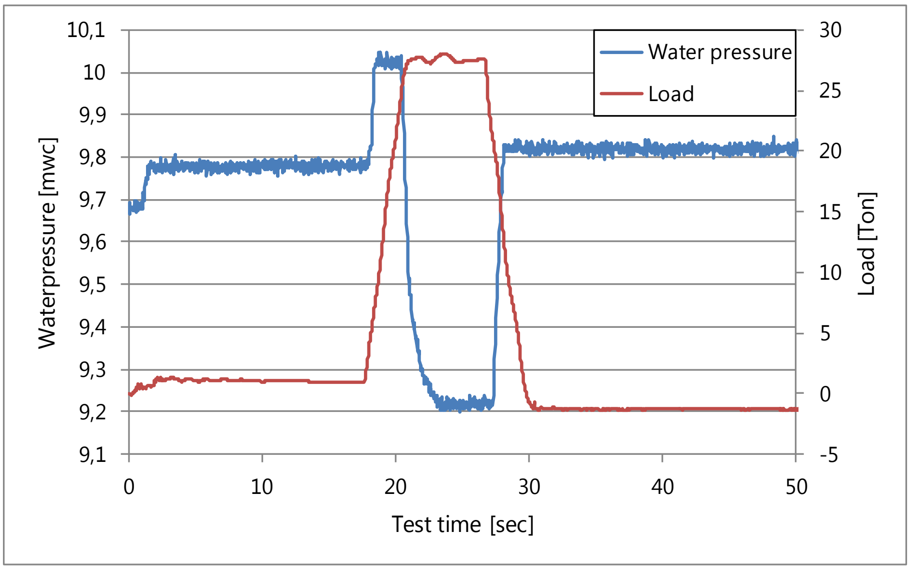

Figure 4.5 - Water pressure registration of the upper water pressure meter near pile 2

However, most measurements did not show such a clear response as in Figure 4.4 and Figure 4.5. Furthermore, during the dynamic tests with a loading of 15 tons, hardly any response was measured.

Soil deformations

To get an indication of the failure behaviour of the soil, the deformations of the soil near the loaded piles were measured during the static failure tests. As soil starts to fail, it will exhibit plastic behaviour and the deformations of the soil will quickly increase. This transition to plastic soil behaviour is also shown by the measurements performed during the static failure tests. The results of the SAAF-measurements made on the passive side of pile 1 are shown in Figure 4.6. The results show a small difference in displacement, which can be explained by the different distance between the tested pile and the SAAFs: SAAF 60467 is located at 1.55 m from the pile whereas SAAF 60470 is located at 1.10 m from the pile. Both measurements show that the passive failure wedge has developed up to approximately NAP -14 m. The results for the other piles show a similar behaviour and are presented in Appendix C.

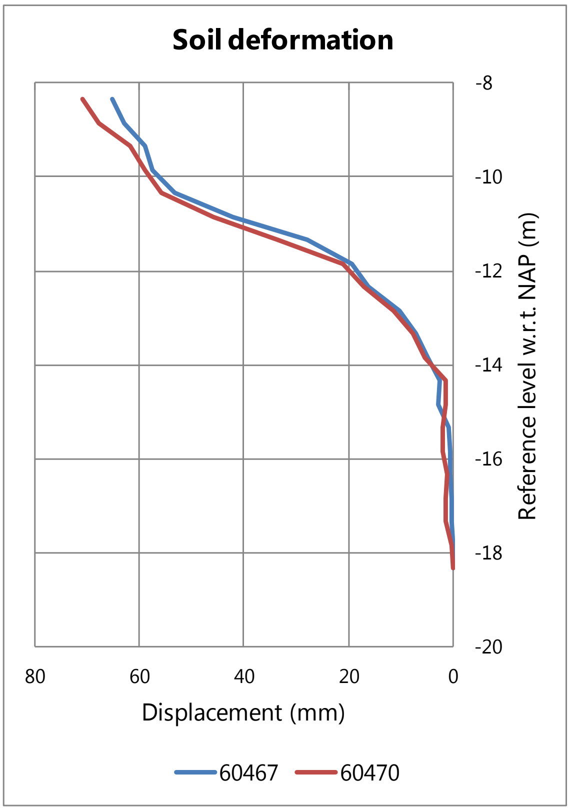

Figure 4.6 - Soil deformation near pile 1

4.3 Model and analysis method

4.3.1 Models vs. Test results

There are different models available that qualify for the design of flexible dolphins. The software models which are most frequently used in the Netherlands are Plaxis 3D, D-Sheet Piling and D-Pile Group. From previous research it appears that Plaxis 3D approaches the behaviour of laterally loaded piles best. Based on a comparison with different tests from literature, Verhoef (2015) shows that the HSsmall model is most appropriate. However, because of the time-consuming calculations and the limitations in performing probabilistic evaluations in combination with the model, Plaxis 3D is not considered to be most appropriate at this stage of this master thesis.

Comparison of D-Sheet Piling and D-Pile Group on complexity of the model and duration of the calculations shows that these models are comparable. Both models have a relatively short calculation time and require a limited amount of input parameters. Although, it can be argued that the input parameters for D-Sheet Piling are a bit more prevalent. The main distinction between the two models is formed by the manner in which the soil behaviour of the soil is modelled. This is reflected by the output of the models. Therefore, a comparison between D-Sheet Piling and D-Pile Group is made based on the results obtained from the performed full scale tests. The models are compared based on bending moments and displacements resulting from a lateral load equal to the failure load of the particular piles. Figure 4.7 compares the two considered models with the results of the tests obtained for pile 1. The results for the other piles show a similar trend and are included in Appendix D.

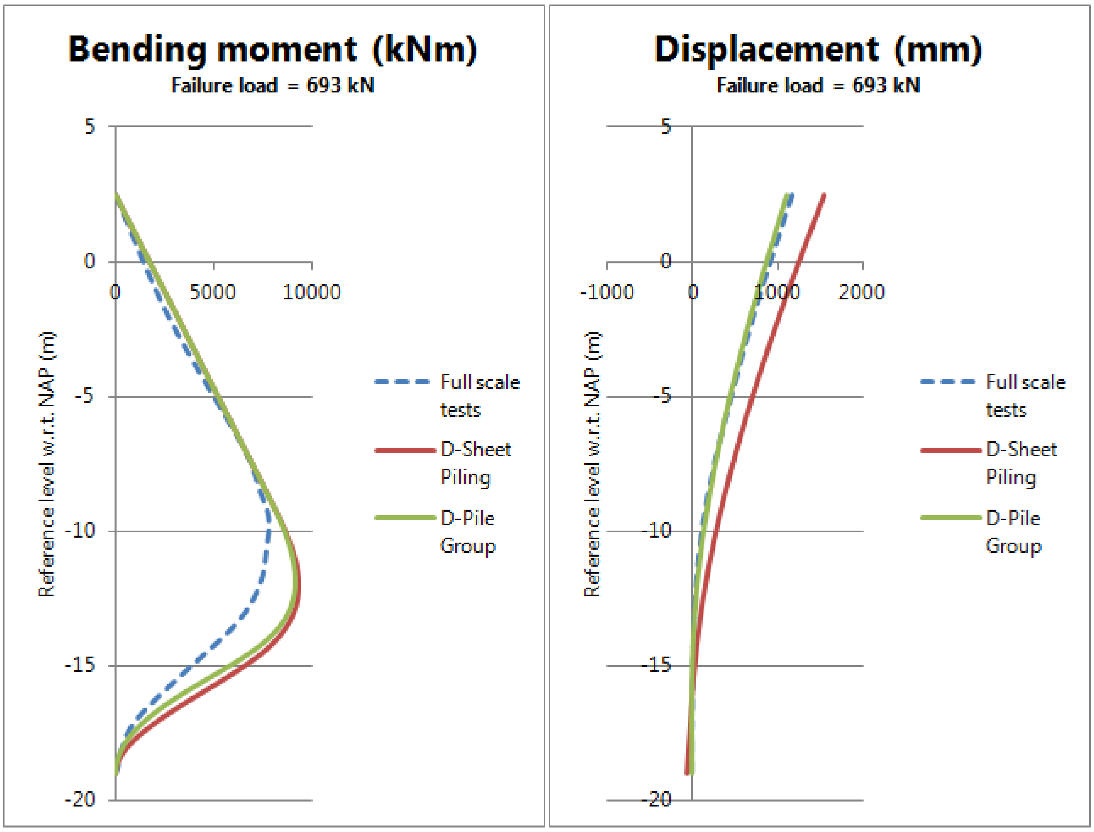

Figure 4.7 - Comparison of the models with the test results (pile 1)

Regarding the bending moments it can be concluded that D-Sheet Piling and D-Pile Group show similar results. Both models tend to overestimate the bending moments that occur in the pile and the depth at which the maximum bending moment occurs. However, D-Pile Group seems to give a smaller overestimation of these results in case cohesive soils have to be considered. This can be explained by the fact that D-Pile Group can take into account the undrained behaviour of clayey soils.

Comparison of the displacements shows that D-Sheet Piling gives an overestimation of the pile displacement due to lateral loading. D-Pile Group gives a more accurate approximation. This is contradictory to the results found by Verhoef (2015), who found that D-Sheet Piling gives the better approximation of the pile behaviour with respect to the deformations. This difference can be explained by the way the soil is modelled. Whereas Verhoef uses the undrained shear strength, the comparison of the models and test results in this section are based on the cohesion of the soil and the angle of internal friction.

In Table 4.3 an overview is given of the compared models. For completeness of the comparison, also the results for Plaxis 3D are included. In the table '-' indicates that the model is considered least suitable for the intended research, whereas '+' indicates that the model is considered most suitable. Comparison of D-Sheet Piling and D-Pile Group shows that both models are almost equally suitable for the design of flexible dolphins and the intended research. Given the available probabilistic analysis methods, it has been decided to use D-Sheet Piling in the determination of the partial safety factors for the parameters which are involved in flexible dolphin design.

Table 4.3 - Comparison of software models ('-' = least suitable; '+'= most suitable)

Criterion	D-Sheet Piling	D-Pile Group	Plaxis 3D
Complexity	+	+	-
Input parameters	+	o	-
Calculation time	+	+	-
Model output – bending moments	-	-	+
Model output – displacements	-	o	+

4.3.2 Model boundaries

D-Sheet Piling is a spring model in which the soil is modelled by bi-linear springs along the pile. The subgrade reaction of the soil is limited by the minimum (active) and maximum (passive) pressure that can develop in the soil, which can be determined using the Brinch-Hansen method. The modulus of subgrade reaction can be determined using the Ménard theory. Modelling the soil by bi-linear springs implies that the stiffness of the soil is independent of stresses and strains. However, in practice the stiffness of the soil decreases with increasing deformation. Furthermore, the stiffness of the soil increases with increasing depth. This increase of stiffness can be accounted for by generating multiple layers for one soil layers with increasing stiffness over the depth.

With D-Sheet Piling it is only possible to consider drained soil behaviour. This means that the model considers the soil to be completely consolidated, which occurs in case of a persistent load. Therefore only static loading can be applied by the model.

Another limitation of D-Sheet Piling is that only horizontal soil layers can be introduced, leaving that sloping ground surfaces cannot be considered. To account for a sloping bottom surface, the modelled surface level has to be raised in case of loading towards to slope or lowered in case of loading from the slope.

4.3.3 Prob2B

The toolbox Prob2B is used to perform probabilistic calculations with D-Sheet Piling (Single Pile module). The toolbox sends stochastic input parameters to the model and uses the output from the model to evaluate the limit state function according to the selected probabilistic method. This loop is repeated as often as is required to obtain the final result of the reliability calculation (Courage & Steenbergen, 2007).

To be able to perform a probabilistic evaluation with Prob2B, first the model and possible additional variables need to be defined. Some of the model parameters and user defined variables may be directly related, which can be included by creating model dependencies. The next step is to define the limit state function, which can be composed out of model output results and user defined variables or values. With Prob2B it is also possible to evaluate multiple limit state functions simultaneously. However, as this may give complications during the evaluation (Courage & Steenbergen, 2007), the limit states will be evaluated individually in this research.

For every individual variable the stochastic properties have to be defined: a type of distribution of the probability density function has to be assigned to the variables and the mean values and standard deviations should be defined. Furthermore, cross-sectional correlations need to be provided to create the joint probability density function (Wolters, 2012).

Finally the reliability calculation method has to be chosen. In this research the FORM-method is used. Prob2B requires some specific settings for this method which are shown in Figure 4.8. The relaxation value determines whether the next step is exactly the calculated point (relaxation value = 1) or a cautious step in between the old and new value (0 < relaxation value < 1) (Wolters, 2012). A smaller value means that smaller steps are taken and that the calculation becomes more time-consuming. However, as a result the method becomes more robust for irregular limit state functions (Courage & Steenbergen, 2007).

The convergence criteria determine whether a satisfying convergence is obtained to in order to find the minimum for the reliability. The convergence criterion for the limit state function is defined as:

$$\left| \frac{Z}{\left\| \frac{dZ}{du} \right\|} \right| < criterion$$

The criterion for the reliability is defined as: $\beta_{n+1} - \beta_n < criterion$

The perturbation value determines which part of the standard deviation is used to calculate the derivative. The perturbation method defines whether this derivative is taken as one or two sides from the point (Wolters, 2012).

During this research, the default values are maintained for the settings for FORM. These values are shown in Figure 4.8.

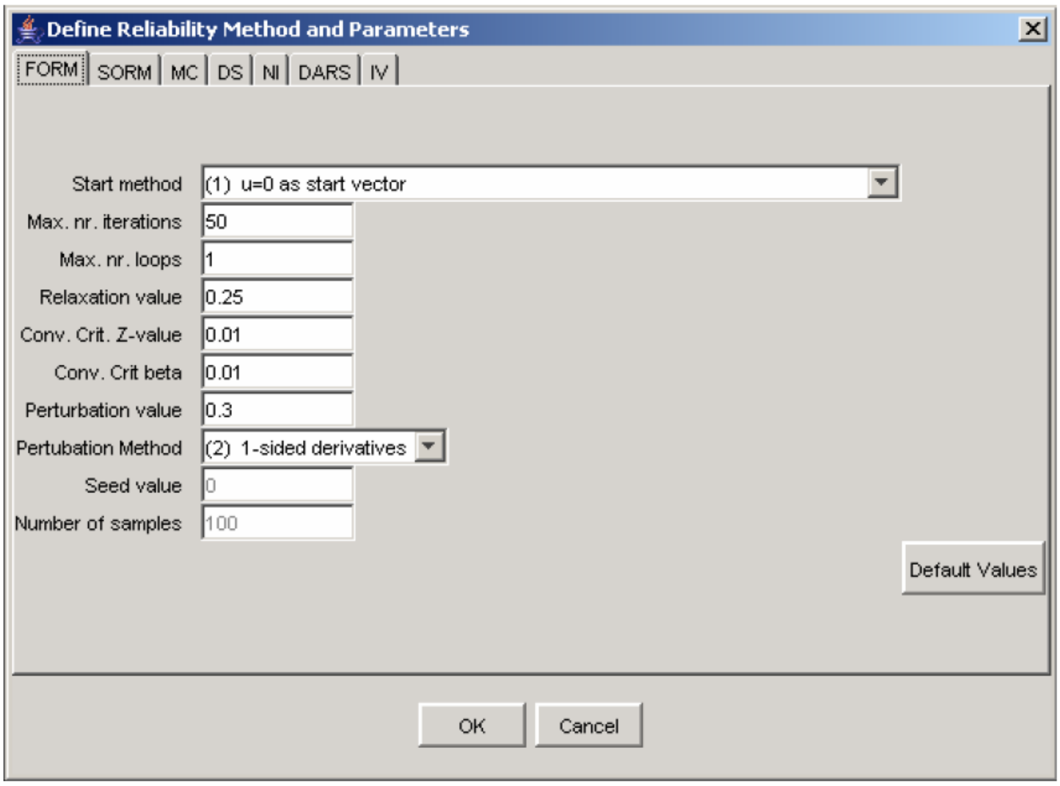

Figure 4.8 - Settings for FORM in Prob2B (Courage & Steenbergen, 2007)

4.4 Input parameters for the model

4.4.1 Soil parameters

4.4.1.1 Unit soil weight

The unit soil weight is defined by the weight of soil per unit volume (Verruijt, 2010). Therefore, this weight for specific types of soils can be determined from soil samples by dividing the weight of the soil by the volume, resulting in equation 4.4 for dry soil:

$$\gamma_{unsat} = \frac{W_d}{V} = (1 - n) \cdot \rho_{grains} \cdot g \tag{4.4}$$

in which the porosity n is defined as the ratio between pore volume and total volume of the soil. The soil that is of influence on the behaviour of flexible dolphins will in most cases be saturated. The unit weight of this saturated soil follows from

$$\gamma_{sat} = \frac{W}{V} = n \cdot \rho_{water} \cdot g + (1 - n) \cdot \rho_{grains} \cdot g \tag{4.5}$$

The coefficient of variation for the unit soil weight is taken from NEN 9997 Table 2.b and is equal to 0.05. This coefficient is relatively small because the unit soil weight can be determined rather accurate (Verruijt, 2010).

4.4.1.2 Cohesion and angle of internal friction

The cohesion and angle of internal friction of soil can be determined from triaxial tests. When at least two tests are performed at different pressure circumstances, the cohesion and angle of internal friction can be derived from the envelope of the different critical stress circles, as is show by Figure 4.9. The envelope is also known as the Mohr-Coulomb failure criterion and can analytically be expressed by

$$\tau_{cr} = c + \sigma_n' \tan \varphi \tag{4.6}$$

in which τ_{cr} is the critical shear stress and σ_n' is the effective normal stress on the considered plane. The criterion shows that the cohesion of soil is linearly dependent on the critical stress whereas the angle of internal friction can be considered as a constant of the material (Verruijt, 2010).

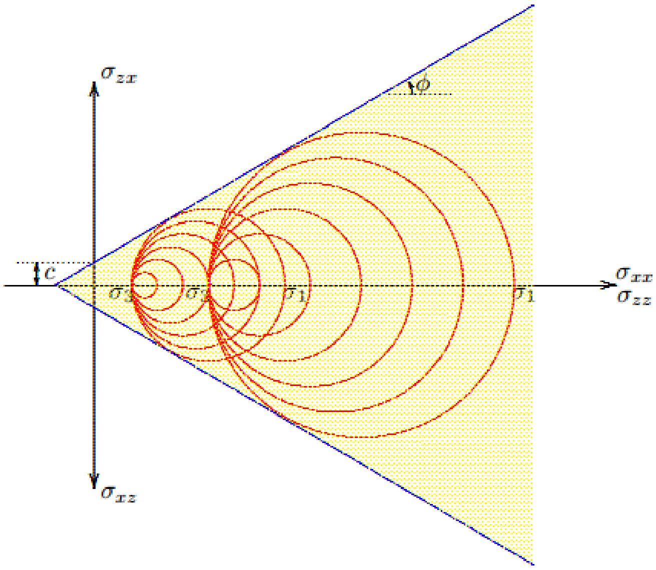

Figure 4.9 - Determination of the cohesion and angle of internal friction from two triaxial tests (Verruijt, 2010)

From equation 4.6 it can be seen that small deviations in the angle of internal friction result in larger variations in cohesion. According to NEN 9997 these different variations have to be taken into account by considering different values for the coefficients of variation. Therefore the coefficient of variation for the cohesion and the angle of internal friction are considered to be respectively 0.2 and 0.1, which is in accordance with NEN 9997 Table 2.b.

Furthermore equation 4.6 and Figure 4.9 show that the cohesion and the angle of internal friction are negatively correlated, as an increasing friction angle implies a decreasing cohesion. This relation is also shown by the results of over 1000 triaxial tests performed by Gemeentewerken Rotterdam (2003). From these tests a correlation coefficient between the cohesion and the angle of internal friction of -0.58 is derived.

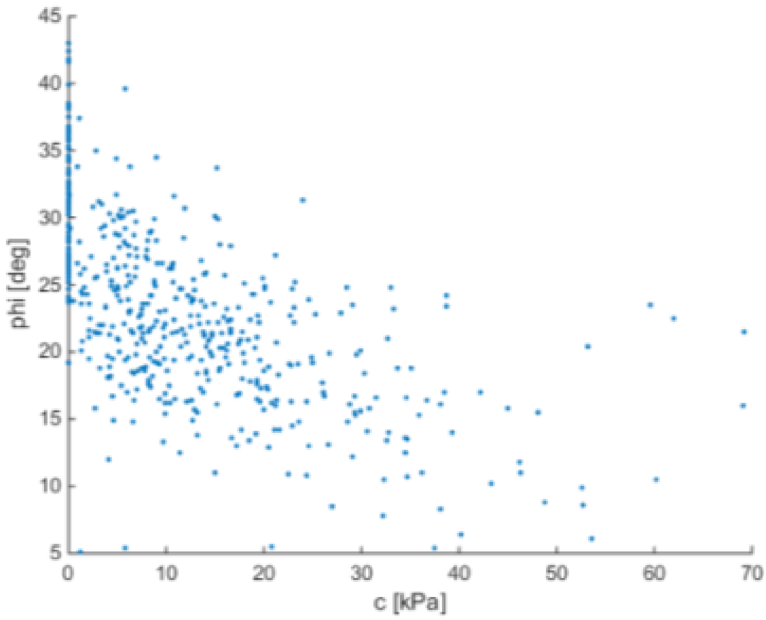

Figure 4.10 - Correlation between cohesion and angle of internal friction

4.4.1.3 Soil stiffness

There are different stiffness parameters that can be used to define the stiffness of soil. D-Sheet Piling requires the input of the pressiometric modulus. Combined with the type of soil, this parameter is used to determine the modulus of subgrade reaction according to Ménard.

The pressiometric modulus can be obtained from pressiometer tests. In these tests a cylindrical element is installed in the soil which is radially stretched in horizontal direction by increasing the uniform pressure in the element in multiple steps. The volume change is measured at three time-intervals and plotted against the measured pressure (CUR-publicatie 211E, 2014). From this graph the pressiometric modulus can be derived as it is equal to the slope of the psuedo-elastic section of the pressiometer curve (Teunissen, 2005).

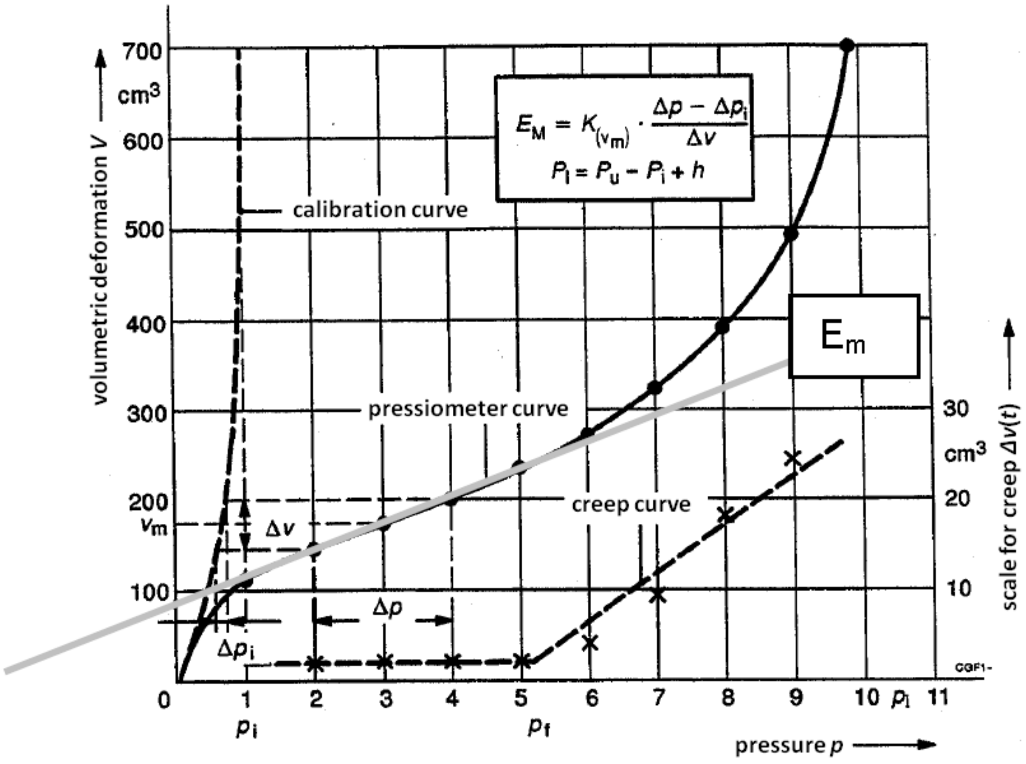

Figure 4.11 - Graph of the results of a Ménard pressiometer test (Teunissen, 2005)

Another way to determine the pressiometric modulus is by using the direct relation between this stiffness parameter and the cone resistance obtained from CPTs. As the pressiometer test is not applied very often, this is a convenient way to find reasonable values for the stiffness of the soil. The relation between the cone resistance (q_c) and the pressiometric modulus is given by $E_M = \beta \cdot q_c$. The values for β depend on the type of soil and are given in Table 4.4.

Table 4.4 - Correlations between pressiometric modulus and cone resistance (Deltares, 2014)

Soil classification	**Correlation β**
Peat	3 – 4
Clay	2 – 3
Loam	1 – 2
Sand	0.7 – 1
Gravel	0.5 – 0.7

As for the other soil parameters, the coefficient of variation for the stiffness parameters is determined based on NEN 9997 Table 2.b, which gives a coefficient of variation equal to 0.1 for stiffness parameters at a reference pressure of 100 kPa. Because no further information is available on the exact relation between E_M and E_M^{ref}, it is assumed that this coefficient also holds for the pressiometric modulus.

4.4.1.4 Overview of the soil parameters

Ideally, all soil parameters are obtained from in-situ soil investigation. The unit soil weight and the strength parameters can be determined from soil samples, and Cone Penetration Tests (CPTs) can be used to derive stiffness parameters. However, in many cases insufficient tests are performed to obtain reliable parameters. In these cases, soil parameter values are determined based on NEN 9997 Table 2.b, which gives characteristic[1] values for the soil parameters for different types of soil.

For a wide variety of soil parameters, a normal distribution can be assumed in geotechnical reliability analysis (Baker & Calle, 2006). However, for parameters with relatively low average values and a large scatter this may lead to physical inconsistencies, such as negative design point values caused by the negative values in the lower tail of a normal distribution. This is particularly the case for the cohesion. Therefore, for the cohesion a lognormal distribution will be applied. For the other soil parameters a normal distribution will be applied because the probability of negative values is negligible.

An overview of the probabilistic distributions and coefficients of variation for each soil parameter is given in Table 4.5. Because the coefficients of variation (CoV = σ/μ) are determined from NEN 9997 Table 2.b, the obtained results can be applied on a larger scale (and do not just hold for one specific location).

Table 4.5 - Soil parameters

Parameter	**Symbol**	**Unit**	**Distribution**	**Coefficient of Variation**
Unsaturated soil weight	γ_{unsat}	[kN/m^3]	Normal	0.05
Saturated soil weight	γ_{sat}	[kN/m^3]	Normal	0.05
Angle of internal friction	φ	[deg]	Normal	0.10
Cohesion	c	[kPa]	Lognormal	0.20
Pressiometric modulus	E_m	[kN/m^2]	Normal	0.10

For each soil layer the different soil parameters are correlated, e.g. an increasing friction angle often implies an increasing soil weight and a decreasing cohesion. The correlations between the parameters are derived from the database of Gemeentewerken Rotterdam (2003), which contains over 1000 triaxial tests taken between 1980 and 2003. The correlation coefficients obtained from this database are given in Table 4.6. It is assumed that these coefficients are also representative for regions outside Rotterdam.

Table 4.6 - Correlation between soil parameters

	γ_{unsat}	γ_{sat}	φ	c	E_m
γ_{unsat}	1.00	1.00	0.53	0.04	0.50
γ_{sat}	1.00	1.00	0.53	0.04	0.50
φ	0.53	0.53	1.00	-0.58	0.27
c	0.04	0.04	-0.58	1.00	0.15
E_m	0.50	0.50	0.27	0.15	1.00

[1] The characteristic value for soil parameters is defined as the parameter value with a probability of exceedance equal to 95% (NEN 9997-1+C1, 2012).

4.4.2 Structural parameters

The flexible rigidity (EI) and the section modulus (W) of the piles are composed of basic random variables. Of these basic random variables, the pile diameter and the wall thickness are considered to have an uniform distribution. Since the piles used for flexible dolphins are mostly cold formed, the considered tolerances on the shape are based on NEN-EN 10219-2. The tolerances on the pile diameter and wall thickness are given Table 4.7. Furthermore, NEN-EN 10219-2 gives tolerances on mass and out of roundness. These parameters both are a function of the pile diameter and wall thickness, what makes it more complex to derive the coefficients of variation for the pile diameter and wall thickness. For this reason the tolerances on mass and out of roundness are disregarded in this master thesis.

Table 4.7 - Tolerances on diameter and wall thickness of piles (NEN-EN10219-2, 2006)

Parameter	**Tolerances**
Pile diameter (*D*)	± 1.0 % with a minimum of ± 0.5 mm and a maximum of ± 10 mm.
Wall thickness (*t*)	*D* ≤ 406.4 mm: *t* ≤ 5 mm: ± 10 % *t* > 5 mm: ± 0.5 mm *D* > 406.4 mm: ± 10 % with a maximum of 2.0 mm

For the other basic random variables the coefficients of variation are taken from the Probabilistic Model Code of the Joint Committee on Structural Safety (JCSS, 2001). Because these parameters have a relatively high average value and a relatively small scatter, it is safe to assume a normal distribution for these parameters. For the composed variables it can also be assumed that the probability that these parameters adopt a negative value is negligible. Therefore, these variables are also assumed to be normally distributed. The coefficients of variation of these parameters are determined by conducting a Monte Carlo simulation. Table 4.8 shows an overview of the distributions and the variations for both the base and the composed pile parameters.

Table 4.8 - Pile parameters

Parameter	**Symbol**	**Unit**	**Distribution**	**Coefficient of Variation**
Pile diameter*	D	[m]	Uniform	0.006
Wall thickness*	t	[mm]	Uniform	0.06
Young's modulus	E	[kN/m^2]	Normal	0.03
Yield strength	f_y	[N/mm^2]	Normal	0.07
Composed parameters*				
Flexible rigidity	EI	[kNm^2]	Normal	0.06
Elastic section modulus	W_{el}	[m^3]	Normal	0.06
*) The given coefficients of variation are derived for a pile with *D* = 914 mm and *t* = 20.6 mm. A change in these parameter values may result in different coefficients of variation.				

The correlations between the pile parameters are derived by performing a Monte Carlo simulation. The results are shown in Table 4.9. Because the tolerances on mass and out of roundness are disregarded, it is found that there exists no correlation between pile diameter and wall thickness.

Table 4.9 - Correlations between pile parameters (for *D* = 914 mm and *t* = 20.6 mm)

	EI	$\mathbf{W_{el}}$	**D**	**t**	**E**
EI	1.00	0.87	0.28	0.83	0.48
$\mathbf{W_{el}}$	0.87	1.00	0.22	0.98	-
D	0.28	0.22	1.00	-	-
t	0.83	0.98	-	1.00	-
E	0.48	-	-	-	1.00

4.4.3 Geometrical parameters

The water levels in a harbour fluctuate due to e.g. ship or wind induced waves and tidal fluctuations. However, these water level fluctuations hardly have any influence on the stability and behaviour of flexible dolphins, because they do not result in the change of the effective stresses in the soil. Therefore, the water levels are chosen as deterministic.

Due to measurement inaccuracies it is difficult to exactly determine the level of the bottom surface. Furthermore, this surface is not flat but contains a lot of irregularities. Therefore, the level of the bottom surface is included as a stochastic variable. The same holds for the levels of the different soil layers. These are mostly determined from CPTs and are therefore very inaccurate. However, brief calculations showed that the levels of the different soil layers hardly have any influence on the reliability of flexible dolphins. Therefore, this level is chosen as deterministic.

It is not possible to install a flexible dolphin such that the pile tip is exactly at the level as is determined in advance. Since the pile tip level may have a significant influence on the reliability of the structure, this parameter is considered to be a stochastic variable. The assumed distribution for this and the other geometrical parameters is given in Table 4.10.

Table 4.10 - Geometrical parameters

Parameter	**Unit**	**Distribution**
Water level	[m NAP]	Deterministic
Bottom surface level	[m NAP]	Normal
Top of soil layers	[m NAP]	Deterministic
Pile tip level	[m NAP]	Normal

4.4.4 Load parameters

4.4.4.1 Mooring loads

According to the desired succumb scenario for flexible mooring dolphins, first the winch on board of the moored vessel has to render, followed by failure of the mooring lines and the bollard, before the steel pile itself is allowed to yield (Havenbedrijf Rotterdam N.V., 2016). This means that the mooring forces acting on a dolphin are usually limited by the load bearing capacity of the vessel's onboard mooring equipment, hence, the winches and ropes (HTG, 2015). The strength of these ropes and winches is expressed by means of the Minimum Breaking Load (MBL) of the mooring lines. Since it is desired that the brakes of the winch are released before the capacity of the mooring lines is reached, the winches on board of a vessel are designed such that the winch renders when the tension in the mooring lines exceeds 60% of its MBL. Therefore the maximum mooring load acting on a flexible dolphin is equal to (HTG, 2015):

$$F_{m,max} = 0.6 \cdot n \cdot F_{MBL} \tag{4.7}$$

In which n is the number of ropes pulling on the dolphin simultaneously in the same direction and F_{MBL} is the minimum breaking load (MBL) of the ropes of the governing vessel.

It can be argued that the maximum mooring load over the lifetime of a dolphin exceeds the maximum load according to equation 4.7. Due to a combination of overdue maintenance and inadvertence winches get jammed, resulting in increasing mooring tensions in the ropes up to their maximum capacity. In the most extreme situation, two winches get jammed simultaneously and the tension in two mooring lines increase up to the minimum breaking load. In this situation the maximum mooring load acting on a flexible dolphin is equal to (Havenbedrijf Rotterdam N.V., 2016):

$$F_{m,max} = 2 \cdot F_{MBL} + (n-2) \cdot 0.6 \cdot F_{MBL} \tag{4.8}$$

The standardized bollards applied in the Port of Rotterdam are designed such that they can hold three hawsers (Havenbedrijf Rotterdam N.V., 2016). Based on this it is assumed that the extreme mooring load acting on a flexible mooring dolphin can best be described by a weibull distribution with a mean value equal to 2.6·MBL and a coefficient of variation equal to 0.15.

4.4.4.2 Berthing loads

Breasting dolphins are designed based on the berthing energy of the governing vessel, which is a function of the characteristics of the vessel, the berthing structure and the berthing manoeuvre (Trellenborg AB, 2015):

$$E_N = \frac{1}{2} m v^2 \cdot C_M \cdot C_E \cdot C_C \cdot C_S \tag{4.9}$$

In which:

E_N	=	Normal berthing energy [kNm]
m	=	Mass of the vessel (displacement in tonne) [t]
v	=	Approach velocity component perpendicular to the berthing line [m/s]
C_M	=	Added mass coefficient, which is a function of the dimensions of the vessel [-]
C_E	=	Eccentricity coefficient, which is a function of the dimensions of the vessel and the angle of approach [-]
C_C	=	Berth configuration coefficient, which is equal to 1.0 for flexible dolphins [-]
C_S	=	Softness coefficient, which is equal to 1.0 for flexible dolphins [-]

The resulting horizontal force acting on the berthing structure is determined by the stiffness of the system, which can be derived from the interaction between the pile, the fender and the subsoil. The typical stress-strain curves for each individual component and the overall system are shown in Figure 4.12. The area underneath the curve for the overall system corresponds to the berthing energy of a vessel (HTG, 2015):

$$E_N = \int_0^s F_R(s)ds \tag{4.10}$$

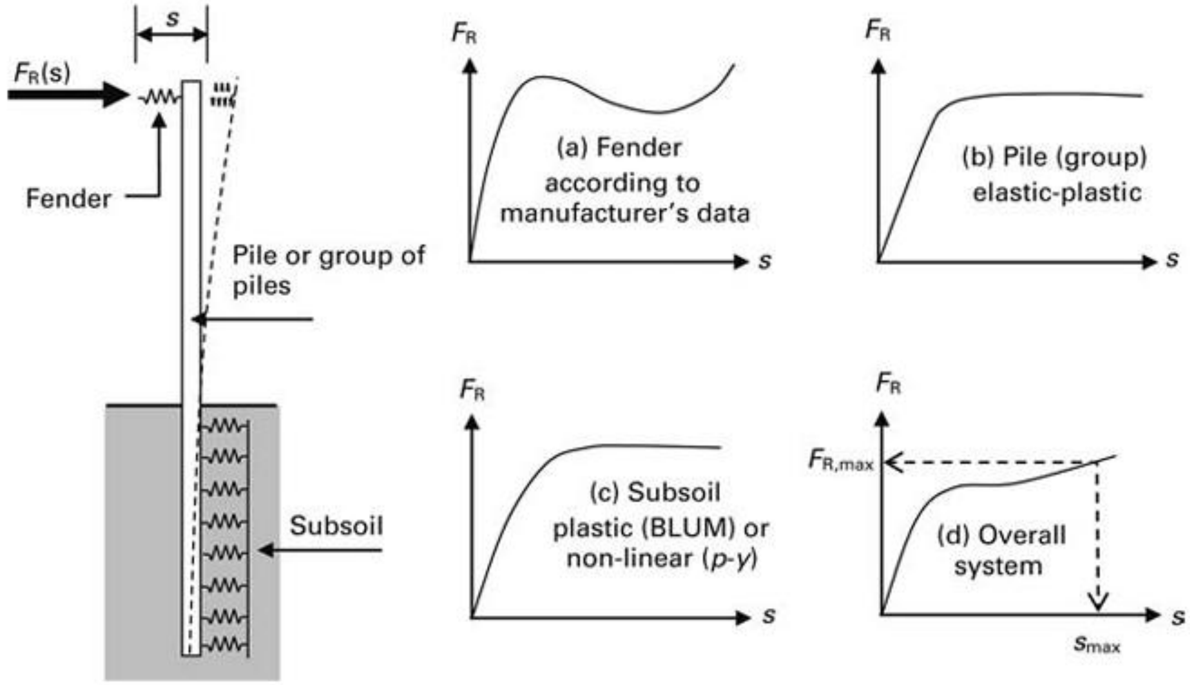

Figure 4.12 - Overview of the structural system of a dolphin with fender and typical stress-strain relations of individual components (a to c) as well as the overall system (d) (HTG, 2015)

The load-deformation behaviour for each type of fender is different, resulting in different reaction forces acting on the dolphin. Therefore, distinction should be made in the probabilistic analysis for flexible berthing dolphins with different types of fenders. The fenders which are most often applied in combination with flexible dolphins are super cone fenders. However, first dolphins without fenders will be considered, which are mainly used by vessels with a low berthing energy.

Dolphins without fenders

In case of flexible dolphins which are not equipped with fenders, the kinetic berthing energy of vessels has to be absorbed completely by deformation of the pile and the subsoil. For both components of this system, the stress-strain behaviour can be approached by an elasto-plastic relation. Under the assumption of a linear load-deformation behaviour, the energy absorbed by the system can be determined with

$$A = \frac{1}{2}Fu \tag{4.11}$$

During the berthing of a vessel, there is a balance between the external energy (the berthing energy of the vessel) and the internal energy (the energy absorbed by the structure). From the energy balance the reaction force acting on the dolphin is derived:

$$F_b = v \cdot \sqrt{m \cdot k_s \cdot C_M \cdot C_E} \tag{4.12}$$

In this equation k_s represents the stiffness of the entire system, which is determined by the stiffness of the pile and the subsoil. The stiffness of the pile is derived from the basic rule for the deformation of a cantilevered beam, for which the level of the clamping can be determined using the method of Blum. For the soil, the stiffness is derived from the theory of Ménard, which is also presented in Appendix A. As the exact contribution of the stiffness of the soil and the pile to the stiffness of the overall system is not exactly known, it is assumed that the contribution of the pile to the overall stiffness is equal to 25%, whereas the contribution of the soil is assumed to be equal to 75%:

$$k_s = 0.25 \cdot k_p + 0.75 \cdot k_h \cdot D \tag{4.13}$$

In which:

$$k_p = \frac{3EI}{l^3} \tag{4.14}$$

$$\frac{1}{k_h} = \frac{1}{3E_m}\left[1.3R_0\left(2.65\frac{D}{2R_0}\right)^{\alpha} + \frac{\alpha D}{2}\right] \tag{4.15}$$

The maximum berthing force acting on a flexible dolphin without fenders can best be described by a weibull distribution. The coefficient of variation for this distribution is determined by performing a Monte Carlo simulation, whereby distinction is made between different vessel classes. As it is often considered that the uncertainty in berthing energy is primarily caused by the uncertainty in berthing velocity, the mass and coefficients are assumed to be deterministic parameters. The distributions for the lifetime maxima of the berthing velocity for different vessel classes are taken from Roubos et al. (2016). Table 4.11 presents an estimation for the different coefficients of variation for different vessel classes, which are based on a pile with a diameter of 914 mm and a wall thickness of 20.6 mm. It should be kept in mind that the coefficients of variation change when the dimensions of the structure change.

Table 4.11 - Coefficients of variation for impact force for dolphins without fenders (*D* = 0.914 m and *t* = 20.6 mm)

Vessel type	Mass [kDWT]	Displacement* x10^3 [t]	C_M* [-]	C_E* [-]	Berthing velocity [m/s]		CoV [-]
					μ	σ	
Tankers							
Panamax	60 – 85	78 – 108	1.7	0.5	0.1283	0.0056	0.062
Suezmax	115 – 165	130 – 205	1.7	0.5	0.1175	0.0054	0.063
VLCC	260 – 319	317 – 388	1.65	0.5	0.1210	0.0058	0.065
Fix. Laser	260 – 319	317 – 388	1.65	0.5	0.0895	0.0043	0.065
Container vessels							
Coasters	7 – 15	10 – 20	1.8	0.6	0.1286	0.0047	0.057
Feeders	15 – 42	20 – 56.8	1.8	0.55	0.1256	0.0068	0.070
Panamax	42 – 70	56.8 – 100	1.8	0.5	0.1115	0.0074	0.080
Post Panamax	70 – 118	100 – 155	1.75	0.5	0.1056	0.0074	0.083
*) The values for the displacement and the coefficients are estimated based on the Fender Application Design Manual of Trellenborg (Trellenborg AB, 2015)							

Dolphins with super cone fenders

Super cone fenders have a highly efficient geometry and a very stable shape (Trellenborg AB, 2015). Therefore, these fenders are most commonly applied in combination with flexible dolphins. Figure 4.13 shows that cone fenders have a strong non-linear behaviour. The impact force which is acting on the dolphin as a result of berthing vessels is reached twice, at a deflection of 35% and 72%. This non-linear relation between deflection and reaction force or energy and reaction force makes it very hard to express the berthing force by means of an analytical solution. As this derivation of the reaction force does not lie within the scope of this master thesis, breasting dolphins in combination with fenders will not be considered any further.

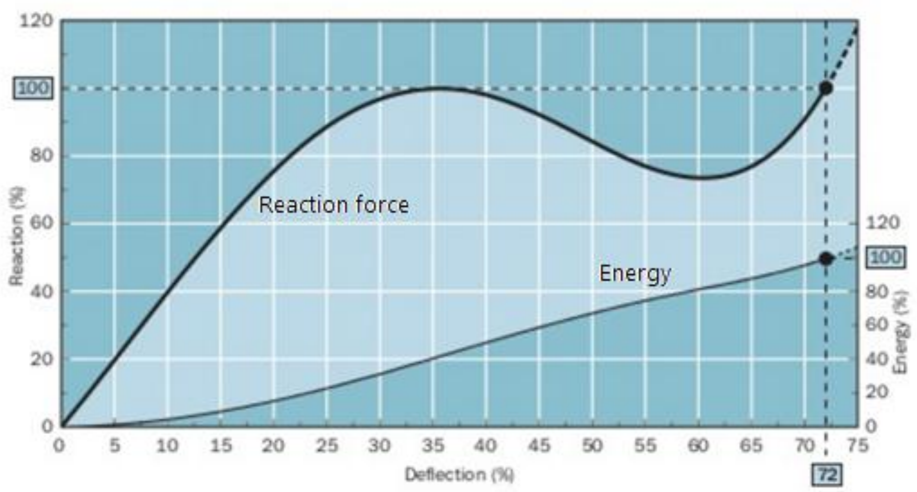

Figure 4.13 - Generic relation between energy, deflection and reaction force for super cone fenders (Trellenborg AB, 2015)

4.5 Limit state functions

4.5.1 Failure mechanisms

With a fault tree, insight is provided in the failure behaviour of structures. It gives a logical succession of all events that lead to one undesired "top event" at the top of the tree (CUR-publicatie 190, 2002). Furthermore, it shows how the different failure mechanisms are related to each other.

The fault tree for flexible dolphins is given by Figure 4.14, which describes failure of the structure as a serial system. The fault tree shows that a dolphin loses its functionality when the deformations of the structure become too large or when the structure itself fails as a result of failure of the tubular pile, lack of equilibrium or failure of the superstructure. The failure mechanisms which are considered most relevant to failure of flexible dolphins are:

- Structural failure (failure of the pile profile)
- Excessive deformations
- Soil mechanical failure (inadequate development of passive resistance)

Therefore, probabilistic evaluations of flexible dolphins will be performed with respect to these three failure mechanisms, for which the limit state functions will be determined sections 4.5.2 to 4.5.4.

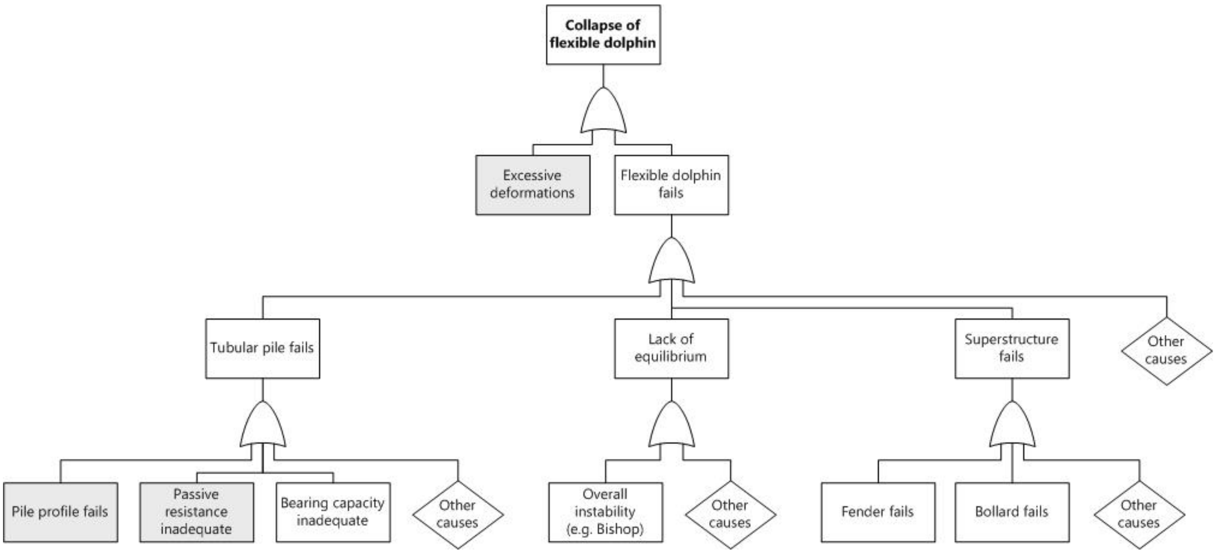

Figure 4.14 - Fault tree for flexible dolphins

4.5.2 Structural failure

In general, the cross-section of flexible dolphins can be classified as semi-compact (class 3) or slender (class 4). For these cross-sections the development of the plastic moment is prevented by local buckling. Furthermore, for slender cross-sections local buckling already occurs before the yield strength of the steel is reached.

According to EN 1993-1-1 an elastic check has to be performed to evaluate the cross-sectional resistance of semi-compact or slender flexible dolphins. For this evaluation the yield criterion given by equation 4.16 can be used. To account for the reduced resistance capacity of slender structures, the characteristics of the effective cross-section have to be used for the evaluation of class 4 cross-sections (NEN-EN 1993-1-1+C2, 2011).

$$\left(\frac{\sigma_{x,Ed}}{\sigma_{x,Rd}}\right)^2 + 3\left(\frac{\tau_{x\theta,Ed}}{\tau_{x\theta,Rd}}\right)^2 \leq 1 \tag{4.16}$$

Because class 4 cross-sections buckle before the elastic resistance capacity is reached, these cross-sections also have to be evaluated on local meridional and/or shear buckling. The criterion for this evaluation in case both types of buckling have to be considered is comparable to the one for the elastic evaluation (NEN-EN 1993-1-6, 2007):

$$\left(\frac{\sigma_{x,Ed}}{\sigma_{x,Rd}}\right)^{k_x} + 3\left(\frac{\tau_{x\theta,Ed}}{\tau_{x\theta,Rd}}\right)^{k_\tau} \leq 1 \tag{4.17}$$

In case only one of the buckling types has to be considered, this criterion can be reduced to equation 4.18 or equation 4.19 for meridional buckling or shear buckling respectively.

$$\sigma_{x,Ed} \leq \sigma_{x,Rd} \tag{4.18}$$

$$\tau_{x\theta,Ed} \leq \tau_{x\theta,Rd} \tag{4.19}$$

For a further elaboration on the evaluation on buckling according to Eurocode, reference is made to Appendix E.

The performed full scale tests reveal that the cross-sectional verification rules according to NEN-EN 1993-1-6 are over-conservative. For all eight tested piles the capacity of the pile exceeds the buckling capacity according to NEN-EN 1993-1-6. This can be explained by the fact that the Eurocode does not consider the effect of the confined soil inside the piles, while earlier performed tests show that this effect is significant (as can also be concluded from Figure 4.15 and Figure 4.16, which show the results of the earlier performed tests). Due to the soil inside the piles, the piles do not easily change their circular shape what makes them less susceptible to buckling. Therefore CUR 211 recommends using the modified Gresnigt method for the evaluation of steel tubular piles. This buckling evaluation method is based on criteria of critical strain rather than on a buckling stress (CUR-publicatie 211E, 2014). The modified Gresnigt method is further elaborated in Appendix E.

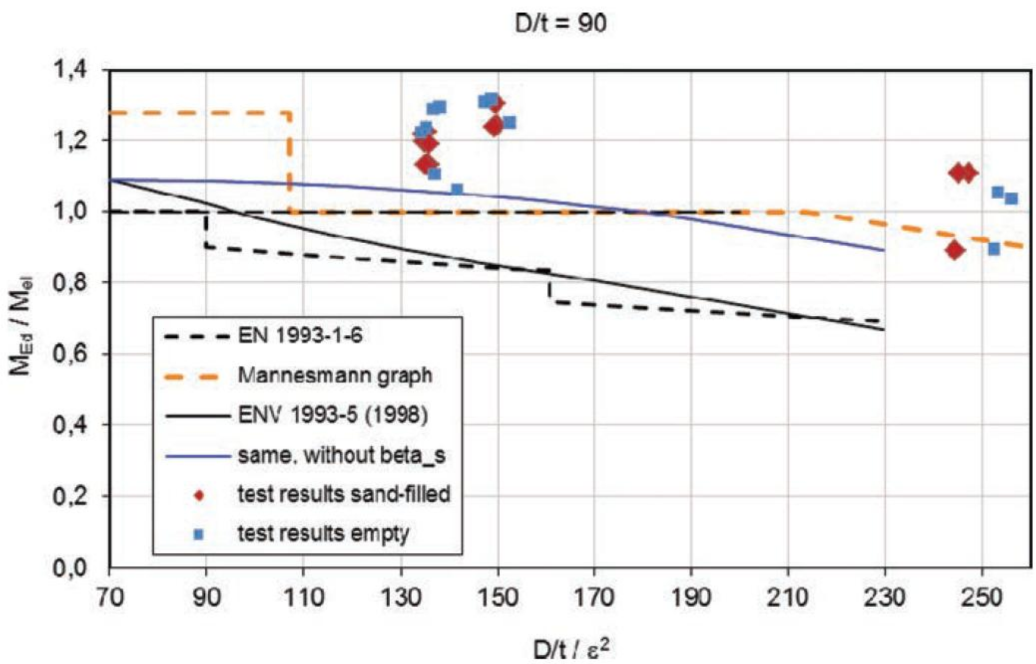

Figure 4.15 - Results of design methods of class 3 and class 4 piles for *D/t* = 90, with plotted test results (*D/t* range of tests: 70 to 120) (CUR-publicatie 211E, 2014)

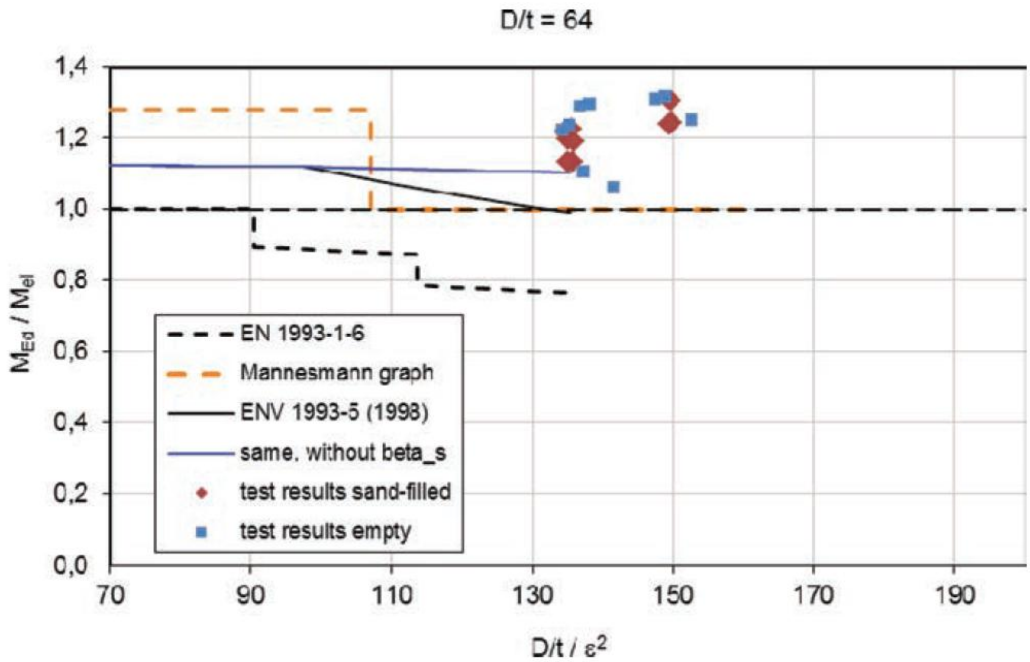

Figure 4.16 - Results of design methods of class 3 and class 4 tubular piles for *D/t* = 64, with plotted test results (*D/t* range of tests: 70 to 120) (CUR-publicatie 211E, 2014)

From the performed tests it is also found that the capacity of the piles also exceed the elastic capacity according to NEN-EN 1993-1-1. This can be explained by the fact that NEN-EN 1993-1-1 considers a class 3 or class 4 pile to fail at yield of the outer fibre of the cross-section. However, in most cases there is enough residual capacity left to withstand higher loads.

The results of the performed full scale tests show that the structural capacity of laterally loaded piles can be best be approach by the modified Gresnigt method. However, many different considerations have to be made during the evaluation of the cross-sectional resistance according to this method, what makes it difficult to express this method by means of a limit state function. Therefore, the considered limit state function regarding structural failure is based on the elastic check. To be able to apply this limit state function, it may be necessary the modify the cross-section of the evaluated structure such that the unity check with respect to cross-sectional verification is close to 1.00.

The cross-section at the level of the maximum bending moment turns out to be the governing cross-section for the elastic cross-sectional verification. Based on equation 4.2 it can be stated that at this level the shear forces in the pile are equal to zero. Practice reveals that the influence of shear forces can indeed be neglected when the bending moments are at a local maximum. Rewriting equation 4.16 therefore results in the following limit state function for the evaluation on structural failure:

$$Z = W_{el} \cdot f_y - M_{max} \tag{4.20}$$

Note that this limit state function is similar to the one obtained from the evaluation on buckling in case only meridional buckling has to be considered.

4.5.3 Excessive deformations

Two of the main functions of flexible breasting dolphins are to provide safe mooring conditions for vessels or to prevent damage to underlying structures as quays or jetties. Therefore, the allowed deflection of flexible dolphins is limited. In case the dolphin has to protect a structure, the maximum allowed deflection of the top of the pile is limited by the distance between the flexible dolphin and the underlying structure. Moreover, according to EAU 2012, BS 6349 and PIANC 2002 the deflection of the top of the pile may not exceed 1500 mm in order to prevent damage to a berthing vessel. Based on these codes and guidelines, the limit state function regarding excessive deformations is expressed as:

$$Z = 1500\ [mm] - \delta_{max} \tag{4.21}$$

4.5.4 Soil mechanical failure

As a result of a lateral loading, a passive failure wedge develops at the rear side of a structure. This wedge is pushed upwards, because the active pressure is larger than the passive resistance that is provided by the weight of the wedge and the friction along its sliding plane. As the load increases, the height of the passive wedge increases and more passive resistance is mobilized. At some point, the resistance is fully mobilized and a further increase of the load will result in soil mechanical failure.

In D-Sheet Piling the mobilized passive resistance is defined as the actual total passive soil reaction divided by the capacity of the total passive soil reaction at full yield (Deltares, 2014). Therefore, the limit state function regarding soil mechanical failure is defined as:

$$Z = 100\ [\%] - mobilized\ passive\ resistance \tag{4.22}$$

However, probabilistic evaluation of this limit state function will introduce complications. As the soil will collapse before a satisfying result is obtained, Prob2B will have difficulties in evaluating this limit state function. Two options to avoid this problem are:

1. Modifying the limit state function by reducing the critical value for the mobilized passive resistance;
2. Defining a limit state function using the D-Sheet Piling definition of a soil body collapse during calculations (ValidCalc).

Reduction of the critical mobilized passive resistance

To be able to perform the probabilistic evaluation regarding soil mechanical failure with the FORM-method, the allowed value for the mobilized passive resistance should be decreased such that the structure will not fail before a satisfying convergence is reached. To correct for this reduction of the critical value of mobilized resistance, the pile should be elongated. The required increase of the embedded pile length can be determined from the relation between the pile length and the mobilized passive resistance, as is illustrated by Figure 4.17.

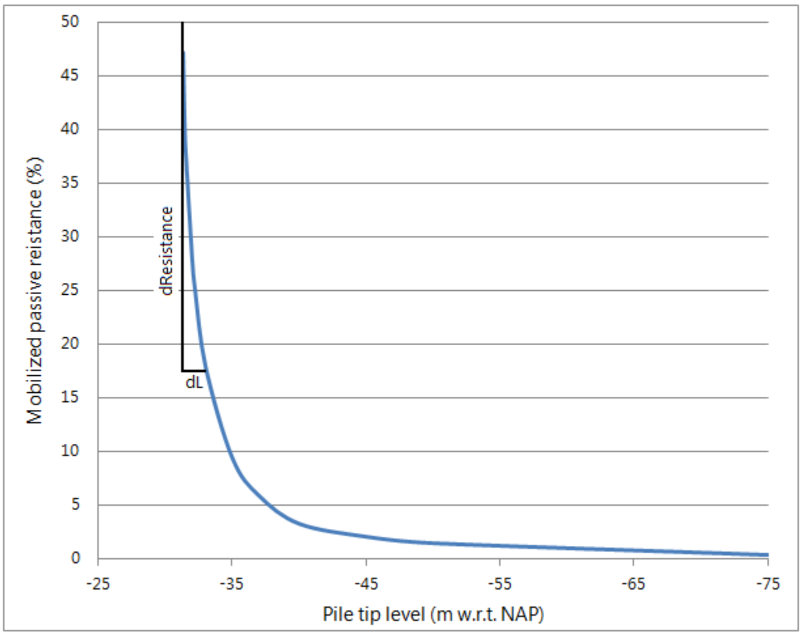

Figure 4.17 - Mobilized passive resistance vs. pile tip level

ValidCalc

With the ValidCalc option, Prob2B gives Z = 1 for a correct calculation and Z = -1 for a calculation that fails (Wolters, 2012). The main disadvantage of this option is that the Z-function is discontinuous. This makes that the influence factors cannot be determined, because it is not possible to determine the derivative of the limit state. This implies that a Monte Carlo based simulation should be used when using the ValidCalc option. However, with this type of probabilistic evaluation only the reliability of the structure can be determined, the influence factors of the parameters will still remain unknown. Based on the reliability, Prob2B can give an estimation of these influence factors, but these may not be accurate enough to determine partial safety factors with.

4.6 Target reliability

The Eurocode prescribes target reliability indices for the design of several types of structures in accordance with the different safety classes. These target reliabilities are related to the allowable probability of failure of the overall structure and should be reached when following the design procedures given in de codes. The recommended reliability indices for flexible dolphins, for which the intended lifetime is 50 years, are given in Table 4.12.

Table 4.12 - Minimum values for the reliability index for flexible dolphin design (NEN-EN 1990+A1+A1/C2, 2011)

Reliability class (RC)	**Minimum value for β**	
	1 year reference period	**50 year reference period**
RC3	5.2	4.3
RC2	4.7	3.8
RC1	4.2	3.3

Each of the considered failure mechanisms contributes differently to the reliability of the overall structure. The required reliability with respect to each of these considered mechanisms can be derived based on the fault tree for flexible dolphins which is shown in Figure 4.14. It shows that the failure of the structure can be described by a serial system, for which the overall probability of failure is bounded:

Lower bound (fully dependent failure mechanisms): $P_f = \max(P_{f,i})$

Upper bound (mutually exclusive failure mechanisms): $P_f = \sum P_{f,i}$

The different failure mechanisms for flexible dolphins can be considered as dependent. However, to derive the correlations between the different mechanisms, a full probabilistic analysis is required, which lies not within the scope of this master thesis. Furthermore, the contribution of each of the failure mechanisms to the overall failure probability is not known. Therefore, it is stated that the probability of occurrence of each of the mechanisms has to comply with the recommended maximum probability of failure according to the Eurocode. The required reliability index with respect to each of the failure mechanisms is assumed to be equal to the reliability index for the overall structure as is given in Table 4.12.

5

BENCHMARK: CALAND CANAL

5.1 Introduction

In this chapter, the probabilistic analysis and results are described for a flexible mooring dolphin from practice, a mooring dolphin which is recently constructed in a bank of the Caland canal. First the characteristics of this structure are established, as well as the parameter values. Furthermore, the significance of the variables is discussed as it appears that not all variables are relevant for the reliability of the structure. In section 5.5 the results of the probabilistic evaluation for the different limit states are presented. It turned out that the embedded length of the initial pile design may be over conservative. Therefore, the probabilistic evaluations are also performed for a shortened pile. The results of these calculations are discussed in section 5.6.

5.2 Characteristics of the structure

The design of the considered mooring dolphin of the Caland canal is detailed in the design report of Volker Staal en Funderingen (2015). Therefore, the characteristics of the considered dolphins are based on this report. The considered mooring dolphin is designed based on reliability class II in accordance with NEN 9997. The desired reliability of this structure therefore equals 3.8.

The soil structure near the considered mooring dolphin is composed out of four different layers of soil. The characteristic values of the soil parameters of these layers are given in Table 5.1. The values for the stiffness parameters are directly derived from CPT's performed near the location of the mooring dolphin. The obtained values are therefore the average parameter values, which are shown in Table 5.2.

Table 5.1 - Characteristic soil parameter values

Layer	Description	Top of layer	γ_{unsat}	γ_{sat}	c′	φ′
[-]	[-]	[m NAP]	[kN/m^3]	[kN/m^3]	[kPa]	[deg]
1	Sandy clay	-18.16	18	18	5	22.5
2	Moderately packed sand	-28.00	18	20	0	32.5
3	Gravel	-31.00	19	21	0	37.5
4	Moderately packed sand	-40.00	18	20	0	32.5

Table 5.2 - Average soil parameter values

Layer	Description	Top of layer	q_c	β	E_m
[-]	[-]	[m NAP]	[MPa]	[-]	[kN/m^2]
1	Sandy clay	-18.16	2	2	4000
2	Moderately packed sand	-28.00	8	0.7	5600
3	Gravel	-31.00	40	0.5	20000
4	Moderately packed sand	-40.00	14	0.7	9800

The steel pile has an outer diameter of 2500 mm and is composed out of multiple sections with different wall thicknesses and steel grades. Within this master thesis the influence of different pile sections on the overall reliability of the structure is neglected. Therefore, mooring dolphin will be modelled as a pile with an uniform cross-section equal to the cross-section at the level of the maximum moment. This governing cross-section has an average wall thickness equal to 41 mm and is composed out of steel with steel grade X70. The length of the pile is equal to 43.0 m.

Taking into account the maintenance margin and the dredging tolerances, the design depth for the considered mooring dolphin is equal to NAP -17.66 m. The representative mooring load is equal to 2000 kN and engages at a level of NAP +6.5 m. In order to obtain the desired reliability, the tip of the pile is at a level of NAP -37.0 m.

The elastic cross-sectional verification of this flexible dolphin according to NEN-EN 1993-1-1 results in an unity check equal to 0.99 (Volker Staal en Funderingen, 2015). Therefore, the initial dolphin design can be used for the limit state evaluation on structural failure, redesign of the cross-section of the considered mooring dolphin is not required.

5.3 Probabilistic input parameters

In probabilistic calculations, mean parameter values are used. Therefore, the characteristic values need to be translated to mean values. For the normally distributed soil parameters this can be done with

$$\mu_i = \frac{X_{char,i}}{1 - 1.64 \cdot V_i} \tag{5.1}$$

The characteristic value for soil parameters is defined as the parameter value which has a probability of non-exceedance equal to 5% (NEN 9997-1+C1, 2012). This definition is used to determine the mean parameter values for the lognormally distributed variables in an iterative way.

An overview of the characteristic and mean values for the soil parameters is given in Table 5.3. Note that only one set of parameters is included for moderately packed sand. This parameter set applies to the first sand layer. Because the pile tip of the considered mooring dolphin does not reach the top of the lower moderately packed sand layer, this soil layer will not be relevant for the reliability of the structure.

Table 5.3 - Characteristic and mean values for soil parameters

Parameter	**Unit**	$X_{char,i}$	V_i	μ_i
$c_{sandy\ clay}$	[kPa]	5.0	0.20	7.1
$E_{m,\ sandy\ clay}$	[kN/m^2]	3344	0.10	4000
$E_{m,\ moderately\ packed\ sand}$	[kN/m^2]	4682	0.10	5600
$E_{m,\ gravel}$	[kN/m^2]	16720	0.10	20000
$\gamma_{sat,\ sandy\ clay}$	[kN/m^3]	18	0.05	19.61
$\gamma_{sat,\ moderately\ packed\ sand}$	[kN/m^3]	20	0.05	21.79
$\gamma_{sat,\ gravel}$	[kN/m^3]	21	0.05	22.88
$\varphi_{sandy\ clay}$	[deg]	22.5	0.10	26.91
$\varphi_{moderately\ packed\ sand}$	[deg]	32.5	0.10	38.88
φ_{gravel}	[deg]	37.5	0.10	44.86

The coefficients of correlation for the soil parameters are given in Table 4.6 in section 4.4.1.4.

The characteristic value of the yield strength of steel is defined as the parameter value with a probability of non-exceedance equal to 2.5%. For this normally distributed parameter the mean value can be determined with

$$\mu_i = \frac{X_{char,i}}{1 - 1.96 \cdot V_i} \tag{5.2}$$

For the other normally distributed structural parameters eq. 5.1 applies, as their characteristic value is defined as the 5% lower bound.

Table 5.4 gives an overview of the characteristic and mean values for the structural parameters. During the design of flexible dolphins it is not usual to express the pile diameter and the wall thickness by means of characteristic values. Possible factors will directly be applied on the mean parameter values. Therefore Table 5.4 only contains the mean values for these parameters.

Table 5.4 - Characteristic and mean values for structural parameters

Parameter	**Unit**	$X_{char,i}$	V_i	μ_i
D	[m]	-	0.002	2.5
t	[mm]	-	0.03	41
E	[kN/m^2]	$200 \cdot 10^6$	0.03	$210 \cdot 10^6$
f_y	[N/mm^2]	483	0.07	559.81
EI	[kNm^2]	$4.699 \cdot 10^7$	0.04	$5.029 \cdot 10^7$
W_{el}	[m^3]	0.18215	0.03	0.19157

The correlations between the structural parameters are presented in Table 5.5. The yield strength of the steel is not included in the table, because this variable is not correlated to any of the other structural parameters.

Table 5.5 - Correlations between structural parameters

	D	t	E	EI	W_{el}
D	1.00	-	-	0.17	0.17
t	-	1.00	-	0.66	0.98
E	-	-	1.00	0.73	-
EI	0.17	0.66	0.73	1.00	0.68
W_{el}	0.17	0.98	-	0.68	1.00

The considered mooring dolphin is located in the sloping bank of the Caland canal. However, within the used model it is not possible to introduce sloping bottom surfaces. To account for the influence of the slope on the behaviour of the structure, an additional margin equal to 0.5 m is applied on top of the design depth. The level of the bottom surface used in the model therefore becomes equal to NAP -18.16 m. During the probabilistic calculations, this modelled depth is regarded as the mean value. Furthermore, possible safety factors or safety margins will directly be applied on this depth.

For geometrical parameters it is more convenient to use absolute changes instead of relative changes. Therefore, the variation of these parameters is expressed by means of standard deviations. The standard deviations used during the probabilistic evaluations are based on assumptions and are given in Table 5.6.

Table 5.6 - Geometrical input parameters

Parameter	**Unit**	**μ**	**σ**
Bottom surface	[m NAP]	-18.16	0.25
Pile tip level	[m NAP]	-37	0.25

The representative load for the considered mooring dolphin, which is usually defined as the load which occurs once in the lifetime of the structure, is equal to 2000 kN. However, there is still some uncertainty about this load, because the development of the moored vessels cannot exactly be predicted. Moreover, practice shows that often more hawsers are held by a mooring dolphin than it is designed for. Furthermore, calculations show that the reliability of the considered mooring dolphin is significantly overestimated in case the representative load is considered to be the characteristic value of the distribution. Therefore, the representative load is considered to be equal to the mean value for the distribution of the maximum mooring loads.

It is often stated that a weibull distribution gives the best approximation of the tail of a maximum value distribution. Therefore, the maximum mooring load is described by a weibull distribution with a shape factor equal to 2.0, as it is assumed that this gives the best approximation to this matter. With a mean value equal to 2000 kN and a coefficient of variation of 0.15, the other parameters for the distribution are determined iteratively, resulting in a value for the scale parameter equal to 2073.7 kN and a value for the location parameter equal to 1426 kN. The characteristic value for the maximum mooring load is assumed to be the value which has a probability of exceedance equal to 5%, resulting in a characteristic parameter value equal to 2547 kN. The probability density function for the mooring load is plotted in Figure 5.1.

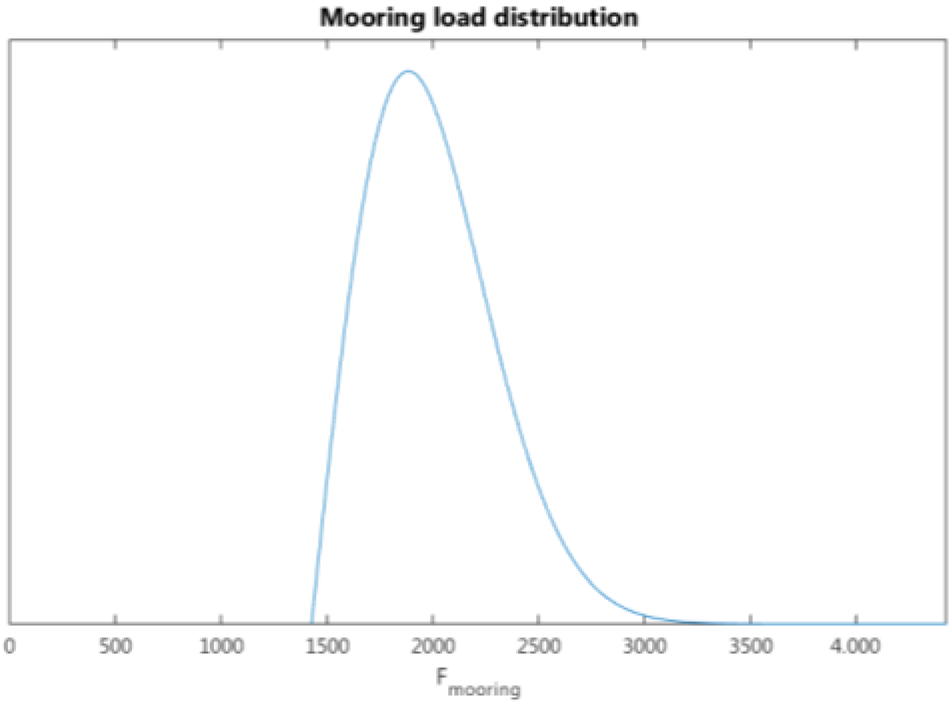

Figure 5.1 - Mooring load distribution

5.4 Significance of the variables

Some parameters have a relatively small influence on the reliability of flexible dolphins. Because it is not relevant to apply partial safety factors on these parameters, they will be eliminated from the probabilistic evaluations. The criterion for a parameter to be eliminated is when they have an influence on the reliability of less than 1% ($\alpha^2 \cdot 100$).

Some of the parameters which are included in flexible dolphin design are correlated to each other. Prob2B takes these correlations into account in the determination of the design values. However, these correlations are not taken into account in the determination of the influence factors. To be able to eliminate parameters from the probabilistic evaluations, therefore first a translation has to take place to influence factors in which the correlations between parameters are taken into account. This is done by first translating the design values (X_i^*) to their standard normal equivalent design values (u_i^*). From these equivalent design values the reliability of the structure based on the correlated parameters is determined ($\beta_{correlated}$), which is used to derive the influence factors in which the correlations are taken into account:

$$\beta_{correlated} = \sqrt{\sum u_i^*} \tag{5.3}$$

$$\alpha_{correlated} = -\frac{u_i^*}{\beta_{correlated}} \tag{5.4}$$

5.5 Limit state evaluations

5.5.1 Structural failure

The limit state function for structural failure is: $Z = W_{el} \cdot f_y - M_{max}$

The first probabilistic calculation contains seventeen stochastic variables. The results of this first calculation are included in Appendix F. They show that most of the variables do not significantly contribute to the reliability of the structure with respect to structural failure. Looking at the soil structure, only the soil above the level of the maximum moment counteracts the development of the bending moment in the pile. However, the influence of this soil on the reliability with respect to structural failure is negligible.

After elimination of the irrelevant variables, the remaining variables for the final calculation are:

- Mooring load: $F_{mooring}$
- Yield strength of steel: f_y
- Wall thickness of the dolphin: t

The results of the final FORM-calculation are shown in Table 5.7. Figure 5.2 presents the influence of the different relevant variables on the reliability as a percentage.

Table 5.7 - Results of the final calculation (LS: structural failure)

Number of calculations: 89					
$\beta_{correlated}$: 4.067					
P_f: $2.383 \cdot 10^{-5}$					
Parameter (X_i)		**Unit**	**V (=σ/μ)**	**$\alpha_{correlated}$**	**X_i* (Design value)**
$F_{mooring}$		[kN]	0.15	-0.84	3257
f_y		[N/mm^2]	0.07	0.51	479.1
t		[mm]	0.03	0.18	39.94
Calculation	Z-value				
1	52300				
89	1.14				

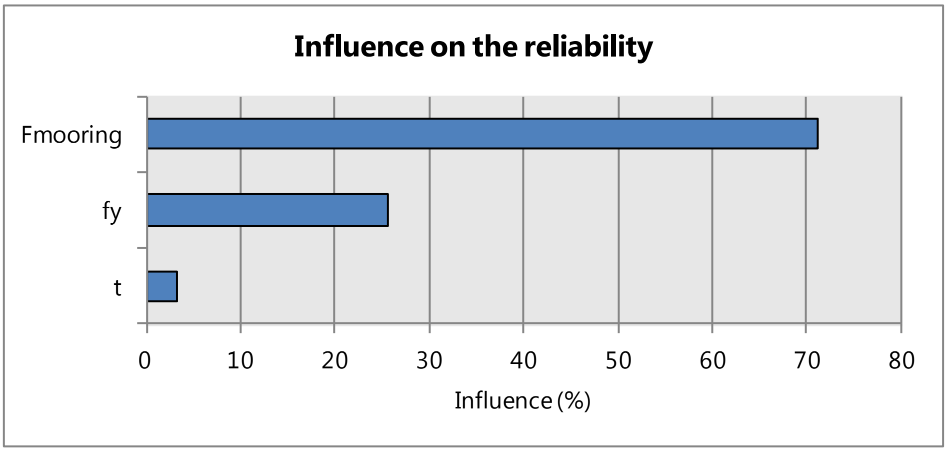

Figure 5.2 - Influence of the relevant parameters on the reliability (LS: structural failure)

From the results of the FORM-calculation, the partial safety factors with respect to the characteristic parameter values can be determined with:

$$\gamma_{R,i} = \frac{X_{char,i}}{X_i^*} \quad \text{for resistance parameters} \tag{5.5}$$

$$\gamma_{S,i} = \frac{X_i^*}{X_{char,i}} \quad \text{for load parameters} \tag{5.6}$$

Besides the partial factors which correspond to the calculated reliability, also the partial safety factors corresponding to reliability class 2 are determined (β_{RC2} = 3.8). To be able to determine the partial factors for a target reliability according to RC2, it is assumed that the influence factors for the relevant parameters do not significantly change (which is a reasonable assumption when $\beta_{calculation} \approx \beta_{RC2}$). The design values corresponding to the target reliability are determined by using:

$$X_{d,i} = \mu_{X_i} - \alpha_i \beta_{RC2} \sigma_{X_i} \quad \text{for normally distributed parameters} \tag{5.7}$$

$$X_{d,i} = a + (b-a)\cdot\Phi(-\alpha_i\beta_{RC2}) \quad \text{for uniformly distributed parameters} \tag{5.8}$$

For the mooring load which has a weibull distribution, the design value corresponding to RC2 is determined iteratively using $F(X_{d,i}) = \Phi(-\alpha_i\beta_{RC2})$.

Table 5.8 presents the partial safety factors, which are determined for both the reliability obtained from the calculation and the target reliability according to RC2.

Table 5.8 - Partial safety factors with respect to structural failure

$\beta_{calculation}$: 4.067						
β_{RC2}: 3.800						
Parameter (X_i)	**Unit**	**$X_{char,i}$**	**X_i***	**$\gamma_{calc,i}$**	**$X_{d,i}$**	**$\gamma_{RC2,i}$**
$F_{mooring}$	[kN]	2547	3257	1.28	3170	1.24
f_y	[N/mm^2]	483	479.1	1.01	484.4	1.00
t	[mm]	41 (μ)	39.94	1.03	40.00	1.03

5.5.2 Excessive deformations

The limit state function for excessive deformations is: $Z = 1500\ [mm] - \delta_{max}$

The first probabilistic calculation contains sixteen stochastic variables. The results of this first calculation are included in Appendix F. They show that many variables are not relevant for the reliability of the structure with respect to excessive deformations. Looking at the resistance parameters it can be concluded that the top soil layer contributes most to the reliability, which can be explained by the non-linear behaviour of the soil.

The variables that contribute significantly to the reliability of the structure with respect to excessive deformations and therefore have to be included in the final calculations as stochastic variables are:

- Pressiometric modulus of sandy clay: $E_{m,\ sandy\ clay}$
- Saturated unit weight of sandy clay: $\gamma_{sat,\ sandy\ clay}$
- Angle of internal friction of sandy clay: $\varphi_{sandy\ clay}$
- Mooring load: $F_{mooring}$
- Pile tip level
- Level of the bottom surface

The results of the final FORM-calculation are given in Table 5.9. Figure 5.3 shows the influence of the stochastic variables on the reliability as a percentage.

Table 5.9 - Results of the final calculation (LS: excessive deformations)

Number of calculations: 141				
$\beta_{correlated}$: 3.402				
P_f: $3.344 \cdot 10^{-4}$				
Parameter (X_i)	**Unit**	**V (=σ/μ)**	**$\alpha_{correlated}$**	**X_i* (Design value)**
$E_{m,\ sandy\ clay}$	[kN/m^2]	0.10	0.15	3783
$\gamma_{sat,\ sandy\ clay}$	[kN/m^3]	0.05	0.29	18.65
$\varphi_{sandy\ clay}$	[deg]	0.10	0.39	23.33
$F_{mooring}$	[kN]	0.15	-0.84	3034
Pile tip level	[m] NAP	0.25 (σ)	-0.12	-36.90
Bottom surface	[m] NAP	0.25 (σ)	0.13	-18.27

Calculation	Z-value	
1	764	
141	1.25	

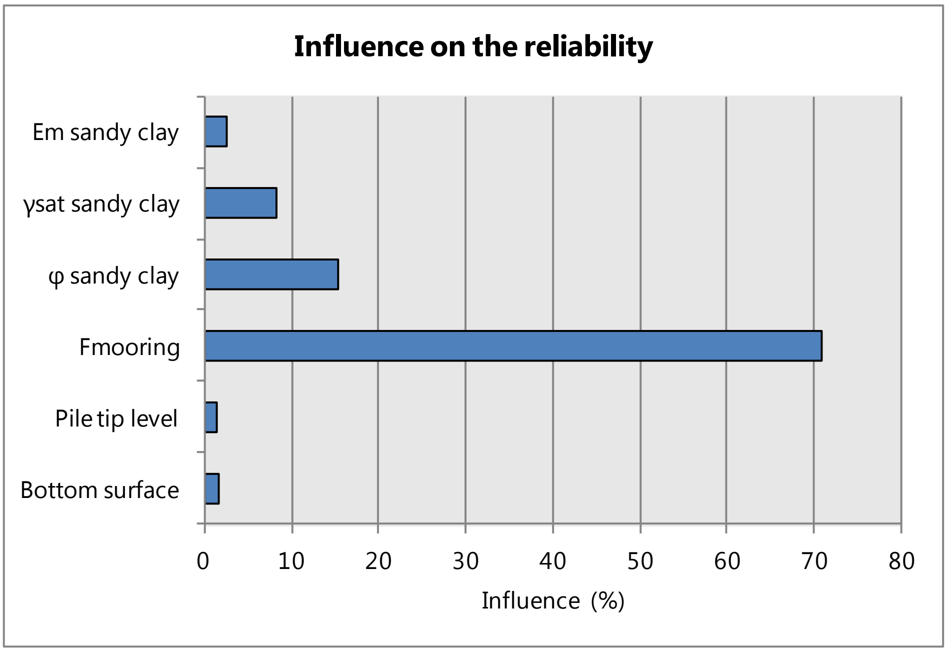

Figure 5.3 - Influence of the relevant parameters on the reliability (LS: excessive deformations)

From the final results partial safety factors can be determined with the equations given in section 5.5.1. The obtained partial factors with respect to the characteristic parameter values are given in Table 5.10. This table also includes the design values and partial factors for geometrical parameters. However, for these parameters it may be more relevant to express the required additional safety by means of an absolute additional margin in metres. For the level of the bottom surface this means that an additional margin equal to 0.12 m should be included for RC2, whereas the embedded pile length should be reduced by 0.11 m.

Table 5.10 - Partial safety factors with respect to excessive deformations

$\beta_{calculation}$: 3.402						
β_{RC2}: 3.800						
Parameter (X_i)	**Unit**	**$X_{char,i}$**	**X_i***	**$\gamma_{calc,i}$**	**$X_{d,i}$**	**$\gamma_{RC2,i}$**
$E_{m,\ sandy\ clay}$	[kN/m^2]	3344	3783	0.88	3758	0.89
$\gamma_{sat,\ sandy\ clay}$	[kN/m^3]	18	18.65	0.97	18.54	0.97
$\varphi_{sandy\ clay}$	[deg]	22.5	23.33	0.96	22.91	0.98
$F_{mooring}$	[kN]	2547	3034	1.19	3165	1.24
Pile tip level	[m] NAP	-37 (μ)	-36.90	1.00	-36.89	1.00
Bottom surface	[m] NAP	-18.16 (μ)	-18.27	0.99	-18.28	0.99

5.5.3 Soil mechanical failure

The limit state function for soil mechanical failure is: $Z = 100\ [\%] - Mobilized\ passive\ resistance\ [\%]$

However, this limit state function cannot be evaluated with Prob2B as the soil will collapse before a satisfying convergence is reached. In that case the model will not produce any useable output and the limit state evaluation cannot be performed. Therefore the limit state function is modified in a way such that Prob2B is able to produce results. To be able to perform a limit state evaluation with respect to soil mechanical failure, the critical percentage of mobilized passive resistance is reduced to 40%. To correct for this reduction, the embedded length of the pile is increased by 0.13 m.

The first probabilistic calculation contains sixteen stochastic variables. The results of this first calculation are presented in Appendix F. They show that the angle of internal friction of the soil at the level of the pile tip has a large influence on the reliability of the structure with respect to soil mechanical failure. Furthermore, the influence of the unit soil weight is significant and unchanged over the depth (after correction for the layer thickness). This can be explained by the fact that the resistance against soil mechanical failure is mainly derived from the weight of the overlying soil and the angle of internal friction.

After elimination of the irrelevant variables, the remaining stochastic variables for the final calculation are:

- Pressiometric modulus of sandy clay: $E_{m,\ sandy\ clay}$
- Saturated unit weight of sandy clay: $\gamma_{sat,\ sandy\ clay}$
- Angle of internal friction of sandy clay: $\varphi_{sandy\ clay}$
- Pressiometric modulus of gravel: $E_{m,\ gravel}$
- Saturated unit weight of gravel: $\gamma_{sat,\ gravel}$
- Angle of internal friction of gravel: φ_{gravel}
- Saturated unit weight of moderately packed sand: $\gamma_{sat,\ moderately\ packed\ sand}$
- Angle of internal friction of moderately packed sand: $\varphi_{moderately\ packed\ sand}$
- Mooring load: $F_{mooring}$
- Pile tip level
- Level of the bottom surface

The results of the final FORM-calculation are shown in Table 5.11 and Figure 5.4 shows the influence of the relevant stochastic variables on the reliability.

Table 5.11 - Results of the final calculation (LS: soil mechanical failure)

Number of calculations: 229				
$\beta_{correlated}$: 5.310				
P_f: $5.473 \cdot 10^{-8}$				
Parameter (X_i)	**Unit**	**V (=σ/μ)**	**$\alpha_{correlated}$**	**X_i* (Design value)**
$E_{m,\ sandy\ clay}$	[kN/m^2]	0.10	0.15	3675
$\gamma_{sat,\ sandy\ clay}$	[kN/m^3]	0.05	0.33	17.91
$\varphi_{sandy\ clay}$	[deg]	0.10	0.34	22.00
$E_{m,\ gravel}$	[kN/m^2]	0.10	0.13	18600
$\gamma_{sat,\ gravel}$	[kN/m^3]	0.05	0.31	21.03
φ_{gravel}	[deg]	0.10	0.57	31.24
$\gamma_{sat,\ moderately\ packed\ sand}$	[kN/m^3]	0.05	0.12	21.07
$\varphi_{moderately\ packed\ sand}$	[deg]	0.10	0.19	35.01
$F_{mooring}$	[kN]	0.15	-0.49	2920
Pile tip level	[m] NAP	0.25 (σ)	-0.13	-36.96
Bottom surface	[m] NAP	0.25 (σ)	0.11	-18.30

Calculation	Z-value	
1	34.4	
229	0.01	

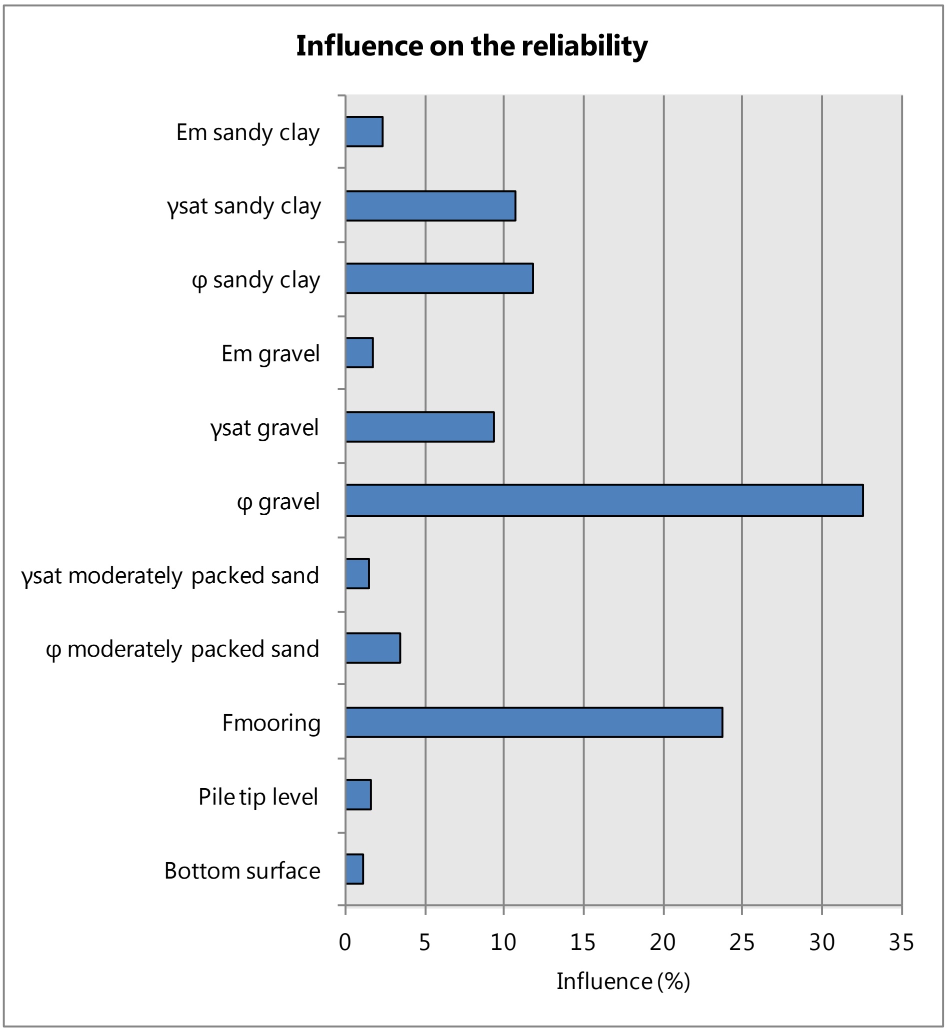

Figure 5.4 - Influence of the relevant parameters on the reliability (LS: soil mechanical failure)

From the results of the final calculation the partial safety factors can be determined with the equations given in section 5.5.1. The obtained partial factors which have to be applied on the characteristic parameter values are given in Table 5.12. Looking at the required absolute additional margins for the geometrical parameters, it is found that this margin for the bottom surface is equal to 0.10 m, whereas the embedded length of the pile should be reduced by 0.12 m for RC2.

Table 5.12 - Partial safety factors with respect to soil mechanical failure

$\beta_{calculation}$: 5.310						
β_{RC2}: 3.800						
Parameter (X_i)	**Unit**	$X_{char,i}$	X_i^*	$\gamma_{calc,i}$	$X_{d,i}$	$\gamma_{RC2,i}$
$E_{m,\ sandy\ clay}$	[kN/m^2]	3344	3675	0.91	3767	0.89
$\gamma_{sat,\ sandy\ clay}$	[kN/m^3]	18	17.91	1.01	18.39	0.98
$\varphi_{sandy\ clay}$	[deg]	22.5	22.00	1.02	23.40	0.96
$E_{m,\ gravel}$	[kN/m^2]	16720	18600	0.90	18998	0.88
$\gamma_{sat,\ gravel}$	[kN/m^3]	21	21.03	1.00	21.56	0.97
φ_{gravel}	[deg]	37.5	31.24	1.20	35.11	1.07
$\gamma_{sat,\ moderately\ packed\ sand}$	[kN/m^3]	20	21.07	0.95	21.27	0.94
$\varphi_{moderately\ packed\ sand}$	[deg]	32.5	35.01	0.93	36.11	0.90
$F_{mooring}$	[kN]	2547	2920	1.15	2626	1.03
Pile tip level	[m] NAP	-37.13 (μ)	-36.96	1.00	-37.01	1.00
Bottom surface	[m] NAP	-18.16 (μ)	-18.30	0.99	-18.26	0.99

5.6 Evaluation of a shortened mooring dolphin

5.6.1 Introduction

The evaluation of the considered mooring dolphin shows that the reliability of the structure with respect to structural failure and excessive deformations approaches the target reliability according to reliability class 2. However, from the evaluation with respect to soil mechanical failure it appears that the required length of the pile may be overestimated. Furthermore, due to the large difference between the calculated reliability and the target reliability it is not possible to obtain accurate partial safety factors for RC2, as it is no longer reasonable to assume that the influence factors do not significantly change. Therefore, the probabilistic calculations will be performed again for a shortened pile. The required pile length is determined iteratively using the method of Blum. The required embedded pile depth according to this method is equal to 16.86 m. The pile tip of the shortened mooring dolphin is therefore chosen to be at a level of NAP -35.0 m.

5.6.2 Structural failure

The results of the first probabilistic calculation regarding structural failure, in which all stochastic variables are included, are given in Appendix F. These results show that most variables do not significantly contribute to the reliability of the structure with respect to structural failure. After elimination of the irrelevant parameters, the remaining variables for the final calculation are:

- Mooring load: $F_{mooring}$
- Yield strength of steel: f_y
- Wall thickness of the dolphin: t

The results of the final calculation are given in Table 5.13 and Figure 5.5. Comparing these results with the results obtained for the initial design of the mooring dolphin, it is found that the reliability of the structure and the influence of the variables on the reliability have not changed. This can be explained by the fact that the level of the pile tip and the soil near this level have no influence on the reliability of the structure with respect to structural failure.

Table 5.13 - Results of the final calculation for a shortened pile (LS: structural failure)

Number of calculations: 89					
$\beta_{correlated}$: 4.067					
P_f: $2.383 \cdot 10^{-5}$					
Parameter (X_i)		**Unit**	**V (=σ/μ)**	**$\alpha_{correlated}$**	**X_i* (Design value)**
$F_{mooring}$		[kN]	0.15	-0.84	3257
f_y		[N/mm^2]	0.07	0.51	479.1
t		[mm]	0.03	0.18	39.94
Calculation	Z-value				
1	52300				
89	1.14				

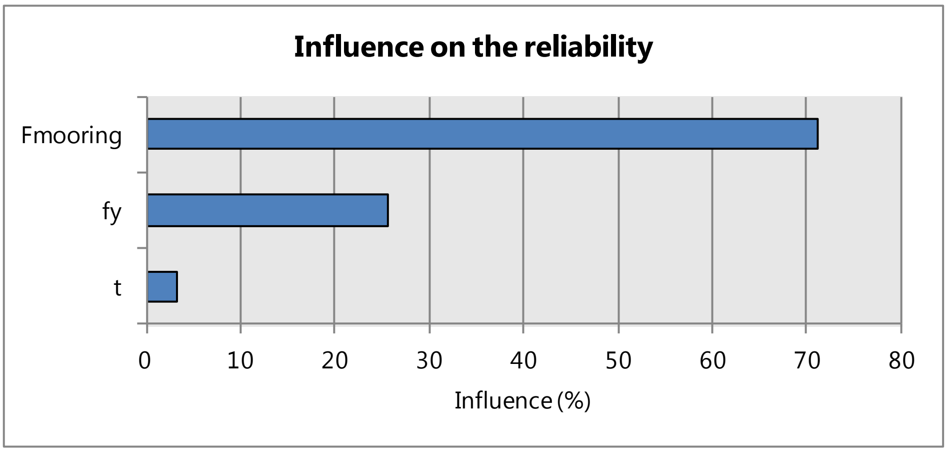

Figure 5.5 - Influence of the relevant parameters on the reliability for a shortened pile (LS: structural failure)

From the final results partial safety factors can be determined with the equations given in section 5.5.1. The obtained partial factors with respect to the characteristic parameter values are presented in Table 5.14. Because the influence factors of the relevant variables have not changed, these partial safety factors are similar to the ones obtained from the initial design of the mooring dolphin.

Table 5.14 - Partial safety factors with respect to structural failure for a shortened pile

$\beta_{calculation}$: 4.067						
β_{RC2}: 3.800						
Parameter (X_i)	**Unit**	**$X_{char,i}$**	**X_i***	**$\gamma_{calc,i}$**	**$X_{d,i}$**	**$\gamma_{RC2,i}$**
$F_{mooring}$	[kN]	2547	3257	1.28	3170	1.24
f_y	[N/mm^2]	483	479.1	1.01	484.4	1.00
t	[mm]	41 (μ)	39.94	1.03	40.00	1.03

5.6.3 Excessive deformations

The results of the first probabilistic calculation regarding excessive deformations, in which all stochastic variables are included, are presented in Appendix F. They show that many variables do not significantly contribute to the reliability of the structure with respect to excessive deformations. Therefore these variables are excluded from the final calculation. The remaining variables which are included in the final calculation are:

- Pressiometric modulus of sandy clay: $E_{m,\ sandy\ clay}$
- Saturated unit weight of sandy clay: $\gamma_{sat,\ sandy\ clay}$
- Angle of internal friction of sandy clay: $\varphi_{sandy\ clay}$
- Mooring load: $F_{mooring}$
- Pile tip level
- Level of the bottom surface

The results of the final calculation are given in Table 5.15 and Figure 5.6. Due to the decreased pile length the displacement of the pile top increases, resulting in a smaller reliability with respect to excessive deformations. Furthermore, it can be concluded that influence of the relevant soil variables and the pile tip level increase as the length of the pile decreases, which can be explained by the non-linear behaviour of the soil.

Table 5.15 - Results of the final calculation for a shortened pile (LS: excessive deformations)

Number of calculations: 120				
$\beta_{correlated}$: 2.087				
P_f: $1.845 \cdot 10^{-2}$				
Parameter (X_i)	**Unit**	**V (=σ/μ)**	**$\alpha_{correlated}$**	**X_i* (Design value)**
$E_{m,\ sandy\ clay}$	[kN/m^2]	0.10	0.18	3846
$\gamma_{sat,\ sandy\ clay}$	[kN/m^3]	0.05	0.34	18.91
$\varphi_{sandy\ clay}$	[deg]	0.10	0.46	24.30
$F_{mooring}$	[kN]	0.15	-0.77	2534
Pile tip level	[m] NAP	0.25 (σ)	-0.15	-34.92
Bottom surface	[m] NAP	0.25 (σ)	0.12	-18.22

Calculation	Z-value	
1	648.0	
120	1.941	

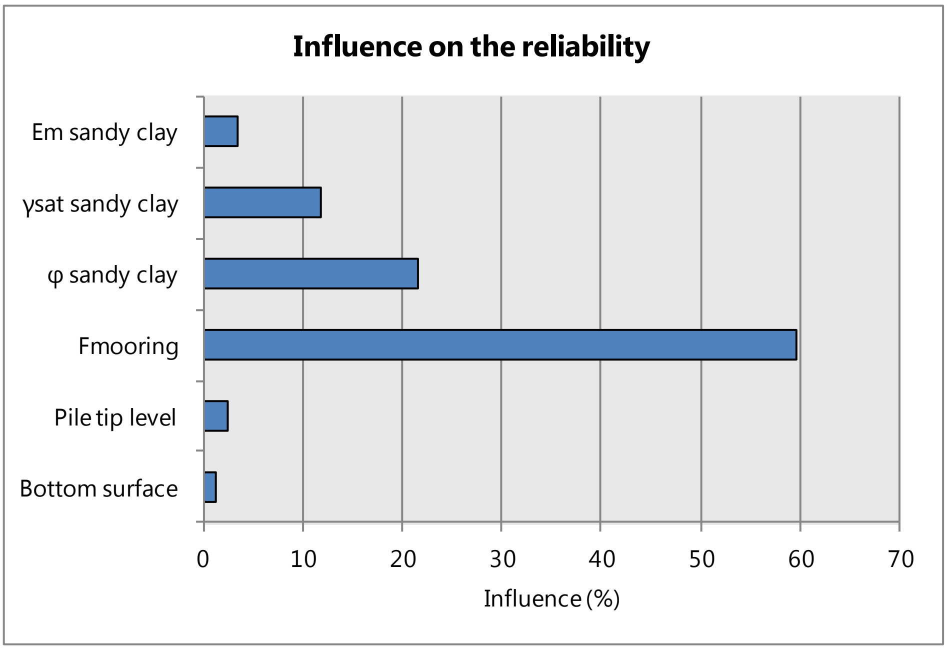

Figure 5.6 - Influence of the relevant parameters on the reliability for a shortened pile (LS: excessive deformations)

From the results of the final calculation the partial safety factors are determined for both the reliability obtained from the calculation and the target reliability as is described in section 5.5.1. However, because there is a relatively large difference between the calculated reliability and the target reliability, it is not reasonable to assume that the influence factors do not significantly change, resulting in unreliable partial safety factors for RC2.

Table 5.16 - Partial safety factors with respect to excessive deformations for a shortened pile

$\beta_{calculation}$: 2.087						
β_{RC2}: 3.800						
Parameter (X_i)	**Unit**	$X_{char,i}$	X_i^*	$\gamma_{calc,i}$	$X_{d,i}$	$\gamma_{RC2,i}$
$E_{m,\ sandy\ clay}$	[kN/m^2]	3344	3846	0.87	3720	0.90
$\gamma_{sat,\ sandy\ clay}$	[kN/m^3]	18	18.91	0.95	18.34	0.98
$\varphi_{sandy\ clay}$	[deg]	22.5	24.30	0.93	22.16	1.02
$F_{mooring}$	[kN]	2547	2534	0.99	3065	1.20
Pile tip level	[m] NAP	-37 (μ)	-34.92	1.00	-34.85	1.00
Bottom surface	[m] NAP	-18.16 (μ)	-18.22	1.00	-18.27	0.99

5.6.4 Soil mechanical failure

The results of the first probabilistic calculations are given in Appendix F. They show that the reliability with respect to soil mechanical failure is mainly determined by the load and the soil structure. After elimination of the irrelevant variables, the remaining stochastic variables for the final calculation are:

- Pressiometric modulus of sandy clay: $E_{m,\ sandy\ clay}$
- Saturated unit weight of sandy clay: $\gamma_{sat,\ sandy\ clay}$

- Angle of internal friction of sandy clay: $\varphi_{sandy\ clay}$
- Pressiometric modulus of gravel: $E_{m,\ gravel}$
- Saturated unit weight of gravel: $\gamma_{sat,\ gravel}$
- Angle of internal friction of gravel: φ_{gravel}
- Saturated unit weight of moderately packed sand: $\gamma_{sat,\ moderately\ packed\ sand}$
- Angle of internal friction of moderately packed sand: $\varphi_{moderately\ packed\ sand}$
- Mooring load: $F_{mooring}$
- Pile tip level
- Level of the bottom surface

The results of the final calculation are given in Table 5.17 and Figure 5.7. Due to the reduced embedded pile length, the reliability of the structure with respect to soil mechanical decreases and approaches the target reliability. Furthermore, the influence of the layer of gravel decreases, whereas the influence of the other relevant parameters on the reliability slightly increases. This is because the effective thickness of the layer of gravel which affects the behaviour of the structure decreases. It may therefore be concluded that the influence factors are dependent on the thickness of the soil layer.

Table 5.17 - Results of the final calculation for a shortened pile (LS: soil mechanical failure)

Number of calculations: 217				
$\beta_{correlated}$: 3.834				
P_f: $6.298 \cdot 10^{-5}$				
Parameter (X_i)	**Unit**	**V (=σ/μ)**	**$\alpha_{correlated}$**	**X_i* (Design value)**
$E_{m,\ sandy\ clay}$	[kN/m^2]	0.10	0.17	3732
$\gamma_{sat,\ sandy\ clay}$	[kN/m^3]	0.05	0.36	18.27
$\varphi_{sandy\ clay}$	[deg]	0.10	0.38	22.96
$E_{m,\ gravel}$	[kN/m^2]	0.10	0.12	19070
$\gamma_{sat,\ gravel}$	[kN/m^3]	0.05	0.26	21.75
φ_{gravel}	[deg]	0.10	0.48	36.61
$\gamma_{sat,\ moderately\ packed\ sand}$	[kN/m^3]	0.05	0.13	21.24
$\varphi_{moderately\ packed\ sand}$	[deg]	0.10	0.21	35.74
$F_{mooring}$	[kN]	0.15	-0.53	2693
Pile tip level	[m] NAP	0.25 (σ)	-0.16	-34.98
Bottom surface	[m] NAP	0.25 (σ)	0.15	-18.30

Calculation	Z-value	
1	31.0	
217	0.0	

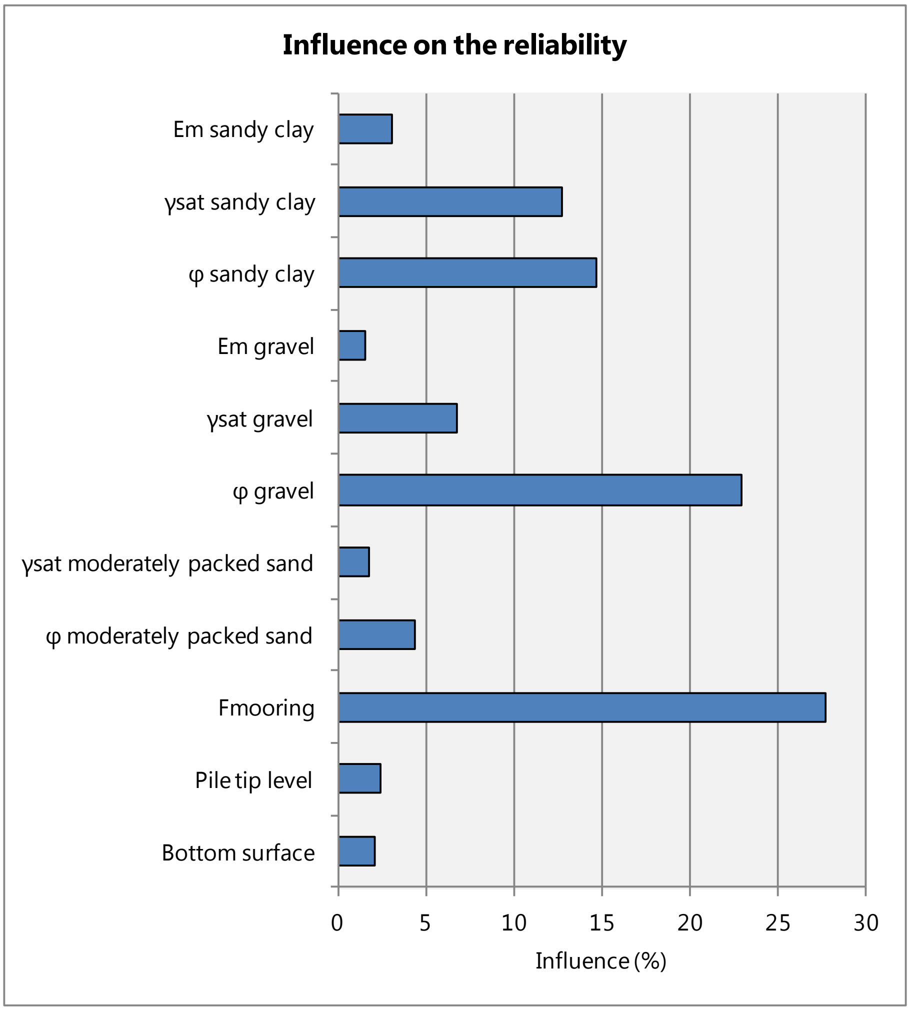

Figure 5.7 - Influence of the relevant parameters on the reliability for a shortened pile (LS: soil mechanical failure)

From the results of the final calculation the partial safety factors with respect to soil mechanical failure are derived for both the calculated reliability and the target reliability as is described in section 5.5.1. Because the calculated reliability approaches the target reliability it is reasonable to assume that the influence factors for the different variables do not significantly change. The results are presented in Table 5.18. Looking at the required absolute safety margins for the geometrical parameters, it is found that this margin for the bottom surface is equal to 0.14 m, whereas the embedded length of the pile should be reduced by 0.15 m for RC2.

Table 5.18 - Partial safety factors with respect to soil mechanical failure for a shortened pile

$\beta_{calculation}$: 3.834

β_{RC2}: 3.800

Parameter (X_i)	Unit	$X_{char,i}$	X_i*	$\gamma_{calc,i}$	$X_{d,i}$	$\gamma_{RC2,i}$
$E_{m,\ sandy\ clay}$	[kN/m^2]	3344	3675	0.90	3734	0.90
$\gamma_{sat,\ sandy\ clay}$	[kN/m^3]	18	17.91	0.99	18.28	0.98
$\varphi_{sandy\ clay}$	[deg]	22.5	22.00	0.98	23.00	0.98
$E_{m,\ gravel}$	[kN/m^2]	16720	18600	0.88	19078	0.88
$\gamma_{sat,\ gravel}$	[kN/m^3]	21	21.03	0.97	21.76	0.97
φ_{gravel}	[deg]	37.5	31.24	1.02	36.68	1.02
$\gamma_{sat,\ moderately\ packed\ sand}$	[kN/m^3]	20	21.07	0.94	21.24	0.94
$\varphi_{moderately\ packed\ sand}$	[deg]	32.5	35.01	0.91	35.77	0.91
$F_{mooring}$	[kN]	2547	2920	1.06	2687	1.05
Pile tip level	[m] NAP	-35.13 (μ)	-36.96	1.00	-34.98	1.00
Bottom surface	[m] NAP	-18.16 (μ)	-18.30	0.99	-18.30	0.99

5.7 Conclusion

From the evaluation of the mooring dolphin which is constructed in the Caland canal, it can be concluded that the reliability of the structure with respect to structural failure and excessive deformations is almost in line with the intended reliability. However, from the performed evaluation with respect to soil mechanical failure it appears that the required pile length may be overestimated. Because the reliability with respect to this limit state is much higher than is intended, it is not possible to obtain accurate partial safety factors for reliability class 2 with respect to soil mechanical failure. Therefore, the probabilistic evaluations are also performed for a shortened pile. As a result, the reliability with respect to excessive deformations becomes much smaller than intended, whereas the reliability with respect to soil mechanical failure is now in line with the target reliability. The results on the reliability for both the initial dolphin design and the shortened pile are summarized in Table 5.19.

Table 5.19 - Reliability of the structure

	Reliability β	
	Pile tip level	
Limit state	**NAP -37.0 m**	**NAP -35.0 m**
Structural failure	4.067	4.067
Excessive deformations	3.402	2.087
Soil mechanical failure	5.310	3.834

To be able to determine the partial safety factors which are in accordance with reliability class 2, it is assumed that the obtained influence factors for the relevant variables do not significantly change. This assumption is only valid when the calculated reliability approaches the target reliability. The results obtained from the initial dolphin design are therefore governing with respect to structural failure and excessive deformations, whereas the results obtained from the modified dolphin design are governing with respect to soil mechanical failure. These governing results are presented in Table 5.20.

Table 5.20 - Overview of the governing results

Parameter	$\alpha_{correlated}$	$\gamma_{RC2,i}$
LS: Structural failure		
$F_{mooring}$	-0.84	1.24
f_y	0.51	1.00
t	0.18	1.03
LS: Excessive deformations		
$E_{m,\ sandy\ clay}$	0.15	0.89
$\gamma_{sat,\ sandy\ clay}$	0.29	0.97
$\varphi_{sandy\ clay}$	0.39	0.98
$F_{mooring}$	-0.84	1.24
Pile tip level	-0.12	1.00
Bottom surface	0.13	0.99
LS: Soil mechanical failure		
$E_{m,\ sandy\ clay}$	0.17	0.90
$\gamma_{sat,\ sandy\ clay}$	0.36	0.98
$\varphi_{sandy\ clay}$	0.38	0.98
$E_{m,\ gravel}$	0.12	0.88
$\gamma_{sat,\ gravel}$	0.26	0.97
φ_{gravel}	0.48	1.02
$\gamma_{sat,\ moderately\ packed\ sand}$	0.13	0.94
$\varphi_{moderately\ packed\ sand}$	0.21	0.91
$F_{mooring}$	-0.53	1.05
Pile tip level	-0.16	1.00
Bottom surface	0.15	0.99

6

SENSITIVITY ANALYSIS OF THE PARTIAL SAFETY FACTORS

6.1 Introduction

The partial safety factors for flexible dolphin design which are derived in chapter 5, are determined based on one specific soil structure and parameter set. However, in practice, different soil structures with different parameter sets can occur. The recommended set of partial safety factors must apply to each of these situations. Therefore, the sensitivity of the obtained partial safety factors to changes in the soil structure and parameter values is analyzed. In this chapter, 4 different variations with respect to the soil structure are evaluated:

- Variation 1: Increased cohesion for the sandy clay (section 6.2)
- Variation 2: Decreased angle of internal friction for the gravel (section 6.3)
- Variation 3: Modified soil structure (section 6.4)
- Variation 4: Increased thickness of the intermediate sand layer (section 6.5)

Furthermore, the coefficient of variation for the stiffness of the soil is not unambiguously defined. Therefore, in section 6.6 a probabilistic evaluation is performed for an increased coefficient of variation for the stiffness of the soil.

6.2 Variation 1: Increased cohesion for sandy clay

6.2.1 Input parameters for the soil structure

From the probabilistic evaluations performed in chapter 5 it is found that the cohesion of clay hardly has any influence on the reliability of the structure. Therefore, it is not required to apply any partial safety factor on the characteristic parameter value of the cohesion. However, the cohesion of the clay included in the model is very small. To be able to form a more general conclusion on the influence of the cohesion on the reliability, the same probabilistic evaluations are performed with an increased cohesion of the sandy clay.

The initial value for the cohesion of the sandy clay is based on Table 2.b of NEN 9997 and equals 5 kPa. For the probabilistic evaluations performed in this paragraph, it is chosen to increase this cohesion to 15 kPa. The parameter values for the other soil parameters are equal to the ones presented in Table 5.1 and Table 5.2.

6.2.2 Limit state evaluations

6.2.2.1 Structural failure

The results of the first probabilistic calculation regarding structural failure are included in Appendix G. They show that most variables can be eliminated as their influence on the reliability is not significant. The remaining variables for the final calculation are:

- Mooring load: $F_{mooring}$
- Yield strength of steel: f_y
- Wall thickness of the dolphin: t

The results of the final calculation are given in Table 6.1 and Figure 6.1. From these results it can be concluded that the reliability with respect to structural failure increases with an increasing strength of the top layer of the soil. This is because the bending moment which develops in the structure becomes smaller. Furthermore, the influence of the mooring load on the reliability of the structure decreases. This can be explained by the fact that the derivative of the limit state in the design point with respect to the mooring load decreases.

Table 6.1 - Results of the final calculation for variation 1: Increased cohesion for sandy clay (LS: Structural failure)

Number of calculations: 93				
$\beta_{correlated}$: 4.313				
P_f: $8.036 \cdot 10^{-6}$				
Parameter (X_i)	**Unit**	**V (=σ/μ)**	**$\alpha_{correlated}$**	**X_i* (Design value)**
$F_{mooring}$	[kN]	0.15	-0.82	3345
f_y	[N/mm^2]	0.07	0.54	468.2
t	[mm]	0.03	0.18	39.87
Calculation	Z-value			
1	54390			
93	0.54			

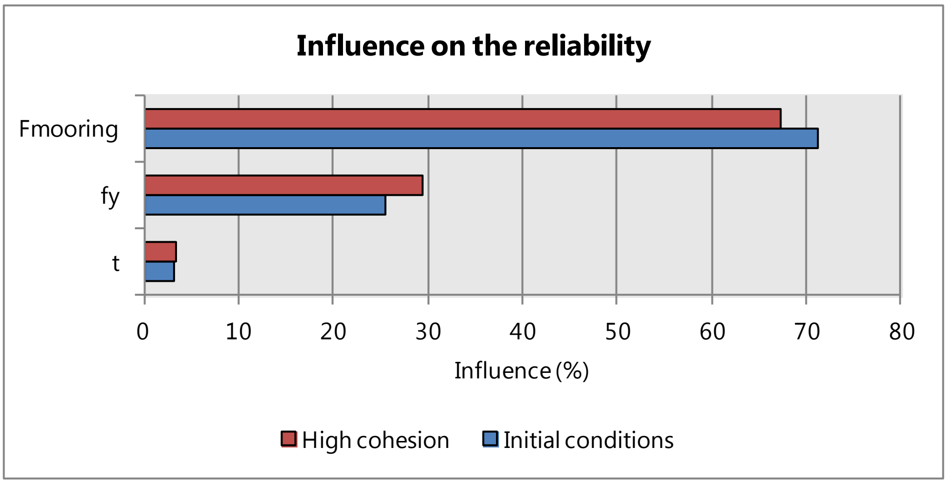

Figure 6.1 - Influence of the relevant parameters on the reliability (LS: Structural failure)

From the results of the FORM-calculation partial safety factors can be determined with:

$$\gamma_{R,i} = \frac{X_{char,i}}{X_i^*} \quad \text{for resistance parameters} \quad (6.1)$$

$$\gamma_{S,i} = \frac{X_i^*}{X_{char,i}} \quad \text{for load parameters} \quad (6.2)$$

Besides the partial factors which correspond to the calculated reliability, also the partial safety factors corresponding to reliability class 2 are determined (β_{RC2} = 3.8). The partial safety factors corresponding to RC2 are determined with the assumption that the influence factors for the relevant parameters do not significantly change. The design values corresponding to the target reliability are determined by using:

$$X_{d,i} = \mu_{X_i} - \alpha_i \beta_{RC2} \sigma_{X_i} \quad \text{for normally distributed parameters} \quad (6.3)$$

$$X_{d,i} = \frac{\mu_{X_i}}{\sqrt{1+V_i}} \exp\left(-\alpha_i \beta_{RC2} \sqrt{ln(1+V_i^2)}\right) \quad \text{for lognormally distributed parameters} \quad (6.4)$$

$$X_{d,i} = a + (b-a) \cdot \Phi(-\alpha_i \beta_{RC2}) \quad \text{for uniformly distributed parameters} \quad (6.5)$$

For the mooring load, which has a weibull distribution, the design value corresponding to RC2 is determined iteratively using $F(X_{d,i}) = \Phi(-\alpha_i \beta_{RC2})$.

Table 6.2 presents the partial safety factors which are derived for both the reliability obtained from the calculation and the target reliability according to RC2.

Table 6.2 - Partial safety factors with respect to structural failure for variation 1: Increased cohesion for sandy clay

$\beta_{calculation}$: 4.313						
β_{RC2}: 3.800						
Parameter (X_i)	**Unit**	**$X_{char,i}$**	**X_i^***	**$\gamma_{calc,i}$**	**$X_{d,i}$**	**$\gamma_{RC2,i}$**
$F_{mooring}$	[kN]	2547	3345	1.31	3145	1.23
f_y	[N/mm^2]	483	468.2	1.03	1.01	1.01
t	[mm]	41 (μ)	39.87	1.03	1.03	1.03

6.2.2.2 Excessive deformations

From the first probabilistic evaluation with respect to excessive deformations it appears that the dimensions of the pile are over conservative. The calculated reliability of the structure is equal to 5.298. Because of the large difference between the calculated reliability and the target reliability, it is no longer reasonable to assume that the influence factors do not significantly change. In order to obtain a reliability which is in line with the target reliability, the pile tip level is altered to NAP -35.0 m. The results of the first probabilistic calculations for this modified pile are included in Appendix G. These results show that many variables do not significantly contribute to the reliability of the structure. The variables which have to be included in the final calculation are:

- Cohesion of sandy clay: $c_{sandy\ clay}$
- Pressiometric modulus of sandy clay: $E_{m,\ sandy\ clay}$
- Saturated unit weight of sandy clay: $\gamma_{sat,\ sandy\ clay}$
- Angle of internal friction of sandy clay: $\varphi_{sandy\ clay}$
- Mooring load: $F_{mooring}$
- Pile tip level
- Level of the bottom surface

The results of the final calculation are presented in Table 6.3 and Figure 6.2. As a result of the variation of the parameter value for the cohesion, the influence of the relevant soil parameters on the reliability is redistributed while the overall influence of the soil only changes a little. It can be seen that the influence of the cohesion of the sandy clay increases as the parameter value increases. This is because the influence factor is proportional to the standard deviation of the considered variable. Furthermore, due to the negative correlation between the cohesion and the angle of internal friction, the influence of the angle of internal friction of the sandy clay on the reliability decreases.

Table 6.3 - Results of the final calculation for variation 1: Increased cohesion for sandy clay (LS: Excessive deformations)

Number of calculations: 153				
$\beta_{correlated}$: 3.786				
P_f: $7.665 \cdot 10^{-5}$				
Parameter (X_i)	**Unit**	**V (=σ/μ)**	**$\alpha_{correlated}$**	**X_i* (Design value)**
$c_{sandy\ clay}$	[kPa]	0.2	0.15	18.64
$E_{m,\ sandy\ clay}$	[kN/m^2]	0.10	0.27	3585
$\gamma_{sat,\ sandy\ clay}$	[kN/m^3]	0.05	0.34	18.34
$\varphi_{sandy\ clay}$	[deg]	0.10	0.25	24.36
$F_{mooring}$	[kN]	0.15	-0.82	3146
Pile tip level	[m] NAP	0.25 (σ)	-0.14	-34.87
Bottom surface	[m] NAP	0.25 (σ)	0.16	-18.31

Calculation	Z-value	
1	827.5	
153	2.747	

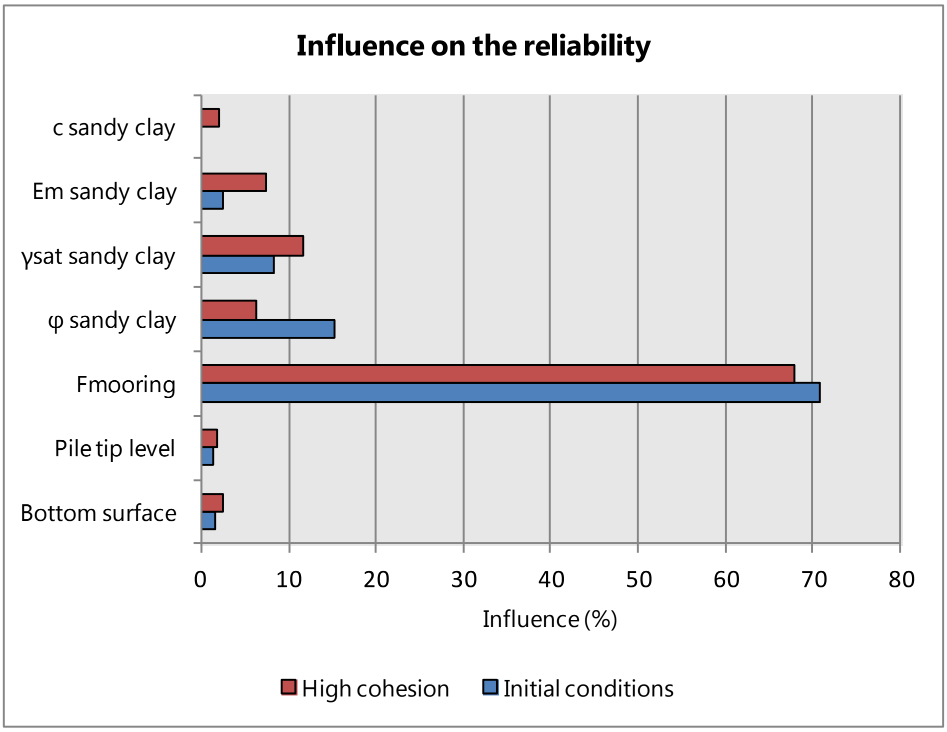

Figure 6.2 - Influence of the relevant parameters on the reliability (LS: Excessive deformations)

From the results of the FORM-calculation, partial safety factors are derived for both the calculated reliability and the target reliability, as is described in section 6.2.2.1. The obtained factors are given in Table 6.4. For the geometrical parameters it may be more relevant to express the required safety by means of an absolute additional margin. For the level of the bottom surface this means that the surface should be lowered by 0.15 m, whereas the pile tip level should be raised by 0.13 m.

Table 6.4 - Partial safety factors with respect to excessive deformations for variation 1: Increased cohesion for sandy clay

$\beta_{calculation}$: 3.786						
β_{RC2}: 3.800						
Parameter (X_i)	**Unit**	$X_{char,i}$	X_i^*	$\gamma_{calc,i}$	$X_{d,i}$	$\gamma_{RC2,i}$
$c_{sandy\ clay}$	[kPa]	15	18.64	0.80	18.63	0.81
$E_{m,\ sandy\ clay}$	[kN/m^2]	3344	3585	0.93	3583	0.93
$\gamma_{sat,\ sandy\ clay}$	[kN/m^3]	18	18.34	0.98	18.34	0.98
$\varphi_{sandy\ clay}$	[deg]	22.5	24.36	0.92	24.35	0.92
$F_{mooring}$	[kN]	2547	3146	1.24	3145	1.23
Pile tip level	[m] NAP	-35 (μ)	-34.87	1.00	-34.87	1.00
Bottom surface	[m] NAP	-18.16 (μ)	-18.31	0.99	-18.31	0.99

6.2.2.3 Soil mechanical failure

To be able to perform the probabilistic evaluation regarding soil mechanical failure, the limit state function as is given in section 4.5.4 has to be modified. It is found that the critical percentage of mobilized resistance has to be reduced to 40%. To correct for this reduction, the embedded length of the pile has to be increased by 0.43 m.

From the first probabilistic evaluation regarding soil mechanical failure it appears that the embedded pile length is over conservative. The calculated reliability of the structure is equal to 6.824. To be able to derive accurate partial safety factors corresponding to RC2, the pile tip level has to be altered to NAP -33.0 m. The results of the first probabilistic calculation for the modified pile are included in Appendix G. They show that some of the variables can be eliminated from the probabilistic calculation. The variables which have to be included in the final calculation are:

- Cohesion of sandy clay: $c_{\text{sandy clay}}$
- Pressiometric modulus of sandy clay: $E_{\text{m, sandy clay}}$
- Saturated unit weight of sandy clay: $\gamma_{\text{sat, sandy clay}}$
- Angle of internal friction of sandy clay: $\varphi_{\text{sandy clay}}$
- Saturated unit weight of gravel: $\gamma_{\text{sat, gravel}}$
- Angle of internal friction of gravel: φ_{gravel}
- Saturated unit weight of moderately packed sand: $\gamma_{\text{sat, moderately packed sand}}$
- Angle of internal friction of moderately packed sand: $\varphi_{\text{moderately packed sand}}$
- Mooring load: F_{mooring}
- Pile tip level
- Level of the bottom surface

The results of the final calculation are shown in Table 6.5 and Figure 6.3. It is found that the influence of the cohesion of the sandy clay on the reliability of the structure increases for an increasing cohesion, while the influence of the angle of internal friction decreases. This can be explained by the negative correlation between these two variables. Furthermore, it can be concluded that the influence of the layer of gravel decreases. Due to the increased strength of the sandy clay layer, the required embedded pile length decreases. As a result, the effective thickness of the layer of gravel decreases and so does the influence of this layer on the reliability of the structure with respect to soil mechanical failure.

Table 6.5 - Results of the final calculation for variation 1: Increased cohesion for sandy clay (LS: Soil mechanical failure)

Number of calculations: 217				
$\beta_{correlated}$: 3.944				
P_f: $4.003 \cdot 10^{-5}$				
Parameter (X_i)	**Unit**	**V (=σ/μ)**	**$\alpha_{correlated}$**	**X_i* (Design value)**
$c_{sandy\ clay}$	[kPa]	0.20	0.12	19.00
$E_{m,\ sandy\ clay}$	[kN/m^2]	0.10	0.24	3610
$\gamma_{sat,\ sandy\ clay}$	[kN/m^3]	0.05	0.41	18.03
$\varphi_{sandy\ clay}$	[deg]	0.10	0.29	23.82
$\gamma_{sat,\ gravel}$	[kN/m^3]	0.05	0.21	21.93
φ_{gravel}	[deg]	0.10	0.39	37.87
$\gamma_{sat,\ moderately\ packed\ sand}$	[kN/m^3]	0.05	0.13	21.22
$\varphi_{moderately\ packed\ sand}$	[deg]	0.10	0.20	35.88
$F_{mooring}$	[kN]	0.15	-0.60	2839
Pile tip level	[m] NAP	0.25 (σ)	-0.16	-33.27
Bottom surface	[m] NAP	0.25 (σ)	0.16	-8.32

Calculation	Z-value	
1	29.4	
217	0.17	

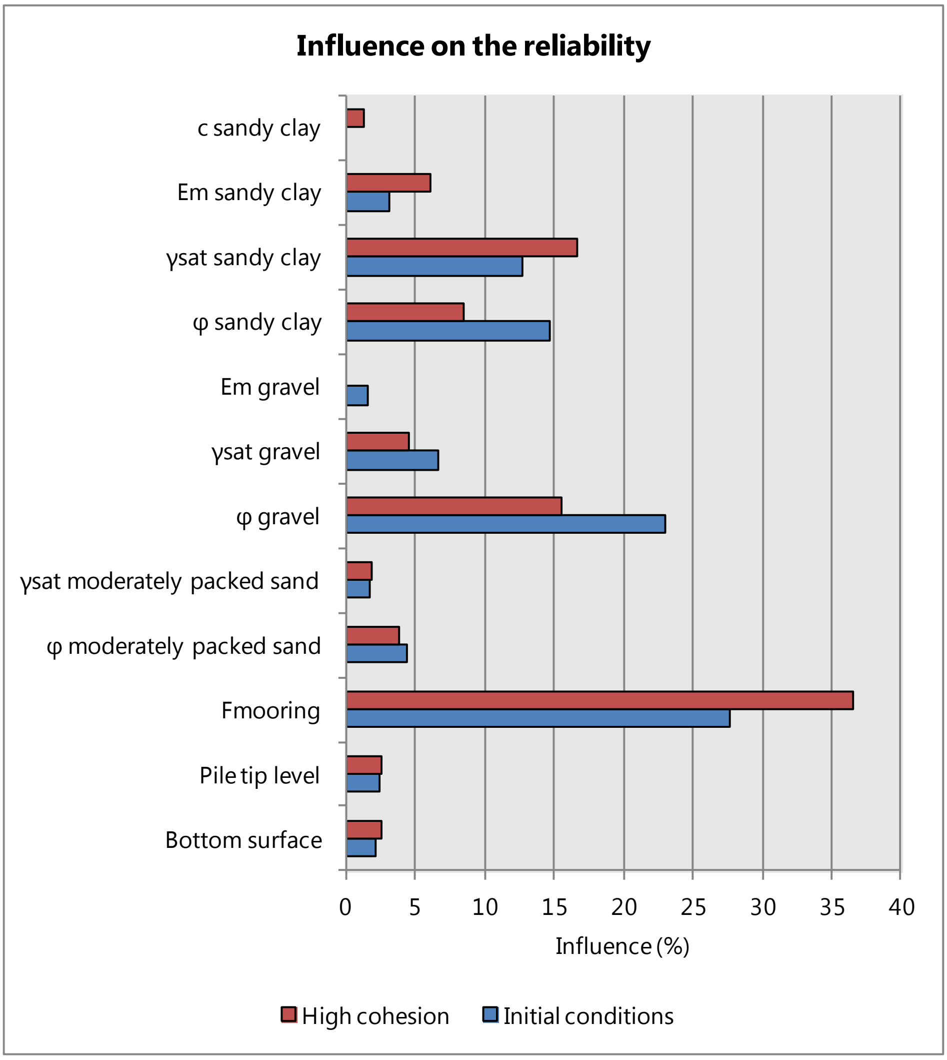

Figure 6.3 - Influence of the relevant parameters on the reliability (LS: Soil mechanical failure)

From the final results, partial safety factors can be derived with the equations given in section 6.2.2.1. The obtained partial factors are presented in Table 6.6. Looking at the required absolute safety margins for the geometrical parameters, it is found that the margin for the bottom surface is equal to 0.15 m, whereas the embedded pile length should be reduced by 0.15 m.

Table 6.6 - Partial safety factors with respect to soil mechanical failure for variation 1: Increased cohesion for sandy clay

$\beta_{calculation}$: 3.944

β_{RC2}: 3.800

Parameter (X_i)	Unit	$X_{char,i}$	X_i*	$\gamma_{calc,i}$	$X_{d,i}$	$\gamma_{RC2,i}$
$c_{sandy\ clay}$	[kPa]	15	19.00	0.79	19.06	0.79
$E_{m,\ sandy\ clay}$	[kN/m^2]	3344	3610	0.93	3624	0.92
$\gamma_{sat,\ sandy\ clay}$	[kN/m^3]	18	18.03	1.00	18.09	1.00
$\varphi_{sandy\ clay}$	[deg]	22.5	23.82	0.94	23.93	0.94
$\gamma_{sat,\ gravel}$	[kN/m^3]	21	21.93	0.96	21.96	0.96
φ_{gravel}	[deg]	37.5	37.87	0.99	38.12	0.98
$\gamma_{sat,\ moderately\ packed\ sand}$	[kN/m^3]	20	21.22	0.94	21.24	0.94
$\varphi_{moderately\ packed\ sand}$	[deg]	32.5	35.88	0.91	35.99	0.90
$F_{mooring}$	[kN]	2547	2839	1.11	2803	1.10
Pile tip level	[m] NAP	-33.43 (μ)	-33.27	1.00	-33.28	1.00
Bottom surface	[m] NAP	-18.16 (μ)	-8.32	0.99	-18.31	0.99

6.3 Variation 2: Decreased angle of internal friction for gravel

6.3.1 Input parameters for the soil structure

From the probabilistic evaluations performed in chapter 5, it is found that the angle of internal friction of the gravel has a large influence on the reliability of the structure with respect to soil mechanical failure. This may be explained by the level of the layer of gravel. Another explanation can be found in the large parameter value for the angle of internal friction. To be able to form a better conclusion on the influence of the lower soil layer on the reliability with respect to soil mechanical failure, the angle of internal friction of the gravel is decreased to 32.5 degrees. Furthermore, the value for the angle of internal friction of the moderately packed sand is decreased from 32.5 degrees to 30.0 degrees, in order to maintain a difference between the soil layers. The parameter values for the other soil parameters are equal to the ones presented in Table 5.1 and Table 5.2.

6.3.2 Limit state evaluations

6.3.2.1 Structural failure

The results of the first probabilistic calculation regarding structural failure are included in Appendix G. They show that most variables do not significantly contribute to the reliability of the structure and therefore can be eliminated from the calculation. The remaining stochastic variables for the final calculation are:

- Mooring load: $F_{mooring}$
- Yield strength of steel: f_y
- Wall thickness of the dolphin: t

The results of the final calculation are presented in Table 6.7 and Figure 6.4. It can be concluded that adjusting the values of the angle of internal friction of the soil below the level of the maximum bending moment does not influence the reliability of the structure with respect the structural failure. This is because it is found that only the soil above the level of the maximum bending moment affects the development of the bending moment in the structure.

Table 6.7 - Results of the final calculation for variation 2: Decreased angle of internal friction for gravel (LS: Structural failure)

Number of calculations: 89					
$\beta_{correlated}$: 4.067					
P_f: $2.383 \cdot 10^{-5}$					
Parameter (X_i)		**Unit**	**V (=σ/μ)**	**$\alpha_{correlated}$**	**X_i* (Design value)**
$F_{mooring}$		[kN]	0.15	-0.84	3257
f_y		[N/mm^2]	0.07	0.51	479.1
t		[mm]	0.03	0.18	39.94
Calculation	Z-value				
1	52300				
89	1.14				

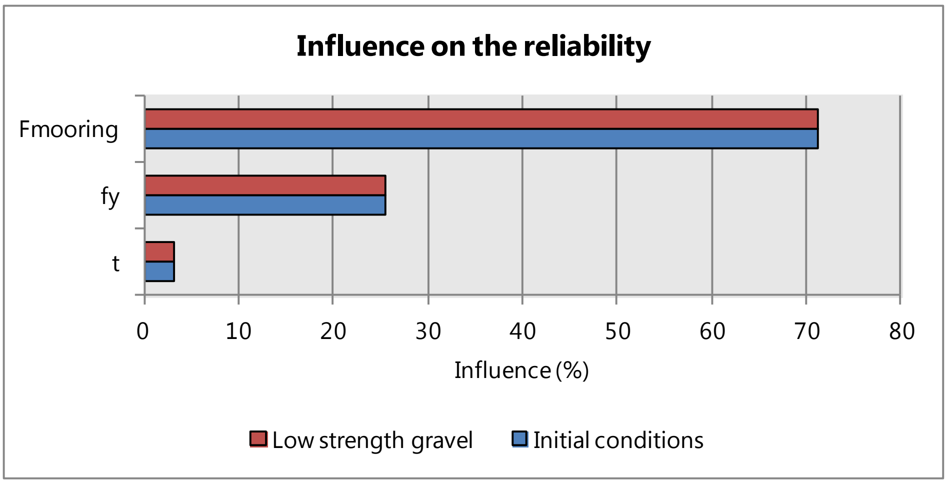

Figure 6.4 - Influence of the relevant parameters on the reliability (LS: Structural failure)

From the final results, partial safety factors can be determined with the equations given in section 6.2.2.1. The obtained partial factors are presented in Table 6.8. Because the influence factors of the relevant variables have not changed, these partial safety factors are similar to the ones obtained from the evaluation with respect to the initial conditions.

Table 6.8 - Partial safety factors with respect to structural failure for gravel with a decreased angle of internal friction

$\beta_{calculation}$: 4.067

β_{RC2}: 3.800

Parameter (X_i)	Unit	$X_{char,i}$	X_i^*	$\gamma_{calc,i}$	$X_{d,i}$	$\gamma_{RC2,i}$
$F_{mooring}$	[kN]	2547	3257	1.28	3170	1.24
f_y	[N/mm^2]	483	479.1	1.01	484.4	1.00
t	[mm]	41 (μ)	39.94	1.03	40.00	1.03

6.3.2.2 Excessive deformations

The results of the first calculation regarding excessive deformations are presented in Appendix G. These results show that many stochastic variables can be eliminated from the probabilistic evaluation, as their influence on the reliability is not significant. The variables which have to be included in the final calculation are:

- Pressiometric modulus of sandy clay: $E_{m,\ sandy\ clay}$
- Saturated unit weight of sandy clay: $\gamma_{sat,\ sandy\ clay}$
- Angle of internal friction of sandy clay: $\varphi_{sandy\ clay}$
- Mooring load: $F_{mooring}$
- Pile tip level
- Level of the bottom surface

The results of the final calculation are presented in Table 6.9 and Figure 6.5. It is found that adjusting the values of the angle of internal friction of the lower soil layers does not result in a change of the reliability. Therefore, it can be concluded that only the angle of internal friction of the top layer of the soil has an influence on the reliability with respect to the deformations, as could also be concluded from previous results.

Table 6.9 - Results of the final calculation for variation 2: Decreased angle of internal friction for gravel (LS: Excessive deformations)

Number of calculations: 120				
$\beta_{correlated}$: 3.402				
P_f: $3.344 \cdot 10^{-4}$				
Parameter (X_i)	**Unit**	**V (=σ/μ)**	**$\alpha_{correlated}$**	**X_i* (Design value)**
$E_{m,\text{ sandy clay}}$	[kN/m^2]	0.10	0.18	3846
$\gamma_{sat,\text{ sandy clay}}$	[kN/m^3]	0.05	0.34	18.91
$\varphi_{\text{sandy clay}}$	[deg]	0.10	0.46	24.30
$F_{mooring}$	[kN]	0.15	-0.77	2534
Pile tip level	[m] NAP	0.25 (σ)	-0.15	-34.92
Bottom surface	[m] NAP	0.25 (σ)	0.12	-18.22

Calculation	Z-value
1	648.0
120	1.941

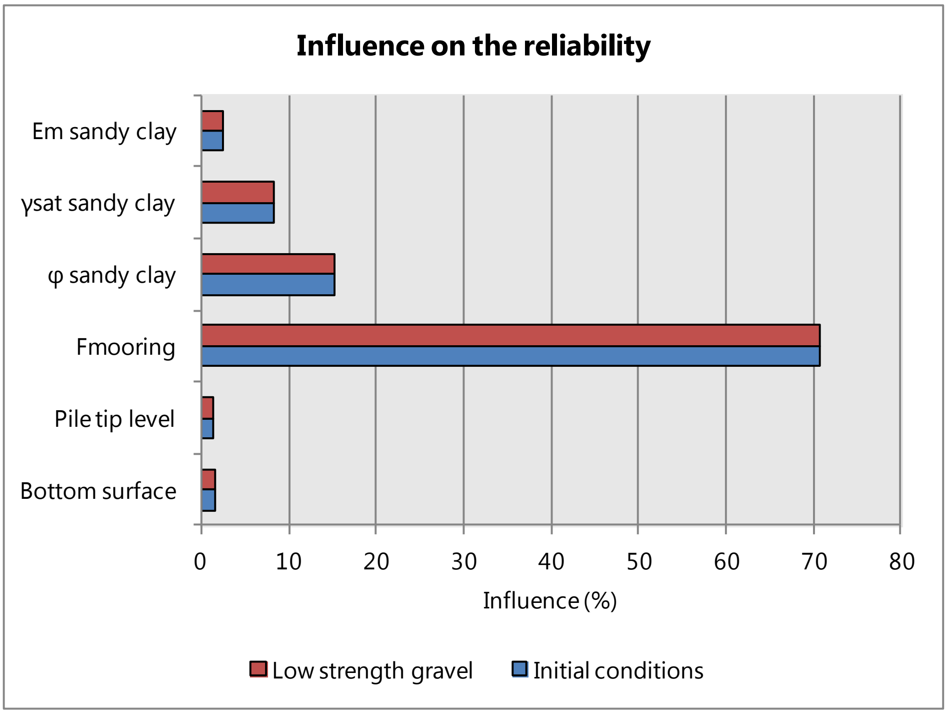

Figure 6.5 - Influence of the relevant parameters on the reliability (LS: Excessive deformations)

From the results of the final calculation, partial safety factors are derived with the equations given in section 6.2.2.1. Table 6.10 presents the obtained factors corresponding to both the reliability obtained from the calculations and the target reliability. Because the influence factors of the relevant variables have not changed, these partial safety factors are similar to the ones obtained from the evaluation with respect to the initial soil conditions.

Table 6.10 - Partial safety factors with respect to excessive deformations for gravel with a decreased angle of internal friction

$\beta_{calculation}$: 3.402

β_{RC2}: 3.800

Parameter (X_i)	**Unit**	$X_{char,i}$	X_i*	$\gamma_{calc,i}$	$X_{d,i}$	$\gamma_{RC2,i}$
$E_{m,\ sandy\ clay}$	[kN/m^2]	3344	3783	0.88	3758	0.89
$\gamma_{sat,\ sandy\ clay}$	[kN/m^3]	18	18.65	0.97	18.54	0.97
$\varphi_{sandy\ clay}$	[deg]	22.5	23.33	0.96	22.91	0.98
$F_{mooring}$	[kN]	2547	3034	1.19	3165	1.24
Pile tip level	[m] NAP	-37 (μ)	-36.90	1.00	-36.89	1.00
Bottom surface	[m] NAP	-18.16 (μ)	-18.27	0.99	-18.28	0.99

6.3.2.3 Soil mechanical failure

The limit state function as is given in section 4.5.4 cannot be evaluated with Prob2B, because the mooring structure will collapse before a satisfying convergence is reached. The be able to perform the probabilistic evaluation regarding soil mechanical failure, the critical percentage of mobilized passive resistance is reduced to 40%. To correct for this reduction, the embedded length of the pile is increased by 0.24 m.

From the first probabilistic calculations it is found that the reliability of the structure in combination with the adjusted soil parameter values is equal to 4.510. This is significantly larger than the target reliability. To be able to derive accurate partial safety factors corresponding to RC2, the pile tip level has to be raised to NAP -36.0 m. The results of the first probabilistic calculation for this modified pile length are included in Appendix G. From these results it can be concluded that some of the variables do not significantly contribute to the reliability and may therefore be eliminated. After elimination of these irrelevant variables, the following variables remain and have to be included in the final calculation:

- Pressiometric modulus of sandy clay: $E_{m,\ sandy\ clay}$
- Saturated unit weight of sandy clay: $\gamma_{sat,\ sandy\ clay}$
- Angle of internal friction of sandy clay: $\varphi_{sandy\ clay}$
- Pressiometric modulus of gravel: $E_{m,\ gravel}$
- Saturated unit weight of gravel: $\gamma_{sat,\ gravel}$
- Angle of internal friction of gravel: φ_{gravel}
- Saturated unit weight of moderately packed sand: $\gamma_{sat,\ moderately\ packed\ sand}$
- Angle of internal friction of moderately packed sand: $\varphi_{moderately\ packed\ sand}$
- Mooring load: $F_{mooring}$
- Pile tip level
- Level of the bottom surface

Table 6.11 and Figure 6.6 show the results of the final calculation. As a result of the reduced strength of the sand and gravel, the influence of these soil layers on the reliability of the structure with respect to soil mechanical failure decreases. However, Figure 6.6 does not confirm this reduction of influence for the variables related to the gravel. This can be explained by the fact that the required embedded pile length increases (with respect to the required length according to section 5.6) as a result of the reduced strength of the soil. Therefore, the thickness of the layer of gravel which affects the behaviour of the structure increases, resulting in an increasing influence of the parameters related to the gravel. It appears that the effect of the decreased strength of the gravel is compensated for by the required additional pile length with respect to the initial pile design.

Table 6.11 - Results of the final calculation for variation 2: decreased angle of internal friction for gravel (LS: Soil mechanical failure)

Number of calculations: 229				
$\beta_{correlated}$: 3.782				
P_f: $7.769 \cdot 10^{-5}$				
Parameter (X_i)	**Unit**	**V (=σ/μ)**	$\alpha_{correlated}$	**X_i* (Design value)**
$E_{m, sandy\ clay}$	[kN/m^2]	0.10	0.17	3744
$\gamma_{sat, sandy\ clay}$	[kN/m^3]	0.05	0.36	18.28
$\varphi_{sandy\ clay}$	[deg]	0.10	0.38	23.00
$E_{m, gravel}$	[kN/m^2]	0.10	0.11	19180
$\gamma_{sat, gravel}$	[kN/m^3]	0.05	0.26	21.77
φ_{gravel}	[deg]	0.10	0.48	31.83
$\gamma_{sat, moderately\ packed\ sand}$	[kN/m^3]	0.05	0.12	21.31
$\varphi_{moderately\ packed\ sand}$	[deg]	0.10	0.18	33.51
$F_{mooring}$	[kN]	0.15	-0.56	2725
Pile tip level	[m] NAP	0.25 (σ)	-0.14	-36.11
Bottom surface	[m] NAP	0.25 (σ)	0.13	-18.28

Calculation	Z-value	
1	29.0	
229	0.02	

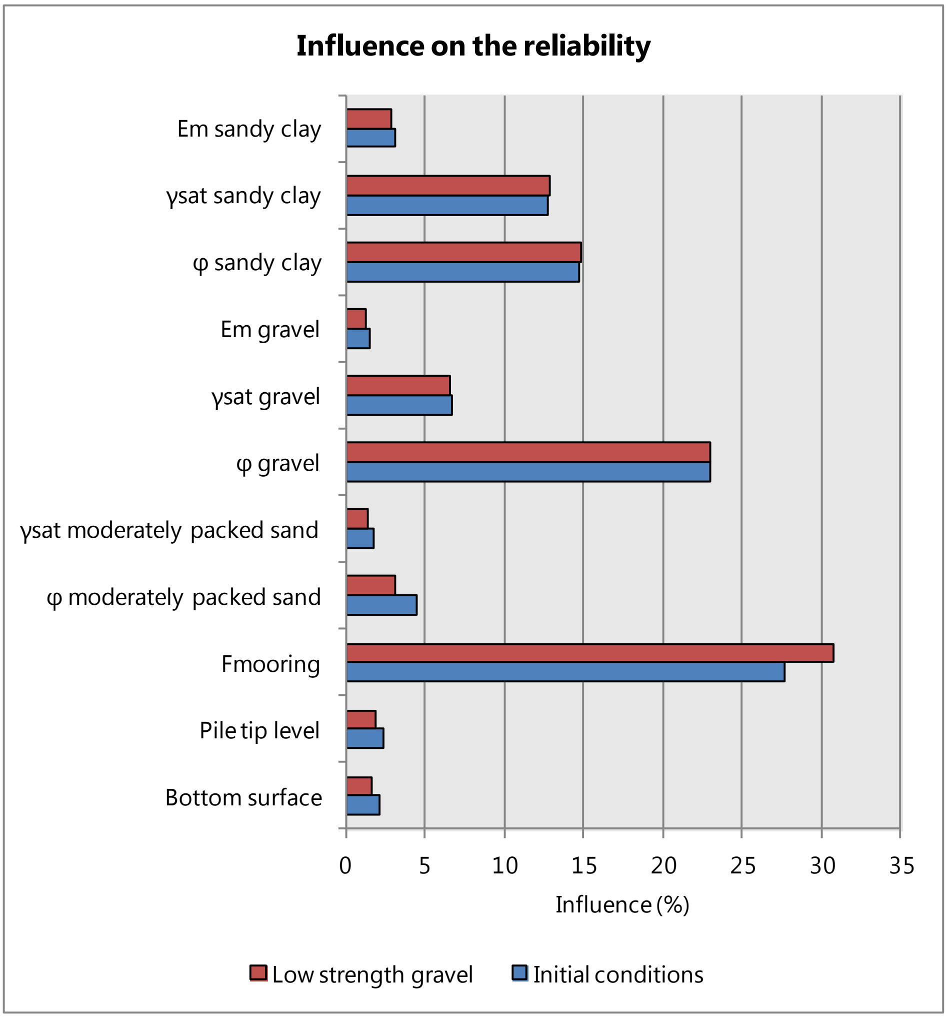

Figure 6.6 - Influence of the relevant parameters on the reliability (LS: Soil mechanical failure)

From the results of the final calculation, partial safety factors are derived with the equations given in section 6.2.2.1. Table 6.12 includes the obtained partial safety factors for both the calculated reliability and the target reliability. For the geometrical parameters it may be more relevant to express the safety by means of an absolute safety margin. For the level of the bottom surface this margin is equal to 0.12 m, whereas the pile tip level should be raised with 0.13 m.

Table 6.12 - Partial safety factors with respect to soil mechanical failure for gravel with a decreased angle of internal friction

$\beta_{calculation}$: 3.782						
β_{RC2}: 3.800						
Parameter (X_i)	**Unit**	$X_{char,i}$	X_i*	$\gamma_{calc,i}$	$X_{d,i}$	$\gamma_{RC2,i}$
$E_{m,\ sandy\ clay}$	[kN/m^2]	3344	3744	0.89	3743	0.89
$\gamma_{sat,\ sandy\ clay}$	[kN/m^3]	18	18.28	0.98	18.27	0.99
$\varphi_{sandy\ clay}$	[deg]	22.5	23.00	0.98	22.98	0.98
$E_{m,\ gravel}$	[kN/m^2]	16720	19180	0.87	19176	0.87
$\gamma_{sat,\ gravel}$	[kN/m^3]	21	21.77	0.96	21.76	0.96
φ_{gravel}	[deg]	32.5	31.83	1.02	31.80	1.02
$\gamma_{sat,\ moderately\ packed\ sand}$	[kN/m^3]	20	21.31	0.94	21.31	0.94
$\varphi_{moderately\ packed\ sand}$	[deg]	30.0	33.51	0.90	33.50	0.90
$F_{mooring}$	[kN]	2547	2725	1.07	2729	1.07
Pile tip level	[m] NAP	-36.24 (μ)	-36.11	1.00	-36.11	1.00
Bottom surface	[m] NAP	-18.16 (μ)	-18.28	0.99	-18.28	0.99

6.4 Variation 3: Modified soil structure

6.4.1 Input parameters for the soil structure

In this section, the sensitivity of the partial safety factors to a change in the soil structure is examined. From the previous evaluations it can be concluded that the soil layers which have most influence on the reliability of the structure with respect to structural failure and excessive deformations, are the upper layers of the soil structure. The influence of the soil layers with respect to these limit states decreases with increasing depth. With respect to soil mechanical failure, it appears that the influence of the unit weight of the soil is constant over the depth, whereas the influence of the angle of internal friction increases with the depth. However, this increasing influence can also be assigned to the increasing strength parameters. To be able to form a better conclusion on the influence of the different soil layers on the reliability with respect to the different limit states, the probabilistic evaluation is performed for a modified soil structure. In order to obtain the most clear results, the strongest and weakest soil layer are exchanged, resulting in a soil structure as is presented in Table 6.13. The properties of the soil layers are similar to the ones presented in Table 5.1 and Table 5.2.

Table 6.13 - Modified soil structure

Layer	**Description**	**Top of layer**
[-]	**[-]**	**[m NAP]**
1	Gravel	-18.16
2	Moderately packed sand	-28.00
3	Sandy clay	-31.00
4	Moderately packed sand	-40.00

6.4.2 Limit state evaluations

6.4.2.1 Structural failure

The results of the first probabilistic calculation regarding structural failure are included in Appendix G. These results show that most of the variables are not relevant for the reliability of the structure and can therefore be eliminated from the probabilistic evaluation. The variables which have to be included in the final calculation are:

- Angle of internal friction of gravel: φ_{gravel}
- Mooring load: $F_{mooring}$
- Yield strength of steel: f_y
- Wall thickness of the dolphin: t

The results of the final calculation are included in Table 6.14 and Figure 6.7. Remarkable is that the influence of the soil on the reliability with respect to structural failure now becomes relevant, although it is still very small. This can be explained by the fact that the influence of the variable is proportional to its standard deviation, which increases with an increasing parameter value.

Table 6.14 - Results of the final calculation for variation 3: Modified soil structure (LS: Structural failure)

Number of calculations: 111				
$\beta_{correlated}$: 4.283				
P_f: $9.221 \cdot 10^{-6}$				
Parameter (X_i)	**Unit**	**V (=σ/μ)**	**$\alpha_{correlated}$**	**X_i* (Design value)**
φ_{gravel}	[deg]	0.1	0.10	42.87
$F_{mooring}$	[kN]	0.15	-0.83	3294
f_y	[N/mm^2]	0.07	0.52	471.9
t	[mm]	0.03	0.18	39.89

Calculation	Z-value
1	56110
111	2.51

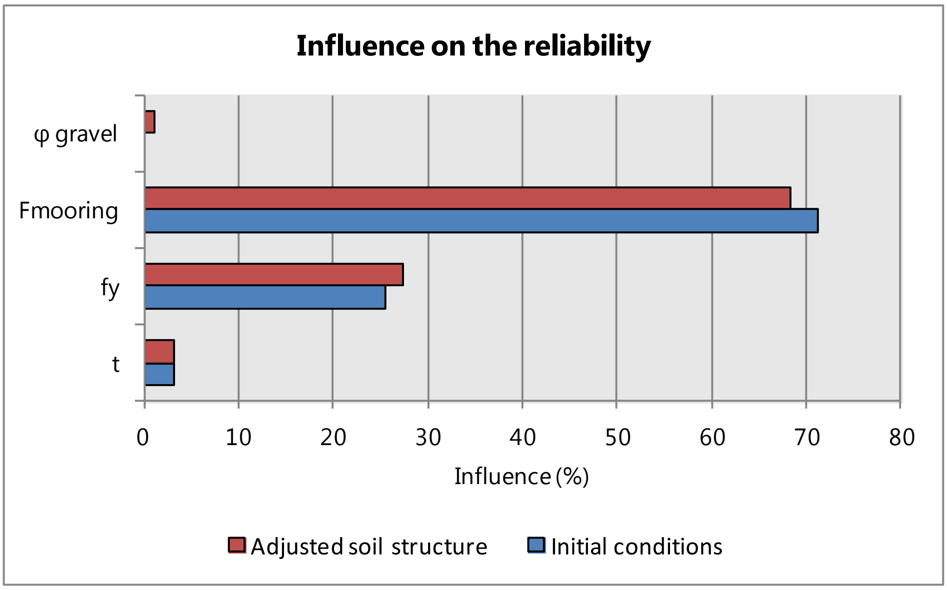

Figure 6.7 - Influence of the relevant parameters on the reliability (LS: Structural failure)

Table 6.15 presents the partial safety factors which are obtained from the results of the final calculation. For the derivation of these factors the equations are used which are presented in section 6.2.2.1.

Table 6.15 - Partial safety factors with respect to structural failure for the modified soil structure

$\beta_{calculation}$: 4.283						
β_{RC2}: 3.800						
Parameter (X_i)	**Unit**	**$X_{char,i}$**	**X_i***	**$\gamma_{calc,i}$**	**$X_{d,i}$**	**$\gamma_{RC2,i}$**
φ_{gravel}	[deg]	37.5	42.87	0.87	43.09	0.87
$F_{mooring}$	[kN]	2547	3294	1.29	3149	1.24
f_y	[N/mm^2]	483	471.9	1.02	481.8	1.00
t	[mm]	41 (μ)	39.89	1.03	40.00	1.03

6.4.2.2 Excessive deformations

Appendix G includes the results of the first probabilistic calculations regarding excessive deformations. They show that most variables do not significantly contribute to the reliability of the structure with respect to the deformations. After elimination of these variables, the following variables remain and have to be included in the final calculation:

- Saturated unit weight of gravel: $\gamma_{sat,\ gravel}$
- Angle of internal friction of gravel: φ_{gravel}
- Mooring load: $F_{mooring}$
- Level of the bottom surface

The results of the final calculation are included in Table 6.16 and Figure 6.8. They again show that regarding the soil only the variables of the upper soil layers have a significant influence on the reliability with respect to the deformations. However, the influence of this layer increases with an increasing strength. Furthermore, the influence of the mooring load decreases, because the sum of the relative influences of the variables always has to be equal to 100%.

Table 6.16 - Results of the final calculation for variation 3: modified soil structure (LS: excessive deformations)

Number of calculations: 96					
$\beta_{correlated}$: 3.612					
P_f: $1.521 \cdot 10^{-4}$					
Parameter (X_i)		**Unit**	**V (=σ/μ)**	**$\alpha_{correlated}$**	**X_i* (Design value)**
$\gamma_{sat,\ gravel}$		[kN/m^3]	0.05	0.37	21.34
φ_{gravel}		[deg]	0.1	0.67	33.97
$F_{mooring}$		[kN]	0.15	-0.62	2782
Bottom surface		[m] NAP	0.25 (σ)	0.16	-18.30
Calculation	Z-value				
1	985.9				
96	5.1				

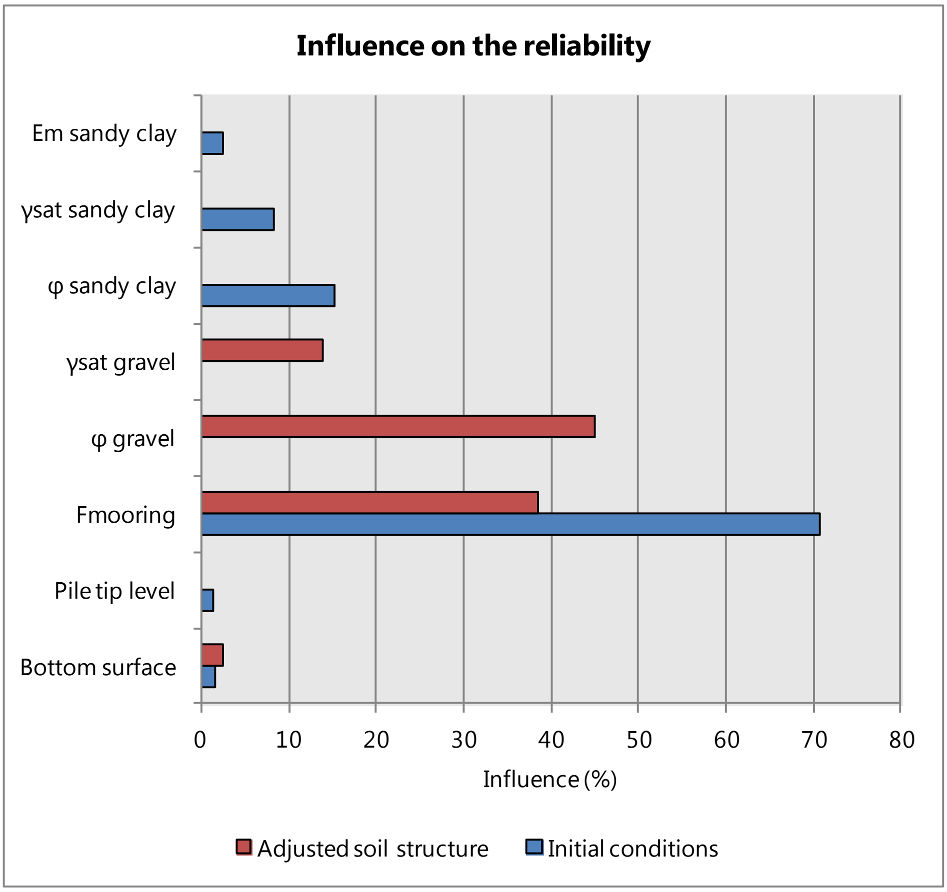

Figure 6.8 - Influence of the relevant parameters on the reliability (LS: Excessive deformations)

From the results of the final calculation, partial safety factors are determined with the equations given in section 6.2.2.1. These factors are presented in Table 6.17. Rewriting the required safety on the level of the bottom surface by means of an absolute margin, results in a required safety margin equal to 0.15 m for RC2.

Table 6.17 - Partial safety factors with respect to excessive deformations for the modified soil structure

$\beta_{calculation}$: 3.612						
β_{RC2}: 3.800						
Parameter (X_i)	**Unit**	$X_{char,i}$	X_i^*	$\gamma_{calc,i}$	$X_{d,i}$	$\gamma_{RC2,i}$
$\gamma_{sat,\ gravel}$	[kN/m^3]	21	21.34	0.98	21.26	0.99
φ_{gravel}	[deg]	37.5	33.97	1.10	33.40	1.12
$F_{mooring}$	[kN]	2547	2782	1.09	2829	1.11
Bottom surface	[m] NAP	-18.16	-18.30	0.99	-18.31	0.99

6.4.2.3 Soil mechanical failure

The limit state function for soil mechanical failure as is defined in section 4.5.4 cannot be evaluated with Prob2B, because collapse of the structure will occur before a satisfying convergence is reached. Therefore, the limit state function needs to be modified. To be able to perform the probabilistic evaluation, the critical percentage of mobilized passive resistance is reduced to 40%, while the embedded pile length is increased by 0.28 m to correct for this reduction.

The results of the probabilistic calculations for the modified soil structure in combination with the initial pile design show that the embedded length of the pile is overestimated. The reliability is equal to 5.513, which strongly deviates from the target reliability. Therefore, the pile tip level has to be altered in order to obtain accurate partial safety factors for RC2. It is found that the new pile tip level should be equal to NAP -34.0 m. The results of the first probabilistic calculations for this new design are given in Appendix G. After elimination of the irrelevant variables, it is found that the following variables have to be included in the final calculation:

- Angle of internal friction of sandy clay: $\varphi_{sandy\ clay}$
- Pressiometric modulus of gravel: $E_{m,\ gravel}$
- Saturated unit weight of gravel: $\gamma_{sat,\ gravel}$
- Angle of internal friction of gravel: φ_{gravel}
- Saturated unit weight of moderately packed sand: $\gamma_{sat,\ moderately\ packed\ sand}$
- Angle of internal friction of moderately packed sand: $\varphi_{moderately\ packed\ sand}$
- Mooring load: $F_{mooring}$
- Pile tip level
- Level of the bottom surface

The results of the final calculation are included in Table 6.18 and Figure 6.9. From these results it can be concluded that the influence of the clayey soil strongly decreases, what can be assigned to the reduction of the required embedded pile length, and therefore to the reduction of the effective thickness of the lower layer of soil. Due to the reduced effective thickness of the lower soil layer and the decreased strength of this layer, its influence on the reliability with respect to soil mechanical failure decreases. The opposite can be concluded for the upper soil layer, which influence increases as a result of the increased strength and layer thickness.

Table 6.18 - Results of the final calculation for variation 3: Modified soil structure (LS: Soil mechanical failure)

Number of calculations: 251				
$\beta_{correlated}$: 3.724				
P_f: $9.805 \cdot 10^{-5}$				
Parameter (X_i)	**Unit**	**V (=σ/μ)**	**$\alpha_{correlated}$**	**X_i* (Design value)**
$\varphi_{sandy\ clay}$	[deg]	0.10	0.17	25.18
$E_{m,\ gravel}$	[kN/m^2]	0.10	0.20	18500
$\gamma_{sat,\ gravel}$	[kN/m^3]	0.05	0.48	20.85
φ_{gravel}	[deg]	0.10	0.57	35.29
$\gamma_{sat,\ moderately\ packed\ sand}$	[kN/m^3]	0.05	0.19	21.03
$\varphi_{moderately\ packed\ sand}$	[deg]	0.10	0.32	34.26
$F_{mooring}$	[kN]	0.15	-0.45	2559
Pile tip level	[m] NAP	0.25 (σ)	-0.11	-34.18
Bottom surface	[m] NAP	0.25 (σ)	0.15	-18.30
Calculation	Z-value			
1	27.2			
251	0.1			

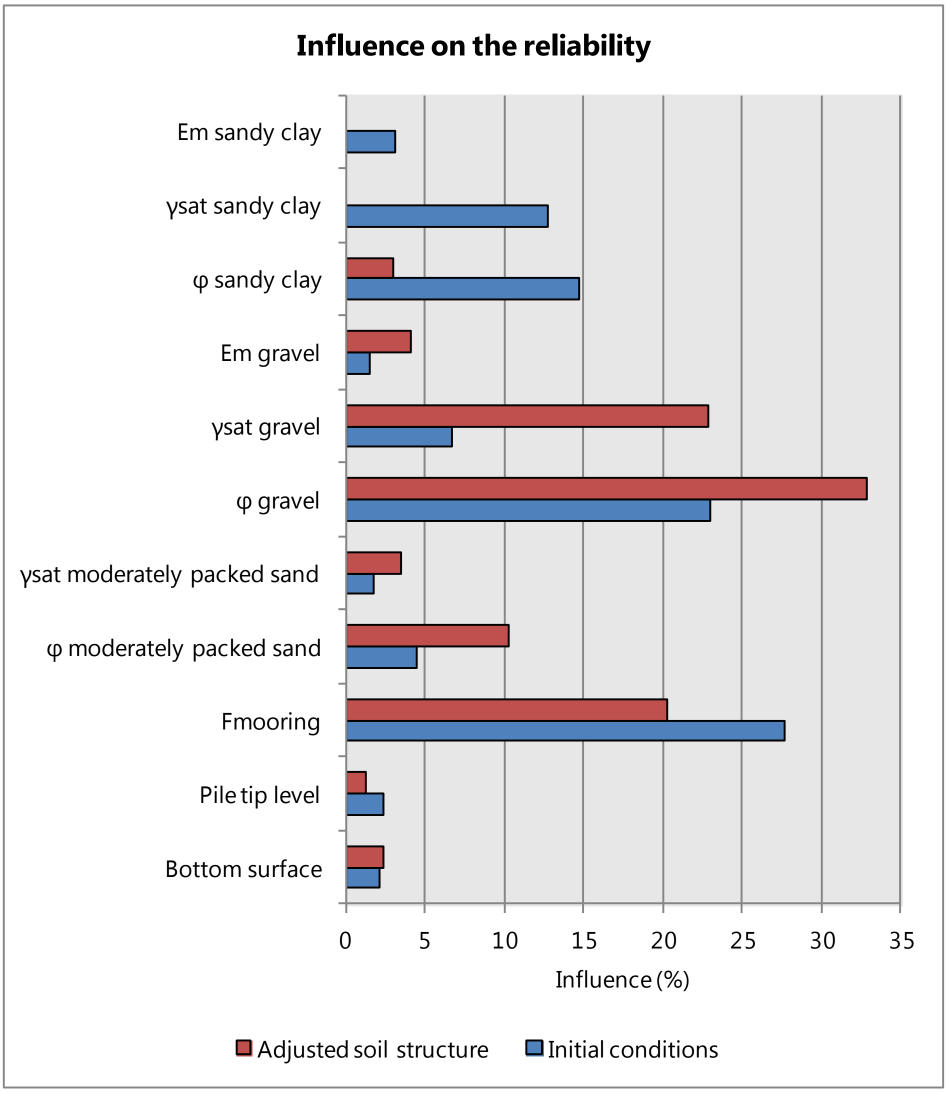

Figure 6.9 - Influence of the relevant parameters on the reliability (LS: soil mechanical failure)

From the results of the final calculation, partial safety factors are derived in a way as is described in section 6.2.2.1. The resulting partial factors for both the calculated reliability and the target reliability are presented in Table 6.19. For the geometrical parameters, these partial factors can be replaced by absolute safety margins equal to 0.14 m and 0.10 m for the level of the bottom surface and the pile tip level respectively.

Table 6.19 - Partial safety factors with respect to soil mechanical failure for the modified soil structure

$\beta_{calculation}$: 3.724

β_{RC2}: 3.800

Parameter (X_i)	Unit	$X_{char,i}$	X_i*	$\gamma_{calc,i}$	$X_{d,i}$	$\gamma_{RC2,i}$
$\varphi_{sandy\ clay}$	[deg]	22.5	25.18	0.89	25.14	0.89
$E_{m,\ gravel}$	[kN/m^2]	16720	18500	0.90	18469	0.91
$\gamma_{sat,\ gravel}$	[kN/m^3]	21	20.85	1.01	20.81	1.01
φ_{gravel}	[deg]	37.5	35.29	1.06	35.09	1.07
$\gamma_{sat,\ moderately\ packed\ sand}$	[kN/m^3]	20	21.03	0.95	21.01	0.95
$\varphi_{moderately\ packed\ sand}$	[deg]	32.5	34.26	0.95	34.17	0.95
$F_{mooring}$	[kN]	2547	2559	1.00	2572	1.01
Pile tip level	[m] NAP	-34.28 (μ)	-34.18	1.00	-34.18	1.00
Bottom surface	[m] NAP	-18.16 (μ)	-18.30	0.99	-18.30	0.99

6.5 Variation 4: Increased thickness of the intermediate sand layer

6.5.1 Input parameters for the soil structure

From the previously performed probabilistic calculations it is learned that the thickness of a soil layer affects its influence on the reliability, the influence of a soil layer appears to increase with an increasing layer thickness. This could possibly explain the small influence of the relatively thin intermediate layer of moderately packed sand. To be able to say more about the influence of the intermediate sand layer on the reliability of the structure, probabilistic calculations are performed with an increased thickness of the moderately packed sand layer. The modified soil structure is presented in Table 6.20. The values for the soil parameters are equal to the ones presented in chapter 5.

Table 6.20 - Soil structure for the modified layer thickness

Layer	Description	Top of layer
[-]	**[-]**	**[m NAP]**
1	Sandy clay	-18.16
2	Moderately packed sand	-26.00
3	Gravel	-32.00
4	Moderately packed sand	-40.00

6.5.2 Limit state evaluations

6.5.2.1 Structural failure

The results of the first probabilistic calculation regarding structural failure are included in Appendix G. These results show that many stochastic variables can be eliminated from the probabilistic evaluation, as their influence on the reliability is not significant. The variables which have to be included in the final calculation are:

- Mooring load: $F_{mooring}$
- Yield strength of steel: f_y
- Wall thickness of the dolphin: t

The results of the final calculation are included in Table 6.21 and Figure 6.10. As a consequence of the modified layer thickness, a small translation of the limit state takes place or its shape is slightly distorted. This results in a minor change of the derivatives in the design point and therefore in a minor change of the influence of the relevant variables on the reliability.

Table 6.21 - Results of the final calculation for variation 4: Increased thickness of the sand layer (LS: Structural failure)

Number of calculations: 111				
$\beta_{correlated}$: 4.034				
P_f: $2.745 \cdot 10^{-5}$				
Parameter (X_i)	**Unit**	**V (=σ/μ)**	**$\alpha_{correlated}$**	**X_i* (Design value)**
$F_{mooring}$	[kN]	0.15	-0.85	3256
f_y	[N/mm^2]	0.07	0.49	482.3
t	[mm]	0.03	0.19	39.89
Calculation	Z-value			
1	52000			
111	0.34			

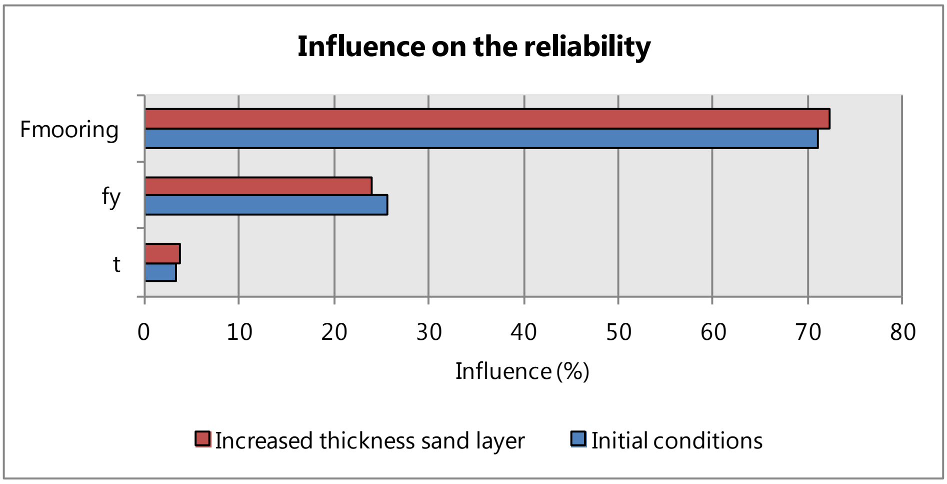

Figure 6.10 - Influence of the relevant parameters on the reliability (LS: Structural failure)

From the results of the final calculation, partial safety factors are derived for both the calculated reliability and the target reliability in accordance with RC2. For this derivation, the equations given in section 6.2.2.1 are applied. The resulting partial safety factors are presented in Table 6.22

Table 6.22 - Partial safety factors with respect to structural failure for the increased thickness of the sand layer

$\beta_{calculation}$: 4.034						
β_{RC2}: 3.800						
Parameter (X_i)	**Unit**	**$X_{char,i}$**	**X_i***	**$\gamma_{calc,i}$**	**$X_{d,i}$**	**$\gamma_{RC2,i}$**
$F_{mooring}$	[kN]	2547	3256	1.28	3190	1.25
f_y	[N/mm^2]	483	482.3	1.00	486.8	0.99
t	[mm]	41 (μ)	39.89	1.03	39.94	1.03

6.5.2.2 Excessive deformations

The results of the first probabilistic calculations regarding excessive deformations are presented in Appendix G. These results show that several variables are not relevant for the reliability of the structure with respect to excessive deformations. After elimination of these variables, the following variables remain:

- Pressiometric modulus of sandy clay: $E_{m,\ sandy\ clay}$
- Saturated unit weight of sandy clay: $\gamma_{sat,\ sandy\ clay}$
- Angle of internal friction of sandy clay: $\varphi_{sandy\ clay}$
- Pressiometric modulus of moderately packed sand: $E_{m,\ moderately\ packed\ sand}$
- Mooring load: $F_{mooring}$
- Young's modulus of the steel: E
- Wall thickness of the dolphin: t

The results of the final calculation are presented in Table 6.23 and Figure 6.11. Due to the upward shift of the boundary between the layers of sandy clay and moderately packed sand, the reliability of the structure with respect to excessive deformations increases. This is because of the higher stiffness of moderately packed sand. Furthermore, the influence of the sandy clay on the reliability decreases due to a decrease in layer thickness, whereas the influence of the moderately packed sand increases. Remarkable is that also the influence of the flexible rigidity of the pile increases as a result of the decreased thickness of the clay layer.

Table 6.23 - Results of the final calculation for variation 4: Increased thickness of the soil layer (LS: Excessive deformations)

Number of calculations: 190				
$\beta_{correlated}$: 3.861				
P_f: $5.642 \cdot 10^{-5}$				
Parameter (X_i)	**Unit**	**V (=σ/μ)**	**$\alpha_{correlated}$**	**X_i* (Design value)**
$E_{m,\ sandy\ clay}$	[kN/m^2]	0.10	0.12	3812
$\gamma_{sat,\ sandy\ clay}$	[kN/m^3]	0.05	0.23	18.73
$\varphi_{sandy\ clay}$	[deg]	0.10	0.31	23.65
$E_{m,\ moderately\ packed\ sand}$	[kN/m^2]	0.10	0.12	5337
$F_{mooring}$	[kN]	0.15	-0.89	3256
E	[kN/m^2]	0.03	0.12	207200000
t	[mm]	0.03	0.12	40.28

Calculation	Z-value	
1	782.0	
190	0.09	

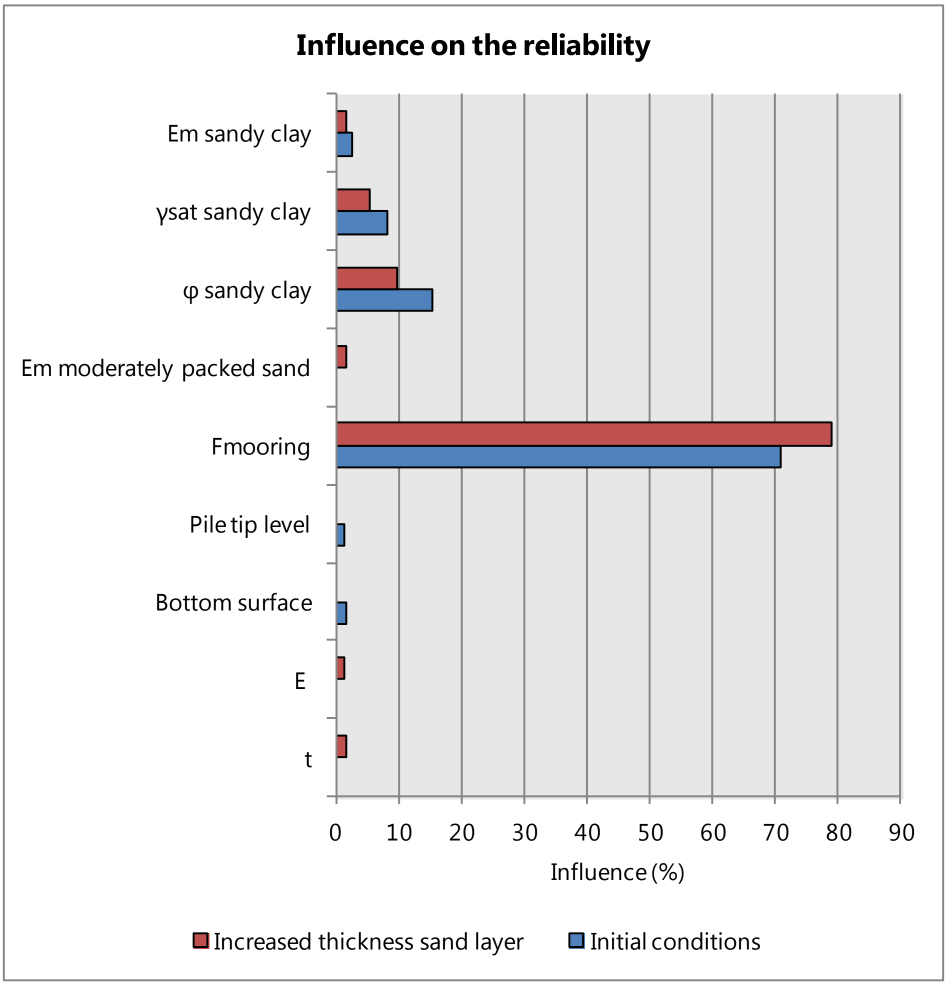

Figure 6.11 - Influence of the relevant parameters on the reliability (LS: Excessive deformations)

Table 6.24 presents the partial safety factors which are obtained from the results of the final calculation. For the derivation of these factors, the equations are used which are given in section 6.2.2.1.

Table 6.24 - Partial safety factors with respect to excessive deformations for the increased thickness of the sand layer

$\beta_{calculation}$: 3.861						
β_{RC2}: 3.800						
Parameter (X_i)	**Unit**	$X_{char,i}$	X_i^*	$\gamma_{calc,i}$	$X_{d,i}$	$\gamma_{RC2,i}$
$E_{m,\ sandy\ clay}$	[kN/m^2]	3344	3812	0.88	3814	0.88
$\gamma_{sat,\ sandy\ clay}$	[kN/m^3]	18	18.73	0.96	18.74	0.96
$\varphi_{sandy\ clay}$	[deg]	22.5	23.65	0.95	23.70	0.95
$E_{m,\ moderately\ packed\ sand}$	[kN/m^2]	4682	5337	0.88	5341	0.88
$F_{mooring}$	[kN]	2547	3256	1.28	3240	1.27
E	[kN/m^2]	199668000	207200000	0.96	207244368	0.96
t	[mm]	41 (μ)	40.28	1.02	40.29	1.02

6.5.2.3 Soil mechanical failure

To be able to perform the probabilistic evaluation regarding soil mechanical failure, the limit state function as is defined in section 4.5.4 needs to be modified. From the relation between the embedded pile length and the mobilized passive resistance it is found that the embedded pile length needs to be increased by 0.27 m in order to account for a reduction of the allowable mobilized passive resistance to 40%.

From the first probabilistic calculations for the modified soil structure in combination with the initial pile design, it can be concluded that the embedded length of the pile can be reduced. It is found that the reliability of the structure with respect to soil mechanical failure is still in compliance with RC2 for a pile tip level equal to NAP -34.5 m. The first calculation results for this modified pile length are included in Appendix G. These results show that some of the variables do not significantly contribute to the reliability, which can therefore be eliminated from the probabilistic evaluation. The variables which have to be included in the final probabilistic calculation are:

- Pressiometric modulus of sandy clay: $E_{m,\ sandy\ clay}$
- Saturated unit weight of sandy clay: $\gamma_{sat,\ sandy\ clay}$
- Angle of internal friction of sandy clay: $\varphi_{sandy\ clay}$
- Saturated unit weight of gravel: $\gamma_{sat,\ gravel}$
- Angle of internal friction of gravel: φ_{gravel}
- Saturated unit weight of moderately packed sand: $\gamma_{sat,\ moderately\ packed\ sand}$
- Angle of internal friction of moderately packed sand: $\varphi_{moderately\ packed\ sand}$
- Mooring load: $F_{mooring}$
- Pile tip level
- Level of the bottom surface

The results of the final calculation are given in Table 6.25 and Figure 6.12. It can be concluded that the influence of the intermediate sand layer increases, as a consequence of the increased layer thickness. Furthermore, the influence of the soil layers for which the thickness is reduced, becomes less significant. Due to the translation and/or deformation of the limit state, the influence of the mooring load significantly increases.

Table 6.25 - Results of the final calculation for variation 4: Increased thickness of the sand layer (LS: Soil mechanical failure)

Number of calculations: 254				
$\beta_{correlated}$: 3.854				
P_f: $5.803 \cdot 10^{-5}$				
Parameter (X_i)	**Unit**	**V (=σ/μ)**	**$\alpha_{correlated}$**	**X_i* (Design value)**
$E_{m, sandy\ clay}$	[kN/m^2]	0.10	0.14	3788
$\gamma_{sat, sandy\ clay}$	[kN/m^3]	0.05	0.30	18.49
$\varphi_{sandy\ clay}$	[deg]	0.10	0.30	23.78
$\gamma_{sat, gravel}$	[kN/m^3]	0.05	0.19	22.04
φ_{gravel}	[deg]	0.10	0.38	38.21
$\gamma_{sat, moderately\ packed\ sand}$	[kN/m^3]	0.05	0.23	20.83
$\varphi_{moderately\ packed\ sand}$	[deg]	0.10	0.40	32.88
$F_{mooring}$	[kN]	0.15	-0.60	2810
Pile tip level	[m] NAP	0.25 (σ)	-0.16	-34.61
Bottom surface	[m] NAP	0.25 (σ)	0.13	-18.29

Calculation	Z-value	
1	30.0	
254	0.09	

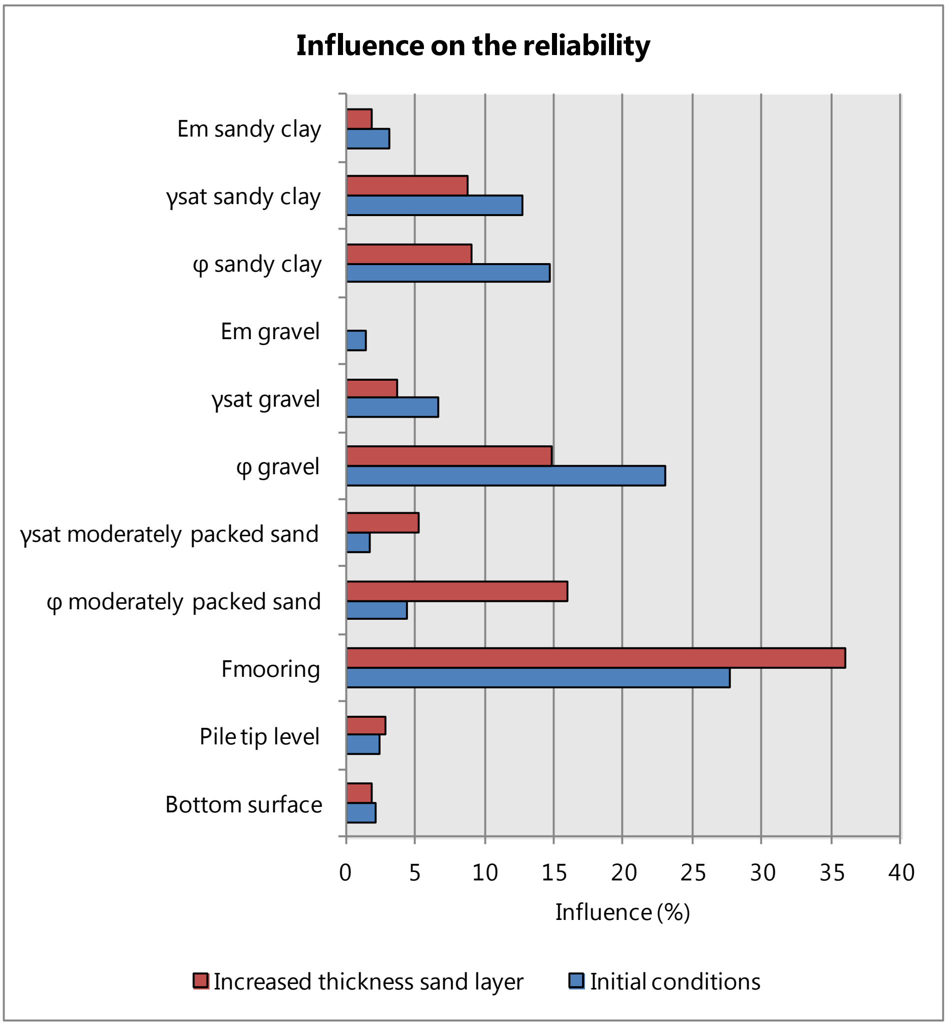

Figure 6.12 - Influence of the relevant parameters on the reliability (LS: Soil mechanical failure)

With the results of the final calculation and the equations given in section 6.2.2.1, the partial safety factors are derived for both the calculated reliability and the target reliability according to RC2. These factors are presented in Table 6.26. For the geometrical parameters it may be more convenient to express the required safety as an absolute additional margin. Translation of the relative margins to absolute margins results in required safety margins equal to 0.13 m and 0.16 m for the level of the bottom surface and the pile tip level respectively.

Table 6.26 - Partial safety factors with respect to soil mechanical failure for an increased thickness of the sand layer

$\beta_{calculation}$: 3.854

β_{RC2}: 3.800

Parameter (X_i)	Unit	$X_{char,i}$	X_i*	$\gamma_{calc,i}$	$X_{d,i}$	$\gamma_{RC2,i}$
$E_{m,\ sandy\ clay}$	[kN/m^2]	3344	3788	0.88	3791	0.88
$\gamma_{sat,\ sandy\ clay}$	[kN/m^3]	18	18.49	0.97	18.51	0.97
$\varphi_{sandy\ clay}$	[deg]	22.5	23.78	0.95	23.82	0.94
$\gamma_{sat,\ gravel}$	[kN/m^3]	21	22.04	0.95	22.05	0.95
φ_{gravel}	[deg]	37.5	38.21	0.98	38.30	0.98
$\gamma_{sat,\ moderately\ packed\ sand}$	[kN/m^3]	20	20.83	0.96	20.84	0.96
$\varphi_{moderately\ packed\ sand}$	[deg]	32.5	32.88	0.99	32.97	0.99
$F_{mooring}$	[kN]	2547	2810	1.10	2797	1.10
Pile tip level	[m] NAP	-34.77 (μ)	-34.61	1.00	-34.61	1.00
Bottom surface	[m] NAP	-18.16 (μ)	-18.29	0.99	-18.29	0.99

6.6 Variation 5: Increased coefficient of variation for the soil stiffness

6.6.1 Input parameters for the soil structure

The coefficients of variation for the soil parameters applied in the previous probabilistic evaluations are based on NEN 9997 Table 2.b. However, also the JCSS Probabilistic Model Code gives some indicative standard deviations of soil properties as a percentage of the expected mean value. Overall, these indications are in line with the coefficients of variation proposed by NEN 9997, with the exception of the variation of the soil stiffness. Whereas NEN 9997 proposes a coefficient of variation for the stiffness equal to 0.10, the Probabilistic Model Codes gives an indicative coefficient of variation between 0.20 and 1.00. Therefore, in this section the probabilistic evaluations are performed with a coefficient of variation for the soil stiffness equal to 0.30.

Due to the increased scatter, it is no longer justified to assume a normal distribution for the pressiometric modulus, as this may lead to physical inconsistencies. Therefore, for the evaluations performed in this paragraph a lognormal distribution is assumed for the stiffness parameters. Consequently, the characteristic values for the pressiometric moduli increase. The new values are presented in Table 6.27. The values for the other soil parameters are similar to their initial values, which are presented in chapter 5.

Table 6.27 - New characteristic and mean values for the pressiometric moduli

Parameter	Unit	$X_{char,i}$	V_i	μ_i
$E_{m,\ sandy\ clay}$	[kN/m^2]	3831	0.30	4000
$E_{m,\ moderately\ packed\ sand}$	[kN/m^2]	5364	0.30	5600
$E_{m,\ gravel}$	[kN/m^2]	19156	0.30	20000

6.6.2 Limit state evaluations

6.6.2.1 Structural failure

The results of the first probabilistic calculation are included in Appendix G. From these results it can be stated that many variables can be eliminated from the probabilistic evaluation, because they do not significantly contribute to the reliability with respect to structural failure. The variables which have to be included in the final calculation are:

- Mooring load: $F_{mooring}$
- Yield strength of steel: f_y
- Wall thickness of the dolphin: t

Table 6.28 and Figure 6.13 present the results of the final calculation. It was already concluded that the influence of the soil on the reliability under the considered conditions can be neglected. This means that the deviation in soil parameter values is no longer relevant, resulting in a reliability index and influence factors similar to the ones obtained for the initial conditions.

Table 6.28 - Results of the final calculation for variation 5: Increased coefficient of variation for the soil stiffness (LS: Structural failure)

Number of calculations: 89				
$\beta_{correlated}$: 4.067				
P_f: $2.383 \cdot 10^{-5}$				
Parameter (X_i)	**Unit**	**V (=σ/μ)**	**$\alpha_{correlated}$**	**X_i* (Design value)**
$F_{mooring}$	[kN]	0.15	-0.84	3257
f_y	[N/mm^2]	0.07	0.51	479.1
t	[mm]	0.03	0.18	39.94
Calculation	Z-value			
1	52300			
89	1.14			

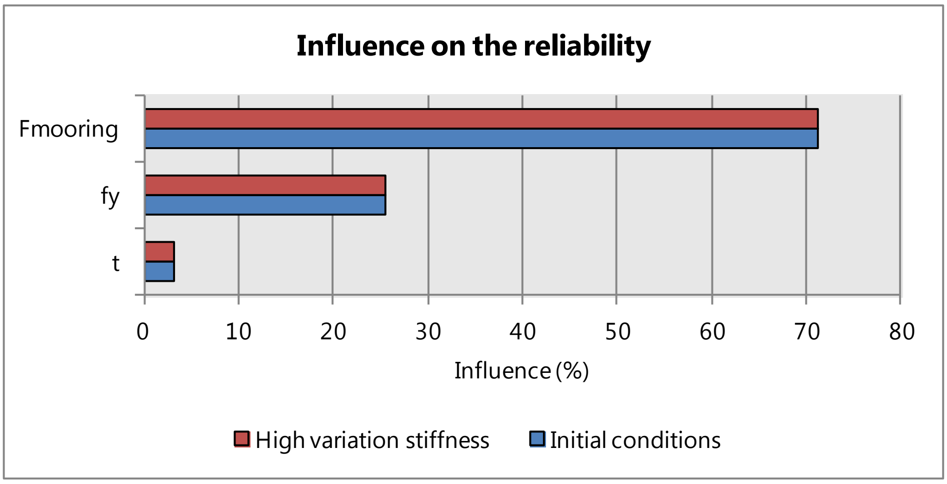

Figure 6.13 - Influence of the relevant parameters on the reliability (LS: Structural failure)

From the results of the final calculation, partial safety factors for both the calculated reliability and the target reliability are determined in accordance with section 6.2.2.1. The resulting partial factors are presented in Table 6.29 and are similar to the obtained factors for the initial conditions.

Table 6.29 - Partial safety factors with respect to structural failure for an increased coefficient of variation for the soil stiffness

$\beta_{calculation}$: 4.067

β_{RC2}: 3.800

Parameter (X_i)	Unit	$X_{char,i}$	X_i^*	$\gamma_{calc,i}$	$X_{d,i}$	$\gamma_{RC2,i}$
$F_{mooring}$	[kN]	2547	3257	1.28	3170	1.24
f_y	[N/mm^2]	483	479.1	1.01	484.4	1.00
t	[mm]	41 (μ)	39.94	1.03	40.00	1.03

6.6.2.2 Excessive deformations

Appendix G includes the results of the first probabilistic calculation with respect to excessive deformations. From these results it can be concluded that several variables can be eliminated from the probabilistic evaluation, as they do not significantly contribute to the reliability of the structure with respect to this limit state. The remaining variables which have to be included in the final calculation are:

- Pressiometric modulus of sandy clay: $E_{m,\ sandy\ clay}$
- Saturated unit weight of sandy clay: $\gamma_{sat,\ sandy\ clay}$
- Angle of internal friction of sandy clay: $\varphi_{sandy\ clay}$
- Pressiometric modulus of gravel: $E_{m,\ gravel}$
- Saturated unit weight of gravel: $\gamma_{sat,\ gravel}$
- Pressiometric modulus of moderately packed sand: $E_{m,\ moderately\ packed\ sand}$
- Mooring load: $F_{mooring}$
- Pile tip level
- Level of the bottom surface

The results of the final calculation are given in Table 6.30 and Figure 6.14. As a consequence of the increased deviation in soil stiffness, the influence of the pressiometric moduli on the reliability increases. This also results in a change of the influence of other soil parameters, due to the correlations between these parameters. Furthermore, the influence of the mooring load decreases, because the sum of the relative influences always equals 100%.

Table 6.30 - Results of the final calculations for variation 5: Increased coefficient of variation for the soil stiffness (LS: Excessive deformations)

Number of calculations: 201				
$\beta_{correlated}$: 3.206				
P_f: $6.719 \cdot 10^{-4}$				
Parameter (X_i)	**Unit**	**V (=σ/μ)**	**$\alpha_{correlated}$**	**X_i* (Design value)**
$E_{m, sandy\ clay}$	[kN/m^2]	0.30	0.21	3150
$\gamma_{sat, sandy\ clay}$	[kN/m^3]	0.05	0.30	18.66
$\varphi_{sandy\ clay}$	[deg]	0.10	0.38	23.60
$E_{m, gravel}$	[kN/m^2]	0.30	0.22	15630
$\gamma_{sat, gravel}$	[kN/m^3]	0.05	0.11	22.49
$E_{m, moderately\ packed\ sand}$	[kN/m^2]	0.30	0.14	4680
$F_{mooring}$	[kN]	0.15	-0.78	2892
Pile tip level	[m] NAP	0.25 (σ)	-0.11	-36.91
Bottom surface	[m] NAP	0.25 (σ)	0.11	-18.25

Calculation	Z-value	
1	759.6	
201	1.1	

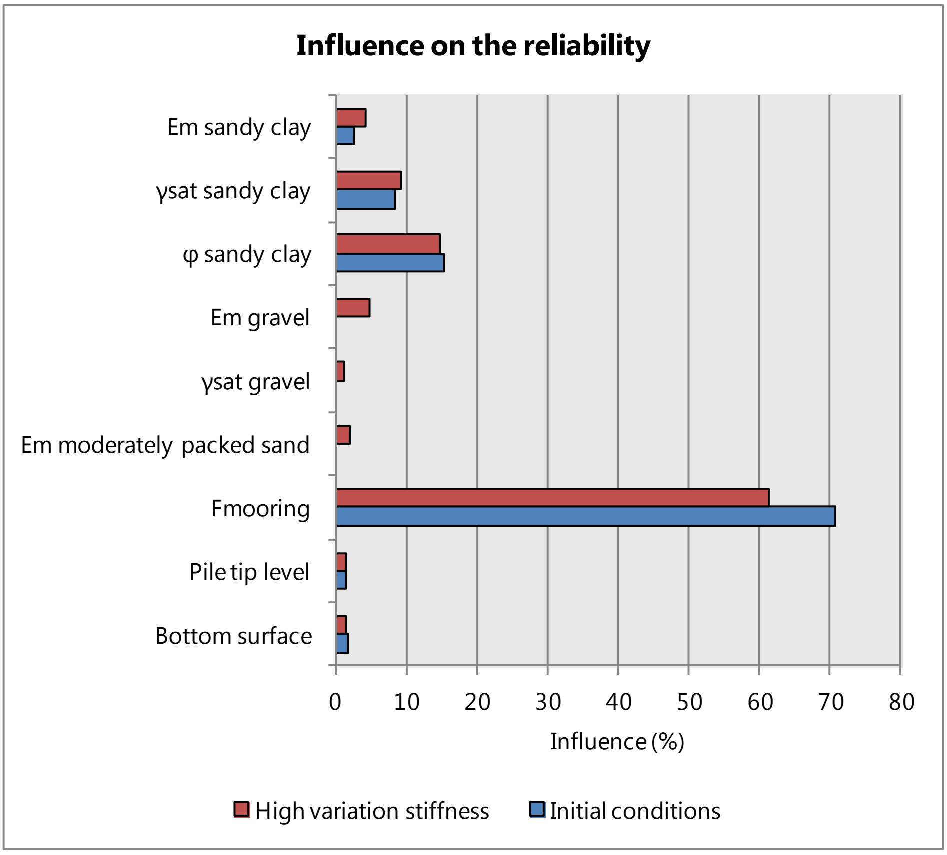

Figure 6.14 - Influence of the relevant parameters on the reliability (LS: Excessive deformations)

From the results of the final calculation, partial safety factors are derived in accordance with section 6.2.2.1. The resulting factors are presented in Table 6.31. Noteworthy are the high partial factors for the pressiometric moduli, what is a consequence of the large spread in the stiffness of the soil. For the geometrical parameters it may be more convenient to express the required additional safety by means of an absolute margin, which should be equal to 0.11 m for both the pile tip level and the level of the bottom surface.

Table 6.31 - Partial safety factors with respect to excessive deformations for an increased coefficient of variation for the soil stiffness

$\beta_{calculation}$: 3.206						
β_{RC2}: 3.800						
Parameter (X_i)	**Unit**	**$X_{char,i}$**	**X_i***	**$\gamma_{calc,i}$**	**$X_{d,i}$**	**$\gamma_{RC2,i}$**
$E_{m,\ sandy\ clay}$	[kN/m^2]	3831	3150	1.22	3038	1.26
$\gamma_{sat,\ sandy\ clay}$	[kN/m^3]	18	18.66	0.96	18.48	0.97
$\varphi_{sandy\ clay}$	[deg]	22.5	23.60	0.95	22.99	0.98
$E_{m,\ gravel}$	[kN/m^2]	19156	15630	1.23	15053	1.27
$\gamma_{sat,\ gravel}$	[kN/m^3]	21	22.49	0.93	22.42	0.94
$E_{m,\ moderately\ packed\ sand}$	[kN/m^2]	5364	4680	1.15	4564	1.18
$F_{mooring}$	[kN]	2547	2892	1.14	3080	1.21
Pile tip level	[m] NAP	-37 (μ)	-36.91	1.00	-36.89	1.00
Bottom surface	[m] NAP	-18.16 (μ)	-18.25	1.00	-18.27	0.99

6.6.2.3 Soil mechanical failure

The limit state function for soil mechanical failure as is defined in section 4.5.4 cannot be evaluated with Prob2B, because the structure will collapse before a satisfying convergence is reached. Therefore, modification of the limit state function is required. It is found that the critical percentage of mobilized passive resistance needs to be reduced to 40%, in order for Prob2B to complete the evaluation. To correct for this reduction, the embedded pile length is increased by 0.13 m.

From the first probabilistic calculations it is found that the reliability of the structure is much higher than the target reliability. Therefore, the pile tip level has to be altered in order to obtain more accurate partial safety factors for reliability class 2. It is found that the embedded pile length needs to be decreased by 2.0 m, resulting in a pile tip level equal to NAP -35.0 m. The results of the first probabilistic calculation for this shortened pile are included in Appendix G. They show that some of the variables do not significantly contribute to the reliability of the structure. After elimination of these irrelevant variables, the following variables remain:

- Pressiometric modulus of sandy clay: $E_{m,\ sandy\ clay}$
- Saturated unit weight of sandy clay: $\gamma_{sat,\ sandy\ clay}$
- Angle of internal friction of sandy clay: $\varphi_{sandy\ clay}$
- Saturated unit weight of gravel: $\gamma_{sat,\ gravel}$
- Angle of internal friction of gravel: φ_{gravel}
- Saturated unit weight of moderately packed sand: $\gamma_{sat,\ moderately\ packed\ sand}$
- Angle of internal friction of moderately packed sand: $\varphi_{moderately\ packed\ sand}$
- Mooring load: $F_{mooring}$
- Pile tip level
- Level of the bottom surface

Influence factors are proportional to the deviation of the parameter value from its mean value. Therefore, it is expected that the influence of the pressiometric moduli on the reliability of the structure increases. However, this is not what is shown be the results of the final calculation, which are presented in Table 6.32 and Figure 6.15. The influence of the different variables on the reliability with respect to soil mechanical failure hardly changes. This is most likely caused by the adaptation of the type of distribution for the stiffness parameters from normal to lognormal.

Table 6.32 - Results of the final calculation for variation 5: Increased coefficient of variation for the soil stiffness (LS: Soil mechanical failure)

Number of calculations: 210					
$\beta_{correlated}$: 3.802					
P_f: $7.170 \cdot 10^{-5}$					
Parameter (X_i)		**Unit**	**V (=σ/μ)**	**$\alpha_{correlated}$**	**X_i* (Design value)**
$E_{m,\ sandy\ clay}$		[kN/m^2]	0.10	0.17	3160
$\gamma_{sat,\ sandy\ clay}$		[kN/m^3]	0.05	0.35	18.29
$\varphi_{sandy\ clay}$		[deg]	0.10	0.38	22.99
$\gamma_{sat,\ gravel}$		[kN/m^3]	0.05	0.27	21.71
φ_{gravel}		[deg]	0.10	0.48	36.62
$\gamma_{sat,\ moderately\ packed\ sand}$		[kN/m^3]	0.05	0.13	21.25
$\varphi_{moderately\ packed\ sand}$		[deg]	0.10	0.21	35.74
$F_{mooring}$		[kN]	0.15	-0.54	2700
Pile tip level		[m] NAP	0.25 (σ)	-0.15	-34.99
Bottom surface		[m] NAP	0.25 (σ)	0.15	-18.30
Calculation	Z-value				
1	31.0				
254	0.03				

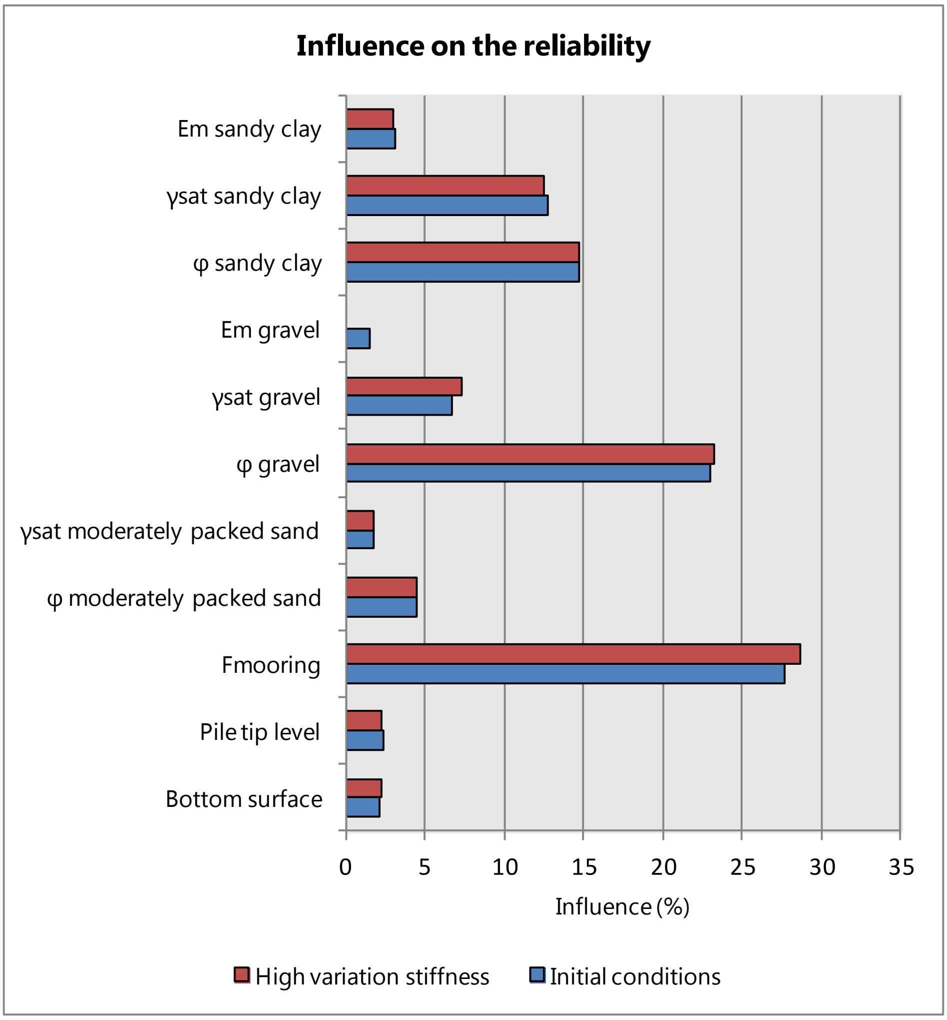

Figure 6.15 - Influence of the relevant parameters on the reliability (LS: Soil mechanical failure)

From the results of the final calculation, partial safety factors are derived for both the calculated reliability and the target reliability in a manner as is elaborated in section 6.2.2.1. The obtained factors are presented in Table 6.33. For the geometrical parameters it may be more convenient to express the required safety by means of an absolute margin. According to this probabilistic evaluation, these margins are equal to 0.14 m for both the pile tip level and the level of the bottom surface.

Table 6.33 - Partial safety factors with respect to soil mechanical failure for an increased coefficient of variation for the soil stiffness

$\beta_{calculation}$: 3.802						
β_{RC2}: 3.800						
Parameter (X_i)	**Unit**	**$X_{char,i}$**	**X_i***	**$\gamma_{calc,i}$**	**$X_{d,i}$**	**$\gamma_{RC2,i}$**
$E_{m,\ sandy\ clay}$	[kN/m^2]	3344	3160	1.21	3161	1.21
$\gamma_{sat,\ sandy\ clay}$	[kN/m^3]	18	18.29	0.98	18.29	0.98
$\varphi_{sandy\ clay}$	[deg]	22.5	22.99	0.98	22.99	0.98
$\gamma_{sat,\ gravel}$	[kN/m^3]	21	21.71	0.97	21.71	0.97
φ_{gravel}	[deg]	37.5	36.62	1.02	36.62	1.02
$\gamma_{sat,\ moderately\ packed\ sand}$	[kN/m^3]	20	21.25	0.94	21.25	0.94
$\varphi_{moderately\ packed\ sand}$	[deg]	32.5	35.74	0.91	35.74	0.91
$F_{mooring}$	[kN]	2547	2700	1.06	2699	1.06
Pile tip level	[m] NAP	-35.13 (μ)	-34.99	1.00	-34.99	1.00
Bottom surface	[m] NAP	-18.16 (μ)	-18.30	0.99	-18.30	0.99

6.7 Overview of the results

6.7.1 Structural failure

Table 6.34 gives an overview of the obtained partial safety factors for RC2 with respect to structural failure. From these results it can be concluded that the reliability of flexible dolphins with respect to structural failure is mainly defined by the mooring load and the structural parameters. The soil hardly has any influence on the reliability on the structure. Only the most upper soil layers have a small influence on the reliability, which becomes significant when the layer has a high strength. Furthermore, it can be concluded that the results with respect to structural failure are hardly sensitive to changes in the soil structure.

Table 6.34 - Overview of the partial safety factors with respect to structural failure in accordance with RC2

Parameter	**Variation**					
	0	**1**	**2**	**3**	**4**	**5**
	Initial conditions	**Increased cohesion for sandy clay**	**Decreased angle of friction for gravel**	**Modified soil structure**	**Increased thickness of the intermediate sand layer**	**Increased coefficient of variation for the soil stiffness**
φ_{gravel}	-	-	-	0.87	-	-
$F_{mooring}$	1.24	1.23	1.24	1.24	1.25	1.24
f_y	1.00	1.01	1.00	1.00	0.99	1.00
t	1.03	1.03	1.03	1.03	1.03	1.03

6.7.2 Excessive deformations

Table 6.35 gives an overview of the obtained partial safety factors for RC2 with respect to excessive deformations. From these results it can be concluded that the mooring load has the largest influence on the reliability with respect to excessive deformations. With respect to the soil parameters it can be concluded that only the upper soil layers are relevant for the reliability of the structure. Furthermore, it can be concluded that the partial safety factors are most sensitive to changes in the soil structure. When the upper soil layer has a high strength, the influence of this layer increases and the influence of the load parameter decreases. As a result, a smaller partial safety factor for the mooring load is obtained for variation 3.

Table 6.35 - Overview of the partial safety factors with respect to excessive deformations in accordance with RC2

Parameter	**Variation**					
	0	**1**	**2**	**3**	**4**	**5**
	Initial conditions	**Increased cohesion for sandy clay**	**Decreased angle of friction for gravel**	**Modified soil structure**	**Increased thickness of the intermediate sand layer**	**Increased coefficient of variation for the soil stiffness**
$c_{\text{sandy clay}}$	-	0.81	-	-	-	-
$E_{\text{m, sandy clay}}$	0.89	0.93	0.89	-	0.88	1.26
$\gamma_{\text{sat, sandy clay}}$	0.97	0.98	0.97	-	0.96	0.97
$\varphi_{\text{sandy clay}}$	0.98	0.92	0.98	-	0.95	0.98
$E_{\text{m, gravel}}$	-	-	-	-	-	1.27
$\gamma_{\text{sat, gravel}}$	-	-	-	0.99	-	0.94
φ_{gravel}	-	-	-	1.12	-	-
$E_{\text{m, mod. sand}}$	-	-	-	-	0.88	1.18
F_{mooring}	1.24	1.23	1.24	1.11	1.27	1.21
Pile tip level	1.00	1.00	1.00	-	-	1.00
Bottom surface	0.99	0.99	0.99	0.99	-	0.99
E	-	-	-	-	0.96	-
t	-	-	-	-	1.02	-

6.7.3 Soil mechanical failure

Table 6.36 presents the partial safety factors for RC2 with respect to soil mechanical failure. It can be concluded that the load parameter is still important for the reliability of the structure. However, in comparison with the results for the other limit state functions, it can be concluded that its influence is smaller. From the table it can also be concluded that the angle of internal friction of the soil layers and the load parameter are most sensitive to changes in the soil structure.

Table 6.36 - Overview of the partial safety factors with respect to soil mechanical failure in accordance with RC2

Parameter	**Variation**					
	0	**1**	**2**	**3**	**4**	**5**
	Initial conditions	**Increased cohesion for sandy clay**	**Decreased angle of friction for gravel**	**Modified soil structure**	**Increased thickness of the intermediate sand layer**	**Increased coefficient of variation for the soil stiffness**
$c_{sandy\ clay}$	-	0.79	-	-	-	-
$E_{m,\ sandy\ clay}$	0.90	0.92	0.89	-	0.88	1.21
$\gamma_{sat,\ sandy\ clay}$	0.98	1.00	0.99	-	0.97	0.98
$\varphi_{sandy\ clay}$	0.98	0.94	0.98	0.89	0.94	0.98
$E_{m,\ gravel}$	0.88	-	0.87	0.91	-	-
$\gamma_{sat,\ gravel}$	0.97	0.96	0.96	1.01	0.95	0.97
φ_{gravel}	1.02	0.98	1.02	1.07	0.98	1.02
$\gamma_{sat,\ mod.\ sand}$	0.94	0.94	0.94	0.94	0.96	0.94
$\varphi_{mod.\ sand}$	0.91	0.90	0.90	0.90	0.99	0.91
$F_{mooring}$	1.05	1.10	1.07	1.01	1.10	1.06
Pile tip level	1.00	1.00	1.00	1.00	1.00	1.00
Bottom surface	0.99	0.99	0.99	0.99	0.99	0.99

7

CONCLUSIONS AND RECOMMENDATIONS

7.1 Conclusions

In this section the results of this master thesis will be discussed in the light of the research questions which were defined in chapter 1. Finally, a set of partial safety factors is recommended for the design of flexible mooring dolphins.

Frequently applied models and guidelines

With the help of the literature review an overview could be obtained of the different design models which are frequently used in Dutch dolphin design. It is found that the different models became more advanced and complex over time. The oldest model is based on empirical relations, which is the method of Blum. It can be concluded that this model is very limited, what makes that it is merely used for preliminary design of dolphins.

The main difference between the more advanced models is the way in which the soil is modelled. With D-Sheet Piling (Single Pile module) the soil is modelled by bi-linear springs and the ultimate soil resistance is determined in accordance with Brinch-Hansen. The soil springs in D-Pile Group are non-linear. They can be user-defined or defined by *API*, with which it is also possible to consider undrained soil behaviour. The most advance method is the finite element method. In Plaxis 3D different models can be used to approach the behaviour of the soil. For different soil layers the model can be applied which approximates the behaviour of that specific soil best.

The codes and guidelines which are most prevalent in Dutch dolphin design are NEN 9997, EAU 2012, BS 6349 and PIANC 2002. These codes and guidelines are based on the Eurocode, but all fill in the blanks in different ways. Each of these codes and guidelines prescribe the use of different design approaches, resulting in different sets of partial safety factors.

Starting points

To be able to obtain the most accurate partial safety factors, it is required to use the model which gives the best approximation of the behaviour of laterally loaded piles. Therefore, a comparison is made between the physical models which are most eligible for dolphin design, namely Plaxis 3D, D-Sheet Piling and D-Pile Group. Verhoef (2015) showed that Plaxis 3D is the most accurate model, it gives the best approximation of the behaviour of laterally loaded piles.

During this master thesis, a more extensive comparison was made between the two spring models, D-Sheet Piling and D-Pile Group. The starting points for this comparison were the results obtained from the performed full scale tests. During these tests the behaviour of laterally loaded piles was measured while they were subjected to static and dynamic loadings. From the results of these tests it can be concluded that the behaviour of a pile which is subjected to a dynamic lateral load quickly approaches the behaviour of a pile which is subjected to a static lateral load when the duration of the dynamic load increases. From the tests it was also found that the level of the maximum bending moment is higher than was expected based on the models.

The two spring models were compared based on the bending moments which developed in the pile and the pile deformations. From this comparison it can be concluded that D-Sheet Piling and D-Pile Group show a similar behaviour of the pile with respect to the development of the bending moments. Both models tend to overestimate the bending moments and the depth at which they occur. Regarding the pile deformations it was found that D-Sheet Piling overestimates the displacements, whereas D-Pile Group gives a more accurate approximation. However, under some circumstance D-Pile Group underestimates the pile deformations and it therefore overestimates the reliability of the structure.

Table 7.1 - Comparison of the software models ('-' = least suitable; '+'= most suitable)

Criterion	**D-Sheet Piling**	**D-Pile Group**	**Plaxis 3D**
Complexity	+	+	-
Input parameters	+	o	-
Calculation time	+	+	-
Model output – bending moments	-	-	+
Model output – displacements	-	o	+

Comparison of the three models shows that Plaxis 3D is the most accurate model. However, because of the limitations of the model and the lack of probabilistic tools, Plaxis 3D is not considered to be most appropriate model for this master thesis. From the comparison between the other two models, it was concluded that D-Sheet Piling is most suitable for the intended research.

There are several methods available to perform a reliability analysis for flexible dolphins. The level III-methods, e.g. Monte Carlo simulations, are fully probabilistic. With these methods the reliability of the structure can be determined most accurate. However, level III-methods cannot be used to determine the influence factors of the parameters, which are important factors for the derivation of partial safety factors. These influence factors can be determined with level II-calculations (FORM), which is therefore considered more appropriate for this master thesis. Because many different variables are involved in flexible dolphin design, it was not desirable to perform the reliability analysis by hand. Therefore, the probabilistic toolbox Prob2B is used to perform the FORM-calculations.

In order to perform the probabilistic evaluation, first the limit state functions had to be derived for the relevant failure mechanisms. The mechanisms which are considered most relevant are structural failure of the cross-section of the pile, excessive deformations and soil mechanical failure. According to Eurocode, the cross-sectional verification should be based on the elastic capacity of the pile, because flexible dolphins can most frequently be classified as class 3 or class 4 piles. However, from the performed full scale tests it can be concluded that the cross-sectional elastic capacity of laterally loaded piles is much higher than the elastic capacity, which can be explained by the residual capacity of the cross-section after yielding of the outer fibre and by the influence of the confined soil in the pile.

Influence of the parameters

The probabilistic evaluation of a flexible mooring dolphin was based on three different failure mechanisms, namely structural failure of the dolphin, excessive deformations and soil mechanical failure. The probabilistic calculations with respect these limit states were performed for a dolphin design from practice. After, the evaluation of the initial mooring dolphin design, modifications were introduced to the soil structure, to examine the sensitivity of the influence factors and partial factors to different soil structures.

From the probabilistic evaluations with respect to structural failure, it can be concluded that the mooring load has the largest influence on the reliability of the structure. In addition, the yield strength of the steel and the wall thickness also have a significant influence on the reliability. Furthermore, it can be concluded that only the soil above the level of the maximum bending moment in the pile has a small influence on the reliability, which in most situations can be disregarded. The sensitivity analysis shows, that the reliability of flexible mooring dolphins with respect to structural failure and the influence factors for the relevant parameters are hardly affected by changes in the soil structure. It can only be concluded that the influence of the top layer of the soil on the reliability increases as the strength increases. However, the influence of the soil still remains rather small.

From the probabilistic evaluations with respect to excessive deformations, it can also be concluded that the mooring load has a very large influence on the reliability of flexible dolphins. Furthermore, it can be concluded that resistance against deformations of the pile is mainly determined by the upper layers of the soil. Of the relevant soil parameters, the angle of internal friction has the largest influence on the reliability with respect to deformations. The sensitivity analysis shows that a redistribution of the influence factors for the soil parameters takes place, when the cohesion of the upper soil layer increases. As the influence of the cohesion increases, the influence of the angle of internal friction of the layer strongly decreases as a result of the negative correlations. Furthermore, it can be concluded that the influence of the upper soil layers is strongly influenced by the strength of the layer. An increasing strength results in an increasing influence of the soil layer. Simultaneously, the influence of the load on the reliability strongly decreases. Finally, it can be concluded that influence factors of the upper soil layers are sensitive for a change in layer thickness. The influence of the soil parameters reduces with a decreasing layer thickness, and vice versa. For a certain thickness of the top layer, the influence of the underlying layer will also become significant. However, this point is not further investigated.

With respect to soil mechanical failure it can be concluded that the mooring load still has a considerable influence on the reliability of flexible mooring dolphins. However, in comparison with the other failure mechanisms, the influence of the load has decreased. Furthermore, it can be concluded that the lower soil layers which are located near the pile tip level have a large influence on the reliability, as well as the weight of the overlying soil layers. However, when the soil layer near the pile tip becomes cohesive, its influence decreases. Furthermore, it can be concluded that influence of a soil layer increases with increasing thickness. However, the sensitivity to changing layer thickness is marginal, as well as the sensitivity to changing soil parameters.

It should be noted that the distribution of the mooring load is mainly based on assumptions. This means that it may be possible that, for example, the coefficient of variation for the mooring load is smaller than is assumed. Consequently, the influence of the load on the reliability would most likely decrease, resulting in a larger influence of the other variables.

Recommended partial factors

From the results obtained from the FORM-calculations, the required partial safety factors for the parameters involved in flexible dolphin design were derived. Even though it was concluded that changes in the soil structure results in a minor change in influence factors, most of these change do not result in changes in the required partial factors. From the obtained results it can be concluded that only a major change in the sequence of the different soil layers introduces an alteration in required safety factors, as well as a change in the coefficients of variation.

The partial safety factors which are recommended for flexible mooring dolphin design in accordance with RC2 are presented in Table 7.2 to Table 7.5. Most of these partial factors should be applied on the characteristic parameter values, which is defined as the 5% upper bound for the extreme mooring load and the 5% lower bound for the soil parameters and the Young's modulus of steel. For the yield strength the characteristic value is defined as the 2.5% lower bound. For the wall thickness, the pile diameter and the geometrical parameters it is not common to define characteristic parameter values, the safety factors can directly be applied on the mean parameter value.

Table 7.2 - Recommended partial safety factors for load parameters

Parameter	γ_{RC2}
Mooring load	1.30

Table 7.3 - Recommended partial safety factor for soil parameters

Parameter	γ_{RC2}
Cohesion	1.00
Angle of internal friction	1.15
Unit soil weight	1.00
Soil stiffness	1.30

Table 7.4 - Recommended partial safety factors for structural parameters

Parameter	γ_{RC2}
Yield strength	1.00
Wall thickness	1.05
Pile diameter	1.00
Young's modulus	1.00

Table 7.5 - Recommended partial safety factors for geometrical parameters

Parameter	γ_{RC2}	**Absolute margin**
Level of the bottom surface	1.00	0.15
Pile tip level	1.00	0.25

7.2 Recommendations

7.2.1 Recommendations on model input

- From the performed evaluations it can be concluded that the mooring load has a very large influence on the reliability of flexible mooring dolphins. However, there is still a lot of indistinctness about the exact probabilistic properties of this load. Because it is likely that an alternation of the mooring load distribution would result in different influence factors, it may be important to perform more research on the behaviour of moored vessels and on the variation of the mooring loads which are exerted on dolphins.
- In this master thesis only flexible mooring dolphins are considered. However, because the distribution for berthing forces may deviate from the mooring load distribution, it is recommended to also perform probabilistic evaluations for breasting dolphins. For these evaluations it is recommended to consider the berthing energy instead of the berthing force.
- In this master thesis, the probabilistic evaluations with respect to structural failure are based on the elastic cross-sectional verification according to NEN-EN 1993-1-1. However, research prevails that the cross-sectional verification according to the modified Gresnigt method is more accurate, as is also discussed in section 4.5.2. Therefore, it is recommended to examine whether both verification methods will result in similar partial factors.
- To be able to perform the probabilistic evaluation with respect to soil mechanical failure, a modification of the limit state was required. However, due to the non-linear relation between the embedded pile length and the mobilized passive resistance, some small inaccuracies may be introduced. These inaccuracies may increase as the required extension of the pile length increases. Therefore, it should be checked if the introduced inaccuracies have a significant influence on the results of the probabilistic evaluations.

7.2.2 Model uncertainties

- From the comparison of the available models with the results obtained from the performed tests, it was found that D-Sheet Piling tends to overestimate the bending moments in and the deformations of laterally loaded piles, resulting in an underestimation of the reliability. Furthermore, it was concluded that Plaxis 3D gives a better approximation of the behaviour of laterally loaded piles. Therefore, it is recommended to perform some probabilistic calculations with Plaxis 3D, as this will result in a more accurate reliability.
- With D-Sheet Piling it is not possible to consider sloping bottom surfaces. However Verhoef (2015) showed that a sloping bottom surface influences the behaviour of laterally loaded piles. Therefore, it is recommended to perform probabilistic calculations with a model in which sloping surfaces can be considered, e.g. Plaxis 3D.
- Due to the simplicity of the model, different inaccuracies are introduced. Therefore, it is recommended to perform future reliability analysis for flexible dolphins with more advanced models. However, more advanced models on their turn also introduce inaccuracies. For some of the input parameters of the advanced models, it is often not unambiguously defined how they should be determined. An increase in required input parameters, therefore also introduces a larger inaccuracies for the results.

7.2.3 Partial safety factors

- Based on the results of the performed evaluations, it was recommended to apply a safety factor equal to 1.05 on the mean wall thickness of the pile. However, in practice it is more common to apply a material factor on the strength parameters of the steel. Therefore, it is desirable to reduce the partial safety factor for the wall thickness to 1.00. As the required partial safety factors are all rounded up, it is expected that this will not cause any problems. However, this should be verified by performing some design calculations.

A

BRINCH-HANSEN AND MÉNARD FOR D-SHEET PILING

A.1 Brinch-Hansen

The passive earth pressure according to Brinch-Hansen is defined by (Brinch-Hansen & Christensen, 1961):

$$\sigma_p = K_q \cdot \sigma_v' + K_c \cdot c, \quad \sigma_a = 0, \quad \sigma_n = 0 \tag{A.1}$$

In this equation K_q and K_c are factors of Brinch-Hansen for piles:

$$K_q = \frac{K_q^0 + K_q^\infty \cdot \alpha_q \cdot \frac{D}{B}}{1 + \alpha_q \cdot \frac{D}{B}} \tag{A.2}$$

$$K_c = \frac{K_c^0 + K_c^\infty \cdot \alpha_c \cdot \frac{D}{B}}{1 + \alpha_c \cdot \frac{D}{B}} \tag{A.3}$$

In which:

D	=	The average depth at the middle of the soil layer [m]
B	=	Diameter of the pile [m]

And where:

$$K_q^0 = e^{\left(\frac{\pi}{2}+\varphi\right)\cdot\tan\varphi} \cdot \cos\varphi \cdot \tan\left(\frac{\pi}{4} + \frac{\varphi}{2}\right) - e^{\left(-\frac{\pi}{2}+\varphi\right)\cdot\tan\varphi} \cdot \cos\varphi \cdot \tan\left(\frac{\pi}{4} - \frac{\varphi}{2}\right)$$

$$K_c^0 = \left[e^{\left(\frac{\pi}{2}+\varphi\right)\cdot\tan\varphi} \cdot \cos\varphi \cdot \tan\left(\frac{\pi}{4} + \frac{\varphi}{2}\right) - 1\right] \cdot \cot\varphi$$

$$K_q^\infty = K_c^\infty \cdot K_0 \cdot \tan\varphi$$

$$K_c^\infty = N_c \cdot d_c^\infty$$

$$d_c^\infty = 1.58 + 4.09 \cdot \tan^4\varphi$$

$$N_c = \left[e^{\pi \cdot \tan\varphi} \cdot \tan^2\left(\frac{\pi}{4} + \frac{\varphi}{2}\right) - 1\right] \cdot \cot\varphi$$

$$K_0 = 1 - \sin\varphi$$

$$\alpha_q = \frac{K_q^0}{K_q^\infty - K_q^0} \cdot \frac{K_0 \cdot \sin\varphi}{\sin\left(\frac{\pi}{4} + \frac{\varphi}{2}\right)}$$

$$\alpha_c = \frac{K_c^0}{K_c^\infty \cdot K_c^0} \cdot 2\sin\left(\frac{\pi}{4} + \frac{\varphi}{2}\right)$$

A.2 Ménard

The modulus of horizontal subgrade reaction according to Ménard is defined by (Ménard, et al., 1971):

$$\frac{1}{k_h} = \begin{cases} \frac{1}{3E_m}\left[1.3R_0\left(2.65\frac{R}{R_0}\right)^\alpha + \alpha R\right] & if \quad R \geq R_0 \\ \frac{2R}{E_m} \cdot \frac{4(2.65)^\alpha + 3\alpha}{18} & if \quad R < R_0 \end{cases} \tag{A.4}$$

In which:

k_h	= Modulus of horizontal subgrade reaction
E_m	= Pressiometric modulus
R_0	= Constant = 0.3
R	= Half width of the pile
α	= Rheological coefficient depending on the kind of soil and the soil conditions

The pressiometric modulus, E_m, can be determined from the cone resistance, q_c, which can be found from CPT's. The relation between these parameters is given by $E_m = \beta \cdot q_c$. The values for β for different kinds of soil is given in Table A.1. In this table also the rheological coefficients for different kinds of soils and soil conditions are given. In D-Sheet Piling the values for normally consolidated soil are applied.

Table A.1 - Correlation between pressiometric modulus and cone resistance; rheological coefficients

Kind of soil	Correlation β	Rheological coefficient α		
		Soil condition		
		Over consolidated	**Normally consolidated**	**Decomposed, weathered**
Peat	3 – 4	-	1	-
Clay	2 – 3	1	2/3	1/2
Loam	1 – 2	2/3	1/2	1/2
Sand	0.7 – 1	1/2	1/3	1/3
Gravel	0.5 – 0.7	1/3	1/4	1/4

B

P-Y CURVES IN D-PILE GROUP

B.1 P-y curves for clay and static lateral loads

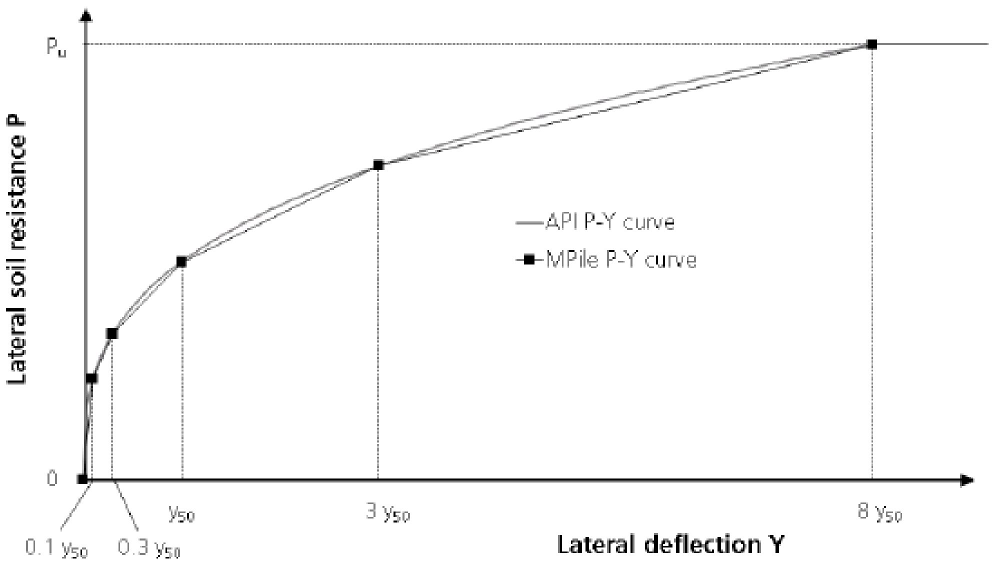

Figure B.1 - Modelling of the p-y curve (API) for clay and static loading (Deltares, 2014)

The *API* p-y curves for clay and static loading used in D-Pile Group is not given as a curve, but defined by a table. The points in this table are lying on the continuous curve defined by eq. B.1.

$$p = \begin{cases} 0.5\, p_u\, (y/y_{50})^{\frac{1}{3}} & for\ y < 8\, y_{50} \\ p_u & for\ y \geq 8\, y_{50} \end{cases} \tag{B.1}$$

In this equation p_u is defined as the ultimate soil resistance at depth *H*, which is defined as the minimum of the ultimate soil resistance at shallow depth, p_{us}, or at greater depth, p_{ud}:

$$p_u = \min\,(p_{us}; p_{ud}) \tag{B.2}$$

With :

$$p_{us} = 3c_u + \gamma H + J c_u \frac{H}{D} \tag{B.3}$$

$$p_{ud} = 9c_u \tag{B.4}$$

Where:

c_u = Undrained shear strength [kN/m^2]
γ = Effective unit weight of the soil [kN/m^3]
J = Dimensionless empirical constant, for which a value between 0.25 and 0.5 is recommended [-]
D = Diameter of the pile [m]

Furthermore, y_{50} is defined as the displacement which occurs at one-half of the maximum stress on laboratory undrained compression tests of undisturbed soil samples:

$$y_{50} = 2.5 \cdot \varepsilon_{50} \cdot D \tag{B.5}$$

The strain which occurs at on-half the maximum stress, ε_{50}, can be determined with Table B.1.

Table B.1 - Determination of ε50 as a function of the undrained cohesion (Deltares, 2014)

C_u [kN/m^2]	ε_{50} [-]
5 – 25	0.020
25 – 50	0.010
50 – 100	0.007
100 – 200	0.005
200 – 400	0.004

B.2 P-y curves for clay and cyclic lateral loads

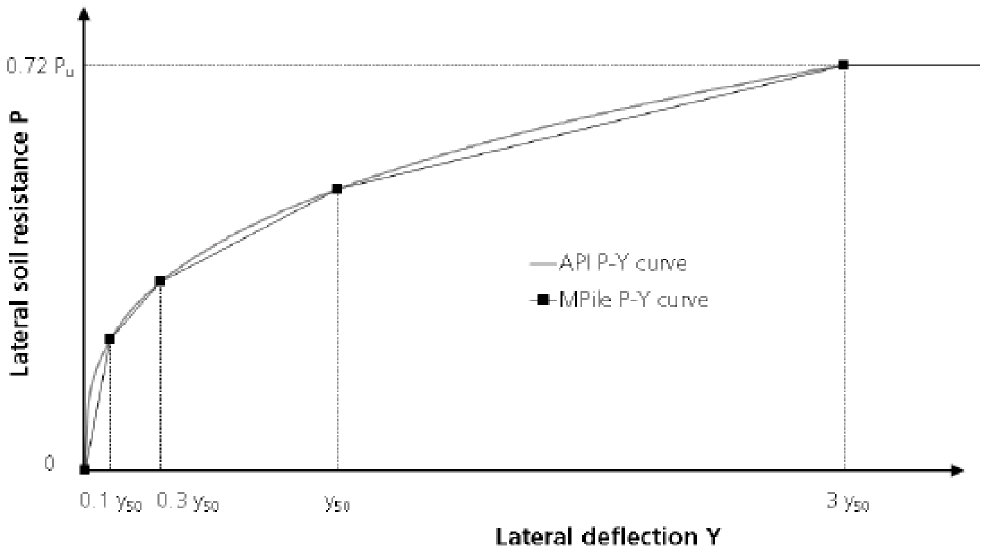

Figure B.2 - Modelling of the p-y curve (*API*) for clay and cyclic loading (Deltares, 2014)

The p-y curves for clay and cyclic lateral loads can be described by similar equations as the ones for clay and static lateral loads. The only difference is that in case of cyclic loading the curves are described by two tables of which the points lay on continuous curves described by eq. B.6 and B.7.

$$\frac{p}{p_u} = \begin{cases} 0.5\,(y/y_{50})^{\frac{1}{3}} & for\ y < 3\,y_{50} \\ 0.72 & for\ y \geq 3\,y_{50} \end{cases} \quad for\ H > H_R \tag{B.6}$$

$$\frac{p}{p_u} = \begin{cases} 0.5\,(y/y_{50})^{\frac{1}{3}} & for\ y < 3\,y_{50} \\ \left(0.06\dfrac{y}{y_{50}} + 0.54\right)\left(\dfrac{H}{H_R} - 1\right) & for\ 15\,y_{50} \geq y \geq 3\,y_{50} \\ 0.72\,(H/H_R) & for\ y > 15\,y_{50} \end{cases} \quad for\ H \leq H_R \tag{B.7}$$

In these equations H_R stands for the depth below the soil surface to the bottom of the reduced resistance zone:

$$H_R = \frac{6D}{\gamma\,D/c + J} \tag{B.8}$$

In D-Pile Group only the case with $H > H_R$ is implemented, because for $H \leq H_R$ a decreasing stiffness is considered which is not possible in D-Pile Group.

B.3 P-y curves for sand and static or cyclic lateral loads

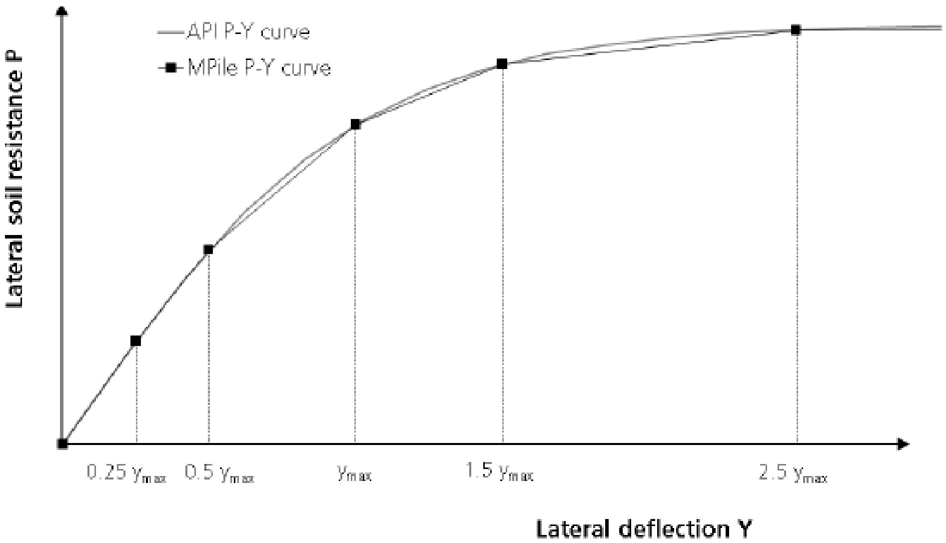

Figure B.3 - Modeling of the p-y curve (API) for sand (Deltares, 2014)

The API p-y curves for sand combined with static or cyclic lateral loading are similar and are defined as

$$p = A\,p_u \tanh\left(\frac{k\,H}{A\,p_u} y\right) \tag{B.9}$$

Where:

P	= Actual lateral soil resistance at depth H [kN/m]
p_u	= Ultimate soil resistance at depth H [kN/m]
k	= Initial modulus of subgrade reaction [kN/m^3]. In D-Pile Group this parameter is determined by linear interpolation of the values given in Table B.2.

H = Depth below soil surface [m]
D = Diameter of the pile [m]
y = Actual lateral pile deflection [m]

In eq. B.9 the factor *A* takes into account the differences for the loading conditions and is defined as:

$$A = \begin{cases} 3 - 0.8\dfrac{H}{D} \geq 0.9 & for\ static\ loads \\ 0.9 & for\ cyclic\ loads \end{cases} \tag{B.10}$$

Table B.2 - Values of k as a function of the internal friction (Deltares, 2014)

Angle of internal fiction [deg]	***k* [kN/m^3]**	
	Dry conditions	**Wet conditions**
29	2715	2715
29.5	6109	5090
30	11199	8145
33	25453	16303
36	42761	25453
38	59051	32580
40	75341	41743

The ultimate soil resistance is defined as the minimum of the ultimate soil resistance at shallow depth, p_{us}, or at greater depth, p_{ud}:

$$p_u = \min\left(p_{us}; p_{ud}\right) \tag{B.11}$$

With:

$$p_{us} = (C_1\, H + C_2\, D_H)\, \gamma H \tag{B.12}$$

$$p_{ud} = C_3\, D_H\, \gamma H \tag{B.13}$$

Where:

C_i = Coefficients which are determined by linear interpolation of the values given in Table B.3.
H = Depth below the soil surface [m]
D_H = Average diameter of the pile from the surface to depth *H* [m]
γ = Effective unit weight of the soil [kN/m^3]

Table B.3 - Values of C1, C2 and C3 inputted in D-Pile Group as function of the angle of internal friction (Deltares, 2014)

Angle of internal friction [deg]	**C_1 [-]**	**C_2 [-]**	**C_3 [-]**
20	0.77	1.58	9.00
25	1.22	2.03	15.50
30	1.90	2.67	28.50
35	3.00	3.45	54.25
40	4.67	4.35	100.00

C

RESULTS OF THE FULL SCALE TESTS

C.1 Section forces and pile displacements

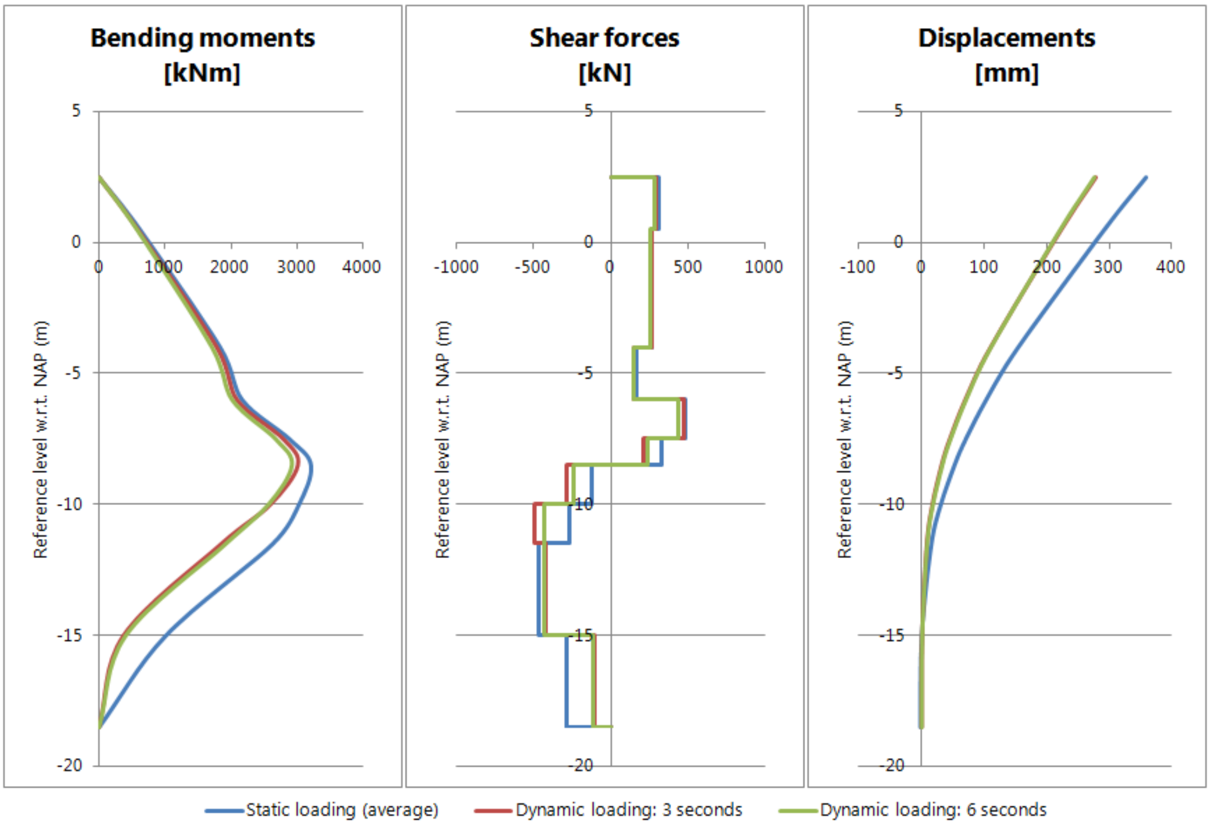

Figure C.1 - Section forces and displacements of pile 2 (F = 30 kN)

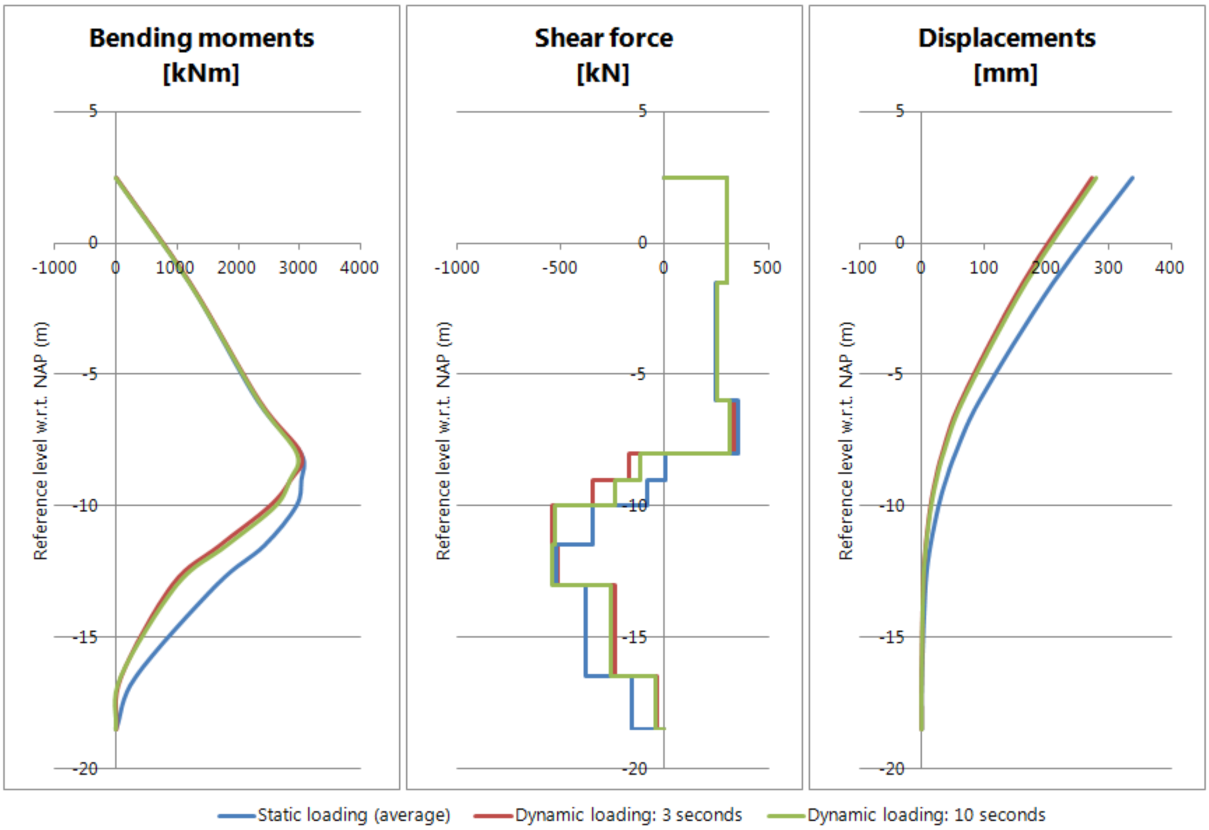

Figure C.2 - Section forces and displacements of pile 3 (F = 30 kN)

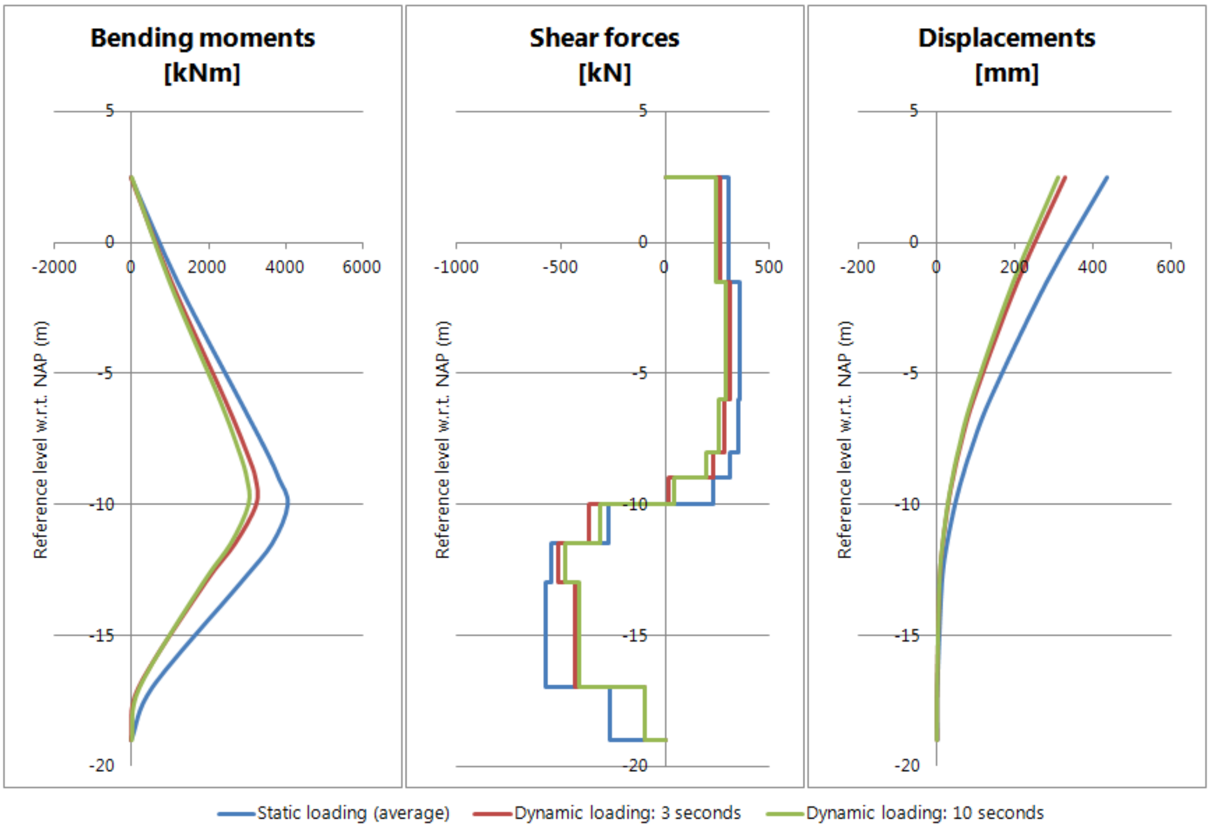

Figure C.3 - Section forces and displacements of pile 4 (F = 30 kN)

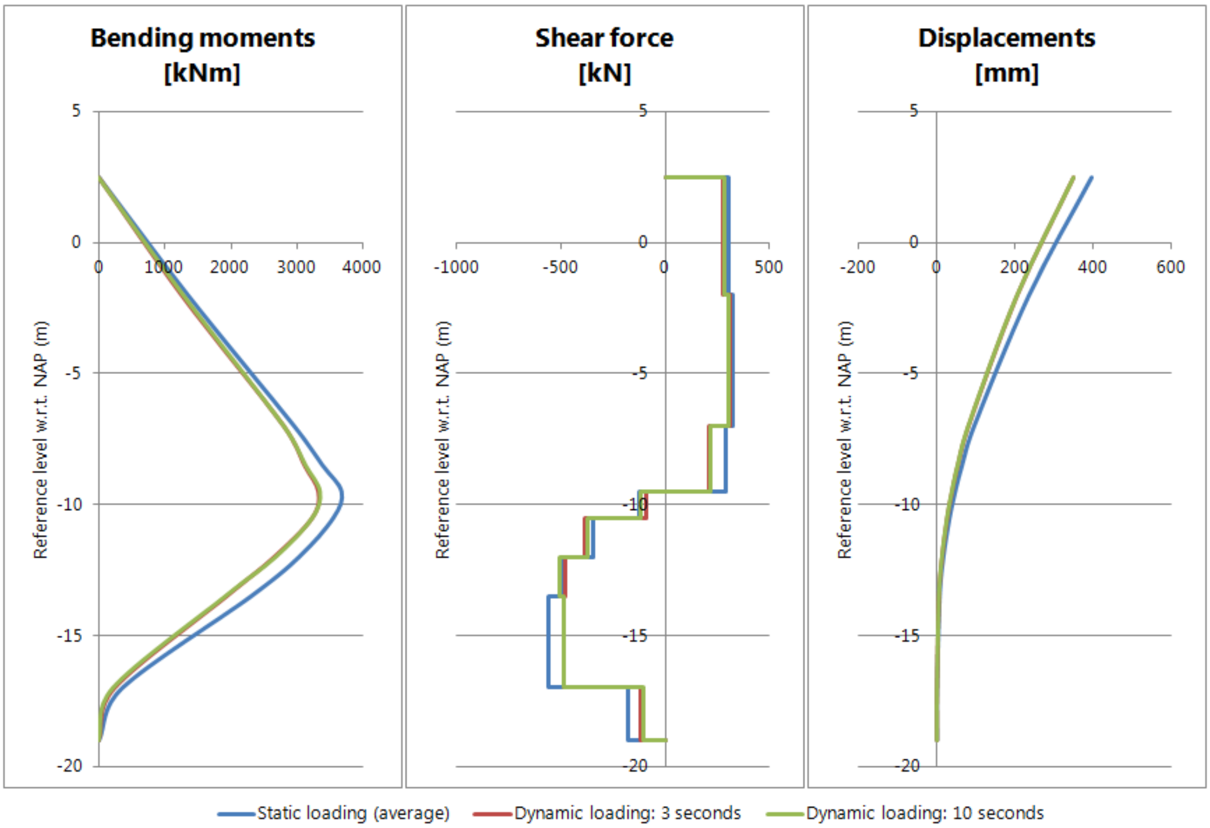

Figure C.4 - Section forces and displacements of pile 5 (F = 30 kN)

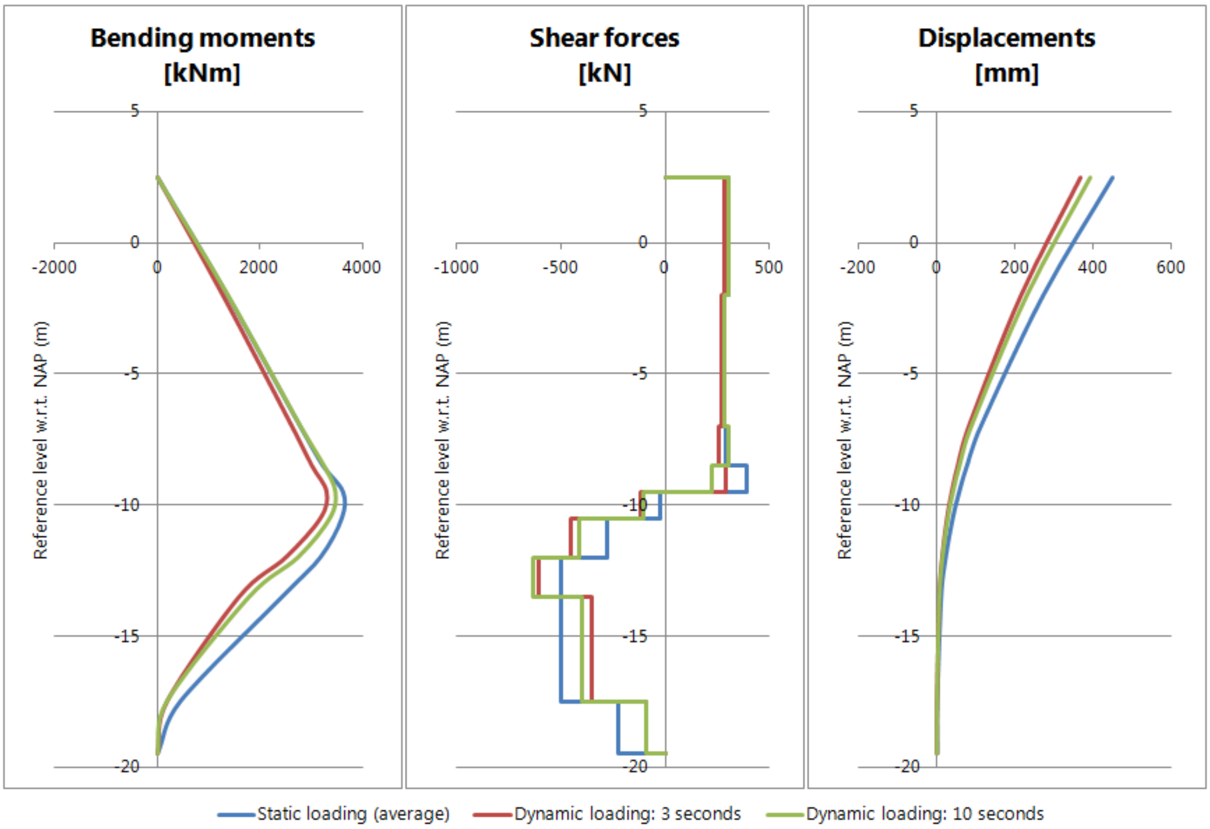

Figure C.5 - Section forces and displacements of pile 6 (F = 30 kN)

C.2 Soil deformations

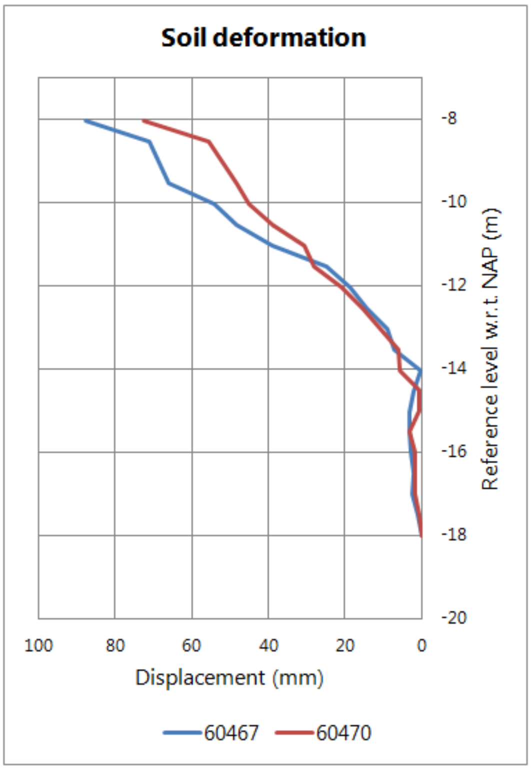

Figure C.6 - Soil deformation near pile 2

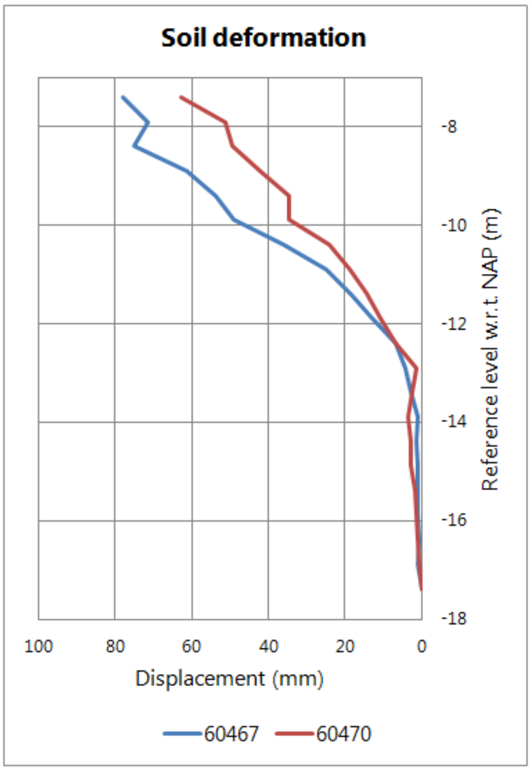

Figure C.7 - Soil deformation near pile 3

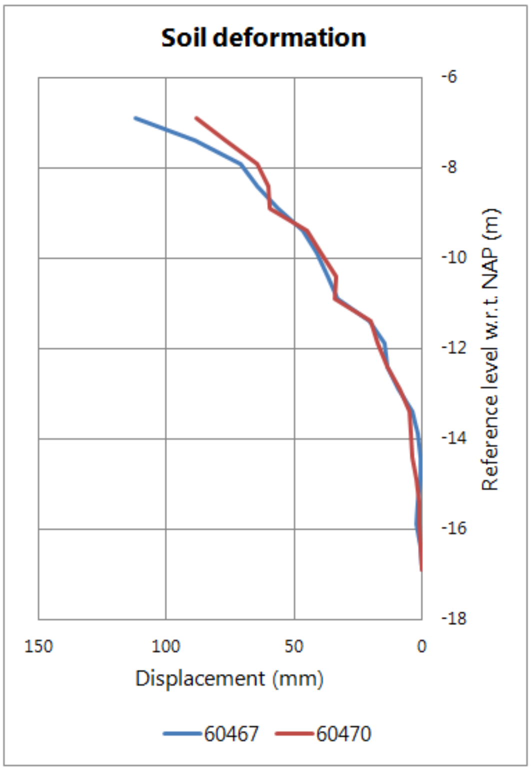

Figure C.8 - Soil deformation near pile 4

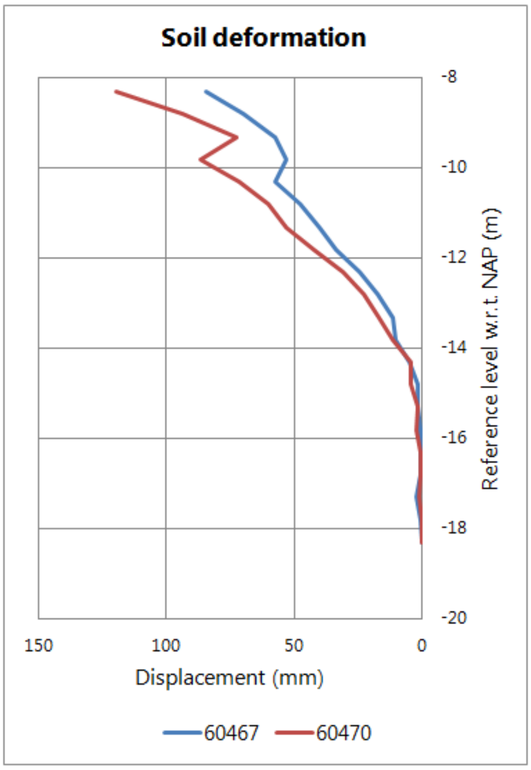

Figure C.9 - Soil deformation near pile 5

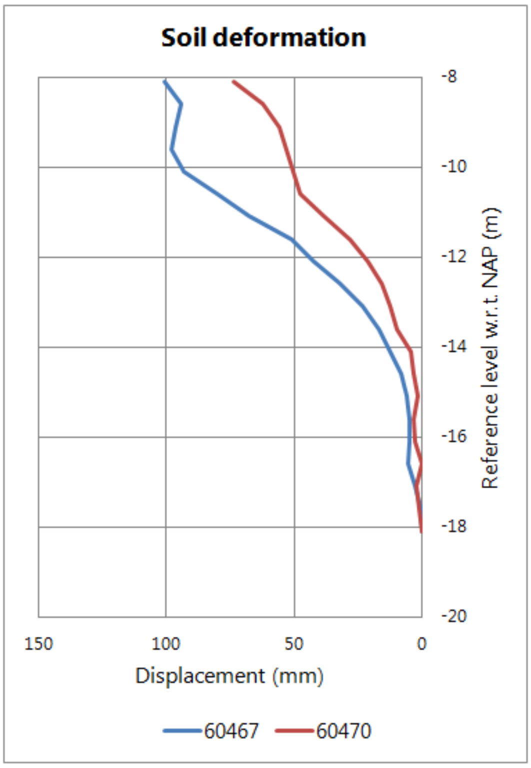

Figure C.10 - Soil deformation near pile 6

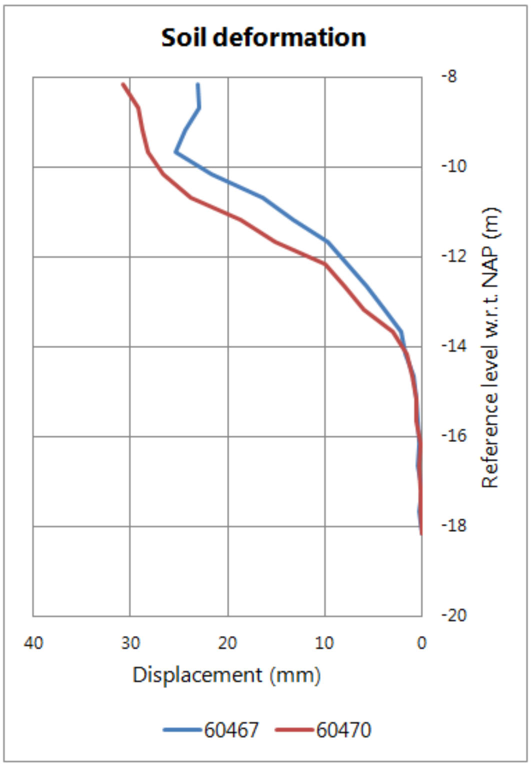

Figure C.11 - Soil deformation near pile 7

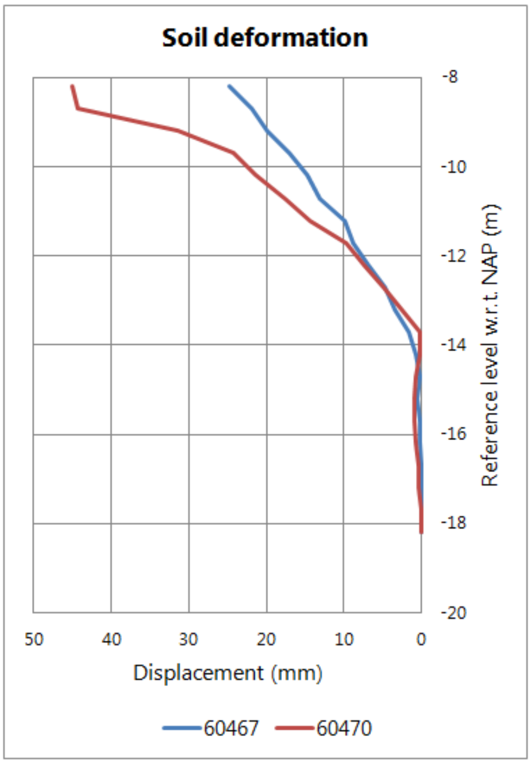

Figure C.12 - Soil deformation near pile 8

D

COMPARISON OF MODELS AND TEST RESULTS

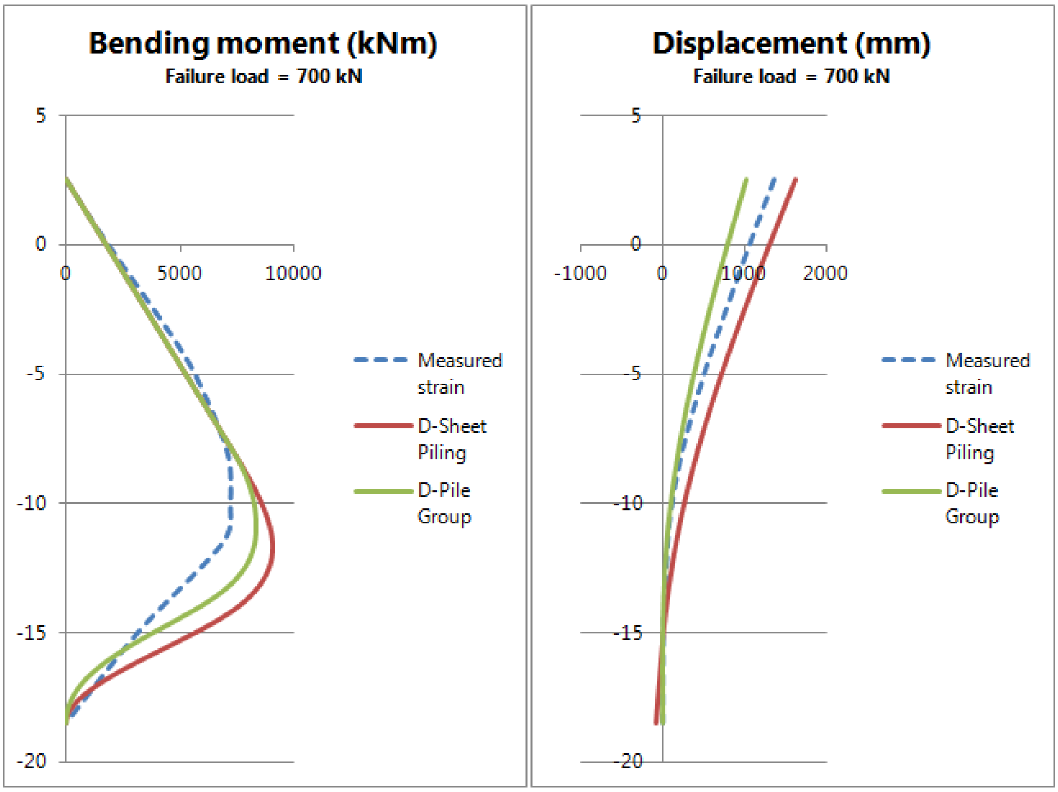

Figure D.1 - Comparison of the models with the test results (pile 2)

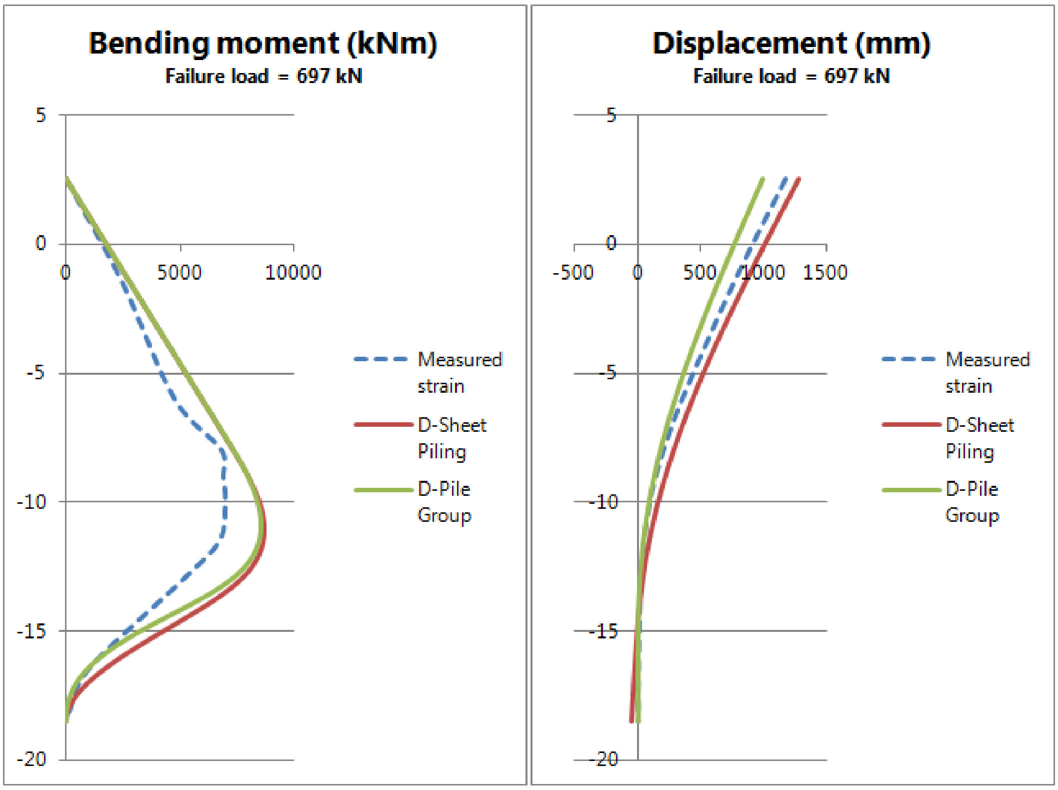

Figure D.2 - Comparison of the models with the test results (pile 3)

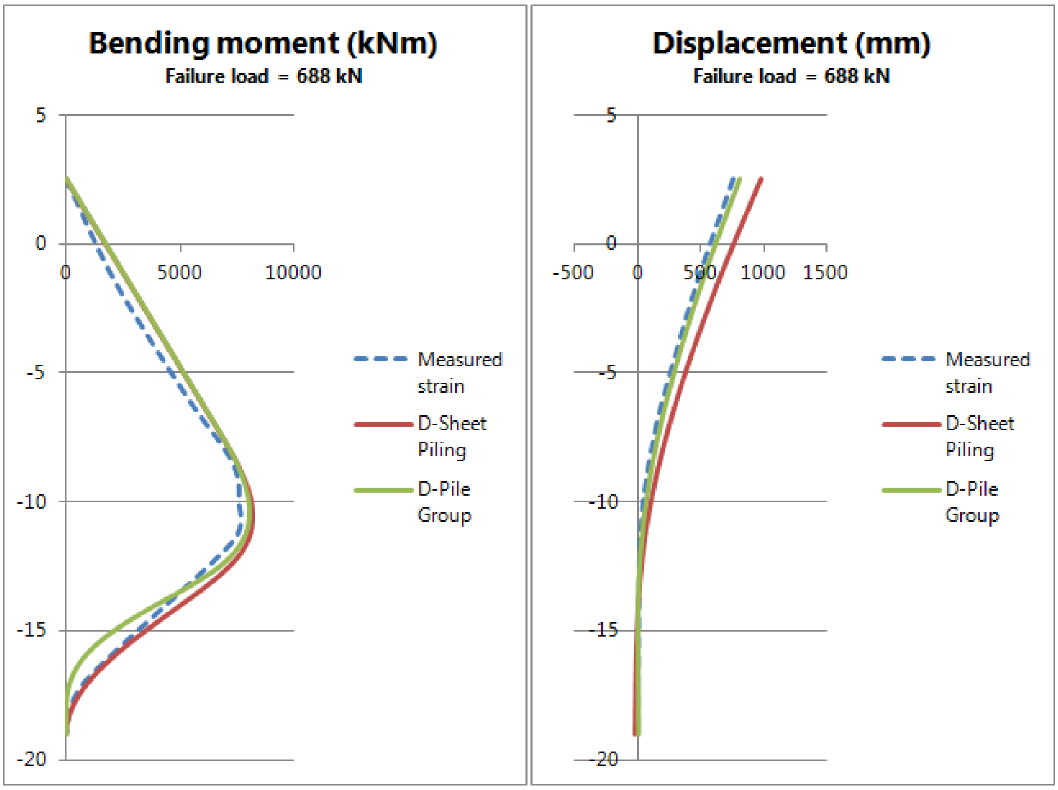

Figure D.3 - Comparison of the models with the test results (pile 4)

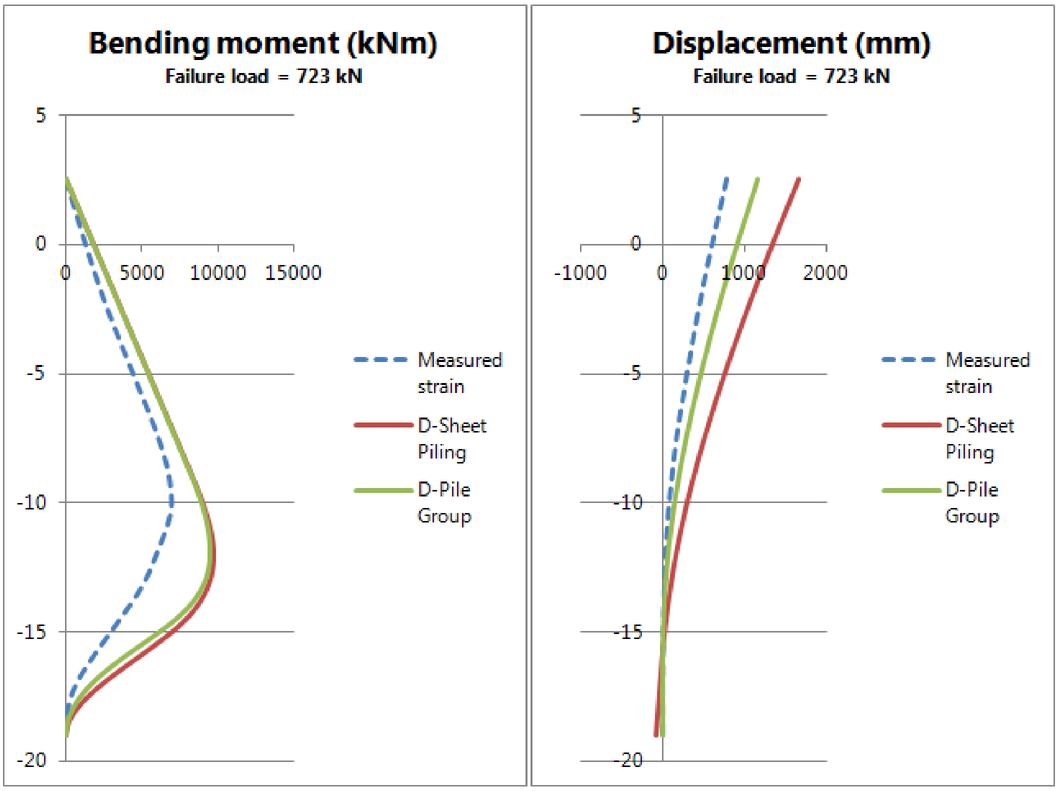

Figure D.4 - Comparison of the models with the test results (pile 5)

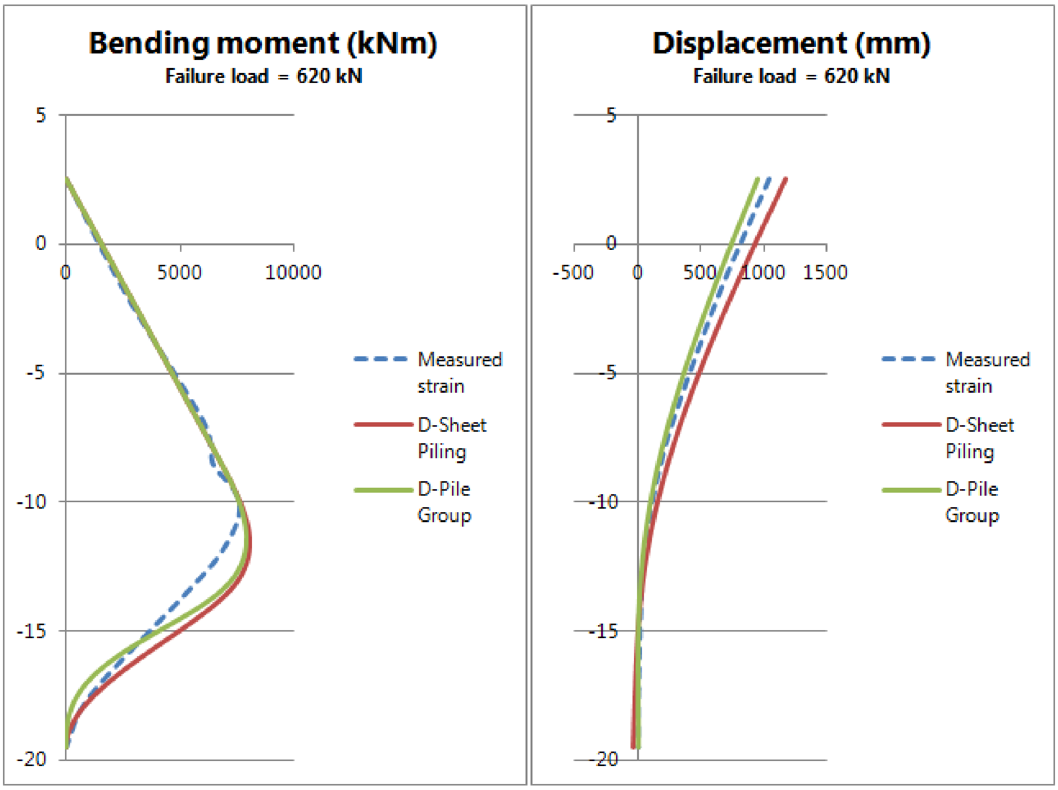

Figure D.5 - Comparison of the models with the test results (pile 6)

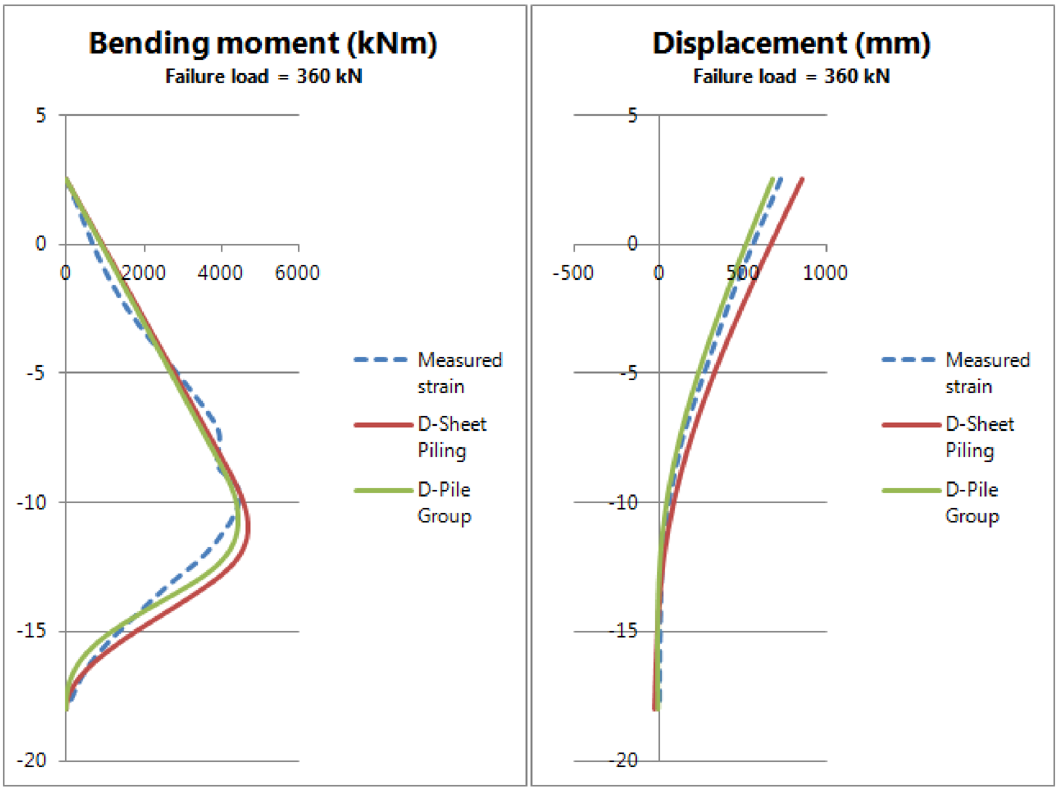

Figure D.6 - Comparison of the models with the test results (pile 7)

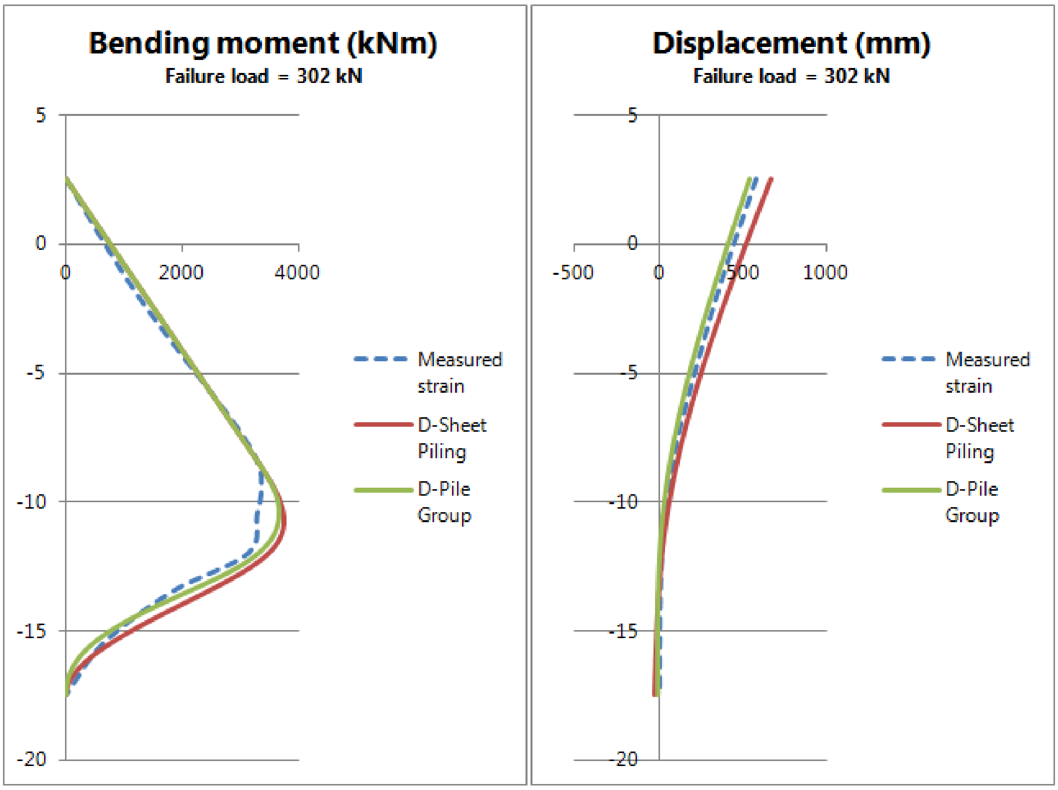

Figure D.7 - Comparison of the models with the test results

E

CROSS-SECTIONAL VERIFICATION METHODS

E.1 Evaluation on buckling according to Eurocode

This elaboration of the evaluation on local buckling is based on NEN-EN 1993-1-6 (2007).

Slender structures have to be evaluated on local buckling, because these cross-sections may buckle before the elastic capacity of the steel is reached. The types of buckling which are most relevant for laterally loaded tubular piles are meridional buckling and shear buckling. Whether these types of buckling have to be considered in the cross-sectional verification, depends on the characteristics of the cross-section.

Meridional buckling

Tubular piles need to be checked against meridional buckling when:

$$\frac{r}{t} > 0.03\,\frac{E}{f_{yk}} \tag{E.1}$$

The design buckling stress is an indirect function of the elastic critical meridional stress. This critical stress can be calculated with:

$$\sigma_{x,Rcr} = 0.605 \cdot E \cdot C_X \cdot \frac{t}{r} \tag{E.2}$$

The value for the factor C_X depends on the length of the tube according to:

$$\begin{array}{llll} \text{Medium length cylinder:} & C_X = 1 & \text{for} & 1.7 \leq \omega \leq 0.5\frac{r}{t} \\ \text{Short cylinder:} & C_X = 1.36 - \frac{1.83}{\omega} + \frac{2.07}{\omega} & \text{for} & \omega \leq 1.7 \\ \text{Long cylinder:} & C_X = 0.60 & \text{for} & \omega > 0.5\frac{r}{t} \end{array} \tag{E.3}$$

in which ω is the dimensionless length parameter:

$$\omega = \frac{l}{r}\sqrt{\frac{r}{t}} = \frac{l}{\sqrt{rt}} \tag{E.4}$$

The design meridional buckling stress can be determined with:

$$\sigma_{x,Rd} = \frac{\chi_x f_{yk}}{\gamma_{M1}} \tag{E.5}$$

In this equation, χ_x is the buckling reduction factor, which should be determined as a function of the relative slenderness of the shell, $\bar{\lambda}_x$:

$$\begin{aligned} &\chi_x = 1 && \text{for} \quad \bar{\lambda}_x \leq \bar{\lambda}_{x0} \\ &\chi_x = 1 - \beta\left(\frac{\bar{\lambda}_x - \bar{\lambda}_{x0}}{\bar{\lambda}_p - \bar{\lambda}_{x0}}\right)^{\eta} && \text{for} \quad \bar{\lambda}_{x0} < \bar{\lambda}_x < \bar{\lambda}_p \\ &\chi_x = \frac{\alpha_x}{\bar{\lambda}_x^2} && \text{for} \quad \bar{\lambda}_p \leq \bar{\lambda}_x \end{aligned} \tag{E.6}$$

In these equations, β is the plastic range factor (= 0.60), η is the interaction exponent (= 1.00) and $\bar{\lambda}_{x0}$ is the squash limit of the relative slenderness (= 0.20). Furthermore, the value of the plastic limit of the relative slenderness $\bar{\lambda}_p$ can be determined with equation E.7. The relative slenderness $\bar{\lambda}_x$ is a function of the elastic critical meridional stress and can be determined with equation E.8.

$$\bar{\lambda}_p = \sqrt{\frac{\alpha_x}{1-\beta}} \tag{E.7}$$

$$\bar{\lambda}_x = \sqrt{\frac{f_{yk}}{\sigma_{x,RCr}}} \tag{E.8}$$

The meridional elastic imperfection reduction factor, α_x, should be obtained from

$$\alpha_x = \frac{0.62}{1 + 1.91\left(\frac{\Delta w_k}{t}\right)^{1.44}} \tag{E.9}$$

In which

$$\Delta w_k = \frac{1}{Q}\sqrt{\frac{r}{t}}\, t \tag{E.10}$$

The value for the fabrication quality parameter Q should be determined from Table E.1. For new tubular piles the value according to Class B – Excellent is often used.

Table E.1 - Values of the fabrication quality parameter Q

Fabrication tolerance quality class	**Q**
Class A – Excellent	40
Class B – High	25
Class C – Normal	16

Shear buckling

Tubular piles need to be checked against shear buckling when:

$$\frac{r}{t} > 0.16\left(\frac{E}{f_{yk}}\right)^{0.67} \tag{E.11}$$

The design buckling stress with respect to shear is an indirect function of the elastic critical shear buckling stress:

$$\tau_{x\theta,Rcr} = 0.75 \cdot E \cdot C_\tau \cdot \sqrt{\frac{1}{\omega}} \cdot \left(\frac{t}{r}\right) \tag{E.12}$$

The value of the factor C_τ depends on the length of the tube according to:

$$\begin{array}{llll} \text{Medium length cylinder:} & C_\tau = 1 & \text{for} & 10 \leq \omega \leq 8.7\frac{r}{t} \\ \text{Short cylinder:} & C_\tau = \sqrt{1 + \frac{42}{\omega^3}} & \text{for} & \omega < 10 \\ \text{Long cylinder:} & C_\tau = \frac{1}{3}\sqrt{\omega\frac{t}{r}} & \text{for} & \omega > 8.7\frac{r}{t} \end{array} \tag{E.13}$$

In equations E.12 and E.13 ω is the dimensionless length parameter, which is already defined by equation E.4.

The design shear buckling stress can be determined with:

$$\tau_{x\theta,Rd} = \frac{\chi_\tau f_{yk}}{\sqrt{3}\,\gamma_{M1}} \tag{E.14}$$

In this equation, χ_τ is the buckling reduction factor, which should be determined as a function of the relative slenderness of the shell, $\bar{\lambda}_\tau$:

$$\begin{array}{lll} \chi_\tau = 1 & \text{for} & \bar{\lambda}_\tau \leq \bar{\lambda}_{\tau 0} \\ \chi_\tau = 1 - \beta\left(\frac{\bar{\lambda}_\tau - \bar{\lambda}_{\tau 0}}{\bar{\lambda}_p - \bar{\lambda}_{\tau 0}}\right)^\eta & \text{for} & \bar{\lambda}_{\tau 0} < \bar{\lambda}_\tau < \bar{\lambda}_p \\ \chi_\tau = \frac{\alpha}{\bar{\lambda}_\tau^2} & \text{for} & \bar{\lambda}_p \leq \bar{\lambda}_\tau \end{array} \tag{E.15}$$

In these equations, β is the plastic range factor (= 0.60), η is the interaction exponent (= 1.00) and $\bar{\lambda}_{\tau 0}$ is the squash limit of the relative slenderness (= 0.40). The value of the plastic limit of the relative slenderness $\bar{\lambda}_p$ is already defined by equation E.7. Furthermore, the relative slenderness $\bar{\lambda}_\tau$ is a function of the elastic critical shear stress and can be determined with:

$$\bar{\lambda}_\tau = \sqrt{\left(\frac{f_{yk}}{\sqrt{3}}\right)/\tau_{x\theta,Rcr}} \tag{E.16}$$

The value for the shear elastic imperfection reduction factor, α_τ, should be determined from Table E.2.

Table E.2 - Values of α_τ based on fabrication quality

Fabrication tolerance quality class	$\boldsymbol{\alpha_\tau}$
Class A – Excellent	0.75
Class B – High	0.65
Class C – Normal	0.50

E.2 Modified Gresnigt method

This elaboration of the modified Gresnigt method is based on the second edition of CUR211E – Quay walls (2014).

The modified Gresnigt method is a buckling evaluation method which is based on the criteria of critical strain. CUR211 advises to use this method for the evaluation of steel tubular piles as it takes into account the influence of the soil surrounding the pile and the possible confined soil inside the pile. However, the applicability of the method is limited to steel grades up to X70, for higher steel grades the method has not been proven yet (CUR-publicatie 211E, 2014).

Piles with a large ratio between the pile diameter and wall thickness tend to adopt an oval shape, what makes a pile more susceptible to buckling as a result of the larger virtual radius. This larger radius is a function of the initial radius of the pile, r, and the ovalization, a:

$$r' = \frac{r}{1 - 3a/r} \tag{E.17}$$

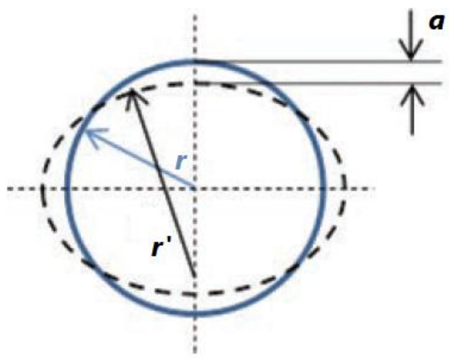

Figure E.1 - Definition of the ovalization, a, and the change of radius (CUR-publicatie 211E, 2014)

For flexible dolphins three types of ovalization have to be taken into account (CUR-publicatie 211E, 2014):

1. Initial out-of-roundness which is allowed for in the production process;

2. Ovalization due to outside soil pressure;
3. Ovalization as a second order effect of tube bending.

The ovalization due to the initial out-of-roundness can be calculated with:

$$a_{initial} = \frac{1}{4} U_r D \tag{E.18}$$

NEN-EN 1993-1-6 recommends values for the out-of-roundness tolerance, U_r. These values are presented in Table E.3.

Table E.3 - Recommended values for out-of-roundness tolerance U_r (NEN-EN 1993-1-6, 2007)

Fabrication class	***D* ≤ 0.50 m**	**0.50 m < *D* < 1.25 m**	**1.25 m ≤ *D***
Class A – Excellent	0.014	0.007 + 0.0093 · (1.25 - *D*)	0.007
Class B – High	0.020	0.010 + 0.0133 · (1.25 - *D*)	0.010
Class C – Normal	0.030	0.015 + 0.0200 · (1.25 -*D*)	0.015

For flexible dolphins the soil pressure is exerted from two opposite sides. For this case the ovalization due to outside soil pressure can be determined with:

$$a_{soil\ pressure} = \frac{1}{12} \frac{qr^4}{EI_{ring}} \tag{E.19}$$

In which q is the effective soil pressure at the level of verification and EI_{ring} is the stiffness of the ring $(= E \cdot 1/12 \cdot t^3)$.

The ovalization as a second order effect of tube bending can be calculated with:

$$a_{2nd} = \frac{\kappa^2 r^5}{t^2} \qquad \text{for} \qquad \sigma_{x,Ed} \leq f_y \tag{E.20}$$

$$a_{2nd} = \frac{\sigma_y}{E} \frac{\kappa r^4}{t^2} \qquad \text{for} \qquad \sigma_{x,Ed} > f_y \tag{E.21}$$

The bending moment capacity of tubular piles is an indirect function of the critical strain, which depends on the slenderness of the pile and the out-of-roundness. The critical strain can be calculated with:

$$\begin{aligned} \varepsilon_{cr} &= 0.25 \frac{t}{r'} - 0.0025 \qquad &\text{for} \qquad \frac{D}{t} < 120 \\ \varepsilon_{cr} &= 0.10 \frac{t}{r'} \qquad &\text{for} \qquad \frac{D}{t} > 120 \end{aligned} \tag{E.22}$$

Dependent on the slenderness and the out-of-roundness, the critical stain will be above or below the yield strain of the steel, which is expressed with the parameter μ:

$$\mu = \frac{\varepsilon_{cr}}{\varepsilon_y} = \frac{\varepsilon_{cr}}{f_y/E} \tag{E.23}$$

In case of pure bending, the position of the yield strain is indicated with the angle θ of the plasticity rate, staring with ½π for plastic strain in the outer fibre and 0 for the full plastic moment.

$$\sin\theta = \frac{1}{\mu} \qquad \text{for} \qquad \mu > 1$$
$$\theta = \frac{\pi}{2} \qquad \text{for} \qquad \mu \leq 1 \tag{E.24}$$

The bending moment as a function of the plasticity rate can be calculated with:

$$M_R = \frac{1}{2}\left(\frac{\theta}{\sin\theta} + \cos\theta\right) \cdot M_{pl;d} \qquad \text{for} \qquad \mu > 1$$
$$M_R = \mu \cdot M_{el;d} \qquad \text{for} \qquad \mu \leq 1 \tag{E.25}$$

with

$$M_{pl;d} = \frac{D^2 t f_y}{\gamma_{M0}} \qquad \text{and} \qquad M_{el;d} = \frac{\pi}{4}\frac{D^2 t f_y}{\gamma_{M0}} \qquad \text{with} \qquad \gamma_{M0} = 1.1$$

To account for the effects of ovalizing bending stresses and deformations, the bending moment has to be reduced with the factors g and β_g respectively. Furthermore, it should be taken into account that local buckling in the elastic area tends to cause sudden failure, without any deformation capacity. This effect is accounted for by the factor β_s. The bending moment capacity of empty tubular piles can be determined with:

$$M_{R,d} = g\beta_g\beta_s M_R \tag{E.26}$$

with

$$g = \frac{c_1}{6} + \frac{2}{3}$$

in which

$$c_1 = \sqrt{4 - 2\sqrt{3}\frac{m_{eff;Ed}}{m_{pl;Rd}}} \qquad \text{with} \qquad m_{eff;Ed} = 0.250 \cdot q \cdot r^2 \qquad \text{and} \qquad m_{pl;Rd} = \frac{1}{4}t^2\frac{f_y}{\gamma_{M0}}$$

and

$$\beta_g = 1 - \frac{2a}{r'}$$

The value for β_s depends on the ratio between the critical strain and the yield strain:

$$\beta_s = 0.75 \qquad \text{for} \quad \mu \leq 1$$
$$\beta_s = 0.625 + 0.125\mu \qquad \text{for} \quad 1 \leq \mu \leq 3$$
$$\beta_s = 1.0 \qquad \text{for} \quad \mu \geq 3$$

When both bending moments and normal forces are acting in a tubular pile, the cross-sectional verification can be performed with equation E.27. In case only bending moments have to be considered, the second term on the left hand side can be neglected.

$$\left(\frac{M_{Ed}}{M_{Rd}}\right) + \left(\frac{N_{Ed}}{N_{Rd}}\right)^{1.7} \leq 1 \tag{E.27}$$

The normal force capacity in this equation equals

$$N_{RD} = gN_{pl;d} \tag{E.28}$$

in which

$$N_{pl;d} = \pi D t \frac{f_y}{\gamma_{M0}}$$

Sand-filled tubular piles

Possible sand fill within tubular piles appears to prevent ovalization of the pile and therefore makes the pile less susceptible to local buckling. In the determination of the ovalization of sand-filled piles, the approach is adopted that the sand fill's resistance against compression provides extra spring stiffness to the steel ring. The ovalization of sand-filled piles can be calculated with:

$$a_{sand-filled} = a_{empty} \frac{k_{steel}}{k_{steel} + k_{sand}} \tag{E.29}$$

in which

$$k_{steel} = \frac{12EI_{ring}}{r^4} \quad \text{with} \quad EI_{ring} = \frac{1}{12}Et^3$$

and

$$k_{sand} = \frac{E_{sand}}{r} \quad \text{with} \quad E_{sand} = 10\ kPa$$

For sand-filled tubes, the critical strain is calculated in a similar way as for empty tubes. Optionally, for sand-filled piles also equation E.30 may be used. However, this equation is only verified within the range $70 < D/t < 120$.

$$\varepsilon_{cr} = 7\left(\frac{t}{r'}\right)^2 \tag{E.30}$$

A proper sand fill also prevents sudden collapse of the piles. Therefore, the deformation capacity reduction factors may be increased, resulting in:

$$\begin{array}{lll} \beta_s = 0.90 & \text{for} & \mu \leq 1 \\ \beta_s = 0.85 + 0.05\mu & \text{for} & 1 \leq \mu \leq 3 \\ \beta_s = 1.0 & \text{for} & \mu \geq 3 \end{array} \tag{E.31}$$

It should be kept in mind that the modified Gresnigt method for sand-filled tubular piles has several limitations. The main limitation for this research is that it should not be used for dolphin piles or for other applications where plastic deformation capacity is required. This means that for this master thesis only the modified Gresnigt method for empty tubular piles is relevant.

F

CALAND CANAL – FIRST CALCULATION RESULTS

F.1 First calculation results for the initial mooring dolphin design

F.1.1 Structural failure

Table F.1 - Results of the first calculation (LS: Structural failure)

Number of calculations: 463				
$\beta_{correlated}$: 4.050				
P_f: $2.556 \cdot 10^{-5}$				
Parameter (X_i)	**Unit**	**V (=σ/μ)**	**$\alpha_{correlated}$**	**X_i* (Design value)**
$c_{sandy\ clay}$	[kPa]	0.20	0.01	6.917
$E_{m,\ sandy\ clay}$	[kN/m^2]	0.10	0.04	3935
$\gamma_{sat,\ sandy\ clay}$	[kN/m^3]	0.05	0.07	19.35
$\varphi_{sandy\ clay}$	[deg]	0.10	0.06	26.25
$E_{m,\ gravel}$	[kN/m^2]	0.10	0.00	20000
$\gamma_{sat,\ gravel}$	[kN/m^3]	0.05	0.00	22.88
φ_{gravel}	[deg]	0.10	0.00	44.86
$E_{m,\ moderately\ packed\ sand}$	[kN/m^2]	0.10	0.00	5600
$\gamma_{sat,\ moderately\ packed\ sand}$	[kN/m^3]	0.05	0.00	21.79
$\varphi_{moderately\ packed\ sand}$	[deg]	0.10	0.00	38.88
$F_{mooring}$	[kN]	0.15	-0.85	3255
Pile tip level	[m] NAP	0.25 (σ)	0.00	-37.00
Bottom surface	[m] NAP	0.25 (σ)	0.04	-18.20
D	[m]	0.002	0.03	2.499
E	[kN/m^2]	0.03	0.00	$2.100 \cdot 10^8$
f_y	[N/mm^2]	0.07	0.49	482.1
t	[mm]	0.03	0.17	39.96

Calculation	Z-value	
1	54990	
463	0.531	

F.1.2 Excessive deformations

Table F.2 - Results of the first calculation (LS: Excessive deformations)

Number of calculations: 401				
$\beta_{correlated}$: 3.366				
P_f: $3.812 \cdot 10^{-4}$				
Parameter (X_i)	**Unit**	**V (=σ/μ)**	**$\alpha_{correlated}$**	**X_i* (Design value)**
$c_{sandy\ clay}$	[kPa]	0.20	-0.01	7.021
$E_{m,\ sandy\ clay}$	[kN/m^2]	0.10	0.20	3737
$\gamma_{sat,\ sandy\ clay}$	[kN/m^3]	0.05	0.30	18.61
$\varphi_{sandy\ clay}$	[deg]	0.10	0.29	24.24
$E_{m,\ gravel}$	[kN/m^2]	0.10	0.08	19470
$\gamma_{sat,\ gravel}$	[kN/m^3]	0.05	0.04	22.73
φ_{gravel}	[deg]	0.10	0.02	44.54
$E_{m,\ moderately\ packed\ sand}$	[kN/m^2]	0.10	0.05	5501
$\gamma_{sat,\ moderately\ packed\ sand}$	[kN/m^3]	0.05	0.03	21.69
$\varphi_{moderately\ packed\ sand}$	[deg]	0.10	0.01	38.70
$F_{mooring}$	[kN]	0.15	-0.85	3036
Pile tip level	[m] NAP	0.25 (σ)	-0.12	-36.90
Bottom surface	[m] NAP	0.25 (σ)	0.12	-18.26
D	[m]	0.002	0.04	2.499
E	[kN/m^2]	0.03	0.10	$2.079 \cdot 10^8$
t	[mm]	0.03	0.09	40.52

Calculation	Z-value	
1	770.7	
401	2.145	

F.1.3 Soil mechanical failure

Table F.3 - Results of the first calculation (LS: Soil mechanical failure)

Number of calculations: 381				
$\beta_{correlated}$: 5.334				
P_f: $4.796 \cdot 10^{-8}$				
Parameter (X_i)	**Unit**	**V (=σ/μ)**	**$\alpha_{correlated}$**	**X_i* (Design value)**
$c_{sandy\ clay}$	[kPa]	0.20	0.00	6.983
$E_{m,\ sandy\ clay}$	[kN/m^2]	0.10	0.18	3610
$\gamma_{sat,\ sandy\ clay}$	[kN/m^3]	0.05	0.34	17.82
$\varphi_{sandy\ clay}$	[deg]	0.10	0.27	22.98
$E_{m,\ gravel}$	[kN/m^2]	0.10	0.13	18580
$\gamma_{sat,\ gravel}$	[kN/m^3]	0.05	0.31	20.99
φ_{gravel}	[deg]	0.10	0.58	31.05
$E_{m,\ moderately\ packed\ sand}$	[kN/m^2]	0.10	0.07	5377
$\gamma_{sat,\ moderately\ packed\ sand}$	[kN/m^3]	0.05	0.13	21.02
$\varphi_{moderately\ packed\ sand}$	[deg]	0.10	0.19	34.91
$F_{mooring}$	[kN]	0.15	-0.49	2926
Pile tip level	[m] NAP	0.25 (σ)	-0.13	-36.96
Bottom surface	[m] NAP	0.25 (σ)	0.12	-18.32
D	[m]	0.002	0.00	2.50
E	[kN/m^2]	0.03	-0.01	$2.104 \cdot 10^8$
t	[mm]	0.03	0.00	41.01

Calculation	Z-value	
1	34.45	
381	0.06	

F.2 First calculation results for the shortened mooring dolphin

F.2.1 Structural failure

Table F.4 - Results of the first calculation for a shortened pile (LS: Structural failure)

Number of calculations: 463				
$\beta_{correlated}$: 4.050				
P_f: $2.556 \cdot 10^{-5}$				
Parameter (X_i)	**Unit**	**V (=σ/μ)**	**$\alpha_{correlated}$**	**X_i* (Design value)**
$c_{sandy\ clay}$	[kPa]	0.20	0.01	6.917
$E_{m,\ sandy\ clay}$	[kN/m^2]	0.10	0.04	3935
$\gamma_{sat,\ sandy\ clay}$	[kN/m^3]	0.05	0.07	19.35
$\varphi_{sandy\ clay}$	[deg]	0.10	0.06	26.25
$E_{m,\ gravel}$	[kN/m^2]	0.10	0.00	20000
$\gamma_{sat,\ gravel}$	[kN/m^3]	0.05	0.00	22.88
φ_{gravel}	[deg]	0.10	0.00	44.86
$E_{m,\ moderately\ packed\ sand}$	[kN/m^2]	0.10	0.00	5600
$\gamma_{sat,\ moderately\ packed\ sand}$	[kN/m^3]	0.05	0.00	21.79
$\varphi_{moderately\ packed\ sand}$	[deg]	0.10	0.00	38.88
$F_{mooring}$	[kN]	0.15	-0.85	3255
Pile tip level	[m] NAP	0.25 (σ)	0.00	-37.00
Bottom surface	[m] NAP	0.25 (σ)	0.04	-18.20
D	[m]	0.002	0.03	2.499
E	[kN/m^2]	0.03	0.00	$2.100 \cdot 10^8$
f_y	[N/mm^2]	0.07	0.49	482.1
t	[mm]	0.03	0.17	39.96

Calculation	Z-value	
1	54990	
463	0.531	

F.2.2 Excessive deformations

Table F.5 - Results of the first calculation for a shortened pile (LS: Excessive deformations)

Number of calculations: 381				
$\beta_{correlated}$: 2.083				
P_f: $1.864{\cdot}10^{-2}$				
Parameter (X_i)	**Unit**	**V (=σ/μ)**	**$\alpha_{correlated}$**	**X_i* (Design value)**
$c_{sandy\ clay}$	[kPa]	0.20	-0.02	7.029
$E_{m,\ sandy\ clay}$	[kN/m^2]	0.10	0.23	3812
$\gamma_{sat,\ sandy\ clay}$	[kN/m^3]	0.05	0.36	18.87
$\varphi_{sandy\ clay}$	[deg]	0.10	0.36	24.91
$E_{m,\ gravel}$	[kN/m^2]	0.10	0.06	19740
$\gamma_{sat,\ gravel}$	[kN/m^3]	0.05	0.03	22.81
φ_{gravel}	[deg]	0.10	0.02	44.70
$E_{m,\ moderately\ packed\ sand}$	[kN/m^2]	0.10	0.05	5538
$\gamma_{sat,\ moderately\ packed\ sand}$	[kN/m^3]	0.05	0.03	21.73
$\varphi_{moderately\ packed\ sand}$	[deg]	0.10	0.01	38.76
$F_{mooring}$	[kN]	0.15	-0.79	2548
Pile tip level	[m] NAP	0.25 (σ)	-0.15	-34.92
Bottom surface	[m] NAP	0.25 (σ)	0.15	-18.24
D	[m]	0.002	0.00	2.499
f_y	[N/mm^2]	0.07	0.08	$2.090{\cdot}10^8$
t	[mm]	0.03	0.04	40.86

Calculation	Z-value	
1	661.0	
381	1.292	

F.2.3 Soil mechanical failure

Table F.6 - Results of the first calculation for a shortened pile (LS: Soil mechanical failure)

Number of calculations: 381				
$\beta_{correlated}$: 3.864				
P_f: $5.567 \cdot 10^{-5}$				
Parameter (X_i)	**Unit**	**V (=σ/μ)**	**$\alpha_{correlated}$**	**X_i* (Design value)**
$c_{sandy\ clay}$	[kPa]	0.20	-0.01	7.039
$E_{m,\ sandy\ clay}$	[kN/m^2]	0.10	0.21	3674
$\gamma_{sat,\ sandy\ clay}$	[kN/m^3]	0.05	0.38	18.17
$\varphi_{sandy\ clay}$	[deg]	0.10	0.32	23.56
$E_{m,\ gravel}$	[kN/m^2]	0.10	0.12	19050
$\gamma_{sat,\ gravel}$	[kN/m^3]	0.05	0.26	21.75
φ_{gravel}	[deg]	0.10	0.48	36.57
$E_{m,\ moderately\ packed\ sand}$	[kN/m^2]	0.10	0.07	5442
$\gamma_{sat,\ moderately\ packed\ sand}$	[kN/m^3]	0.05	0.14	21.22
$\varphi_{moderately\ packed\ sand}$	[deg]	0.10	0.21	35.68
$F_{mooring}$	[kN]	0.15	-0.53	2708
Pile tip level	[m] NAP	0.25 (σ)	-0.16	-34.98
Bottom surface	[m] NAP	0.25 (σ)	0.14	-18.30
D	[m]	0.002	0.00	2.50
E	[kN/m^2]	0.03	0.02	$2.094 \cdot 10^8$
t	[mm]	0.03	0.01	40.96

Calculation	Z-value	
1	31.21	
381	0.14	

G

SENSITIVITY ANALYSIS – FIRST CALCULATION RESULTS

G.1 Variation 1: Increased cohesion for sandy clay

G.1.1 Structural failure

Table G.1 - Results of the first calculation for variation 1: Increased cohesion for sandy clay (LS: Structural failure)

Number of calculations: 484				
$\beta_{correlated}$: 4.289				
P_f: $8.959 \cdot 10^{-6}$				
Parameter (X_i)	**Unit**	**V (=σ/μ)**	**$\alpha_{correlated}$**	**X_i* (Design value)**
$c_{sandy\ clay}$	[kPa]	0.20	0.02	20.36
$E_{m,\ sandy\ clay}$	[kN/m^2]	0.10	0.02	3959
$\gamma_{sat,\ sandy\ clay}$	[kN/m^3]	0.05	0.03	19.47
$\varphi_{sandy\ clay}$	[deg]	0.10	0.02	26.67
$E_{m,\ gravel}$	[kN/m^2]	0.10	0.00	20000
$\gamma_{sat,\ gravel}$	[kN/m^3]	0.05	0.00	22.88
φ_{gravel}	[deg]	0.10	0.00	44.86
$E_{m,\ moderately\ packed\ sand}$	[kN/m^2]	0.10	0.00	5600
$\gamma_{sat,\ moderately\ packed\ sand}$	[kN/m^3]	0.05	0.00	21.79
$\varphi_{moderately\ packed\ sand}$	[deg]	0.10	0.00	38.88
$F_{mooring}$	[kN]	0.15	-0.83	3345
Pile tip level	[m] NAP	0.25 (σ)	0.00	-37.00
Bottom surface	[m] NAP	0.25 (σ)	0.06	-18.22
D	[m]	0.002	0.03	2.499
E	[kN/m^2]	0.03	0.00	$2.099 \cdot 10^8$
f_y	[N/mm^2]	0.07	0.53	471.5
t	[mm]	0.03	0.19	39.83

Calculation	Z-value	
1	56900	
484	3.414	

G.1.2 Excessive deformations

Table G.2 - Results of the first calculation for variation 1: Increased cohesion for sandy clay (LS: Excessive deformations)

Number of calculations: 401				
$\beta_{correlated}$: 3.768				
P_f: $8.223 \cdot 10^{-5}$				
Parameter (X_i)	**Unit**	**V (=σ/μ)**	$\boldsymbol{\alpha_{correlated}}$	**X_i* (Design value)**
$c_{sandy\ clay}$	[kPa]	0.20	0.14	18.68
$E_{m,\ sandy\ clay}$	[kN/m^2]	0.10	0.27	3595
$\gamma_{sat,\ sandy\ clay}$	[kN/m^3]	0.05	0.34	18.37
$\varphi_{sandy\ clay}$	[deg]	0.10	0.25	24.41
$E_{m,\ gravel}$	[kN/m^2]	0.10	0.05	19590
$\gamma_{sat,\ gravel}$	[kN/m^3]	0.05	0.03	22.76
φ_{gravel}	[deg]	0.10	0.01	44.61
$E_{m,\ moderately\ packed\ sand}$	[kN/m^2]	0.10	0.03	5529
$\gamma_{sat,\ moderately\ packed\ sand}$	[kN/m^3]	0.05	0.02	21.72
$\varphi_{moderately\ packed\ sand}$	[deg]	0.10	0.01	38.75
$F_{mooring}$	[kN]	0.15	-0.82	3129
Pile tip level	[m] NAP	0.25 (σ)	-0.13	-34.88
Bottom surface	[m] NAP	0.25 (σ)	0.17	-18.32
D	[m]	0.002	0.03	2.499
E	[kN/m^2]	0.03	0.06	$2.085 \cdot 10^8$
t	[mm]	0.03	0.07	40.56
Calculation	Z-value			
1	827.5			
401	0.821			

G.1.3 Soil mechanical failure

Table G.3 - Results of the first calculation for variation 1: Increased cohesion for sandy clay (LS: Soil mechanical failure)

Number of calculations: 361				
$\beta_{correlated}$: 3.972				
P_f: $3.568 \cdot 10^{-5}$				
Parameter (X_i)	**Unit**	**V (=σ/μ)**	$\alpha_{correlated}$	**X_i* (Design value)**
$c_{sandy\ clay}$	[kPa]	0.20	0.12	18.94
$E_{m,\ sandy\ clay}$	[kN/m^2]	0.10	0.25	3601
$\gamma_{sat,\ sandy\ clay}$	[kN/m^3]	0.05	0.41	18.03
$\varphi_{sandy\ clay}$	[deg]	0.10	0.29	23.86
$E_{m,\ gravel}$	[kN/m^2]	0.10	0.10	19210
$\gamma_{sat,\ gravel}$	[kN/m^3]	0.05	0.21	21.94
φ_{gravel}	[deg]	0.10	0.39	37.85
$E_{m,\ moderately\ packed\ sand}$	[kN/m^2]	0.10	0.06	5470
$\gamma_{sat,\ moderately\ packed\ sand}$	[kN/m^3]	0.05	0.12	21.25
$\varphi_{moderately\ packed\ sand}$	[deg]	0.10	0.19	35.99
$F_{mooring}$	[kN]	0.15	-0.60	2836
Pile tip level	[m] NAP	0.25 (σ)	-0.16	-33.27
Bottom surface	[m] NAP	0.25 (σ)	0.17	-18.33
D	[m]	0.002	0.03	2.499
E	[kN/m^2]	0.03	0.01	$2.097 \cdot 10^8$
t	[mm]	0.03	-0.01	41.09

Calculation	Z-value	
1	29.41	
361	0.26	

G.2 Variation 2: Decreased angle of internal friction for gravel

G.2.1 Structural failure

Table G.4 - Results of the first calculation for variation 2: Decreased angle of internal friction for gravel (LS: Structural failure)

Number of calculations: 463				
$\beta_{correlated}$: 4.050				
P_f: $2.556 \cdot 10^{-5}$				
Parameter (X_i)	**Unit**	**V (=σ/μ)**	**$\alpha_{correlated}$**	**X_i* (Design value)**
$c_{sandy\ clay}$	[kPa]	0.20	0.01	6.917
$E_{m,\ sandy\ clay}$	[kN/m^2]	0.10	0.04	3935
$\gamma_{sat,\ sandy\ clay}$	[kN/m^3]	0.05	0.07	19.35
$\varphi_{sandy\ clay}$	[deg]	0.10	0.06	26.25
$E_{m,\ gravel}$	[kN/m^2]	0.10	0.00	20000
$\gamma_{sat,\ gravel}$	[kN/m^3]	0.05	0.00	22.88
φ_{gravel}	[deg]	0.10	0.00	44.86
$E_{m,\ moderately\ packed\ sand}$	[kN/m^2]	0.10	0.00	5600
$\gamma_{sat,\ moderately\ packed\ sand}$	[kN/m^3]	0.05	0.00	21.79
$\varphi_{moderately\ packed\ sand}$	[deg]	0.10	0.00	38.88
$F_{mooring}$	[kN]	0.15	-0.85	3255
Pile tip level	[m] NAP	0.25 (σ)	0.00	-37.00
Bottom surface	[m] NAP	0.25 (σ)	0.04	-18.20
D	[m]	0.002	0.03	2.499
E	[kN/m^2]	0.03	0.00	$2.100 \cdot 10^8$
f_y	[N/mm^2]	0.07	0.49	482.1
t	[mm]	0.03	0.17	39.96

Calculation	Z-value	
1	54990	
463	0.531	

G.2.2 Excessive deformations

Table G.5 - Results of the first calculation for variation 2: Decreased angle of internal friction for gravel (LS: Excessive deformations)

Number of calculations: 401				
$\beta_{correlated}$: 3.366				
P_f: $3.812 \cdot 10^{-4}$				
Parameter (X_i)	**Unit**	**V (=σ/μ)**	**$\alpha_{correlated}$**	**X_i* (Design value)**
$c_{sandy\ clay}$	[kPa]	0.20	-0.01	7.021
$E_{m,\ sandy\ clay}$	[kN/m^2]	0.10	0.20	3737
$\gamma_{sat,\ sandy\ clay}$	[kN/m^3]	0.05	0.30	18.61
$\varphi_{sandy\ clay}$	[deg]	0.10	0.29	24.24
$E_{m,\ gravel}$	[kN/m^2]	0.10	0.08	19470
$\gamma_{sat,\ gravel}$	[kN/m^3]	0.05	0.04	22.73
φ_{gravel}	[deg]	0.10	0.02	44.54
$E_{m,\ moderately\ packed\ sand}$	[kN/m^2]	0.10	0.05	5501
$\gamma_{sat,\ moderately\ packed\ sand}$	[kN/m^3]	0.05	0.03	21.69
$\varphi_{moderately\ packed\ sand}$	[deg]	0.10	0.01	38.70
$F_{mooring}$	[kN]	0.15	-0.85	3036
Pile tip level	[m] NAP	0.25 (σ)	-0.12	-36.90
Bottom surface	[m] NAP	0.25 (σ)	0.12	-18.26
D	[m]	0.002	0.04	2.499
E	[kN/m^2]	0.03	0.10	$2.079 \cdot 10^8$
t	[mm]	0.03	0.09	40.52

Calculation	Z-value	
1	770.7	
401	2.145	

G.2.3 Soil mechanical failure

Table G.6 - Results of the first calculation for variation 2: Decreased angle of internal friction for gravel (LS: Soil mechanical failure)

Number of calculations: 381				
$\beta_{correlated}$: 3.808				
P_f: $7.012 \cdot 10^{-5}$				
Parameter (X_i)	**Unit**	**V (=σ/μ)**	**$\alpha_{correlated}$**	**X_i* (Design value)**
$c_{sandy\ clay}$	[kPa]	0.20	0.00	6.970
$E_{m,\ sandy\ clay}$	[kN/m^2]	0.10	0.20	3694
$\gamma_{sat,\ sandy\ clay}$	[kN/m^3]	0.05	0.38	18.19
$\varphi_{sandy\ clay}$	[deg]	0.10	0.31	23.73
$E_{m,\ gravel}$	[kN/m^2]	0.10	0.11	19150
$\gamma_{sat,\ gravel}$	[kN/m^3]	0.05	0.27	21.72
φ_{gravel}	[deg]	0.10	0.49	31.67
$E_{m,\ moderately\ packed\ sand}$	[kN/m^2]	0.10	0.07	5447
$\gamma_{sat,\ moderately\ packed\ sand}$	[kN/m^3]	0.05	0.13	21.26
$\varphi_{moderately\ packed\ sand}$	[deg]	0.10	0.18	33.40
$F_{mooring}$	[kN]	0.15	-0.56	2734
Pile tip level	[m] NAP	0.25 (σ)	-0.14	-36.11
Bottom surface	[m] NAP	0.25 (σ)	0.12	-18.27
D	[m]	0.002	0.00	2.50
E	[kN/m^2]	0.03	0.02	$2.096 \cdot 10^8$
t	[mm]	0.03	0.00	41.02

Calculation	Z-value	
1	29.20	
381	0.16	

G.3 Variation 3: Modified soil structure

G.3.1 Structural failure

Table G.7 - Results of the first calculation for variation 3: Modified soil structure (LS: Structural failure)

Number of calculations: 463				
$\beta_{correlated}$: 4.276				
P_f: $9.525 \cdot 10^{-6}$				
Parameter (X_i)	**Unit**	**V (=σ/μ)**	**$\alpha_{correlated}$**	**X_i* (Design value)**
$c_{sandy\ clay}$	[kPa]	0.20	0.00	6.962
$E_{m,\ sandy\ clay}$	[kN/m^2]	0.10	0.00	4000
$\gamma_{sat,\ sandy\ clay}$	[kN/m^3]	0.05	0.00	19.61
$\varphi_{sandy\ clay}$	[deg]	0.10	0.00	26.91
$E_{m,\ gravel}$	[kN/m^2]	0.10	0.03	19710
$\gamma_{sat,\ gravel}$	[kN/m^3]	0.05	0.07	22.52
φ_{gravel}	[deg]	0.10	0.11	42.68
$E_{m,\ moderately\ packed\ sand}$	[kN/m^2]	0.10	0.00	5600
$\gamma_{sat,\ moderately\ packed\ sand}$	[kN/m^3]	0.05	0.00	21.79
$\varphi_{moderately\ packed\ sand}$	[deg]	0.10	0.00	38.88
$F_{mooring}$	[kN]	0.15	-0.83	3295
Pile tip level	[m] NAP	0.25 (σ)	0.00	-37.00
Bottom surface	[m] NAP	0.25 (σ)	0.06	-18.22
D	[m]	0.002	0.03	2.499
E	[kN/m^2]	0.03	0.00	$2.101 \cdot 10^8$
f_y	[N/mm^2]	0.07	0.51	475.0
t	[mm]	0.03	0.19	39.85

Calculation	Z-value	
1	55910	
463	-0.919	

G.3.2 Excessive deformations

Table G.8 - Results of the first calculation for variation 3: Modified soil structure (LS: Excessive deformations)

Number of calculations: 621				
$\beta_{correlated}$: 3.579				
P_f: $1.725 \cdot 10^{-4}$				
Parameter (X_i)	**Unit**	**V (=σ/μ)**	**$\alpha_{correlated}$**	**X_i* (Design value)**
$c_{sandy\ clay}$	[kPa]	0.20	0.01	6.916
$E_{m,\ sandy\ clay}$	[kN/m^2]	0.10	0.06	3911
$\gamma_{sat,\ sandy\ clay}$	[kN/m^3]	0.05	0.03	19.50
$\varphi_{sandy\ clay}$	[deg]	0.10	0.02	26.75
$E_{m,\ gravel}$	[kN/m^2]	0.10	0.05	19630
$\gamma_{sat,\ gravel}$	[kN/m^3]	0.05	0.37	21.37
φ_{gravel}	[deg]	0.10	0.71	33.48
$E_{m,\ moderately\ packed\ sand}$	[kN/m^2]	0.10	0.00	5602
$\gamma_{sat,\ moderately\ packed\ sand}$	[kN/m^3]	0.05	0.00	21.79
$\varphi_{moderately\ packed\ sand}$	[deg]	0.10	0.00	38.88
$F_{mooring}$	[kN]	0.15	-0.57	2704
Pile tip level	[m] NAP	0.25 (σ)	-0.07	-36.94
Bottom surface	[m] NAP	0.25 (σ)	0.15	-18.29
D	[m]	0.002	0.00	2.50
E	[kN/m^2]	0.03	0.02	$2.095 \cdot 10^8$
t	[mm]	0.03	0.03	40.83

Calculation	Z-value
1	992.8
621	0.307

G.3.3 Soil mechanical failure

Table G.9 - Results of the first calculation for variation 3: Modified soil structure (LS: Soil mechanical failure)

Number of calculations: 521				
$\beta_{correlated}$: 3.760				
P_f: $8.484 \cdot 10^{-5}$				
Parameter (X_i)	**Unit**	**V (=σ/μ)**	**$\alpha_{correlated}$**	**X_i* (Design value)**
$c_{sandy\ clay}$	[kPa]	0.20	-0.07	7.353
$E_{m,\ sandy\ clay}$	[kN/m^2]	0.10	0.08	3886
$\gamma_{sat,\ sandy\ clay}$	[kN/m^3]	0.05	0.11	19.20
$\varphi_{sandy\ clay}$	[deg]	0.10	0.17	25.21
$E_{m,\ gravel}$	[kN/m^2]	0.10	0.18	18610
$\gamma_{sat,\ gravel}$	[kN/m^3]	0.05	0.46	20.89
φ_{gravel}	[deg]	0.10	0.57	35.22
$E_{m,\ moderately\ packed\ sand}$	[kN/m^2]	0.10	0.08	5434
$\gamma_{sat,\ moderately\ packed\ sand}$	[kN/m^3]	0.05	0.18	21.05
$\varphi_{moderately\ packed\ sand}$	[deg]	0.10	0.31	34.28
$F_{mooring}$	[kN]	0.15	-0.46	2581
Pile tip level	[m] NAP	0.25 (σ)	-0.11	-34.18
Bottom surface	[m] NAP	0.25 (σ)	0.11	-18.26
D	[m]	0.002	0.00	2.50
E	[kN/m^2]	0.03	0.00	$2.099 \cdot 10^8$
t	[mm]	0.03	0.00	40.98

Calculation	Z-value
1	27.00
521	0.18

G.4 Variation 4: Increased thickness of the intermediate sand layer

G.4.1 Structural failure

Table G.10 - Results of the first calculation for variation 4: Increased thickness of the intermediate sand layer (LS: Structural failure)

Number of calculations: 463				
$\beta_{correlated}$: 3.977				
P_f: $4.486{\cdot}10^{-5}$				
Parameter (X_i)	**Unit**	**V (=σ/μ)**	**$\alpha_{correlated}$**	**X_i* (Design value)**
$c_{sandy\ clay}$	[kPa]	0.20	0.01	6.920
$E_{m,\ sandy\ clay}$	[kN/m^2]	0.10	0.04	3940
$\gamma_{sat,\ sandy\ clay}$	[kN/m^3]	0.05	0.07	19.35
$\varphi_{sandy\ clay}$	[deg]	0.10	0.06	26.27
$E_{m,\ gravel}$	[kN/m^2]	0.10	0.00	20000
$\gamma_{sat,\ gravel}$	[kN/m^3]	0.05	0.00	22.88
φ_{gravel}	[deg]	0.10	0.00	44.86
$E_{m,\ moderately\ packed\ sand}$	[kN/m^2]	0.10	0.00	5600
$\gamma_{sat,\ moderately\ packed\ sand}$	[kN/m^3]	0.05	0.00	21.79
$\varphi_{moderately\ packed\ sand}$	[deg]	0.10	0.00	38.88
$F_{mooring}$	[kN]	0.15	-0.84	3239
Pile tip level	[m] NAP	0.25 (σ)	0.00	-37.00
Bottom surface	[m] NAP	0.25 (σ)	0.07	-18.23
D	[m]	0.002	0.03	2.499
E	[kN/m^2]	0.03	0.00	$2.101{\cdot}10^8$
f_y	[N/mm^2]	0.07	0.49	483.8
t	[mm]	0.03	0.19	39.90

Calculation	Z-value	
1	54740	
463	-10.47	

G.4.2 Excessive deformations

Table G.11 - Results of the first calculation for variation 4: Increased thickness of the intermediate sand layer (LS: Excessive deformations)

Number of calculations: 401				
$\beta_{correlated}$: 3.791				
P_f: $7.507 \cdot 10^{-5}$				
Parameter (X_i)	**Unit**	**V (=σ/μ)**	**$\alpha_{correlated}$**	**X_i* (Design value)**
$c_{sandy\ clay}$	[kPa]	0.20	-0.01	7.040
$E_{m,\ sandy\ clay}$	[kN/m^2]	0.10	0.14	3781
$\gamma_{sat,\ sandy\ clay}$	[kN/m^3]	0.05	0.24	18.70
$\varphi_{sandy\ clay}$	[deg]	0.10	0.24	24.45
$E_{m,\ gravel}$	[kN/m^2]	0.10	0.05	19600
$\gamma_{sat,\ gravel}$	[kN/m^3]	0.05	0.03	22.77
φ_{gravel}	[deg]	0.10	0.01	44.62
$E_{m,\ moderately\ packed\ sand}$	[kN/m^2]	0.10	0.11	5364
$\gamma_{sat,\ moderately\ packed\ sand}$	[kN/m^3]	0.05	0.06	21.54
$\varphi_{moderately\ packed\ sand}$	[deg]	0.10	0.05	38.11
$F_{mooring}$	[kN]	0.15	-0.88	3238
Pile tip level	[m] NAP	0.25 (σ)	-0.09	-36.91
Bottom surface	[m] NAP	0.25 (σ)	0.13	-18.28
D	[m]	0.002	0.03	2.499
E	[kN/m^2]	0.03	0.11	$2.074 \cdot 10^8$
t	[mm]	0.03	0.13	40.22

Calculation	Z-value	
1	787.5	
401	0.647	

Table G.12 - Results of the second calculation for variation 4: Increased thickness of the intermediate sand layer (LS: Excessive deformations)

Number of calculations: 211				
$\beta_{correlated}$: 3.779				
P_f: $7.864 \cdot 10^{-5}$				
Parameter (X_i)	**Unit**	**V (=σ/μ)**	**$\alpha_{correlated}$**	**X_i* (Design value)**
$E_{m,\ sandy\ clay}$	[kN/m^2]	0.10	0.12	3821
$\gamma_{sat,\ sandy\ clay}$	[kN/m^3]	0.05	0.23	18.77
$\varphi_{sandy\ clay}$	[deg]	0.10	0.31	23.77
$E_{m,\ moderately\ packed\ sand}$	[kN/m^2]	0.10	0.12	5338
$F_{mooring}$	[kN]	0.15	-0.89	3243
Bottom surface	[m] NAP	0.25 (σ)	0.10	-18.25
E	[kN/m^2]	0.03	0.11	$2.074 \cdot 10^8$
t	[mm]	0.03	0.13	40.27

Calculation	Z-value	
1	782.0	
211	0.495	

G.4.3 Soil mechanical failure

Table G.13 - Results of the first calculation for variation 4: Increased thickness of the intermediate sand layer (LS: Soil mechanical failure)

Number of calculations: 441				
$\beta_{correlated}$: 3.882				
P_f: $5.176 \cdot 10^{-5}$				
Parameter (X_i)	**Unit**	**V (=σ/μ)**	**$\alpha_{correlated}$**	**X_i* (Design value)**
$c_{sandy\ clay}$	[kPa]	0.20	0.01	6.908
$E_{m,\ sandy\ clay}$	[kN/m^2]	0.10	0.16	3751
$\gamma_{sat,\ sandy\ clay}$	[kN/m^3]	0.05	0.32	18.41
$\varphi_{sandy\ clay}$	[deg]	0.10	0.24	24.43
$E_{m,\ gravel}$	[kN/m^2]	0.10	0.09	19320
$\gamma_{sat,\ gravel}$	[kN/m^3]	0.05	0.20	22.01
φ_{gravel}	[deg]	0.10	0.39	38.13
$E_{m,\ moderately\ packed\ sand}$	[kN/m^2]	0.10	0.09	5400
$\gamma_{sat,\ moderately\ packed\ sand}$	[kN/m^3]	0.05	0.23	20.81
$\varphi_{moderately\ packed\ sand}$	[deg]	0.10	0.40	32.77
$F_{mooring}$	[kN]	0.15	-0.59	2799
Pile tip level	[m] NAP	0.25 (σ)	-0.16	-34.61
Bottom surface	[m] NAP	0.25 (σ)	0.15	-18.31
D	[m]	0.002	0.00	2.50
E	[kN/m^2]	0.03	0.01	$2.098 \cdot 10^8$
t	[mm]	0.03	0.00	40.97

Calculation	Z-value	
1	30.16	
441	0.09	

Table G.14 - Results of the second calculation for variation 4: Increased thickness of the intermediate sand layer (LS: Soil mechanical failure)

Number of calculations: 253				
$\beta_{correlated}$: 3.865				
P_f: $5.553 \cdot 10^{-5}$				
Parameter (X_i)	**Unit**	**V (=σ/μ)**	**$\alpha_{correlated}$**	**X_i* (Design value)**
$E_{m,\ sandy\ clay}$	[kN/m^2]	0.10	0.13	3802
$\gamma_{sat,\ sandy\ clay}$	[kN/m^3]	0.05	0.29	18.50
$\varphi_{sandy\ clay}$	[deg]	0.10	0.30	23.78
$E_{m,\ gravel}$	[kN/m^2]	0.10	0.09	19310
$\gamma_{sat,\ gravel}$	[kN/m^3]	0.05	0.20	22.00
φ_{gravel}	[deg]	0.10	0.39	38.05
$\gamma_{sat,\ moderately\ packed\ sand}$	[kN/m^3]	0.05	0.23	20.83
$\varphi_{moderately\ packed\ sand}$	[deg]	0.10	0.39	32.97
$F_{mooring}$	[kN]	0.15	-0.59	2804
Pile tip level	[m] NAP	0.25 (σ)	-0.17	-34.61
Bottom surface	[m] NAP	0.25 (σ)	0.13	-18.29
Calculation	Z-value			
1	29.98			
253	0.20			

G.5 Variation 5: Increased coefficient of variation for the soil stiffness

G.5.1 Structural failure

Table G.15 - Results of the first calculation for variation 5: Increased coefficient of variation for the soil stiffness (LS: Structural failure)

Number of calculations: 463				
$\beta_{correlated}$: 4.050				
P_f: $2.556 \cdot 10^{-5}$				
Parameter (X_i)	**Unit**	**V (=σ/μ)**	**$\alpha_{correlated}$**	**X_i* (Design value)**
$c_{sandy\ clay}$	[kPa]	0.20	0.01	6.917
$E_{m,\ sandy\ clay}$	[kN/m^2]	0.10	0.04	3935
$\gamma_{sat,\ sandy\ clay}$	[kN/m^3]	0.05	0.07	19.35
$\varphi_{sandy\ clay}$	[deg]	0.10	0.06	26.25
$E_{m,\ gravel}$	[kN/m^2]	0.10	0.00	20000
$\gamma_{sat,\ gravel}$	[kN/m^3]	0.05	0.00	22.88
φ_{gravel}	[deg]	0.10	0.00	44.86
$E_{m,\ moderately\ packed\ sand}$	[kN/m^2]	0.10	0.00	5600
$\gamma_{sat,\ moderately\ packed\ sand}$	[kN/m^3]	0.05	0.00	21.79
$\varphi_{moderately\ packed\ sand}$	[deg]	0.10	0.00	38.88
$F_{mooring}$	[kN]	0.15	-0.85	3255
Pile tip level	[m] NAP	0.25 (σ)	0.00	-37.00
Bottom surface	[m] NAP	0.25 (σ)	0.04	-18.20
D	[m]	0.002	0.03	2.499
E	[kN/m^2]	0.03	0.00	$2.100 \cdot 10^8$
f_y	[N/mm^2]	0.07	0.49	482.1
t	[mm]	0.03	0.17	39.96

Calculation	Z-value	
1	54990	
463	0.531	

G.5.2 Excessive deformations

Table G.16 - Results of the first calculation for variation 5: Increased coefficient of variation for the soil stiffness (LS: Excessive deformations)

Number of calculations: 401				
$\beta_{correlated}$: 3.212				
P_f: $6.599 \cdot 10^{-4}$				
Parameter (X_i)	**Unit**	**V (=σ/μ)**	**$\alpha_{correlated}$**	**X_i* (Design value)**
$c_{sandy\ clay}$	[kPa]	0.20	0.00	6.967
$E_{m,\ sandy\ clay}$	[kN/m^2]	0.10	0.25	3013
$\gamma_{sat,\ sandy\ clay}$	[kN/m^3]	0.05	0.32	18.61
$\varphi_{sandy\ clay}$	[deg]	0.10	0.29	24.40
$E_{m,\ gravel}$	[kN/m^2]	0.10	0.21	15770
$\gamma_{sat,\ gravel}$	[kN/m^3]	0.05	0.10	22.51
φ_{gravel}	[deg]	0.10	0.06	44.05
$E_{m,\ moderately\ packed\ sand}$	[kN/m^2]	0.10	0.14	4721
$\gamma_{sat,\ moderately\ packed\ sand}$	[kN/m^3]	0.05	0.07	21.56
$\varphi_{moderately\ packed\ sand}$	[deg]	0.10	0.04	38.42
$F_{mooring}$	[kN]	0.15	-0.79	2902
Pile tip level	[m] NAP	0.25 (σ)	-0.11	-36.91
Bottom surface	[m] NAP	0.25 (σ)	0.12	-18.26
D	[m]	0.002	0.00	2.50
E	[kN/m^2]	0.03	0.08	$2.083 \cdot 10^8$
t	[mm]	0.03	0.10	40.52

Calculation	Z-value	
1	766.4	
401	0.816	

G.5.3 Soil mechanical failure

Table G.17 - Results of the first calculation for variation 5: Increased coefficient of variation for the soil stiffness (LS: Soil mechanical failure)

Number of calculations: 381				
$\beta_{correlated}$: 3.859				
P_f: $5.683 \cdot 10^{-5}$				
Parameter (X_i)	**Unit**	**V (=σ/μ)**	**$\alpha_{correlated}$**	**X_i* (Design value)**
$c_{sandy\ clay}$	[kPa]	0.20	-0.01	7.023
$E_{m,\ sandy\ clay}$	[kN/m^2]	0.10	0.22	3001
$\gamma_{sat,\ sandy\ clay}$	[kN/m^3]	0.05	0.38	18.17
$\varphi_{sandy\ clay}$	[deg]	0.10	0.32	23.58
$E_{m,\ gravel}$	[kN/m^2]	0.10	0.10	17110
$\gamma_{sat,\ gravel}$	[kN/m^3]	0.05	0.25	21.79
φ_{gravel}	[deg]	0.10	0.47	36.64
$E_{m,\ moderately\ packed\ sand}$	[kN/m^2]	0.10	0.10	4797
$\gamma_{sat,\ moderately\ packed\ sand}$	[kN/m^3]	0.05	0.15	21.16
$\varphi_{moderately\ packed\ sand}$	[deg]	0.10	0.22	35.59
$F_{mooring}$	[kN]	0.15	-0.53	2709
Pile tip level	[m] NAP	0.25 (σ)	-0.16	-34.98
Bottom surface	[m] NAP	0.25 (σ)	0.13	-18.29
D	[m]	0.002	0.03	2.499
E	[kN/m^2]	0.03	0.00	$2.099 \cdot 10^8$
t	[mm]	0.03	0.00	40.97

Calculation	Z-value	
1	31.24	
381	0.22	

REFERENCES

Baecher, G. B. & Christian, J. T., 2003. *Reliability and statistics in geotechnical engineering.* Hoboken, New Jersey: Wiley.

Baker, J. & Calle, E., 2006. *JCSS Probabilistic Model Code. Section 3.7: Soil Properties.* Revised version August 2006 red. sl:Joint Committee on Structural Safety.

Blum, H., 1932. Wirtschaftliche dalbenformen und deren berechnung. *Bautechnik, Heft 5.*

Brinch-Hansen, J. & Christensen, N., 1961. *The ultimate resistance of rigid piles against transversal forces; Model tests with transversally loaded rigid piles in sand.* s.l.:Geoteknisk Institut.

Brinkgreve, R. B. J., Kumarswamy, S. & Swolfs, W. M., 2015. *Plaxis 2015 - General information.* Delft: Plaxis bv.

BS6349-2, 2010. *Maritime works - Part 2: Code of practice for the design of quay walls, jetties and dolphins.* London: British Standards Institution.

BS6349-4, 1994. *Maritime structures - Part 4: Code of practice for design of fendering and mooring systems.* London: British Standards Institution.

BS-EN1997-1, 2004. *UK National Annex to Eurocode 7: Geotechnical design - Part 1: General rules.* London: British Standards Institution.

Courage, W. M. G. & Steenbergen, H. M. G. M., 2007. *Prob2B: Variables, Expressions and Excel Installation and Getting Started.* Delft: TNO Built Environment and Geoscience.

CUR-publicatie 190, 2002. *Kansen in de civiele techniek, Deel 1: Probabilistisch ontwerpen in theorie.* 2e druk ed. Gouda: Stichting CUR.

CUR-publicatie 211E, 2014. *Quay walls.* Second edition ed. Leiden: CRC Press/Balkema.

Deltares, 2014. *D-Pile Group, 3D modelling of single piles and pile groups.* Version 14.1 ed. Delft: Deltares.

Deltares, 2014. *D-Sheet Piling, Design of diaphragm and sheet pile walls, User Manual.* Version 14.1 ed. Delft: Deltares.

Fleming, K., Weltman, A., Randolph, M. & Elson, K., 2008. *Piling engineering.* s.l.:CRC Press.

Havenbedrijf Rotterdam N.V., 2016. *Bolderbelastingen Standaardisatie Rotterdam, versie 1.1,* Rotterdam: Havenbedrijf Rotterdam N.V..

HTG, 2015. *Recommendations of the Committee for Waterfront Structures, Harbours and Waterways: EAU 2012.* 9th edition ed. Hoboken, New Jersey: Wiley.

JCSS, 2001. *JCSS Probabilistic Model Code.* sl:Joint Committee on Structural Safety.

Maier, H. R., Lence, B. J., Tolson, B. A. & Foschi, R. O., 2001. First-order reliability method for estimating reliability, vulnerability and resilience. *Water resources research,* Vol. 37(No. 3), pp. 779-790.

Ménard, L., Bourdon, G. & Gambin, M., 1971. Methode generale de calcul d'un rideau ou d'un pieu sollicite horizontalement en fonction des resultats pressiometrique. *Sols Soils,* Issue vol. 6, no. 22/23.

NEN 9997-1+C1, 2012. *Geotechnical design of structures - Part 1: General rules.* Delft: Nederlands Normalisatie-instituut.

NEN-EN 1990+A1+A1/C2, 2011. *Eurocode - Basis of structural design.* Delft: Nederlands Normalisatie-instituut.

NEN-EN 1993-1-1+C2, 2011. *Ontwerp en berekening van staalconstructies - Deel 1-1: Algemene regels en regels voor gebouwen,* sl: Nederlands Normalisatie-instituut.

NEN-EN 1993-1-6, 2007. *Ontwerp en berekening van staalconstructies - Deel 1-6: Algemene regels - Sterkte en Stabiliteit van Staalconstructies,* sl: Nederlands Normalisatie-instituut.

NEN-EN 1997-1, 2005. *Eurocode 7: Geotechnical design - Part 1: General rules.* Delft: Nederlands Normalisatie-instituut.

NEN-EN10219-2, 2006. *Koudvervaardigde gelaste buisprofielen voor constructiedoeleinden van ongelegeerde en fijnkorrelige staalsoorten - Deel 2: Toleranties, afmetingen en profieleigenschappen.* Delft: Nederlands Normalisatie-instituut.

PIANC, 2002. *Guidelines for the Design of Fender Systems: 2002.* Brussels: International Navigation Association.

Plaxis bv, 2015. *Plaxis 3D - Material Models Manual.* Delft: Plaxis bv.

Plaxis bv, n.d. *Plaxis 3D - Reference manual.* Anniversary edition ed. Delft: Plaxis bv.

Reese, L. C., Isenhower, W. M. & Wang, S. T., 2006. *Analysis and design of shallow and deep foundations.* Hoboken, New Jersey: John Wiley & Sons, Inc.

Reese, L. C. & Van Impe, W. F., 2001. *Single piles and pile groups under lateral loading.* Rotterdam: A.A. Balkema.

Roubos, A. A., Groenewegen, L. & Peters, D. J., 2016. *Berthing energy, berthing impact and partial safety factors for maritime structures (concept version),* sl: sn

Ruigrok, J. A. T., 2010. *Laterally loaded piles, Models and Measurements,* Delft: Delft University of Technology.

Schweckendiek, T., 2006. *Structural reliability applied to deep excavations; Coupling reliability methods with finite elements,* Delft: Delft University of Technology.

Technische Adviescommissie voor de Waterkeringen [TAW], 2004. *Technisch Rapport Kistdammen en Diepwanden in Waterkeringen,* Delft: TAW.

Teunissen, M. N. H., 2005. *Kwaliteitscrontrole van gestabiliseerde grondkolommen,* Delft: TU Delft.

Trellenborg AB, 2015. *Fender Application Design Manual.* Sweden: Trellenborg Marine Systems.

Trellenborg AB, 2015. *Fender systems - Product brochure,* Sweden: Trellenborg Marine Systems.

Van der Meer, J. & Peters, D. J., 2015. *Static and dynamic lateral load tests on Flexible Dolphins - Factual and interpretation report (Final draft report, internal report),* Rotterdam: Witteveen+Bos and HaskoningDHV Nederland BV.

Verhoef, R. M., 2015. *Laterally loaded piles in sloping ground,* Delft: Delft University of Technology.

Verruijt, A., 2010. *Grondmechanica.* Delft: VSSD.

Volker Staal en Funderingen, 2015. *Ligplaatsen Calandkanaal. Dimensionering buispalen en energiebeschouwing van de meerpalen en trospalen van de ligplaatsen 79b / 82 / 83,* Rotterdam: VSF.

Wolters, H. J., 2012. *Reliability of quay walls,* Delft: Delft University of Technology.

Yang, Z. & Jeremic, B., n.d. Study of soil layering effects on lateral loading behavior of piles. *ASCE Journal of Geotechnical and Geoenvironmental Engineering.*